Aus dem Institut für Laboratoriumsmedizin und Pathobiochemie,
Molekulare Diagnostik
Geschäftsführender Direktor: Prof. Dr. Harald Renz
des Fachbereichs Medizin der Philipps-Universität Marburg

An immunoinformatics approach for identification and characterization of T cell-mediated heterologous immunity between RNA viruses and allergens

Inaugural-Dissertation zur Erlangung
des Doktorgrades der Naturwissenschaften
dem Fachbereich Medizin der Philipps-Universität Marburg

vorgelegt von

Kathrin Jana Balz
aus Frankfurt
Marburg, 2022

Angenommen vom Fachbereich Medizin der Philipps-Universität Marburg am: 23.05.2022

Gedruckt mit Genehmigung des Fachbereichs Medizin

Dekanin: Prof. Dr. Denise Hilfiker-Kleiner
Referentin: PD Dr. Chrysanthi Skevaki
Korreferent: Prof. Dr. Alexander Visekruna

„Man sieht nur mit dem Herzen gut. Das Wesentliche ist für die Augen unsichtbar."

-Antoine de Saint-Exupéry-

Table of Contents

Table of Contents IV

I. Abbreviations IX

II. List of Figures XIII

III. List of Tables XVI

1. Introduction 1

1.1 The allergy epidemic 1

1.2 The evolution of the hygiene hypothesis 2

1.3 Asthma 5

1.3.1 Epidemiology 5

1.3.2 Risk factors 6

1.3.3 Phenotypes and endotypes of asthma 10

1.3.4 Diagnosis and treatment 15

1.4 Heterologous immunity 16

1.4.1 Virus-induced T cell mediated heterologous immunity 18

1.5 Hypothesis and aims 19

2. Materials 21

2.1 Cell lines 21

2.2 Virus 21

2.3 Animals 21

2.4 Anesthetics 21

2.5 Allergens 22

2.6 Adjuvants/Vaccines 22

2.7 Antibodies 22

2.8 Pentamers 23

2.9 Peptides 23

2.10 Cell culture media 25
2.11 Primer 25
2.12 Kits 25
2.13 Chemicals 26
2.14 Plastic ware 27
2.15 Devices 27
2.16 Softwares 28
3. Methods 29
3.1 Murine models 29
3.1.1 RSV A2 infection 29
3.1.2 Influenza vaccination 29
3.1.3 Peptide immunization 29
3.1.4 HDM- induced experimental asthma 30
3.1.5 *Asp f*-induced experimental asthma 30
3.2 Serum preparation 30
3.3 Bronchoalveolar lavage acquisition and cytology 31
3.4 Lung histology preparation 31
3.4.1 H&E & PAS stainings 32
3.4.2 Immunofluorescence 33
3.5 Preparation of cell suspensions from murine organs 34
3.5.1 Lung 34
3.5.2 Spleen 34
3.5.3 Lymph nodes 35
3.6 *Ex-vivo* T cell stimulation assays 35
3.7 CFSE proliferation assay 35
3.8 Immunological methods 36
3.8.1 IgG Enzyme-linked immunosorbent assay 36

3.8.2 IFNγ Enzyme-linked immunosorbent assay 36
3.8.3 Cytometric bead array 37
3.8.4 Flow cytometry staining 37
3.8.5 *In-vitro* MHC stabilization assay 38
3.9 Molecular biology methods 38
3.9.1 RNA Isolation 38
3.9.2 cDNA production 39
3.9.3 Quantitative real-time PCR 39
3.9.4 Standard curve for strand-specific qPCR 40
3.10 Virome analysis 40
3.11 Cell biology methods 41
3.11.1 Cell culture 41
3.11.2 Freezing and thawing of cells 41
3.11.3 RSV propagation 41
3.11.4 RSV titration 42
3.11.5 UV-inactivation of RSV 42
3.12 *In-silico* prediction of potentially cross-reactive T cell epitopes 43
3.12.1 Bioinformatics pipeline 43
3.12.2 Scoring system 44
3.13 Statistical analysis 45
4. Results 46
4.1 A bioinformatics approach identified potentially cross-reactive T cell epitope pairs between several RNA viruses and allergens 46
4.2 Several predicted T cell epitopes were able to bind to MHC molecules *in-vitro* 49
4.3 RSV-induced inflammation in mice peaks between 4 and 12 dpi and is cleared upon 35 dpi 51

4.4 Cross-reactivity between predicted RSV A2- and allergen-derived epitopes following viral infection and virus peptide immunization 55

4.4.1 *Ex-vivo* stimulation of splenocytes and lung cell homogenates with the predicted allergen peptides results in enhanced $CD8^+$ T cell response following RSV infection 55

4.4.2 Long-lasting virus- and allergen- double positive $CD8^+$ memory T cells in the lung 57

4.4.3 Cross-reactive T cell response to *Asp f*-derived epitopes in virus-peptide immunized mice 59

4.5 Prior RSV A2 infection attenuates T2 response in mice subjected to *Asp f*-induced experimental asthma 60

4.5.1 Virome diversity and composition are altered in *Asp f*-induced experimental asthma 67

4.6 Predicted cross-reactive T cell epitopes are partly responsible for virus-mediated attenuation of *Asp f*-induced experimental asthma 71

4.7 Beneficial heterologous immune response against allergens is also induced by prior influenza vaccination 76

4.7.1 Intraperitoneal vaccination of mice with the seasonal quadrivalent influenza vaccine induces B- and T cell response 76

4.7.2 Predicted virus-and allergen derived T cell epitopes induce activation of $CD8^+$ T cells upon *ex-vivo* stimulation of splenocytes from influenza-vaccinated mice 78

4.7.3 Influenza vaccination reduces eosinophilic airway inflammation and mucus production in mice with HDM-induced experimental asthma 79

5. Discussion 85

5.1 A suitable RSV infection model for investigation of heterologous T cell response was established 85

5.2 An immunoinformatics approach identified cross-reactive T cell epitope pairs between RNA viruses and environmental allergens 87

5.3 Type 2 immune response in experimental asthma is attenuated by preceding virus infection 91
5.3.1 Changes in lung virome composition may also contribute to heterologous immune response 95
5.4 Immunization with the predicted RSV-derived peptides partially contribute to attenuation of experimental asthma 96
5.5 T2 inflammation is attenuated in experimental asthma via prior influenza vaccination 99
5.6 Conclusion and outlook 102
6. Summary 105
7. Zusammenfassung 107
8. References 109
9. Supplementary figures 136
10. Appendix 138
Curriculum vitae ..... **Fehler! Textmarke nicht definiert.**
Verzeichnis der akademischen Lehrer 139
Danksagung 140
Ehrenwörtliche Erklärung ..... **Fehler! Textmarke nicht definiert.**

I. Abbreviations

A

AAI	Allergic airway inflammation
Asp f	*Aspergillus fumigatus*
ACK	Ammonium-chloride-potassium
AEC2	Angiotensin-converting enzyme2
AHR	Airway hyperresponsiveness
APC	Antigen presenting cell
AW	Airway

B

BAL	Bronchoalveolar lavage
BSA	Bovine serum albumin
BV	Blood vessel

C

CBA	Cytometric bead array
CD	Cluster of differentiation
CFSE	Carboxyfluorescein succinimidyl ester
COPD	Chronic obstructive pulmonary disease
CoV	Coronavirus
COVID-19	Coronavirus disease 2019

D

DC	Dendritic cell
DENV	Dengue virus
Der p	*Dermatophagiodes pternoyssinus*
Der f	*Dermatophagiodes farinae*
DMEM	Dulbecco′s Modified Eagle′s Medium
DMSO	Dimethyl sulfoxide
Dpi	Days post infection

E

EDTA	Ethylenediaminetetraacetic acid
AERD	Aspirin-exacerbated respiratory disease
EIA	Exercise-induced asthma
ELISA	Enzyme-Linked Immunosorbent Assay
EoA	Early-onset asthma
EoE	Eosinophilic esophagitis

F

Fab	Fragment antigen binding
FEV1	Forced expiratory volume in 1 second
FVC	Forced vital capacity

G

GINA	Global Initiative for Asthma

H

HAV	Hepatitis A virus
HDM	House dust mite
H&E	Hematoxylin & eosin
HLA	Human leukocyte antigen
HRP	Horseradish peroxidase

I

IAV	Influenza A virus
ICS	Inhaled corticosteroids
IFNγ	Interferon gamma
Ig	Immunoglobulin
IL	Interleukin
ILC	Innate lymphoid cell
i.n.	Intranasal
i.p.	Intraperitoneal

L

LAIV	Live Attenuated Influenza Vaccine

M

MCT	Microcrystalline tyrosine
MEM	Minimal Essential Medium
MERS	Middle East Respiratory Syndrom
MHC	Major histocompatibility complex

N

NEAA	Non-essential amino acids

O

OD	Optical density
OVA	Ovalbumin

P

PAS	Periodic acid Schiff
PCR	Polymerase chain reaction
Phl p	*Phleum pratense*
PBMCs	peripheral blood mononuclear cells
PBS	Phosphate-buffered saline
PFA	Paraformaldehyde
PMA	Phorbol 12-myristate 13-acetate

Q

QIV 19/20	Quadrivalent influenza vaccine 2019/2020

R

rpm	Revolutions per minute
RPMI	Roswell Park Memorial Institute
RSV	Respiratory syncytial virus
RT	Room temperature

RV	Rhinovirus

S

SABA	Short-acting beta-2 agonists
SARS	Severe acute respiratory syndrome
s.c.	Subcutaneous

T

TCR	T cell receptor
Tem	T effector memory cell
Tfh	Follicular T helper cell
TLR	Toll-like receptor
TNFα	Tumor necrosis factor alpha
Treg	T regulatory cell
Trm	Tissue-resident memory T cells
TSLP	Thymic stromal lymphopoietin

U-Z

VE-H_20	Deionized water
VPP	Virus peptide pool
ZIKV	Zika virus

II. List of Figures

Figure 1: Schematic representation of the concept of “atopic march”, demonstrating the development of allergic diseases over 15 years of age (Kabashima, 2012) 2
Figure 2: Contrary development of infectious diseases and immune disorders over a period of 50 years within industrialization (Bach, 2002) 4
Figure 3: Schematic overview of pre- and postnatal risk factors in the process of asthma and allergy development (Renz, Skevaki 2021) 6
Figure 4: Correlation of wheezing within the first 3 years of life by rhinovirus (RV), respiratory syncytial virus (RSV) or both and development of asthma at the age of 6 years (Jackson 2008) 8
Figure 5: Phenotypes and endotypes of asthma (Wenzel, 2012) 12
Figure 6: Mechanisms of T2- driven allergic asthma (Fahy, 2015) 13
Figure 7: Mechanisms of T cell-mediated heterologous immune response (Pusch et al., 2018) 17
Figure 8: Virus-induced heterologous immune response towards allergen exposure [adapted from (Pusch et al., 2018)] 20
Figure 9: Schematic overview of the bioinformatics pipeline and calculation of the pair combined score 44
Figure 10: Scoring system for further prioritization of the selected top 30 potentially cross-reactive allergen- and virus- derived T cell epitope pairs 45
Figure 11: Predicted candidate epitopes as per pair combined score and allergen proteins families 47
Figure 12: Predicted peptides bind to the mouse Balb/c H-2-Kd MHC molecule *in-vitro* 50
Figure 13: RSV A2 replicates in the lung until 4 dpi and induces virus-specific IgG response 52
Figure 14: Airway inflammation peaks between 6 and 12 days after RSV A2 infection 52
Figure 15: Virus infection induces long lasting T effector memory response in the lung as well as virus-specific T cells in lung and mediastinal lymph nodes 53
Figure 16: Lung inflammation can be observed in parallel with presence of RSV A2 in lung histology sections 54

Figure 17: Enhanced CD8+ T cell activation and cytokine production upon *ex-vivo* stimuation with the predicted virus-and allergen derived peptides of RSV A2 primed lung cells at 12 dpi 56
Figure 18: CD8+ T cells produce more intracellular cytokines upon *ex-vivo* stimulation with the predicted allergen peptide pool in RSV-primed splenocytes at 35 dpi 57
Figure 19: Dual pentamer staining of RSV-primed lung cells demonstrate long-lasting virus-and allergen specific CD8+ T cells 58
Figure 20: Predicted *Asp f*- derived peptides induce cross-reactive T cell response 60
Figure 21: Experimental set-up and detection of immunoglobulins 61
Figure 22: RSV A2 infection reduces eosinophilic response in BAL of *Asp f*-treated mice 62
Figure 23: Cytokines are reduced in BAL supernatant of *Asp f*- treated mice upon RSV A2 infection 63
Figure 24: Immune cell composition in *Asp f*- treated mice is altered upon a prior RSV A2 infection 64
Figure 25: Reduced IL-5+ T cells in lung homogenates of RSV/*Asp f* mice 65
Figure 26: Lung inflammation and mucus production are reduced in RSV/*Asp f* mice 66
Figure 27: Principal Component Analysis (PCoA) reveals differences in lung tissue between asthmatic and non-asthmatic groups of animals 68
Figure 28: Lung samples contain higher virome diversity compared to BAL, which is reduced in asthmatic mice 69
Figure 29: Virome composition is altered upon allergen treatment in lung tissue of mice 70
Figure 30: Experimental set-up 71
Figure 31: Virus peptide immunization reduces numbers of eosinophils in the BAL of *Asp f*-treated mice 72
Figure 32: Immune cells in the lung are not affected by virus peptide immunization 73
Figure 33: Virus peptide immunization increases intracellular IFNγ in CD8+ T cells 74

Figure 34: Lung histology is not altered in VPP/*Asp f* group compared to Mock/*Asp f*.....75
Figure 35: Immunization with QIV in mice induced T- and B cell response.....77
Figure 36: Predicted peptide pools induces activation of $CD8^+$ T cells in spleen cells of QIV immunized mice 78
Figure 37: Experimental set-up and detection of immunoglobulins.....79
Figure 38: Influenza vaccination in mice reduces eosinophilia in BAL of HDM-treated animals.....80
Figure 39: Increased TNFα but no changes in T2 cytokines in HDM-treated mice upon QIV immunization 81
Figure 40: Altered abundance of immune cell subsets in the lung of QIV/HDM mice compare to Mock/HDM animals 82
Figure 41: Reduced $CD4^+$ $IL\text{-}13^+$ T cells in lung of QIV/HDM- treated mice.....83
Figure 42: Influenza vaccination significantly reduced lung inflammation and mucus secretion in lung histology sections of HDM-treated mice 84
Figure 43: Binding of predicted RV1b peptides to the mouse Balb/c H-2-Kd MHC molecule *in-vitro* 136
Figure 44: Binding of predicted QIV 19/20 peptides to the mouse Balb/c H-2-Kd MHC molecule *in-vitro*.....137

III. List of Tables

Table 1: Anesthetics 21
Table 2: Allergens 22
Table 3: Adjuvants and Vaccines 22
Table 4: Antibodies 22
Table 5: Pentamers 23
Table 6: Peptides 24
Table 7: Composition of cell culture media 25
Table 8: Primer 25
Table 9: Kits 25
Table 10: Chemicals 26
Table 11: Plastic ware 27
Table 12: Devices 27
Table 13: Softwares 28
Table 14: Peptides used for virus-peptide immunization experiment 30
Table 15: H&E and PAS staining protocols 32
Table 16: Amounts of reagents used for cDNA production 39
Table 17: Amounts of reagents used for qPCR 39
Table 18: qPCR settings 39
Table 19: Settings for the RT-PCR for production of a standard curve 40
Table 20: The top 5 candidate human T cell epitope pairs for potential cross-reactivity between SARS-CoV-2 and aero - and food-allergens for HLA class I 48
Table 21: The top 5 candidate human T cell epitope pairs for potential cross-reactivity between SARS-CoV-2 and aero - and food-allergens for HLA class II; 48
Table 22: The top 5 candidate mouse T cell epitope pairs for potential cross-reactivity between RV1b and aero - and food-allergens 50
Table 23: The top 5 candidate mouse T cell epitope pairs for potential cross-reactivity between RSV A2 and aero - and food-allergense 51
Table 24: The top 5 candidate mouse T cell epitope pairs for potential cross-reactivity between QIV 19/20 and aero - and food-allergens 51

1. Introduction

1.1 The allergy epidemic

The concept of atopy was first described in 1923 in order to distinguish between normal and abnormal hypersensitivity (Coca, Cooke, 1923). Nowadays, atopy is defined as a genetic predisposition of atopic individuals to develop one or more allergic diseases, such as allergic asthma, allergic rhinitis and atopic dermatitis (Verschoor, Gunten, 2019). Additionally, food allergy, eosinophilic esophagitis (EoE), or allergic conjunctivitis are also often encountered among atopic patients (Han et al., 2017). The main feature of these atopic diseases is an exaggerated immune response upon contact with environmental stimuli, mostly resulting in allergen-specific Immunoglobulin E (IgE) production (Verschoor, Gunten, 2019). However, non-IgE-mediated allergies are known as well, mainly in the area of food allergy. Food allergy may be mediated by different immune mechanisms. Besides of IgE-mediated food allergies, non-IgE-mediated diseases are existing, as well as such characterized by a mixed IgE/non-IgE response. Non-IgE-mediated diseases are suggested to be initiated by T cells (Cianferoni, 2020, Labrosse et al., 2020). However, exact mechanisms are not fully investigated yet.

Atopic diseases naturally develop during the life of predisposed individuals in a specific order, known as “the atopic march” (Figure 1) (Cantani, 1999, Schäfer et al., 1996). The latter begins early in life with the development of atopic dermatitis and food allergies, followed by allergic rhinitis and allergic asthma (Han et al., 2017). Approximately half of the predisposed children start developing atopic dermatitis under the age of six months, with increasing prevalence until the age of five years. The clinical features of atopic dermatitis are chronic skin inflammation and a disturbed skin barrier (Yang et al., 2020). Skin barrier disruptions may be initiated by genetic mutations and polymorphisms in genes relevant for a balanced immune system, but also by environmental influences (Hill, Spergel, 2018). Subsequent contact of allergens with the damaged skin results in chronic inflammation and sensitization, which is defined as “transcutaneous sensitization”. Repeated allergen exposures facilitate progression of allergic asthma, allergic rhinitis and food allergy (Han et al., 2017). Of note, food allergy can as well promote allergic rhinitis and asthma

development independently of atopic dermatitis (Hill et al., 2016). Additionally, allergic rhinitis and asthma may influence each other and coexist (Leynaert et al., 2004). Another important atopic disease is EoE, representing a chronic esophageal inflammatory disease, which is caused by allergens or pollen. Several studies demonstrated positive correlations between EoE and other allergic diseases, suggesting this to be also involved in the mechanisms of the atopic march. However, EoE may also occur independently of atopy and larger studies are needed to confirm relationships between these diseases (Yang et al., 2020).

Generally, the mechanisms of the atopic march are still not completely investigated and multiple phenotypes of the diseases are described which do not follow these progressions.

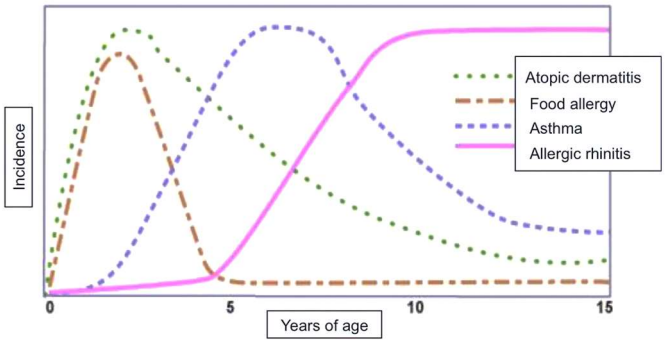

Figure 1: Schematic representation of the concept of "atopic march", demonstrating the development of allergic diseases over 15 years of age (Kabashima, 2012)

1.2 The evolution of the hygiene hypothesis

Since the 1950s, the prevalence of allergic diseases has increased in the developed countries. This is especially prominent for asthma, having gained a fourfold higher incidence since then (Lambrecht, Hammad, 2017). The rise in asthma prevalence goes along with an increase in other immune diseases, such as multiple sclerosis, Type 1 diabetes mellitus and Crohn's disease. On the other hand, the incidence of infectious diseases, including measles, Hepatitis A and tuberculosis, constantly decreases (Bach, 2002) (Figure 2). The hygiene hypothesis was originally described by David Strachan in 1989, suggesting an inverse correlation between family size and personal hygiene in childhood and the development of hay fever and eczema (Strachan, 1989). Further studies showed an increasing prevalence of allergic diseases in west Germany compared to east Germany. Environment and western lifestyle,

including nutrition and housing, have been hypothesized and investigated as contributing factors (Heinrich et al., 2002, Wichmann, 1996). Several conducted studies focused on a protective effect of pet exposure to the prevalence of allergic rhinitis and asthma, although the results were quite inconsistent. The Multicenter Allergy Study (MAS) correlated levels and ratio of cat-specific IgE/IgG to either development of allergic diseases or protection (Lau et al., 2005, Pfefferle et al., 2009). Important evidence regarding the association between lifestyle and allergy development were delivered by farming studies. The SCARPOL study in Switzerland demonstrated a 50 % lower risk of children born and raised on farms to develop allergic diseases compared to non-farming children (Braun-Fahrländer et al., 1999). Subsequent farming studies correlated environmental burden, including exposure to cowsheds, endotoxin, helminths and lactobacilli, with protection towards allergic diseases (Rook, 2009). It has been shown for example, that specific bacteria, such as *Acinetobacter lwoffii* or *Lactococcus lactis* were found in cowshed, being able to shift the adaptive immunity from T2 to T1 response and therefore protecting from asthma (Debarry et al., 2007). The original hygiene hypothesis was then extended, claiming that microbes in the urban environment have been present throughout evolution and are recognized by the innate immune system as "old friends", dampening a regulatory T cell (T_{reg}) response and therefore leading to progressive disease. This "old friends hypothesis" includes mycobacteria, lactobacilli, helminths and viruses (Rook et al., 2004). Later, it was demonstrated that not only the microbes, but also the microbial diversity and living environment in general („biodiversity hypothesis") contribute to a protection against allergy and autoimmune diseases (Ege et al., 2011, Hanski et al., 2012, Hertzen et al., 2011, Rook, 2009). Such an environmental diversity could as well enrich the human microbiota, resulting in an enhanced immune balance and therefore protection from allergic diseases (Haahtela, 2019). A prominent example is the bacterium *Helicobacter pylori* in the gastrointestinal area, whose prevalence is decreasing in industrialized countries. Notably, exposure to this bacterium is associated with a reduced risk for allergic diseases. The microbiota of healthy human consists of different species, including bacteria (microbiome), viruses (virome), fungi and archaea and is considered as stable, resistant and resilient (Barcik et al., 2020). The human virome comprises a huge number of commensal and non-pathogenic viruses, which are suggested to play a

role in disease susceptibility (Sullivan et al., 2016). For example, *Anelloviridae*, but also *Caudovirales* and *Picornaviridae* were associated with a possible protective role for wheezing and rhinitis in human (Tay et al., 2021). Thus, the role of the airway virome and asthma is currently extensively investigated.

The mechanisms behind the hygiene hypothesis are quite complex. In the late 20th century it was known that there is a T2 bias early in life, which gradually shifts in non-atopic individuals due to contact with microbes and further leads to a higher T1 response (Barrios et al., 1996, Prescott et al., 1998). The role of dendritic cells and toll-like receptor signaling became more important, triggering T1 and T_{reg} response after microbial contact (Haspeslagh et al., 2018). Indeed, an increase in T_{reg} frequency upon contact with viruses, bacteria and also parasites was shown in several experimental studies, being associated with protective mechanisms against autoimmune diseases (Bach, 2018).

However, the mechanisms of the immune system and asthma development are highly complex, including several different T cell subsets, but also cells of the innate immune system and epigenetic mechanisms (Holgate, 2012). Therefore, further investigations are needed to support the hygiene hypothesis and its underlaying mechanisms.

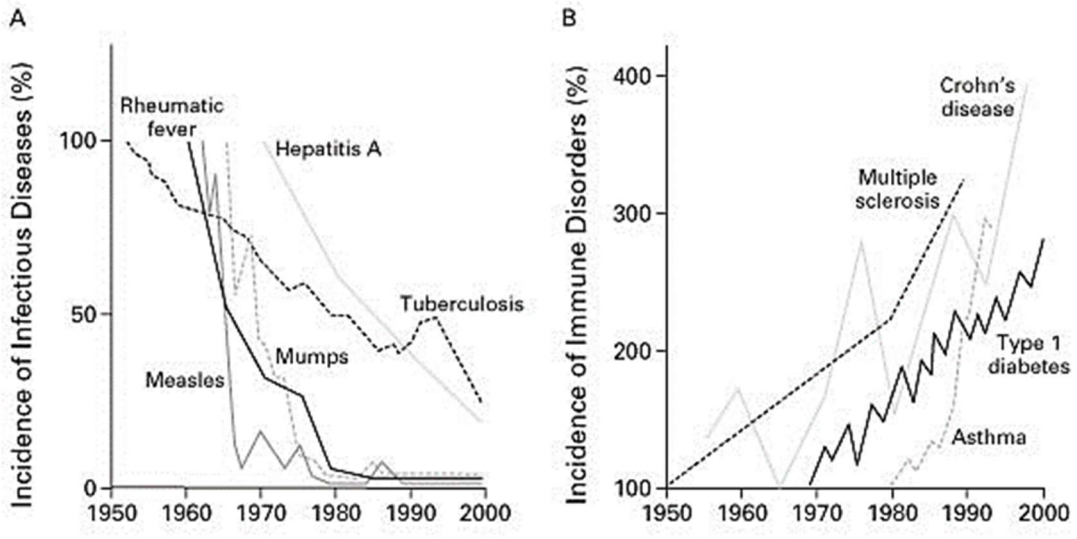

Figure 2: Contrary development of infectious diseases and immune disorders over a period of 50 years within industrialization (Bach, 2002)

While most studies focus on the protective role of bacteria and their products, exposure to respiratory and non-respiratory viruses have been shown to contribute to asthma protection as well (Bach, 2002). Matricardi et al. measured specific IgE

response, skin sensitization and diagnosis of allergic diseases in Hepatitis A virus (HAV) seropositive versus seronegative individuals. After adjustment to environmental criteria, the prevalence of atopy in seropositive individuals was lower compared to seronegative individuals (Matricardi et al., 1997, Matricardi et al., 2002). In contrast, this could not be shown for mumps, rubella, chickenpox, herpes simplex virus type 1 and cytomegalovirus, suggesting a protective role for orofecal infections but not for airborne viruses (Matricardi et al., 2000). A mouse study provided evidence of protection towards development of experimental asthma in a mouse model of T2-response in airways but not lung (Wohlleben et al., 2003). In addition, Skevaki et al. showed that mice, which were previously infected with Influenza A Virus (IAV), were protected from asthma development in a murine model of ovalbumin (OVA) and house dust mite (HDM)-induced experimental asthma (Skevaki et al., 2018). However, a protective effect of respiratory virus infections towards allergic diseases remains controversial, as respiratory virus infections, especially with rhinovirus (RV) or respiratory syncytial virus (RSV), are also known to cause asthma exacerbations (Jackson et al., 2008, Lemanske et al., 2005, Smits et al., 2016).

1.3 Asthma

1.3.1 Epidemiology

Asthma is one of the major chronic inflammatory disorders, affecting about 262 million people worldwide. In 2019, asthma caused 461.000 deaths (World Health Organization, 2021). Due to the heterogeneity of the disease, it is often challenging to differentiate between asthma and other respiratory diseases, such as chronic obstructive pulmonary disease (COPD) later in life (Holgate et al., 2015). The prevalence of asthma is highest in western countries (e.g. Australia 20 %), compared to developing countries (e.g. China 0,2 %) (Papi et al., 2018). However, there is no linear correlation between the gross national product and asthma (Kuruvilla et al., 2019b). Further, immunological factors, sex and age can influence asthma development. Among children, the prevalence is higher in boys, while in adults the prevalence is higher in women compared to men. The reasons for this are not clear, but hormones and environmental settings might be important. In addition, the onset of

new asthma developed in adults tends to be more severe compared to the disease developed already in childhood (Holgate et al., 2015).

1.3.2 Risk factors

Asthma is well believed to result from gene-environment interactions, whereby environmental risk factors mostly include allergens, tobacco smoke, air pollution, obesity, microbes and virus infections (Holgate et al., 2015). There are many other prenatal and postnatal risk factors that correlate with urbanization, westernized lifestyle and industrialization, such as use of antibiotics, diets and indoor time or time of sports (Figure 3). The risk of developing asthma starts already in pregnancy, especially in presence of maternal allergic diseases. After birth, early respiratory tract infections represent a major risk (Renz, Skevaki, 2021) .

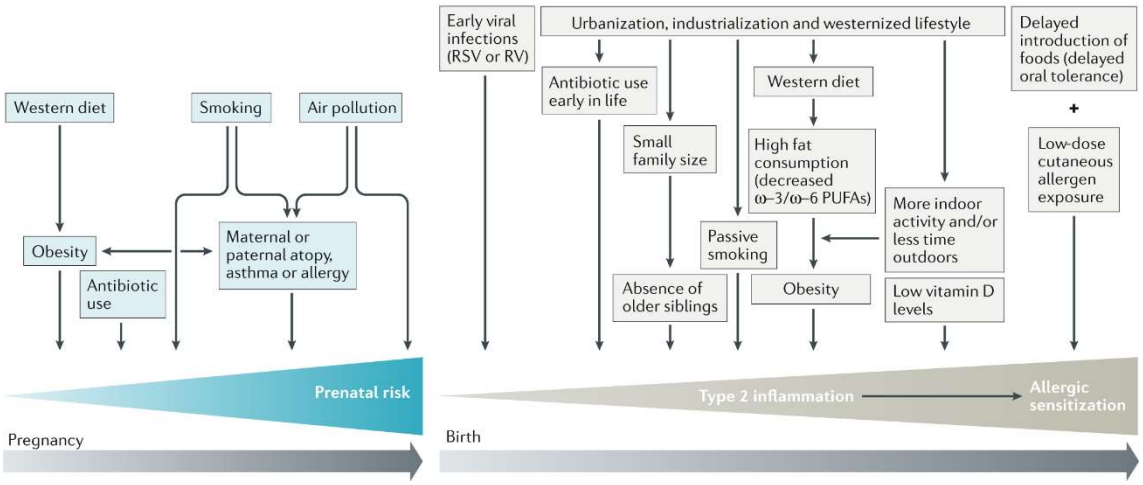

Figure 3: Schematic overview of pre- and postnatal risk factors in the process of asthma and allergy development (Renz, Skevaki 2021)

Genes that have been identified to be associated with asthma include the beta2adrenergic receptor gene, but also cytokines, transcription factors, receptors and signaling proteins, such as *IL4*, *IL4RA*, *IFNG*, *IFNGR1*, *STAT6*, *GATA3,* and *TBX21* (Toskala, Kennedy, 2015). Genetic factors, such as single nucleotide polymorphisms, have also been intensively investigated in genome-wide association studies over the last decades (Lee et al., 2015).

Indoor and outdoor pollutant are increasing risk factors for asthma development particularly in urbanized areas. The most important pollutants include traffic related air pollution, airborne particulate matter, volatile organic compounds

(formaldehyde, acetaldehyde, benzene, toluene, ethylbenzene, and xylenes) and gases (ozone and nitrogen oxide) (Guarnieri, Balmes, 2014, Hulin et al., 2010). Pollutants have been shown to induce airway responsiveness, as well as oxidative stress, leading to epithelial damage and inflammation and subsequently resulting in asthma exacerbation or even development of new-onset asthma (Guarnieri, Balmes, 2014). In addition to the above-mentioned substances, tobacco smoke represents a major air pollutant. A 10-years follow up study pointed out that active smoking was strongly correlated in a dose-dependent manner with new-onset asthma in patients with allergic rhinitis (Polosa et al., 2008). Furthermore, secondhand tobacco smoking has been evaluated in several studies to induce a 20-80 % increased risk of wheezing and asthma in children that were passively exposed to tobacco smoke (Burke et al., 2012).

Overweight and obesity in childhood, but also adults, were assessed to be associated with a higher risk of asthma development in meta-analyses and systematic reviews (Beuther, Sutherland, 2007, Mebrahtu et al., 2015). Obesity-associated asthma has also been accepted as a separate phenotype, however, the knowledge about mechanisms is still inconsistent (Miethe et al., 2020).

Another important risk factor for asthma is exposure to environmental allergens. Especially higher levels of IgE towards house dust mites (*Der p* and *Der f*) were correlated with a higher asthma burden (Kovac et al., 2007). A cross-sectional study in the US pointed out that multiple allergens are common in homes, including house dust mites, cats (*Fel d 1*), dogs (*Can f 1*) and cockroaches (*Bla g 1*). The higher the allergen levels, the higher the association with asthma burden in allergen-sensitized individuals (Salo et al., 2008). In another study, IgE levels to common indoor allergens and symptoms were assessed in school-age children. Asthmatic children, which were sensitized to *Penicillium*, *Der p 1*, *Fel d 1* or *Can f 1,* had a higher risk of increased disease burden (Gent et al., 2012).

1.3.2.1 Respiratory viruses as a risk factor for asthma

Respiratory virus infection, especially RV and RSV, are highly associated with asthma development and are the major cause of asthma exacerbations (Holgate et al., 2015). In the Childhood Origins of Asthma (COAST)- Study, including 289 new born children with high risk for asthma development, wheezing illness due to RSV or RV infections within the first three years of life was demonstrated to significantly

increase the risk of asthma development at the age of six years. It was also shown that RV infection alone induced the same risk compared to cumulative RSV and RV infections and was significantly higher compared to RSV infection alone (Figure 4) (Jackson et al., 2008). Furthermore, this risk dramatically increased from wheezing in the first year of life until wheezing in the third year (Jackson, Lemanske, 2010).
RSV-induced bronchiolitis has been associated with childhood asthma in several prospective long-term studies (Jartti, Gern, 2017). A retrospective cohort study showed that especially children, which were born three month before the RSV season, had a greater risk of hospitalization because of lower respiratory tract infections, as well as a higher risk of asthma development at the age of four to five years (Wu et al., 2008). However, data from a twin study in Denmark suggest that severe RSV wheezing illness can lead to short-term recurrent wheezing within two months after RSV hospitalization and induces bronchial hyperresponsiveness, but not long-term asthma later in life. In the same study, asthmatic patients were shown to have a three-fold risk of severe RSV hospitalization. This bidirectional association of RSV and asthma suggests a common genetic predisposition and environmental exposure (Stensballe et al., 2009).

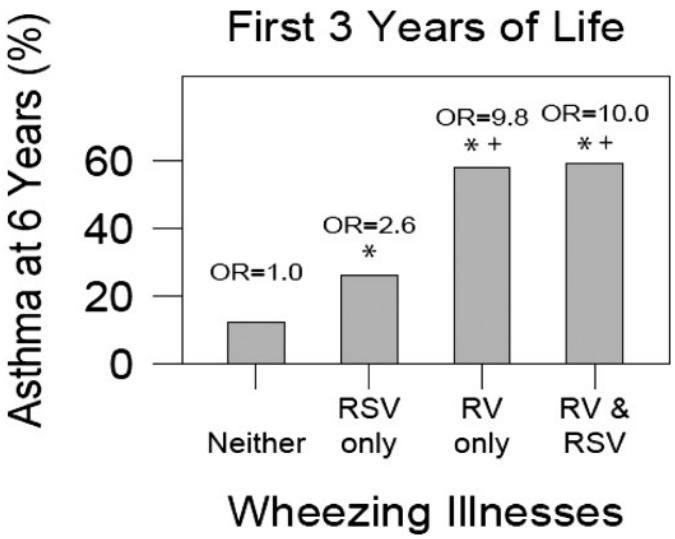

Figure 4: Correlation of wheezing within the first 3 years of life by rhinovirus (RV), respiratory syncytial virus (RSV) or both and development of asthma at the age of 6 years (Jackson 2008) OR=odds ratio

Several studies correlated asthma exacerbations in children with the peak of RV season, which is mainly spring and fall and, moreover, it was linked to prior allergen sensitizations (Dulek, Peebles, 2011). Additionally, RV is the most common cause of asthma exacerbations, being responsible for up to 60 % of the virus-induced asthma

exacerbations. The remaining asthma exacerbations linked to virus infections are caused by RSV and influenza (Wark et al., 2018). On the other hand, asthma is defined to be a high risk of developing severe illness after influenza infection. Thus, influenza vaccination in asthmatic patients has been recommended since 1964 by the Advisory Committee on Immunization Practice (Dulek, Peebles, 2011, World Health Organiszation, 2012).

1.3.2.2 Mechanisms of virus-allergen interactions

Several possible mechanisms of virus and allergen interactions are discussed, including abnormalities in the epithelial cell barrier, which were associated with disrupted tight junctions, impaired innate immunity and attenuated antioxidant properties (Gavala et al., 2013). A damaged epithelial cell barrier can be caused by viral infections, thereby leading to an enhanced sensitivity towards virus infections and allergen exposure. On the one hand, such a damage leads to an increased induction of T2 alarmins, including Interleukin (IL)-25, IL-33 and thymic stromal lymphopoietin (TSLP), thereby promoting differentiation and activation of innate lymphoid cells 2 (ILC2) as well as suppression of T_{reg}s (Gavala et al., 2013). The latter one may enhance susceptibility to allergens but also result in worse anti-viral immune responses (Gavala et al., 2013, Krishnamoorthy et al., 2012). Additionally, several studies showed decreased interferon type I and III response in atopic individuals towards virus infections. Bronchial epithelial cells suppressed production of these interferons due to T2 cytokines and IgE crosslinking in atopic patients (Bufe et al., 2002, Edwards et al., 2017). This leads to suppression of T2 inflammation and activation of ILC2s by plasmacytoid dendritic cell-derived type I and type III interferons. Clinically, impaired interferon production would result in inadequate viral clearance and therefore establishment of virus-induced inflammation and activation of eosinophilic pathways (Edwards et al., 2017, Renz, Skevaki, 2021). Such a reciprocal interaction between antiviral immune responses and allergy would imply a beneficial response of anti T2-biologicals, including anti-IgE or anti-IL-5 antibodies, not only to reduce allergic inflammation, but also enhance viral clearance. Indeed, first investigations of Omalizumab (anti-IgE)-treated asthmatic children provide evidence for increased interferon responses towards rhinovirus and influenza stimulations (Gill et al., 2017, Renz, Skevaki, 2021).

Another mechanism of virus-allergen interaction may result from synergistic effects of virus infection and allergen exposure. Lungs of allergen-sensitized individuals are more susceptible to virus infections (Jackson et al., 2012). Virus infections induce massive neutrophilic influx into the lung, which cause airway inflammation through activation of the inflammasome, thereby leading to lung injury (Renz, Skevaki, 2021). Neutrophils produce IL-9, leading to a massive migration of long-living mast cells into lung tissue, which contributes to airway hyperresponsiveness and pathogenesis of asthma development. In addition, neutrophils can release proteolytic enzymes, such as elastase, but also reactive oxygen species, promoting lung damage (Geerdink et al., 2015). Neutrophil extracellular tap formation upon viral infection has also been shown to destroy alveolar epithelium and endothelial cells (Narasaraju et al., 2011, Saffarzadeh et al., 2012). Finally, neutrophils promote mucus production and therefore airway obstruction. This has been shown in a mouse model of RSV infection, in which depletion of neutrophils in the mice led to a lower mucus production as well as TNFα levels (Stokes et al., 2013).

1.3.3 Phenotypes and endotypes of asthma

Asthma is a complex and heterogenous disease, which typically results in airway inflammation and hyperresponsiveness. During the last years, multiple phenotypes were described. A phenotype reflects the clinical characteristics, simply describing observable properties which result from interactions of environmental influences and genotypes. The underlying biological mechanisms and pathways of the different phenotypes are defined as endotypes (Koczulla et al., 2017). Although the symptoms are mainly similar, reactivity towards therapeutics may differ. Thus, considering the phenotype/endotype classification is important in precision medicine (Figure 5) (Kuruvilla et al., 2019a). Additionally, severity of different phenotypes within one endotype ranges from mild to severe. So far, only two endotypes are described for asthma, mainly referred to as “T2-type” and “non-T2/T2-low-type”, which are both equally represented among asthmatic patients (Hammad, Lambrecht, 2021, Woodruff et al., 2009). Due to the high overlap of characteristics, classification of the asthmatic phenotypes is quite difficult (Kuruvilla et al., 2019a).

T2-driven asthmatic phenotypes are mostly classified as early-onset allergic asthma (eoA), exercise-induced asthma (EIA), late-onset eosinophilic asthma and aspirin-

exacerbated respiratory disease (EARD) (Kuruvilla et al., 2019a, Wenzel, 2012). EoA is the most common type of asthma and represents the best studied phenotype, although the definition is vague as no cut-off age has been determined (Koczulla et al., 2017, Wenzel, 2012). This type is distinguished from other T2-driven phenotypes by elevated serum IgE in combination with a positive skin-prick test to define allergy (Kuruvilla et al., 2019a). However, some cases have been reported in children with low IgE levels and no response to corticosteroids, suggesting also another form of non-T2 childhood asthma. Additionally, early infections with RSV are co-modulators for eoA, thereby influencing T_{reg} function and increasing the susceptibility to allergic asthma via the IL-4 receptor pathway. Late-onset eosinophilic asthma is linked to T2 inflammation based on eosinophils, mast cells and basophils and is more severe from the early onset on (Koczulla et al., 2017). These patients are also resistant to treatment with corticosteroids and show comorbidities with chronic rhinosinusitis with nasal polyps. A more severe form of this phenotype is AERD, which is additionally characterized by COX-1 inhibitor-induced respiratory reactions (Kuruvilla et al., 2019a). So far, the classification of EIA as a separate phenotype is discussed, as the symptoms were also found in individuals with no asthmatic diagnosis (Koczulla et al., 2017).

Non-T2 phenotypes are characterized by neutrophilic inflammation. Although the mechanisms are not yet fully understood, activation of T1/T17 cells through toll like receptor (TLRs) is known to play a role. Factors leading to activation of such TLRs include viral infections and environmental pollutants, but this neutrophilic asthma is mainly linked to cigarette smoke (Suraya et al., 2021). Furthermore, obesity-associated asthma belongs to the non-T2-types of asthma. It is known to be non-allergic, late onset and predominantly present in women (Koczulla et al., 2017).

Several other phenotypes are described in the literature and more suggestions for subclassifications arise, thereby all of them are hypothesis-based, taking specific characteristics into account to differentiate the phenotypes, although there are also high overlaps. Thus, for example “-omics” approaches are now more frequently used to define asthmatic phenotypes in a more precise manner (Kuruvilla et al., 2019a).

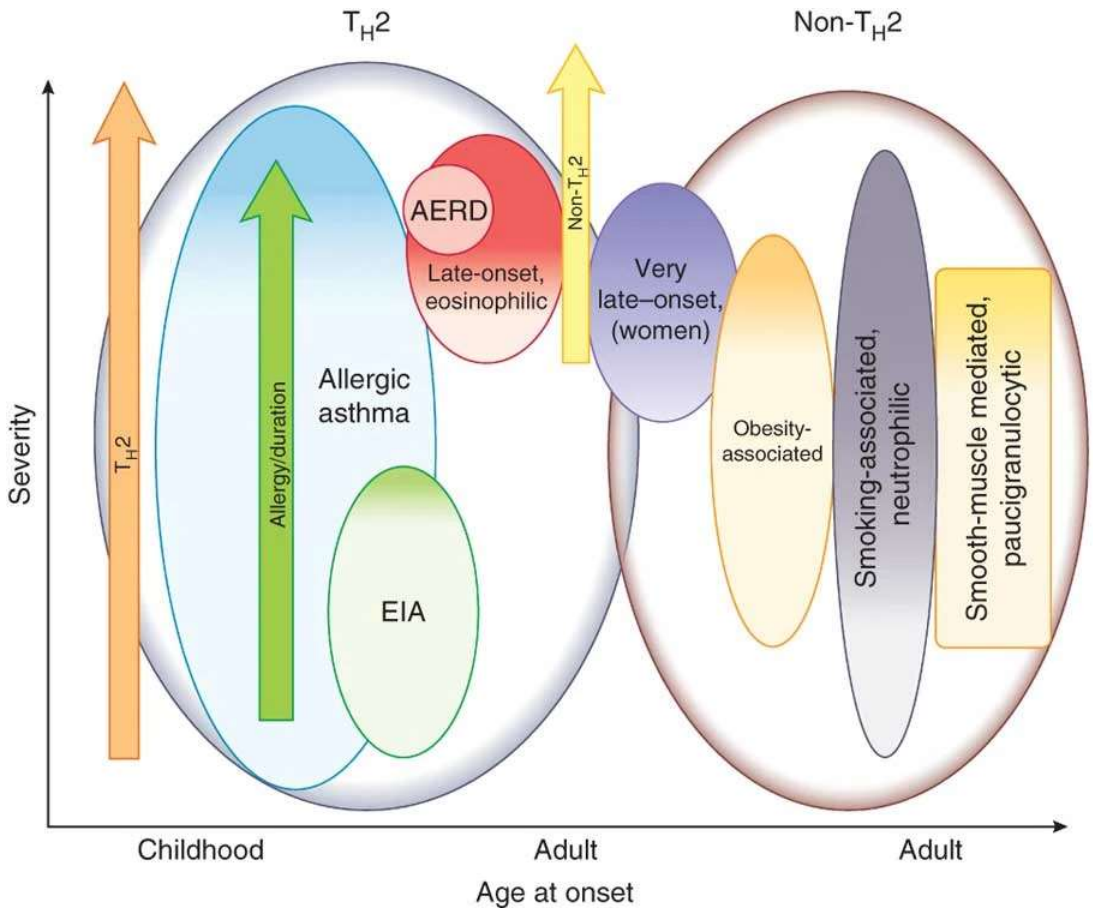

Figure 5: Phenotypes and endotypes of asthma (Wenzel, 2012)

1.3.3.1 Pathophysiology of T2-driven allergic asthma

The development of T2-driven allergic asthma is initiated by the uptake of allergen proteins at the lung epithelial cell barrier. Epithelial cells express pattern recognition receptors (PRR), such as TLRs, which recognize the antigen and initiate the release of IL-25, IL-33 and TSLP (Hammad, Lambrecht, 2021, Holgate et al., 2015). These alarmins activate ILC2, which release the T2 cytokines IL-5, IL-9 and IL-13 (Lambrecht, Hammad, 2015). Additionally, upon antigen uptake, antigen-presenting cells (APC) are activated, such as dendritic cells (DC) and macrophages, which in turn move to the regional lymph nodes and present the processed peptides to naïve T cells via major histocompatibility complex (MHC) class II presentation (Suraya et al., 2021). Subsequently, naïve T cells differentiate into T2 cells with the help of IL-4, and secrete the T2 cytokines IL-3, IL-4, IL-5, IL-9, IL-13 and granulocyte-macrophage colony-stimulating factor (GM-CSF). These cytokines activate B cells to produce IgE (Gandhi et al., 2016, Holgate et al., 2015). Especially IL-4 increases B cell proliferation and differentiation into plasma cells. IL-5 helps B cells to differentiate

and perform the isotype switch of immunoglobulins to IgE and further promotes basophil differentiation and histamine release (Regateiro et al., 2021). IgE binds specifically to the mast cells via high-affinity IgE receptors (FcεRI), leading to degranulation and release of mediators, such as histamine, leucotriens and cytokines, which in turn leads to the recruitment of eosinophils and neutrophils as classical characteristics of allergic asthma (Holgate et al., 2015, Suraya et al., 2021). However, besides of airway inflammation, airway remodeling is known to be a major part in asthma pathogenesis. Once the airways are sensitized to the allergen, the released cytokines, mainly IL-13, drive goblet cell hyperplasia and mucus production, as well as smooth muscle cell contraction, fibroblast proliferation and activation of macrophages, thus leading to airway hyperresponsiveness (Regateiro et al., 2021, Suraya et al., 2021). A schematic illustration of the type 2-immune mechanisms is displayed in Figure 6.

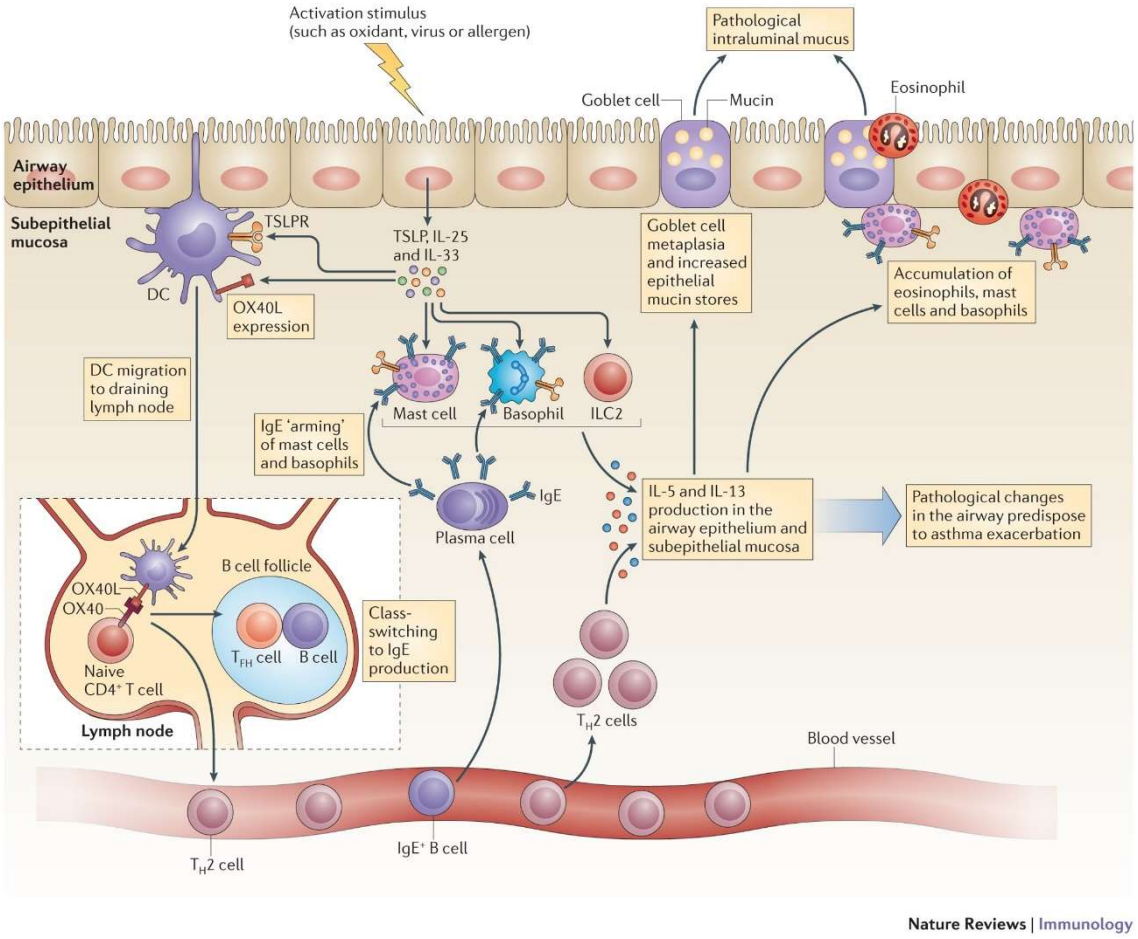

Figure 6: Mechanisms of T2- driven allergic asthma (Fahy, 2015)

1.3.3.2 The role of T cells in asthma pathogenesis

The cellular and molecular mechanisms of asthma pathogenesis are much more complicated as described above and are still not fully understood. Especially the contribution of different T cell subsets is increasingly investigated, as they control the inflammatory cell profile (Holgate et al., 2015). Upon the first contact with the allergen, cells are sensitized and cause an immune response, but no symptoms. In this phase, T cells are primed for the specific allergen. Only after subsequent exposure, these T cells migrate to the affected airway and release T2 cytokines, resulting in bronchoconstriction and airway hyperresponsiveness (Holgate et al., 2015, León, 2017). Not only the classical T2, T1 and T17 $CD4^+$ T cells, but also T9 cells, as well as T_{reg}s, follicular T helper cells (T_{FH}) and tissue resident memory cells (T_{RM}) were shown to contribute to asthma pathogenesis (Hammad, Lambrecht, 2021, Regateiro et al., 2021). The major cytokine produced by T9 cells is IL-9, a pleiotropic cytokine affecting different cells subsets, thereby promoting asthma progression (Koch et al., 2017). T_{FH} cells are suggested to be highly involved in the process of IgE production and control by secretion of different cytokines, including not only its typical IL-21, but also T1 and T2 cytokines (Yao et al., 2021). T_{reg}s are supposed to work as suppressor cells for potentially harmful immune responses, thereby avoiding diseases. An impaired function of these cells might contribute to allergic asthma development. Therefore, aiming on enhancing T_{reg} function may display a potential mechanism for therapeutic strategies (Robinson, 2009, Sun et al., 2021). T_{RM} cells are also gaining more interest, as they acquire a T2-phenotype, persist in the lung and are activated upon allergen re-challenge, with associated proliferation and induction of T2 response (Rahimi et al., 2020, Yuan et al., 2021).

Importantly, subsets of $CD8^+$ T cells have also been demonstrated to be able to differentiate into similar subsets as $CD4^+$ T cells, which are characterized by the corresponding cytokine profile and effector function (Huber, Lohoff, 2015). The majority of $CD8^+$ T cells are characterized by secretion of T1 cytokines (T_c1 cells), but $CD8^+$ T cells producing IL-4, IL-5 and IL-10 (T_c2 cells) are also known (Stock et al., 2004). Several studies investigated a contribution of $CD8^+$ T cells to allergic inflammation, but also a beneficial effect of $CD8^+$ T cells in asthma pathogenesis was observed in several studies (Betts, Kemeny, 2009). Stock et al. were able to demonstrate an organ-specificity of the T_c1 and T_c2 subtypes, whereby antigen-specific $CD8^+$ T cells in

the lungs of ovalbumin (OVA)-sensitized animals showed a dominant T2 response (IL- 4, IL-5 and IL-10, but only a low amount of IFNγ); on the other hand, only IFNγ was secreted in $CD8^+$ T cells in spleen (Stock et al., 2004). Such T_c2 cells were able to promote eosinophilia and airway hyperresponsiveness (AHR) in rodents and therefore contributing to allergic inflammation (Betts, Kemeny, 2009). Indeed, T2-cytokine (IL-13, IL-5, IL-4) expressing *Der p 1*-specific $CD8^+$ T cells were detected in PBMC´s of atopic patients, showing higher frequencies with increase in disease severity (Hinks et al., 2019, Seneviratne et al., 2002). A recent study using RNA-Sequencing technology identified elevated levels of $CD8^+$ T cells in bronchoalveolar lavage (BAL) fluid of patients with asthma exacerbations (Li et al., 2021a).
Taking the diversity and complexity of T cells in asthma pathogenesis and its different phenotypes and endotypes into consideration, generation of pathway-targeting biologicals displays important an strategy for treatment of asthma (Hammad, Lambrecht, 2021).

1.3.4 Diagnosis and treatment

The Global Initiative for Asthma (GINA) defines asthma as "a heterogeneous disease, which is characterized by chronic airway inflammation. This includes respiratory symptoms, such as wheezing, shortness of breath, chest tightness and cough, as well as variable expiratory airflow limitation, varying over time and intensity" (Global Initiative for Asthma - GINA, 2021). There is no gold standard test for diagnosis; pattern and history of the different symptoms in combination with measurement of airway obstruction and lung function on a spirometer are taken into consideration by physicians. Spirometry measures forced expiratory volume in one second (FEV1) and the ratio of FEV1 to forced vital capacity (FVC), which can be used to distinguish between restriction and obstruction. Lung obstruction is indicated by a decreased FEV1/FVC ratio (Brigham, West, 2015, Stern et al., 2020). Airway hyperresponsiveness can also be measured by a methacholine provocation test, which is mainly used in asymptomatic patients (Buhl et al., 2021). Detailed recommendations for asthma diagnosis are found in GINA (Global Initiative for Asthma - GINA, 2021) and the National Institute for Health and Care Excellence Quality Standard for Asthma (National Institute for Health and Care Excellence., 2018).

The treatment strategy of asthma in adults underlies the general asthma guidelines from GINA and other initiatives, usually being classified into five steps. Depending on the symptoms, comorbidities and other factors which are assessed before starting a therapy, the first on-demand therapy usually starts with low-dose inhaled corticosteroids (ICS) in combination with the beta-2 agonists formoterol. The next recommended steps comprise long-term therapy with increasing doses of ICS in combination with short-acting beta-2 agonists (SABA) or, depending on severity, application of additional long-acting beta-2 agonists. In case of an uncontrolled and exacerbated disease, phenotype-dependent add-on treatment is recommended, such as anti- IL-5 therapy in eosinophilic asthma (Global Initiative for Asthma - GINA, 2021). However, considering the complexity and heterogeneity of the diseases, the identification of novel therapeutic strategies fitting to the individual asthma phenotype is quite important, especially in patients with no response to corticosteroids. In addition, treatment of children under five years is more complex, as the symptoms are not as clear as in adults and the evidence for effective ICS-SABA treatment is low (Holgate et al., 2015).

1.4 Heterologous immunity

Heterologous immunity is considered as a consequence of previous infections, which alter the immune response to a subsequent exposure with a different pathogen (Welsh, Selin, 2002). This effect is likely to happen between closely related antigens, but could also occur among unrelated pathogens, including bacteria, viruses, protozoa and parasites (Mathurin et al., 2009, Selin et al., 1998, Sharma, Thomas, 2014). Altered immune response can result in protective immunity or lead to an impaired immunopathology (Selin et al., 1998, Sharma, Thomas, 2014). As this mechanism requires immune memory, heterologous immunity is mainly linked to cells of the adaptive immune system, underlaying different mechanisms (Pusch et al., 2018). Antibodies recognize an antigen on the paratope of the fragment antigen binding (Fab) domain. One Fab-domain contains multiple paratopes, making it capable of binding multiple epitopes of different pathogens. Additionally, cross-reactive protection upon binding of epitopes with similar sequences at the same paratope has been shown (van Regenmortel, 2014). However, antibodies may react to self-antigens by means of molecular mimicry, therefore eliciting autoreactive

immunopathology (Barnett, Fujinami, 1992). One of the mechanisms with respect to T cell-mediated heterologous immunity displays T cell receptor (TCR)- mediated cross-reactivity (Figure 7). It is suggested that the human T cell receptor repertoire is smaller than the pool of potential presented antigens, thus, cross-reactivity is important for an appropriate immune response (Arstila et al., 1999, Mason, 1998, Sewell, 2012). Importantly, TCRs may recognize highly similar peptides, but also peptides with a lower degree of similarity and even autoantigens (Welsh et al., 2010). As a consequence, memory T cells are expanded and result in a modified memory pool with an altered immune response, which is highly dependent on the private infection history of each individual (Selin et al., 1998). Of note, an unspecific activation of memory T cells was also observed, for example through cytokines and interferon signaling (Pusch et al., 2018). In addition to the role of T- and B- cells in heterologous immunity, innate immune cells were recently shown to be able to adapt to antigen exposure, leading to innate immune memory, also known as trained immunity (Martin, 2014). Notably, heterologous immune responses may not be reciprocal and might result in loss of specific memory T cells or alteration of immunodominance and T_H-polarization (Pusch et al., 2018).

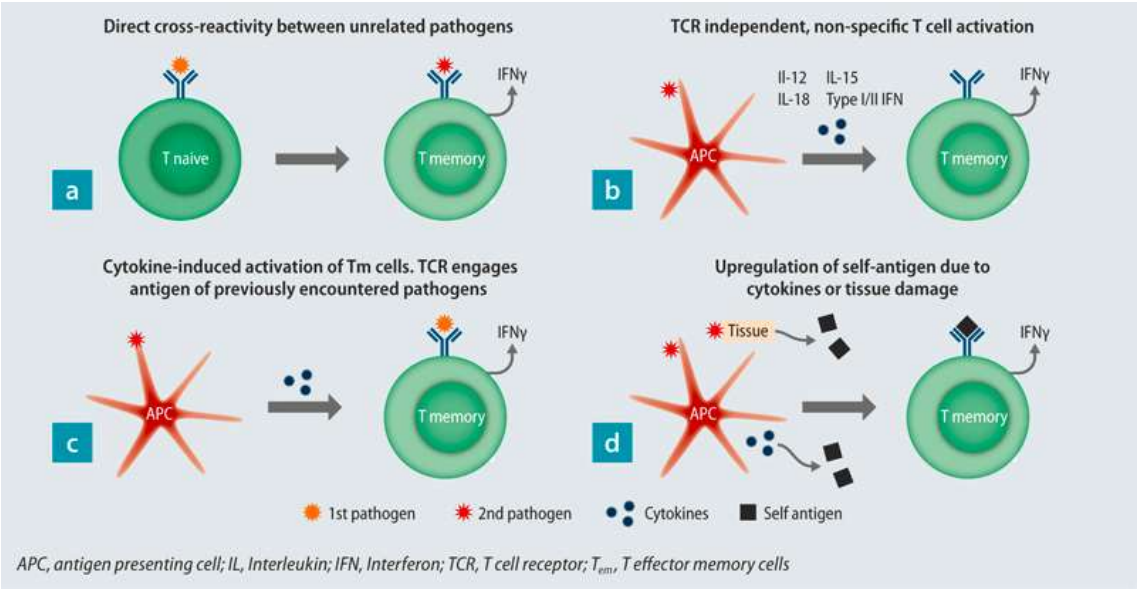

Figure 7: Mechanisms of T cell-mediated heterologous immune response (Pusch et al., 2018)

1.4.1 Virus-induced T cell mediated heterologous immunity

Heterologous immune responses are known for respiratory and non-respiratory viruses. The latter ones include for example flaviviruses, hepatitis C virus and human immunodeficiency virus (Pusch et al., 2018). For example, flaviviruses exhibit a high degree of genetic similarity, which has been shown to induce protective immunity, but also aggravates the immune response (Slon Campos et al., 2018). This is mainly known for dengue virus (DENV), where a second infection with the same serotype induces long protection, but a heterogenous serotype infection results in severe disease (Elong Ngono, Shresta, 2019). Additionally, $CD8^+$ memory T cells of DENV seropositive patients induced antigen-specific cytokine production upon stimulation with zika virus (ZIKV) peptides, which is modulated by the status of ZIKV-infection (Grifoni et al., 2017). In the field of respiratory viruses, heterologous immunity was frequently demonstrated for coronaviruses (CoV) and influenza virus. In a mouse study, intranasal application of a conserved severe acute respiratory syndrome (SARS)-CoV $CD4^+$ T cell epitope resulted in production of CoV specific memory T cells, which protected mice from infection with the heterosubtypic Middle East respiratory syndrome (MERS)-CoV (Zhao et al., 2016). More recently, the new emerged SARS-CoV-2 causes a coronavirus disease 2019 (COVID-19) pandemic. Importantly, SARS-CoV-2 specific T cells were found in patients with no SARS or SARS-CoV-2 infection history. These T cells frequently targeted NSP7 epitopes of proteins that are known to be conserved among betacoronaviruses (Le Bert et al., 2020). Another group identified and further characterized SARS-CoV-2 T cell epitopes of various HLA types, which revealed cross-reactive T cell response in 81 % of unexposed individuals, providing evidence for heterologous immune response against common cold coronaviruses (Nelde et al., 2021). During the influenza pandemic 2009, patients with pre-existing conserved $CD8^+$ T cells were correlated to a less severe disease, suggesting cross-protective heterologous immune response (Sridhar et al., 2013). Additionally, intranasal application of the live attenuated influenza vaccine (LAIV) in mice induced long-lasting tissue resident memory cells in the lung, which protected mice from a heterosubtypic virus infection (Zens et al., 2016). Of note, heterologous immune response between an IAV and allergens was demonstrated recently. Mice previously infected with the pandemic strain A/Hamburg/5/2009 were protected from development of experimental asthma in murine models of OVA and

HDM, leading to reduced airway inflammation, hyperresponsiveness and T2 immune response. This effect was further dependent on the presence of $CD4^+$ and $CD8^+$ T effector memory cells (T_{EM}) and an *in-silico* approach followed by *ex-vivo* stimulation assays identified cross-reactive T cell epitopes between the virus and OVA proteins (Skevaki et al., 2018).

1.5 Hypothesis and aims

Asthma is a major chronic inflammatory airway disease, affecting about 262 million people worldwide and causing more than 460.000 deaths (2019), representing also a socioeconomic burden (World Health Organization, 2021, Stern et al., 2020). The heterogeneity of the disease leads to a failure of the classical treatment strategies including ICS, demonstrating the importance of a better understanding of the underlaying endotypes and phenotypes in order to develop specific therapeutics. Exposure to environmental allergens is a major risk factor for allergic asthma. In addition, respiratory viruses are highly associated with asthma development and exacerbations (Holgate et al., 2015).
Heterologous immunity is a naturally occurring phenomenon, by which the immune response can be altered upon antigen exposure as a result of previous infections. Virus-induced heterologous immune responses have been described in the context of similar virus strains, but also between distinct virus subtypes and even among unrelated pathogens. Studies also showed heterologous immune responses upon vaccination, leading to protection against distinct virus strains or even to beneficial effects with respect to other diseases. One mechanism of heterologous immune response is based on cross-reactive T cell response, mediated by the TCR. Thus, development of vaccines that induce cross-reactive T cells is of great interest (Balz et al., 2020).

Previous work of our research group showed a protective effect of a preceding influenza A H1N1 virus infection towards development of experimental asthma in a murine model. This effect was further mediated by cross-reactive $CD4^+$ and $CD8^+$ T effector memory cells and it was the first time demonstrating heterologous immune response between viruses and allergens (Skevaki et al., 2018).

The hypothesis of this project is that heterologous immune response might be a broadly applicable concept for several RNA viruses and environmental allergens. More precisely, a preceding RNA virus infection might offer a long-lasting protection against allergen-induced experimental asthma through memory T cells, which react in a T1-driven immune response upon allergen exposure due to its virus-shaped phenotype (Figure 8). During the course of this work, a comprehensive immunoinformatic approach should identify and characterize potential cross-reactive T cell epitopes between different clinically relevant respiratory RNA viruses and allergens.

Specifically, the following aims were approached:

- Predict potentially cross-reactive T cell epitopes between multiple RNA viruses and allergens using an *in-silico* approach
- Validate MHC binding of predicted T cell epitopes by means of *in-vitro* MHC stabilization assay
- Assess the immunogenic potential of the predicted epitopes in previously infected or immunized animals
- Analyze a cross-reactive T cell response between the virus-and allergen derived T cell epitopes by functional T cell assays and pentamer double staining
- Characterize phenotypic changes in a potential protective effect of virus infection or vaccination towards development of experimental asthma
- Investigate a contribution of the predicted T cell epitopes in the setting of asthma protection by virus peptide immunization
- Identify the composition and diversity of the airway virome and its potential contribution to asthma protection

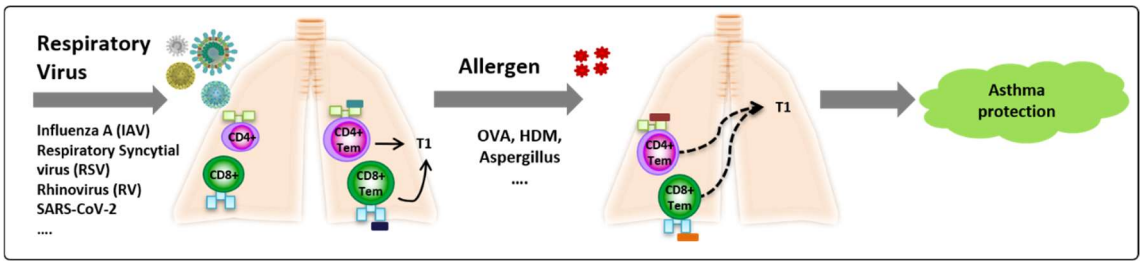

Figure 8: Virus-induced heterologous immune response towards allergen exposure [adapted from (Pusch et al., 2018)]

2. Materials

2.1 Cell lines

Hep-2: Provided from: Institute of Virology, Eva Friebertshäuser, Philipps University Marburg (UMR)
Hep-2 cells are epithelial carcinoma cells and derive from HeLa cell contaminations (Gartler, 1968).

Vero76: Provided from: Institute of Virology, Eva Friebertshäuser, Philipps University Marburg (UMR)
Vero76 cells originally derive from Vero cells, which were obtained from monkey kidney (Steffen et al., 1980, Waldeck, Sauer, 1977).

RMA-S^{Kd}: Provided from: Institute of Immunology, Stefan Bauer, Philipps University Marburg (UMR)
The RMA-S cell line is a murine lymphoma mutant cell line, which has been described to be used for the analysis of MHC class I peptide interactions (Ljunggren et al., 1990). RMA-S cells were stably transfected with the mouse MHC class I allele H-2-Kd by Stefan Bauer.

2.2 Virus

The human Respiratory Syncytial Virus stain A2 (RSV A2) was kindly provided by Jürgen Schwarze (University of Edinburgh, UK).

2.3 Animals

Wildtype Balb/c mice were purchased from The Jackson Laboratory, Sulzfeld, DE.

2.4 Anesthetics

Table 1: Anesthetics

Name	Provider
Ketamin	Medistar, Ascheberg, DE
Rompun 2% (Xylazine)	Bayer, Leverkusen, DE

2.5 Allergens

Table 2: Allergens

Name	Provider
Aspergillus fumigatus	DST Diagnostics, DE
House dust mite*s*	Stallergenes Greer Laboratories, USA

2.6 Adjuvants/Vaccines

Table 3: Adjuvants and Vaccines

Name	Provider
Imject™ Alum Adjuvant	Thermo Fisher Scientific, Rockford, IL, US
InfluSplit 2019/2020 (QIV 19/20)	GlaxoSmithKline (GSK), Brentford, UK
MCT®	Allergy Therapheutics, UK

2.7 Antibodies

Table 4: Antibodies

Name	Conjugate	Clone	Dilution	Provider
CD4	PerCPCy5.5	RM4-5	1:500	Biolegend, US
CD4	V450	RM4-5	1:500	BD Bioscience
CD8α	BV510	53.6.7	1:500	Biolegend, US
CD8α	FITC	53-6.7	1:500	Biolegend, US
CD11b	FITC	M1/70	1:500	Biolegend, US
CD11c	BV510	N418	1:500	Biolegend, US
CD27	PE-Cy7	LG.3A10	1:500	Biolegend, US
CD44	PE	IM7	1:500	Biolegend, US
CD62L	APC-Cy7	MEL-14	1:500	Biolegend, US
CD69	PE	H1.2F3	1:500	Biolegend, US
CD69	BV421	H1.2F3	1:500	Biolegend, US
B220	BV421	RA3-6B2	1:500	Biolegend, US
Siglec F	PE	E50-2440	1:500	BD Bioscience
Ly6C	APC	HK1.4	1:500	Biolegend, US
Ly6G	PerCPCy5.5	1A8	1:500	Biolegend, US
IL-5	BV421	TRFK5	1:300	Biolegend, US
IL-6	APC	MP5-20F3	1:300	Biolegend, US
IL-13	PE	W17010B	1:300	Biolegend, US
IL-17	AF647	TC11-18H10.1	1:300	Biolegend, US
TNFα	PE-Cy7	MP6.XT22	1:300	Biolegend, US
IFNγ	BV750	XMG1.2	1:300	Biolegend, US

IFNγ	AF488	XMG1.2	1:300	Biolegend, US
H-2-K_d	PE	SF1-1.1	1:500	BD Pharmingen™
Mouse αCD16/αCD32 (Fc block)		93	1:500	Biolegend, US
Zombie NIR dye			1:2000	Biolegend, US
Goat anti-mouse IgG	HRP		1:2000	Dako Agilent, CA, US
Goat anti- RSV			1:200	Abcam, Cambridge, UK
Rabbit anti-goat IgG H&L	HRP		1:2000	Abcam, Cambridge, UK
Goat anti-mouse Ig			1 µg/ml	SouthernBiotech, AL, US
Mouse IgG			500 ng/ml	SouthernBiotech, AL, US
rat anti-mouse IgE			1 µg/ml	BD Pharmingen™
purified mouse IgE Isotype			500 ng/ml	BD Pharmingen™
Biotin rat anti-mouse	Biotin		1 µg/ml	BD Pharmingen™

2.8 Pentamers

Associated Class I pentamers were purchased from Proimmune and were ready-to use, labelled with APC or PE.

Table 5: Pentamers

Name	Sequence	Conjugate
RSV A2 $M2_{81-90}$	SYIGSINNI	PE
Influenza A $HA_{533-541}$	IYSTVASSL	PE
RSV A2 $L_{356-364}$	FYNSMLNNI	APC
Asp f $4_{192-200}$	WYGNSALTI	PE

2.9 Peptides

MHC class I peptides were purchased from Proimmune. MHC class II T helper peptide $HepCore_{128-140}$ was purchased from GenScript. The purity was >95 % based on HPLC. Lyophilized peptides were stored at -80 °C until dissolving in sterile H_2O.

Aliquots were prepared in order to avoid freeze-thawing cycles and stored at -20 °C or -80 °C.

Table 6: Peptides

Name	Sequence
HBV$_{28-39}$	IPQSLDSWWTSL
HepCore$_{128-140}$	TPPAYRPPNAPIL
Influenza A HA$_{533-541}$	IYSTVASSL
Protein L$_{356-364}$	FYNSMLNNI
NS1$_{124-132}$	NYMNQLSEL
Protein L$_{605-613}$	SYLNNPNHV
Protein L$_{356-364}$	FYNSMLNNI
Protein L$_{605-614}$	SYLNNPNHVV
F0$_{32-40}$	FYQSTCSAV
Asp f 4$_{201-209}$	WYGNSALTI
Cor a 9$_{485-493}$	KYNRQETTL
Asp f 5 $_{44-52}$	KYVNATETV
Asp f 4$_{201-209}$	AYTAALAAV
Asp f 5$_{66-75}$	SYVEVATQHV
Gal d 6$_{805-813}$	FYYSSVTKV
PA$_{457-466}$	KYVLFHTSL
NA$_{216-224}$	SYAKNILRT
PB1$_{323-331}$	TYITRNQPE
PA$_{457-466}$	KYVLFHTSLL
PB2$_{743-751}$	RYSALSNDI
HA$_{550-558}$	YYSTAASSL
Asp f 6$_{179-187}$	SYAKGIWNV
Der p 14$_{1044-1052}$	KYMSSHFPI
Der p 14$_{1044-1053}$	KYMSSHFPIL
Blo t 11$_{542-550}$	KYQAQITEL
Ves a 1$_{133-141}$	SYAASNTRL
Protein 2C$_{1195-1203}$	LYNKCSNII
Polymerase 2$_{124-2132}$	VYEDFSSKI
Protease A2$_{862-870}$	LYVHVGNLI
Pol$_{2141-2149}$	LYIPPYDLL
Asp f 4$_{43-51}$	VYATMNGVL
Asp f 4$_{43-51}$	VYATINGVL
Cha o 1$_{105-113}$	LYIAGNKTI
Tri a 21$_{108-116}$	KYLQPQQPI

2.10 Cell culture media

Table 7: Composition of cell culture media

Name	Composition
Full RPMI medium	RPMI 1640, 2mM L-glutamine, 100 U/mL penicillin and streptomycin, 10 % FCS
Vero76 culture medium	DMEM, 10 % FCS, 2 mmol/L L-glutamine, 100 U/ml penicillin and streptomycin
RMA-S^{Kd} culture medium	RPMI 1640, 10 % FCS, 2 mM L-glutamine, 100 U/ml penicillin and streptomycin, 0,5 mM 2-Mercaptoethanol, 0,5 mg/ml Hygromycin B.
Hep-2 culture medium	MEM, 10 % FCS, 2 mM L-glutamine, 100 U/mL penicillin and streptomycin, 1 % NEAA
Hep-2 infection medium	MEM, 5 % FCS, 2 mM L-glutamine, 100 U/mL penicillin and streptomycin, 1 % NEAA

2.11 Primer

All primers were purchased from Metabion International AG.

Table 8: Primer

Name	Sequence
qPCR_RSV_N_forward	ATGGGAGAGGTAGCTCCAGA
qPCR_RSV_N_reverse	AGCTCTCCTAATCACGGCTG
cDNA_RSV A2_N_reverse	TCCTCGGTGTACCTCTGTACT

2.12 Kits

Table 9: Kits

Name	Provider
Mouse IFNγ Duo-Set	R&D Systems, Minneapolis, MN, US
Mouse magnetic luminex® assay	R&D Systems, Minneapolis, MN, US
OmniScript RT Kit	Qiagen, Hilden, DE
OneStep RT-PCR Kit	Qiagen, Hilden, DE
RNeasy plus mini kit	Qiagen, Hilden, DE
Rotor-Gene SYBR Green PCR Kit	Qiagen, Hilden, DE
QIAamp Viral RNA Mini Kit	Qiagen, Hilden, DE

2.13 Chemicals

Table 10: Chemicals

Name	Provider
ABTS	Life Technologies, Carlsbad, CA, US
Avicell	Virologie, Philipps University Marburg
β-mercaptoethanol for RNA Isolation	Carl Roth, Karlsruhe, DE
β-mercaptoethanol for cell culture	Gibco, Grand Island, NY, US
Brefeldin A	Biolegend, US
Bovine serum albumin (BSA)	Anprotec, Bruckberg, DE
CASYton	OmniLife, Bremen, DE
CFSE	Sigma-Aldrich, Steinheim, DE
citric acid-monohydrate	Carl Roth, Karlsruhe, DE
Collagenase D from *chlostridium histo-lyticum*	Roche, Mannheim, DE
cOmplete™ protease inhibitor cocktail	Roche, Mannheim, DE
Deoxyribonuclease I from bovine pan-creas	Sigma-Aldrich, Steinheim, DE
Diff-Quick®-Solutions Stain set	RAL Diagnositics, Martillac, FR
DMEM	Anprotec, Bruckberg, DE
DMSO	Carl Roth, Karlsruhe, DE
Entellan mounting medium	Merck, Darmstadt, DE
Eosin	Carl Roth, Karlsruhe, DE
Ethanol 100 %	Carl Roth, Karlsruhe, DE
Ethylenediaminetetraaceticacid(EDTA)	Sigma-Aldrich, Steinheim, DE
Fetal calf serum	Anprotec, Bruckberg, DE
Fluoroshild™	Sigma Aldrich, St. Louis, MO, USA
Formaldehyde 37%	Sigma Aldrich, St. Louis, MO, USA
Glacial acetic acid	Acros Organics, Geel, BE
Glycin	Carl Roth, Karlsruhe, DE
Hematoxylin	Merck, Darmstadt, DE
Horse serum	Capricorn, Ebsdorfergrund, DE
Hygromycin B	Thermo Scientific, Rockford, IL, US
Ionomycin	Sigma-Aldrich, Steinheim, DE
L-Glutamin	Capricorn, Ebsdorfergrund, DE
Liquid nitrogen	Linde, Gablingen, DE
MEM medium	Gibco, Grand Island, NY, US
MEM nonessential amino acids 100x (NEAA)	Capricorn, Ebsdorfergrund, DE
Peptivator Influenza HA	Miltenyi, Bergisch-Gladbach, DE
Penicillin/streptavidin	Capricorn, Ebsdorfergrund, DE
Periodic acid	Carl Roth, Karlsruhe, DE

Phosphate-buffered saline (PBS)	Sigma Aldrich, St. Louis, MO, USA
Phorbol 12-myristate 13-acetate (PMA)	Sigma-Aldrich, Steinheim, DE
PM Blue POD substrate	Roche, Mannheim, DE
Rabbit serum	Capricorn, Ebsdorfergrund, DE
RPMI medium	Anprotec, Bruckberg, DE
Roti-ClearTM	Carl Roth, Karlsruhe, DE
Saponin	Sigma-Aldrich, Steinheim, DE
Schiff's reagent	Carl Roth, Karlsruhe, DE
Sulfric acid	Carl Roth, Karlsruhe, DE
Triton-X-100	Merck, Darmstadt, DE
Tween®20	Carl Roth, Karlsruhe, DE

2.14 Plastic ware

Table 11: Plastic ware

Name	Provider
24-well suspension plate	Greiner AG, Kremsmünster, AUT
24 well cell culture plate	Nunc, Roskilde, DNK
30 µm & 100 µm strainer	Miltenyi Biotec, Bergisch Gladbach, DE
96-well flat bottom plate	Nunc, Roskilde, DNK
96-well half well plate	Corning, New York, US
96-well u bottom plates	Greiner AG, Kremsmünster, AUT
96-well v bottom plates, polypropylen	Corning, New York, US
96-well thin-wall hard-Shell PCR Plates	Bio-Rad Laboratories GmbH, CA, US
Centrifuge tubes 15 ml, 50 ml	Sarstedt, Nümbrecht, DE
Cryotubes 1.5 ml	Sarstedt, Nümbrecht, DE
Flow cytometry tubes 5 ml, 75x12 mm	Sarstedt, Nümbrecht, DE
gentleMACS C tubes	Miltenyi Biotec, Bergisch Gladbach, DE
Pipette tips (10µl, 200 µl, 1000 µl)	Sarstedt, Nümbrecht, DE
Reaction tubes (0,5 ml, 1,5 ml, 2,0 ml)	Sarstedt, Nümbrecht, DE
Serological pipets (5 ml; 10 ml; 25 ml)	Sarstedt, Nümbrecht, DE
(Superfrost) microscopy slides	Thermo Scientific, Rockford, IL, US

2.15 Devices

Table 12: Devices

Name	Provider
37 °C shaker	LAUDA-GFL, Burgwedel, DE
Attune™ NxT Flow Cytometer	Life Technologies, Carlsbad, CA, US
BD Aria III Sorter	BD, Heidelberg, DE
BD Canto II	BD, Heidelberg, DE

Bio-Plex® 200	Miltenyi Biotec, Bergisch Gladbach, DE
CASY Cell Counter and Analyzer TT	Omni Life Science, Bremen, DE
Centrifuge- Megafuge 1.0R	Heraeus, Haunau, DE
Counter AC-8	Assistent, Sondheim, DE
Cytocentrifuge Cytospin 3	Shandon, DE
Cytoflex LX	Beckman Coulter, CA, US
Freezer	Liebherr, Ochsenhausen, DE
gentleMACS™ Dissociator	Miltenyi Biotec, Bergisch Gladbach, DE
Leica DFC365 FX	Leica Microsystems, Wetzlar, DE
Leica DM5500 B	Leica Microsystems, Wetzlar, DE
LSRFortessa	BD, Heidelberg, DE
Microm, HM 3555	Thermo Scientific, Rockford, IL, US
Mr. Frosty freezing system	Sigma-Aldrich, Steinheim, DE
UV lamp 16W, 230V, 50/60 Hz	Vilber Lourmat GmbH, DE
Vortexer- MS1 Mini	IKA, Staufen, DE
Waterbath	GFL, Burgwedel, DE

2.16 Softwares

Table 13: Softwares

Name	Provider
BioPlex Manager Software 6.1	Bio-Rad Laboratories GmbH, CA, US
Bio-Rad CFX Manager 3.1	Bio-Rad Laboratories GmbH, CA, US
GraphPad Prism 8®	GraphPad, San Diego, CA, US
Fiji/ImageJ	https://imagej.net/software/fiji/
FlowJo 10.7.1	BD, Ashland, US
Leica Application Suite Advanced Fluo-rescence	Leica Microsystems, Wetzlar, DE
Magellan V7.2	Tecan, Crailsheim, DE
Nanodrop 2000/2000c 1.4.2	Thermo Scientific, Rockford, IL, US

3. Methods

3.1 Murine models

All animal studies were approved by the Federal Authorities for Animal Research of the Regierungspraesidium Giessen, Hessen, Germany, protocols G48/2016, G87/2017, G61/2019 and G27/2020. Adult 6-8 weeks old female Balb/c were purchased and kept under specific pathogen-free housing conditions in the animal facility of the Faculty of Medicine at the Marburg University. A 12 h/12 h day/night rhythm was controlled automatically and mice had constant access to food and water.

3.1.1 RSV A2 infection

Mice were mildly anesthetized by intraperitoneal injection of 50 mg/kg Ketamin and 15 mg/kg Rompun and infected intranasally with $1x10^6$ pfu RSV A2. Mock mice were treated similarly with PBS. Mice were sacrificed as indicated or subjected to the experimental asthma protocol 35 dpi.

3.1.2 Influenza vaccination

Mice were immunized with the InfluSplit 2019/2020 (QIV 19/20) once a week for three consecutive weeks intraperitoneally with a total of 1,5 µg HA protein/virus strain in PBS. Mock immunized mice received a control solution containing the components of the vaccine solution. Animals were sacrificed or subjected to the experimental asthma protocol 35 days after the last immunization.

Vaccine control solution: 3, 75 mg NaCl, 1,3 mg $NaPO_4$ x 12 H_20, 0,2 mg KH_2PO_4, 0,1 mg KCl

3.1.3 Peptide immunization

Mice were immunized subcutaneously at the cervical region with 100 µg virus peptide pool in PBS, using MCT® as an adjuvant in a final concentration of 2 mg, together with 100 µg of the Hepatitis B Virus Core Peptide ($HepCore_{128-140}$; TPPAYRPPNAPIL) as a T helper epitope. The virus peptides for the pool derived from the *in-silico* analysis of RSV A2 included: FYNSMLNNI, SYLNNPNHV, SYLNNPNHVV. Mock immunized mice received only MCT and HepCore peptide.

Treatment was performed twice with a 2-week interval in between. Animals were sacrificed two weeks after the last immunization or subjected to the experimental asthma protocol.

Table 14: Peptides used for virus-peptide immunization experiment (indicated in red)

allergen epitope	allergen	allergen protein family	viral epitope	viral protein	MHC allele	pcs	final score
WYGNSALTI	Asp f 4	Unclassified	FYNSMLNNI	RNA-directed RNA polymerase L	H-2-K^d	1310	1804
KYVNATETV	Asp f 5	Fungalysin metalloprotease	SYLNNPNHV	RNA-directed RNA polymerase L	H-2-K^d	2369	782
SYVEVATQHV	Asp f 5	Fungalysin metalloprotease	SYLNNPNHVV	RNA-directed RNA polymerase L	H-2-K^d	844	458

3.1.4 HDM- induced experimental asthma

HDM allergen whole-body extracts from the common HDM species *Dermatophagoides pteronyssinus* (*Der p*) and *Dermatophagoides farinae* (*Der f*) were used to induce experimental asthma. Mice were mildly sedated by means of intraperitoneal injection of 50 mg/kg Ketamin and 15 mg/kg Rompun and treated with a mixture of 25 µg *Der p* and 25 µg *Der f* in PBS for four times, with a one-week interval in between. Mock animals were treated similarly with PBS. Animals were sacrificed 24 h after the last treatment.

3.1.5 *Asp f*-induced experimental asthma

Mice were treated with 20 µg *Aspergillus fumigatus* (*Asp f*) + 2 mg Alum twice with a one-week interval in between. 11 days after the second treatment they were mildly sedated by means of intraperitoneal injection of 50 mg/kg Ketamin and 15 mg/kg Rompun and challenged intranasally with 100 µg *Asp f* for three consecutive days once daily. Animals were sacrificed 24 h after the last treatment.

3.2 Serum preparation

Mice were sacrificed by injecting 400 mg/kg Ketamin and 40 mg/kg Rompun and after the mice starting to fall into narcosis, final blood was taken from the vena axialliaris. The blood was incubated at room temperature for 2 h and subsequently centrifuged for 20 minutes at 4000 rpm, 4 °C. The serum was frozen at -80 °C.

3.3 Bronchoalveolar lavage acquisition and cytology

BAL acquisition was performed with 1 ml lavage buffer by means of a tracheal cannula. The BAL was centrifuged for 10 minutes at 1300 rpm, 4 °C. Cell-free supernatant was frozen at -20 °C for cytokine detection. Cells were resuspended in 1 ml BAL sample buffer and total leucocyte cells were counted with an automated cell counter (CASY cell counter). Cytospins were prepared by mixing the cell suspension 1:2 with BAL sample buffer and 200 µl diluted BAL was used for centrifugation onto a glass slide with a cytocentrifuge at 700 rpm for 5 minutes. The slides were dried for at least 1 h before staining with the RAL Diff-Quick staining set for differential cell counting. Staining was performed as following: 30 seconds Fixation-Solution; 30 seconds Diff-Quick I; 1 minute Diff-Quick II. Standard microscopical and morphological criteria were used to identify cell types.

Lavage buffer: 50 ml PBS with 1 tablet cOmplete
BAL sample buffer: PBS, 1 % BSA

3.4 Lung histology preparation

Before removing from the animal, lungs were perfused with PBS ones and the left lobe was tied up for lung histology preparation. The smallest lobe of the right lung was snap-frozen for later RNA isolation or virus titration. The remaining lobes were used for preparation of cell suspension.

The left lobe was fixed with 6 % PFA by means of a tracheal cannula and stored in 6 % PFA for at least 24 h at 4 °C. Afterwards, heart and trachea were removed and the lung was put into warm 2 % agar dissolved in VE water. After 1 h at 4 °C, the lung inside the hardened agar block was cut into pieces and transferred into an embedding cassette. The embedding of the lungs in paraffin took place in the Institute of Pathology of the University. Paraffin blocks were cut into 3 µm section with a Microtome and dried for one day at room temperature (RT) before staining.

3.4.1 H&E & PAS stainings

For detection of inflammatory cells, paraffin-embedded lung sections were stained for haematoxylin and eosin (H&E). The average number of inflammatory cells on an external tangent line between neighboring airway and blood vessel sections was counted and the average score was calculated by dividing the counted cells by the length of the line.

For detection of mucus producing cells, paraffin-embedded lung sections were stained with periodic acid, schiff´s reagent and hematoxylin (PAS). PAS positive cells in the airways were scored as following: <5 % = 0; 5-25 % =1; 25-50 % = 2; 50-75 %= 3; >75 % = 4. A minimum of 6 airways per animal were analyzed for both stainings.

The steps of the stainings are described in the following table.

Table 15: H&E and PAS staining protocols

H&E staining	PAS staining
• 5 min PBS	• 5 min PBS
• rinse VE-H2O	• rinse VE-H2O
• 3 min hematoxylin	• 10 min periodic acid 0,5 %
• 5 min running tap water	• 3 min running tap water
• rinse VE-H2O	• rinse VE-H2O
• 2 min eosin with glacial acetic acid	• 15 min Schiff's reagent
• rinse VE-H2O	• 15 min running tap water
• 1 min 70 % ethanol	• rinse VE-H2O
• 1 min 80 % ethanol	• 1 min 70 % ethanol
• 1 min 96 % ethanol	• 1 min 80 % ethanol
• 2 x 1 min 100 % ethanol	• 1 min 96 % ethanol
• 2 x 10 min Roti-Clear	• 1 min 100 % ethanol
• mount coverslip using Entellan	• 15 min Roti-Clear
	• mount coverslip using Entellan

3.4.2 Immunofluorescence

Immunofluorescence (IF) staining was used as a direct detection method for the presence of RSV in murine lung. The antibody is directed against specific epitopes of RSV strains A and B, although the producer does not provide more information about the exact epitope specifity. In this work, an indirect IF method was used, detecting the primary antibody by means of a secondary fluorescence labelled antibody. The stainings were performed together with the Bachelor student Anita Stanczlik (Biopharmaceutical technology, Technische Hochschule Mittelhessen (THM) Gießen, 2019).

Paraffin-embedded lungs were cut into 3, 5 µm sections and put on superfrost microscope slides. In a first step, the slides were incubated twice for 10 minutes each in Roti-Clear™ (Xylol-Substitute) and a decreasing ethanol series was performed, starting with twice incubation for 5 minutes in 100 % ethanol, following 5 minutes incubation in each, 96 %-, 80 %- and 70 %- ethanol. Slides were washed for 5 minutes in PBS before incubation at 80 °C in 10 mM citrate buffer. After another 2 washing steps in PBS, incubation for 15 minutes in PBS, 100 mM glycine in PBS was performed twice, permeabilization in PBS, 0,1 % Triton-X- 100 for 10 minutes at RT, another washing step in PBS for 5 minutes and blocking for 2 h at RT. Afterwards, the primary goat anti-RSV antibody was diluted 1:200 in PBS, 1 % BSA and incubated over night at 4 °C in a humidity chamber. The specific epitope of the antibody is not disclosed by the company. The slides were washed 3 x for 5 minutes each with PBS and incubated with the secondary rabbit anti-goat IgG antibody H&L Alexa Fluor 488 (diluted 1:2000 in PBS, 1 % BSA) together with DAPI staining (diluted 1:1000) for 1 h at RT in the humidity chamber. After 3 final washing steps for 5 minutes in PBS each, the samples were covered with Fluoroshild™ and a coverslip. Slides were stored at 4 °C in the dark before analyzing on a Leica DM5500B with the Software Leica Application Suite Advanced Fluorescence.

Citrate buffer: VE H_20, 10 mM citric acid-monohydrate, 0,05 % Tween 20, pH 6,0
Permeabilization buffer for immunofluorescence: PBS, 0,1 % Triton-X- 100
Dilution buffer: PBS, 1 % BSA
Blocking buffer: PBS, 10 % rabbit serum, 1 % BSA

3.5 Preparation of cell suspensions from murine organs

3.5.1 Lung

Lung pieces of the right lobe were transferred into 5 ml digestion media into gentleMACS C tubes and subsequently dissociated for 16 s, 415 rounds per run, on a gentleMACS dissociator, using the pre-set program m_spleen_03.02. Lungs were incubated for 30 minutes at 37 °C on a shaker. Subsequently, they were once more dissociated with the gentleMACS dissociator and further mashed through a 100 µM cell strainer, using full RPMI medium to prepare a single cell suspension. After centrifugation for 5 minutes at 1300 rpm, 4 °C, red blood cell lysis was performed by resuspending the pellet in 2 ml ACK lysis buffer and incubation for 2 minutes at RT. The reaction was stopped with 8 ml full medium and filtered through a 30 µM cell strainer. The cell suspension was centrifuged again and the cell pellet was resuspended in an appropriate amount of full RMPI medium.

Digestion medium: Full RPMI, 20 µg/ml DNase I, 100 µg/ml collagenase D, 10 % Sodium-pyruvate
ACK lysis buffer: H_2O, 0.15 M ammonium chloride, 10 mM potassium hydrogen carbonate, 0.5 mM EDTA, pH 7,2

3.5.2 Spleen

Spleens were mashed through a 100 µM cell strainer using full RPMI medium to prepare a single cell suspension. After centrifugation for 5 minutes at 1300 rpm, 4 °C, red blood cell lysis was performed by resuspending the pellet in 2 ml ACK lysis buffer and incubating for 2 minutes at RT. The reaction was stopped with 8 ml full medium and filtered through a 30 µM cell strainer. The cell suspension was centrifuged again and the cell pellet was resuspended in an appropriate amount of full RMPI medium.

ACK lysis buffer: H_2O, 0.15 M ammonium chloride, 10 mM potassium hydrogen carbonate, 0.5 mM EDTA, pH 7,2

3.5.3 Lymph nodes

Respective lymph nodes were isolated and mashed through a 100 µM cell strainer, using full RPMI medium to prepare a single cell suspension. After centrifugation for 5 minutes at 1300 rpm, 4 °C, the cell pellet was resuspended in an appropriate amount of full RMPI medium.

3.6 *Ex-vivo* T cell stimulation assays

0,2-1x10^6 isolated cells from either lung or spleen were incubated in 96 well u bottom plates in full RPMI medium. Specific negative stimulation was done with 10 µg/ml unrelated control peptide (HBV_{28-39}). Specific positive stimulation was performed with 10 µg/ml UV-inactivated RSV, 1 µg/ml Peptivator HA or influenza vaccine. Stimulation of interest were pools of the respective virus- or allergen peptides, both with 100 µg/ml in total. Used peptides for the pools included all tested peptide pairs that were positive (strong and weak binder) on the MHC binding assay as shown in Table 23 and Table 24. Detection of intracellular cytokines was performed in flow cytometry after 9 h and 24 h stimulation, detection of activation marker after 24 h.

3.7 CFSE proliferation assay

Proliferation was measured by CFSE (Carboxyfluorescein succinimidyl ester) staining. CFSE is a cell permeable dye, which covalently binds to intracellular amines, resulting in production of green fluorescence. Upon cell division, CFSE is divided to the daughter cells and fluorescence intensity decreases with each cell division. Cells were resuspended in 1 ml PBS with a concentration of 1x10^6 cells and stained with 1 ml of 5 µM CFSE in PBS for 5 minutes at RT. The reaction was stopped with PBS, 5 % FCS, cells were centrifuged for 5 minutes at 1300 rpm, resuspended in medium and stimulated for 6 days. Flow cytometry staining was performed for discrimination of $CD4^+$ and $CD8^+$ T cells.

3.8 Immunological methods

3.8.1 IgG Enzyme-linked immunosorbent assay

Immunoglobulins were detected in Enzyme-linked immunosorbent assay (ELISA) For virus-specific IgG detection, 96-well half-well flat bottom plates were coated with 1µg/ml UV-inactivated RSV or QIV 19/20 in coating buffer at 4 °C over night (o/n). Standard curve was coated with a polyclonal goat-anti mouse IgG antibody with 1 µg/ml. Plates were washed four times and blocked for 2h at RT. After washing, serum samples were diluted 1:10 (RSV) or 1:50 (QIV) in dilution buffer and incubated at RT for 2 h. A two-fold standard curve was prepared, using a recombinant mouse-IgG antibody, starting at 500 ng/ml. Following another four times washing step, secondary antibody goat anti-mouse–HRP antibody (1:2000 in dilution buffer) was applied for 2 h at RT. Plates were washed six times and signal was developed with ABTS. Absorbance was read at 405 nm on TECAN microplate reader.

Coating buffer: 500 ml H_2O, 4,2 g $NaHCO_3$, pH 8,3
Washing buffer (PBS-T): PBS, 0,1 % Tween-20
Blocking buffer: PBS, 2 % BSA
Dilution buffer: Washing buffer, 10 % horse serum

3.8.2 IFNγ Enzyme-linked immunosorbent assay

Mouse IFNγ in BAL supernatant was measured using a commercially available mouse IFNγ ELISA DuoSet (R&D). Experimental procedure was performed according to the manufacturers protocol, using a 96 well flat bottom plate. Absorbance was read at 450 nm on a TECAN microplate reader.

Coating buffer: PBS
Washing buffer: PBS, 0,1 % Tween-20
Blocking buffer: PBS, 1 % BSA
Dilution buffer: PBS, 1 % BSA

3.8.3 Cytometric bead array

Cytokines were measured from 50 µl cell-free supernatant with a mouse-specific cytometric bead array (CBA) according to the manufacturer's instructions. Cytokine measurements were performed using the BioPlex-200 (Bio-Rad). The standard curve and respective cytokine concentrations were calculated with the BioPlex Manager Software 6.1 (Bio-Rad).

3.8.4 Flow cytometry staining

For staining of surface markers, 0,2-1x10^6 cells were seeded in a 96-well polypropylene v-bottom plate, washed with FACS buffer and Fc receptors were blocked with an αCD16/αCD32 antibody (anti-mouse Fc block) for 10 minutes at 4 °C. Afterwards, cells were stained with the indicated set of surface FACS antibodies for 20 minutes at 4 °C in FACS buffer. When indicated, H-2-Kd-specific pentamer staining was performed for 10 minutes at RT before staining with the FACS antibodies. After centrifugation at 4 °C, 1500 rpm for 3 minutes, fixation of the cells was performed by resuspending in fixation buffer and incubating for 20 minutes at 4 °C. Cells were centrifuged, finally resuspended in FACS buffer and stored at 4 °C in the dark until acquisition.

For intracellular cytokine staining after organ preparation, cells were put into restimulation medium for 4 h and incubated at 37 °C. Cells of *ex-vivo* stimulation were only subjected to Brefeldin A (5 µg/ml) for the last 4 h of stimulation before proceeding with staining. Surface staining was performed in the same way as described above. Subsequently after fixation, cells were washed twice with permeabilization buffer before incubation with the respective antibodies for 30 minutes at 4 °C. Cells were finally washed once with permeabilization buffer and once with FACS buffer and stored in the latter at 4 °C in the dark until acquisition. Flow cytometric analysis was performed using a Canto II flow cytometer, Aria III cell sorter, LSRFortessa, Attune Nxt or Cytoflex LX. Data analysis was done with FlowJo V.10 software.

FACS buffer: PBS, 0,5 % BSA, 2 mM EDTA

Fixation buffer: 2 % PFA in VE H_20

Permeabilization buffer: PBS, 1 % FCS, 0,3 % Saponin

Restimulation medium: 50 ng/ml PMA, 1 µg/ml Ionomycin, 5 µg/ml Brefeldin A in RPMI full medium

3.8.5 *In-vitro* MHC stabilization assay

In order to proof binding of the predicted peptides to the H-2-Kd molecule, an MHC stabilization assay was used. Therefore, RMA-S cells, already stably transfected with the H-2-Kd allele, were used. These cells have a deficient TAP transporter, being unable to express their MHC molecules on the cell surface for a longer time at 37 °C. Incubation at 26 °C leads to expression of their MHC molecules, but also exogenous peptides which bind to the MHC molecules, lead to a stable expression.
The MHC stabilization assay was performed together with the medical student Max Schultheiß (Medicine, Justus-Liebig-University Gießen, 2019/2020). 100 µl RMA-S^{Kd} cells were seeded at a density of 10^6 cells per well on a 96-well u bottom plate and incubated for 16 h at 26 °C. Serum-free medium containing the peptide of interest was prepared (medium-peptide mix). The H-2-Kd specific known immunogenic influenza virus peptide IYSTVASSL (IAV $HA_{533-541}$) was used as a positive control and an unrelated H-2-Ld- specific Hepatitis B virus peptide IPQSLDSWWTSL (HBV_{28-39}), as well as a sample without any peptide served as negative controls. All peptides were used at a concentration of 10 µM. Following incubation, cells were pelleted by centrifugation at 1300 rpm for 5 minutes, resuspended in medium-peptide mix or medium-control peptides and incubated for 30 minutes at 26 °C. Cells were washed with serum free medium without peptides three times to remove non-bound peptides. Resuspended in medium with serum, cells were incubated for different time points (60, 120 & 180 minutes) at 37 °C. Flow cytometry staining was performed using a PE Anti-Mouse H-2-Kd antibody as described in 3.8.4.

3.9 Molecular biology methods

3.9.1 RNA Isolation

Frozen lungs of infected animals were crushed with a mortar to a fine powder and 600 µl of lysis buffer were added. Further RNA isolation was performed according to the manufacturer's instructions for the RNAeasy Plus Mini Kit form Qiagen. RNA from virus stock was isolated with the QIAamp Viral RNA Mini Kit, according to the manufacturer´s protocol.

Lysis buffer: RTL buffer, 1 % 2-Mercaptoethanol

3.9.2 cDNA production

cDNA was produced using the Qiagen OmniScript RT Kit. For detection of the replicative virus, cDNA was prepared using the reverse primer for the positive strand of RSV. All reactions were performed using a thermocycler at 37 °C for 1 h and cDNA samples were stored at -20 °C.

Table 16: Amounts of reagents used for cDNA production

Reagent	Amount per sample
RT buffer	2 µl
dNTP´s	2 µl
Primer (10 µM)	2 µl
ORT	1 µl
Nuclease-free water	3 µl
RNA	10 µl

3.9.3 Quantitative real-time PCR

In order to detect and quantify viral load in lung, quantitative real-time polymerase chain reaction (qPCR) was used. Therefore, cDNA was used and the reaction was set up using SYBR Green MasterMix, following the manufacturer´s instructions. Forward and reverse primers were used in the reaction. A non-template control using water instead of cDNA was performed for each primer pair. cDNA was used undiluted.

Table 17: Amounts of reagents used for qPCR

Reagent	Amount per sample
SYBR Green Mix	5 µl
Primer forward (10 pmol/µl)	0,5 µl
Primer reverse (10 pmol/µl)	0,5 µl
Nuclease-free water	3 µl
cDNA	1 µl

Table 18: qPCR settings

Steps	Temperature	Time	Cycles
Initiation	95 °C	3 min	
Denaturation	95 °C	5 sec	40
Annealing and Elongation (Fl measurement)	60 °C	10 sec	40
Melt curve (Fl measurement)	65 °C - 95 °C	0,5 °C, 5 sec	

3.9.4 Standard curve for strand-specific qPCR

In order to quantify the amount of strain-specific virus RNA in the samples, a calibration curve with defined numbers of fragments was created and run in parallel to the samples. Thus, the obtained cycle numbers could be correlated with the numbers of detected fragments.
RNA was isolated from virus as described and further processed in a OneStep RT-PCR Kit to obtain cDNA. A 10x standard curve was prepared starting from $1x10^9$ molecules/µl. This was applied for each qPCR run. The number of obtained transcripts per µl was calculated with the following formula:

Weight of one DNA-monophosphate	$M_{DNA} = 327$ g/mol
Length of the DNA transcripts	L_T (#nucleotides)
cDNA concentration as measured by nanodrop	$Cm = g/\mu l$
Molar weight of one transcript	$M_{SST}\,(g/mol) = M_{DNA} * L_T$
Mass of one transcript	$m_{sst}\,(g) = \frac{M_{SST}}{Avogadro\ constant}$
Number of transcripts per µl	$x\ (molecule/\mu l) = \frac{Cm}{m_{SST}}$

The program used for the RT-PCR is the following:

Table 19: Settings for the RT-PCR for production of a standard curve

Steps	Temperature	Time	Cycles
Reverse Transcription	50 °C	30 min	
Initiation	95 °C	15 min	
Denaturation	94 °C	30 sec	40
Annealing	55 °C	10 sec	40
Extension	72 °C	1:30 min	40
Final extension	72 °C	10 min	

3.10 Virome analysis

Total BAL and lung from RSV/ *Asp f* experiment were collected, snap frozen in liquid nitrogen and stored at -80 °C until processing. Five samples from each group were used. Further processing was performed by Dr. Roland Liu at the University California San Diego (UCSD) in the lab from Prof. David Pride. Samples were homogenized

and filtered through a 0,4 µm CA filter to remove eukaryotic and bacterial cells. Benzonase and micrococcal nuclease treatment was performed to remove host RNAs from cell lysis and subsequently cells were lysed and viral RNA and DNA was extracted. cDNA libraries were created by a WTA2 transcriptome amplification kit and tagmented to ~500 bp fragments and barcoded. Viral cDNA libraries were then normalized, pooled and sequenced with an Illumina NG sequencer. For analysis, paired-end reads were trimmed to retain only sequence reads between 100 and 301 bp. Sequence reads were mapped to common bacterial contaminant genomes to ensure samples were not grossly contaminated. Resulting unmapped reads are likely viral sequence reads and underwent contig assembly, which were further BLASTed. Finally, virome data were compared and analyzed among samples.

3.11 Cell biology methods

3.11.1 Cell culture

All cells were cultured in their respective medium (2.10) at 37 °C in a humidified atmosphere containing 5 % CO_2.

3.11.2 Freezing and thawing of cells

$1x10^7$ cells were frozen in freezing medium at -80 °C, using a Mr. Frosty system (gradual freezing of -1 °C/minute). After 24 h, cells were transferred to liquid nitrogen for long-term storage. For thawing, cells were put into a water bath at 37 °C until they were almost thawn and subsequently transferred into 9 ml of the appropriate cell culture medium. After centrifugation for 10 minutes at 1300 rpm, 4 °C, the pellet was resuspended in cell culture medium and cells were counted using an automated Casy cell counter.

Freezing medium: 90 % FCS, 10 % DMSO

3.11.3 RSV propagation

For RSV propagation, Hep-2 cells were seeded 1:2 o/n, washed three times with PBS and infected with 0,1 MOI RSV A2 in infection medium (MEM+ 5 % FCS) in a total volume of 5 ml in a T75 cell culture flask. After 3 h incubation at 37 °C, 15 ml

infection medium were added. 24 h post infection (p.i.), the medium was changed to 20 ml fresh infection medium and cells were harvested 48 h post infection. 10 x virus stabilization solution was added in a final concentration of 1 x and cells were centrifuged for 10 minutes at 4 °C, 900 g and the supernatant was stored on ice. The pellet was vortexed for 3 minutes to release virus, centrifuged again and the supernatants were fused and frozen at -80 °C.

Virus stabilization buffer: 11 g $MgSO_4$, 25 ml 1M HEPES, 25 ml H_20

3.11.4 RSV titration

For virus titration, Vero76 cells were seeded on a 24-well plate and grown o/n. The virus was thawn and a serial dilution from 10^{-1} to 10^{-6} was prepared in infection medium. Cells with virus were incubated for 1 h at 37 °C before the virus was removed, each well covered with 500 µl 1 x Avicell in infection medium and incubated for 72 h in an incubator. The Avicell was removed, cells were washed twice with PBS and fixed for 30 minutes at 4 °C with 4 % PFA in PBS. Afterwards, cells were incubated with 0,3 % Triton-X-100 for 20 minutes at RT, following staining with the primary goat anti-RSV antibody (diluted 1:200 in dilution buffer) for 1 h at RT. After three times washing with PBS, the secondary anti-mouse HRP antibody (diluted 1:4000 in dilution buffer) was incubated for 1 h at RT in the dark, washed away with PBS three times and TrueBlue Substrate was added for 15-30 minutes until plaques were able to be detected. Plaques per well were counted and plaque forming units per milliliter (pfu/ml) were calculated by means of the formula: plaques x 10 x reciprocal value of dilution=x pfu/ml

Dilution buffer: PBS, 10 % Horse serum, 0,1 % Tween-80

3.11.5 UV-inactivation of RSV

The RSV A2 stock that was used for mouse infection was UV- inactivated using a lamp (230 Volt, 8-Watt, 254 nm tube, 16-Watt power, distance 25 cm) for 30 minutes on ice and frozen at -80 °C. Inactivation of virus suspension was confirmed via subsequent titration.

3.12 *In-silico* prediction of potentially cross-reactive T cell epitopes

3.12.1 Bioinformatics pipeline

The development of the bioinformatics pipeline was done in cooperation with the bioinformatics department of Prof. Franz Cemic at the THM Gießen.
Allergen protein sequences were downloaded (10.09.2017) from Allergen Online (Mari et al., 2006, Mari et al., 2009, Mari, Scala, 2006) and virus protein sequences from Uniprot (RSV A2, RV1b, SARS-CoV-2) (The universal protein resource [UniProt], 2008) and Gisaid (Influenza strains) . Viral T cell epitope prediction was performed using smm (Peters, Sette, 2005), ann (Buus et al., 2003) and consensus (Moutaftsi et al., 2006) algorithm tools for MHC class I (IC50 threshhold <=5000nm), and netMHCII (Nielsen, Lund, 2009) for MHC class II (affinity score rank for strong binders: 0.500 %; for weak binders: 2.000 %). Epitopes predicted by all methods were aligned against all allergen proteins with NCBI protein blast platform (Camacho et al., 2009). Allergen proteins associated with an alignment e-value <10 were further processed for T cell epitope prediction using netMHC (Nielsen et al., 2003) and netMHCpan (Hoof et al., 2009) for MHC class I, and netMHCII and netMHCIIpan (Andreatta et al., 2015) for MHC class II prediction (affinity score threshold for strong binders: 0.500; for weak binders: 2.000). Viral and allergen epitopes were pairwise aligned with a Biopython module pairwise 2 (Cock et al., 2009) and pairs with a score > 8 were further evaluated. A final pair combined score was automatically calculated, taking the binding affinity of predicted viral and allergen epitopes to MHC molecules into consideration, as well as the score from the pairwise alignment and cross-entropy (cut-off 0,8). A schematic illustration of the pipeline is provided in Figure 9.

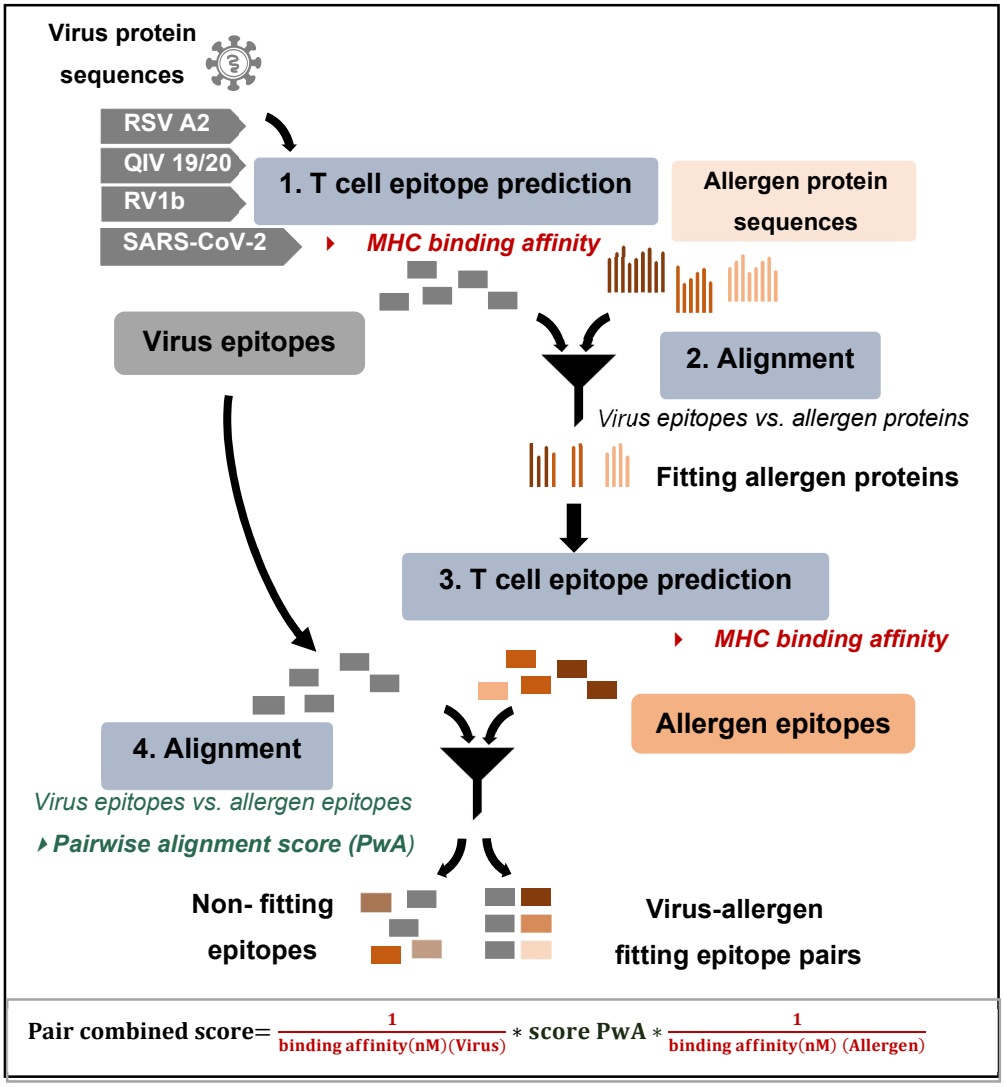

Figure 9: Schematic overview of the bioinformatics pipeline and calculation of the pair combined score

3.12.2 Scoring system

The top 30 candidate epitope pairs, as per pair combined score, were further assessed. A scoring system was developed and five categories of criteria were formed, summing up the scores of individual criteria in one group (Figure 10), based on:

- Category 1: whether they are included in the commercially available diagnostic assays ImmunoCAP ISAC®112 or ALEX® and evoked IgE production in >50 % of patients with associated clinical allergy as per WHO/IUIS Allergen Nomenclature Sub-committee (http://allergen.org/index.php)
- Category 2: pair combined score; defined in 4 ranges, with the help of percentiles: ≤ 10 % = 0; [20-50 %] = 1; [50-90 %] = 2; [90-100 %]
- Category 3: whether they achieve more than 100 entries when entering the epitope sequence in Uniprot and whether the specific epitope sequence is also contained in proteins of other allergen sources

- Category 4: abundance of the allergen component within the top 30 candidates
- Category 5: abundance of the allergen source within the top 30 candidates

As a next step, five different combinations of the aforementioned categories were defined and the cumulative score was calculated for each allergen epitope. Additionally, the cumulative score was calculated three more times, each time multiplying another category by a factor of 3 in order to critically compare alternative weighing of the associated criteria. The new top 5 candidate epitope pairs were subsequently ranked based on the frequency of achieving the maximum score in each of the separately weighed scoring approaches as described above.

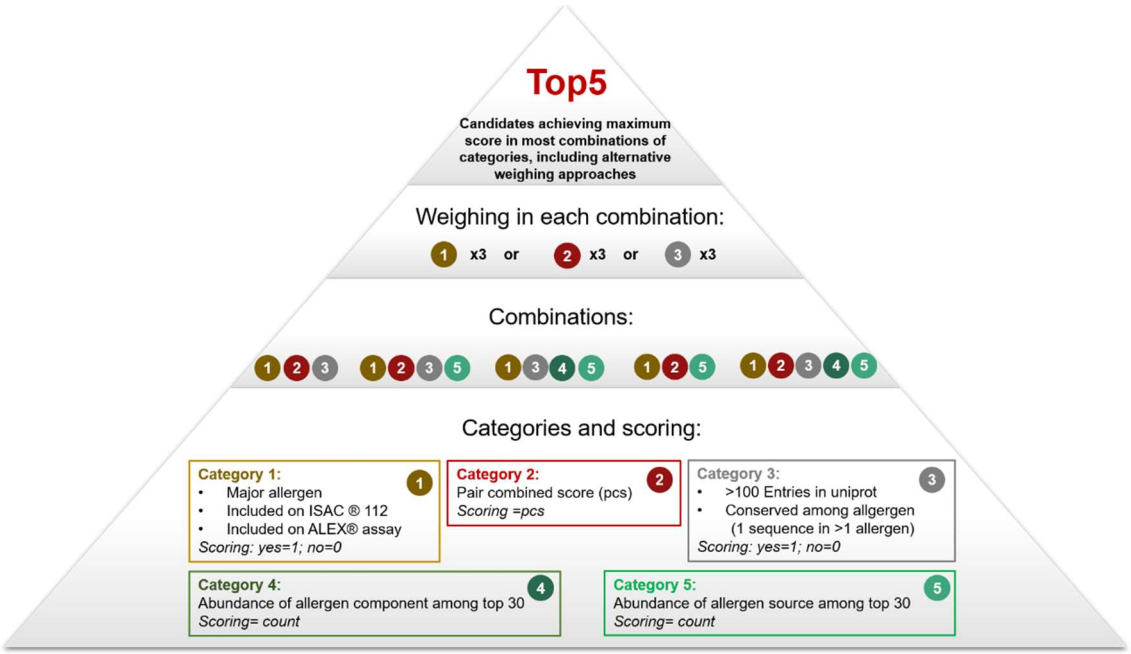

Figure 10: Scoring system for further prioritization of the selected top 30 potentially cross-reactive allergen- and virus- derived T cell epitope pairs

3.13 Statistical analysis

Data analysis was performed using the GraphPad Prism 8 software. Outliers were identified by ROUT (Q=1). All data were log transformed. When comparing multiple groups, one-way ANOVA and Tukey´s multiple comparisons test was used. When comparing more than one group against a control group, one-way ANOVA and Dunetts´ multiple comparison test was used. Unpaired t-test was used when comparing two groups. P values were defined as following: * ≤0,05; ** p≤0,01; *** p≤0,001; **** p≤0,0001.

4. Results

4.1 A bioinformatics approach identified potentially cross-reactive T cell epitope pairs between several RNA viruses and allergens

In order to investigate cross-reactivity between several RNA viruses and allergens, a robust bioinformatics pipeline for prediction of potentially cross-reactive T cell epitopes was developed (Figure 9). Several available tools for epitope prediction and alignment were used as described in the methods 3.12.1. The pipeline is able to predict T cell epitopes on the basis of MHC binding affinity of individual epitopes for both, virus and allergen proteins, as well as detection of sequence similarity of the predicted epitopes. The pipeline works as a filtering system, first predicting T cell epitopes of the respective virus, before aligning these against all available allergen proteins. Only matching allergen proteins are further processed for epitope prediction. Finally, predicted allergen epitopes are aligned against predicted virus epitopes. The pipeline was performed for the most important respiratory viruses with regard to allergy and asthma development, focusing on the strains that are available for mouse models; RV1b, RSV A2 and the strains of the seasonal quadrivalent influenza vaccine 2019/2020 (further referred to as QIV). Analyses were done for both, MHC class I and II on the background of the mouse Balb/c strain, as well as the most frequent human HLA alleles. Interestingly, predictions for MHC class II achieved only a few candidate pairs with relatively low pair combined scores as compared to candidate pairs of MHC class I predictions (up to 500 x lower score, data not shown). Therefore, they were not further assessed. The allergen epitopes of the MHC class I top 30 candidates as per pair combined score were further assessed in a comprehensive scoring system as shown in Figure 10. By doing so, clinical relevance was considered for the allergen epitopes. The epitope pairs that were most likely to play a role in the context of allergy and viruses were used for further *in-vitro*, *ex-vivo* and *in-vivo* analyses. Figure 11 A- C compares the pair combined scores of all candidates from all analyses, highlighting the top 30 candidates in green, as well as the top five candidates that were arising from the scoring systems in red. Interestingly, candidates from RV1b achieved lower scores as compared to RSV A2 or QIV. Overall, scores from the latter ones were relatively similar. For the

purpose of further analysis of the allergen counterpart of the top 30 candidates, protein families of each allergen component were assessed by using AllFam (Radauer et al., 2008) and displayed in Figure 11 D. An overlap between predicted protein families was observed between human and mouse analyses for all viruses. Especially epitopes from lipoprotein, cupin and enolase were predicted frequently. Concurrently, allergen-derived epitopes potentially cross-reactive to RSV A2-derived epitopes in the mouse Balb/c MHC context showed the highest diversity of associated protein family sources, suggesting a high probability of different allergen sources to cross-react with T cell epitopes from this virus. In this thesis, only the mouse candidate pairs were further evaluated for these viruses.

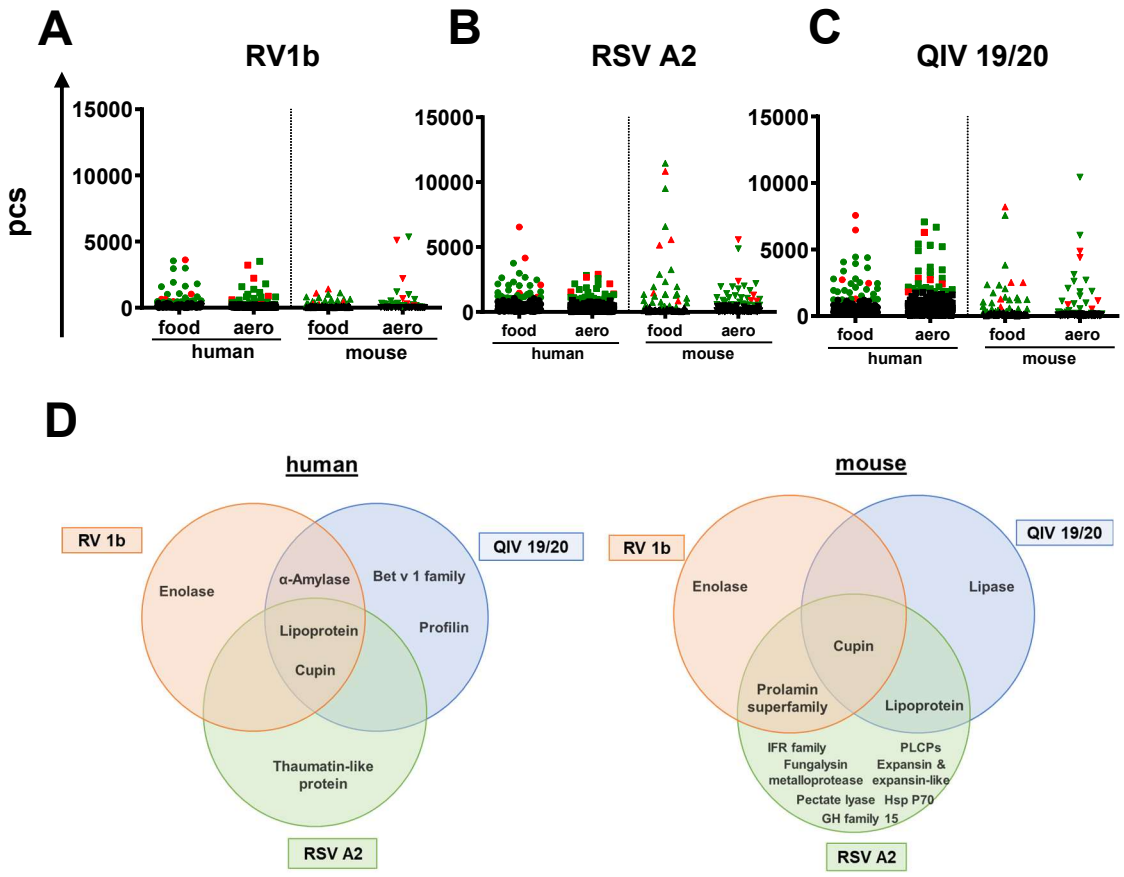

Figure 11: Predicted candidate epitopes as per pair combined score and allergen proteins families
A-C: Scores of the predicted candidate pairs for MHC class I, top 30 candidates as per pair combined score are depicted in green, top 5 candidate pairs as per scoring system are depicted in red **D:** Protein families of the allergen counterpart for the top 30 candidates for MHC class I prediction.; pcs=pair combined score, QIV=quadrivalent influenza vaccine, RV=rhinovirus, RSV=respiratory syncytial virus

With the start of the COVID-19 pandemic, potentially cross-reactive T cell-epitopes between SARS-CoV-2 and allergens for the most important human HLA alleles were additionally identified using the aforementioned comprehensive *in-silico* pipeline. These data complement all prior analyses with the inclusion of an additional

clinically relevant virus. Due to the ongoing pandemic at this time, this part of the project was based on the human context, thus, this analysis was only performed on the background of human HLA alleles including both HLA class I and II (Table 20 and Table 21). Interestingly, the predicted HLA class II epitope pairs again scored much lower compared to the predicted HLA class I pairs, being in line with the results from the other viruses. However, associated food allergen epitopes for both MHC classes derived mainly from chicken and more specifically belonging to the allergen protein family of lipoproteins. This protein family was also found to be most frequent in the predictions of epitope pairs on the human HLA background for RV1b, RSV A2 and QIV 19/20 (Figure 11). Predicted aero-allergens for HLA class I indicated a high diversity of allergen sources for HLA class I alleles, including mouse, fungi and timothy grass. Interestingly, HLA class II predicted aeroallergen epitopes mainly derived from timothy grass, specifically *Phleum pratense* 5 (*Phl p* 5).

Table 20: The top 5 candidate human T cell epitope pairs for potential cross-reactivity between SARS-CoV-2 and aero (upper table)- and food-allergens (lower table) for HLA class I; pcs=pair combined score

	allergen epitope	allergen	allergen protein family	viral epitope	viral protein	HLA allele	pcs	final score
Nr. 1	GSNTFTILK	Mus m 1	Lipocalin	TSNSFDVLK	Papain-like proteinase	HLA-A_11_01	8188	1810
Nr. 2	MLYEVLWNL	Asp f 5	Fungalysin met-alloprotease	YLYALVYFL	ORF3a	HLA-A_02_01	5974	782
Nr. 3	SGVSPVSYQK	Aln g 1	Bet v 1 family	ATSRTLSYYK	Membrane protein	HLA-A_11_01	2413	138
Nr. 4	KYKTFVATF	Phl p 5	Group 5/6 grass pollen allergen	MFDAYVNTF	Papain-like proteinase	HLA-A_24_02	1910	154
Nr. 5	GSNTFTILK	Mus m 1	Lipocalin	VTNNTFTLK	Non-structural protein 2 (nsp2)	HLA-A_11_01	3286	138

Nr. 1	FLGHFIYSV	Gal d 5	Serum albumin	TMADLVYAL	RNA-directed RNA polymerase (RdRp)	HLA-A_02_01	1408	1282
Nr. 2	YLLDLLPAA	Gal d 6	Lipoprotein	TLMNVLTLV	Non-structural protein 6 (nsp6)	HLA-A_02_01	4185	1180
Nr. 3	RPAYRRYLL	Gal d 6	Lipoprotein	RPPLNRNYV	Helicase (Hel)	HLA-B_07_02	2274	556
Nr. 4	APHGGGSIL	Cor a 1	Bet v 1 family	VPGLPGTIL	Non-structural protein 4 (nsp4)	HLA-B_07_02	2571	462
Nr. 5	KVFRFSMFK	Gal d 6	Lipoprotein	LVASIKNFK	RNA-directed RNA polymerase (RdRp)	HLA-A_11_01	1194	432

Table 21: The top 5 candidate human T cell epitope pairs for potential cross-reactivity between SARS-CoV-2 and aero (upper table)- and food-allergens (lower table) for HLA class II; pcs=pair combined score

	allergen epitope	allergen	allergen protein family	viral epitope	viral protein	HLA allele	pcs	final score
Nr.1	YNTFVAT-FGAASNKA	Phl p 5	Group 5/6 grass pollen allergen	VNTFSSTFNVP-MEKL	Papain-like proteinase	HLA-DRB1_04_01	87	1882
Nr. 2	MLLLTALAAGS AVAR	Asp f 4	Unclassified	PLIVTALRAN-SAVKL	Non-structural protein 8 (nsp8)	HLA-DRB1_01_01	479	752
Nr. 3	KTFVAT-FGAASNKAF	Phl p 5	Group 5/6 grass pollen allergen	DAYV-NTFSSTFNVPM	Papain-like proteinase	HLA-DRB1_04_01	53	658
Nr.4	RTFVAT-FGPASNKAF	Phl p 5	Group 5/6 grass pollen allergen	DAYV-NTFSSTFNVPM	Papain-like proteinase	HLA-DRB1_04_01	29	658
Nr. 5	DAAFKVAATAA-NAAP	Phl p 5	Group 5/6 grass pollen allergen	DAYV-NTFSSTFNVPM	Papain-like proteinase	HLA-DRB1_04_01	38	634

Nr. 1	RHPFLYA-PAILSFAV	Gal d 5	Serum albumin	KSAFYILPSI-ISNEK	Papain-like proteinase	HLA-DRB1_01_01	299	1646
Nr. 2	ILMILVDAVLKE PSM	Gal d 6	Lipoprotein	FACVVADA-VIKTLQP	Papain-like proteinase	HLA-DRB1_03_01	113	1244
Nr. 3	FKPVYSDVPIEK IQV	Gal d 6	Lipoprotein	FACVVADA-VIKTLQP	Papain-like proteinase	HLA-DRB1_03_01	29	696
Nr. 4	KEGDVFIM-PAAHPVA	Ara h 1	Cupin	QQESPFVMM-SAPPAQ	Papain-like proteinase	HLA-DRB1_01_01	258	462
Nr. 5	RHPFLYA-PAILSFAV	Gal d 5	Serum albumin	LFFFLYENAFLP FAM	Non-structural protein 6 (nsp6)	HLA-DRB1_01_01	81	398

4.2 Several predicted T cell epitopes were able to bind to MHC molecules *in-vitro*

Since the candidate epitopes were predicted *in-silico* but not yet described as T cell epitopes in The Immune Epitope Database (IEDB, www.iedb.org), MHC binding ability for the mouse epitopes for RV1b, RSV A2 and QIV analyses was analyzed in an *in-vitro* MHC stabilization assay. Since inhaled allergens are more clinically relevant in the context of asthma, we prioritized on testing all top five candidate pairs including aeroallergens on the background of H-2-Kd MHC allele. This MHC allele was chosen, because the further experiments were performed in Balb/c mice and this allele is specific for Balb/c mice. Furthermore, the available RMA-S cells are stably transfected with this MHC allele and several predicted candidate pairs were predicted on this background. Additionally, the food-allergen pair with the highest pair combined score for each virus analysis was tested. Peptides were synthesized for these epitopes and further tested. RSV A2 candidates are shown in Figure 12, results for candidates of QIV and RV1b are displayed in the supplements in Figure 43 and Figure 44. Peptides binding to the MHC molecule with a similar strength as the positive control were considered as strong binders. Weak peptides were considered to also bind to the MHC molecule compared to the negative control with a lower strength compared to the positive control, whereas non-binders showed the same trend as the negative control. Out of six tested peptide pairs for RSV A2, only one peptide pair was considered as non-binder. Three out of six tested candidate pairs from the QIV analysis were also able to bind to the MHC molecule. Interestingly, among the non-binder pairs, mostly the virus peptide was not able to achieve good MHC binding results. From the tested candidate pairs of RV1b, only two were able to bind to the MHC molecule. Therefore, further experimental testing was only done for peptides from RSV A2 and QIV. All top five candidate pairs for aero- and food- allergens, including the results of the *in-vitro* testing, are depicted in Table 22 (RV1b), Table 23 (RSV A2), and Table 24 (QIV 19/20). Interestingly, each analysis pointed out different patterns of allergen sources of the predicted peptides. For RSV A2 and RV1b, several top aeroallergen peptides derived from *Aspergillus fumigatus*. Candidates from QIV analysis showed a prevalence in inhaled allergens from house dust mites, mainly *Der p*. This suggests an important role of the respective allergen in combination with the specific virus.

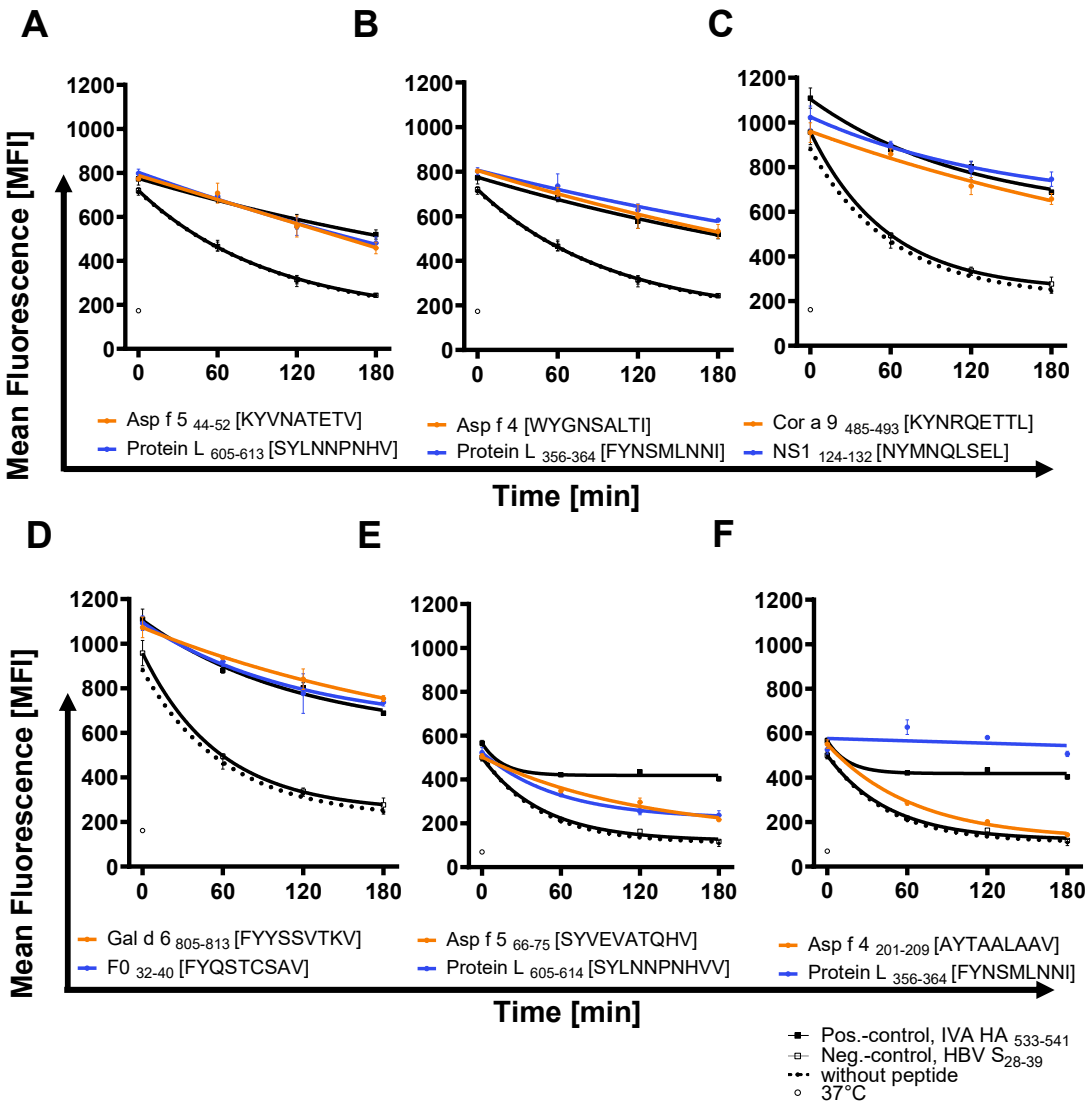

Figure 12: Predicted peptides bind to the mouse Balb/c H-2-Kd MHC molecule *in-vitro*

H-2-Kd expressing RMA-S cells were incubated with 10 µM of the respective peptides of RSV A2 analysis or control peptides for 3 h at 26 °C. Mean fluorescence intensity of H-2-Kd expression was measured by flow cytometry and are shown as ± SD, n=3 **A-D:** strong binder pairs **E:** weak binder pair **F:** non-binder pairs; IVA HA= Hemagglutinin of Influenza A virus, HBV S= surface protein of Hepatitis B virus

Table 22: The top 5 candidate mouse T cell epitope pairs for potential cross-reactivity between RV1b and aero (upper table)- and food-allergens (lower table); pcs=pair combined score

	allergen epitope	allergen	allergen protein family	viral epitope	viral protein	MHC allele	pcs	final score
Nr. 1	VYATMNGVL	Asp f 4	Unclassified	LYNKCSNII	P2-C	H-2-K^d	694	1960
Nr. 2	KPYVLPVPF	Asp f 22	Enolase	VPYVNAVPM	VP2	H-2-L^d	289	916
Nr. 3	VYATINGVL	Asp f 4	Unclassified	VYEDFSSKI	Polymerase	H-2-K^d	140	636
Nr. 4	KPLKGPFTI	Cyn d 1	Expansin and expansin-like	KPFDSRFVL	P2-C	H-2-L^d	5111	350
Nr. 5	LYIAGNKTI	Cha o 1	Pectate lyase	LYVHVGNLI	P2-A	H-2-K^d	2207	326

Nr. 1	VYIPPYCTI	Tri a 21	Prolamin superfamily	LYIPPYDLL	Polymerase	H-2-K^d	1104	2020
Nr. 2	LPYPQPQPF	Tri a 21	Prolamin superfamily	LPAMNRRFF	P2-C	H-2-L^d	431	700
Nr. 3	KYLQPQQPI	Tri a 21	Prolamin superfamily	LYIPPYDLL	Polymerase	H-2-K^d	1413	696
Nr. 4	LPYSQPQPF	Tri a 21	Prolamin superfamily	LPAMNRRFF	P2-C	H-2-L^d	247	672
Nr. 5	KFYTVISSL	Gal d 3	Transferrin	TYYEVAGGV	Polymerase	H-2-K^d	276	378

Table 23: The top 5 candidate mouse T cell epitope pairs for potential cross-reactivity between RSV A2 and aero (upper table)- and food-allergens (lower table); pcs=pair combined score

	allergen epitope	allergen	allergen protein family	viral epitope	viral protein	MHC allele	pcs	final score
Nr. 1	WYGNSALTI	Asp f 4	Unclassified	FYNSMLNNI	RNA-directed RNA polymerase L	H-2-K^d	1310	1804
Nr. 2	KYNRQETTL	Cor a 9	Cupin, 11S seed storage globulin	NYMNQLSEL	Non-structural protein 1	H-2-K^d	5565	986
Nr. 3	KYVNATETV	Asp f 5	Fungalysin metalloprotease	SYLNNPNHV	RNA-directed RNA polymerase L	H-2-K^d	2369	782
Nr. 4	AYTAALAAV	Asp f 4	Unclassified	FYNSMLNNI	RNA-directed RNA polymerase L	H-2-K^d	883	580
Nr. 5	SYVEVATQHV	Asp f 5	Fungalysin metalloprotease	SYLNNPNHVV	RNA-directed RNA polymerase L	H-2-K^d	844	458

Nr. 1	KFYTVISSL	Gal d 3	Transferrin	PYFTLIHMI	Small hydrophobic protein	H-2-K^d	1455	1142
Nr. 2	FYYSSVTKV	Gal d 6	Lipoprotein	FYQSTCSAV	Fusion glycoprotein F0	H-2-K^d	10837	908
Nr. 3	KPQLSLTGF	Mal d 2	Thaumatin-like protein	NPKASLLSL	Nucleoprotein	H-2-L^d	846	814
Nr. 4	KYNRQETTL	Cor a 9	Cupin, 11S seed storage globulin	NYMNQLSEL	Non-structural protein	H-2-K^d	5565	486
Nr. 5	SYAAHMSII	Act d 1	Papain-like cysteine protease	NYMNQLSEL	Non-structural protein	H-2-K^d	5148	426

Table 24: The top 5 candidate mouse T cell epitope pairs for potential cross-reactivity between QIV 19/20 and aero (upper table)- and food-allergens (lower table); pcs=Pair combined score

	allergen epitope	allergen	allergen protein family	viral epitope	viral protein	virus strain	MHC allele	pcs	final score
Nr. 1	KYMSSHFPI	Der p 14	Lipoprotein	KYVLFHTSL	PA	B/Colorado/2017, B/Phuket/2013	H-2-K^d	4404	1516
Nr. 2	SYAKGIWNV	Asp f 6	Fe/Mn superoxide dis-	SYAKNILRT	NA	B/Phuket/2013	H-2-K^d	859	554
Nr. 3	KYMSSHFPI	Der p 14	Lipoprotein	TYITRNQPE	PB1	A/Brisbane/2018	H-2-K^d	1153	492
Nr. 4	KYMSSHFPIL	Der p 14	Lipoprotein	KYVLFHTSLL	PA	B/Colorado/2017, B/Phuket/2013	H-2-K^d	534	468
Nr. 5	KYQAQITEL	Blo t 11	Myosin heavy chain	RYSALSNDI	NA	B/Colorado/2017, B/Phuket/2013	H-2-K^d	4885	450

Nr. 1	SYAASNTRL	Ves a 1	Lipase	YYSTAASSL	HA	B/Colorado/2017, B/Phuket/2013	H-2-K^d	8203	1616
Nr. 2	SYHSNNERI	Act d 5	Unclassified	GYHANNSTD	HA	A/Brisbane/2018	H-2-K^d	2523	772
Nr. 3	SYAASNTRL	Ves a 1	Lipase	IFLAMTERI	PB1	B/Colorado/2017, B/Phuket/2013	H-2-K^d	1278	592
Nr. 4	YSYAASNTRL	Ves a 1	Lipase	LYYSTAASSL	HA	B/Colorado/2017, B/Phuket/2013	H-2-K^d	688	568
Nr. 5	SYTNGPQEI	Gly m 6	Cupin	KYTSGRQEK	PB2	A/Brisbane/2018, A/Kansas/2017	H-2-K^d	2527	248

4.3 RSV-induced inflammation in mice peaks between 4 and 12 dpi and is cleared upon 35 dpi

In order to further investigate the immunogenic and cross-reactive potential of the candidate pairs from RSV A2 in virus-infected animals, a suitable mouse model of RSV infection needed to be established. The model should show signs of acute viral infection, leading to a memory T cell response, but not resulting in a chronic disease. We thus infected mice with $1x10^6$ pfu RSV A2 and performed a time course to investigate the phases of acute viral infection and memory response.

Replication of the virus could be proven by detection of the replicative strand in qPCR of lung homogenates and calculating observed numbers of molecules of the viral N gene per mg of lung based on a standard curve (3.9.4). The virus replicated until 4 dpi, further decreased and was not detectable anymore after 8 dpi (Figure 13 A). RSV-specific IgG production started at 6 dpi and could be detected until 35 dpi in serum of infected mice. (Figure 13 B).

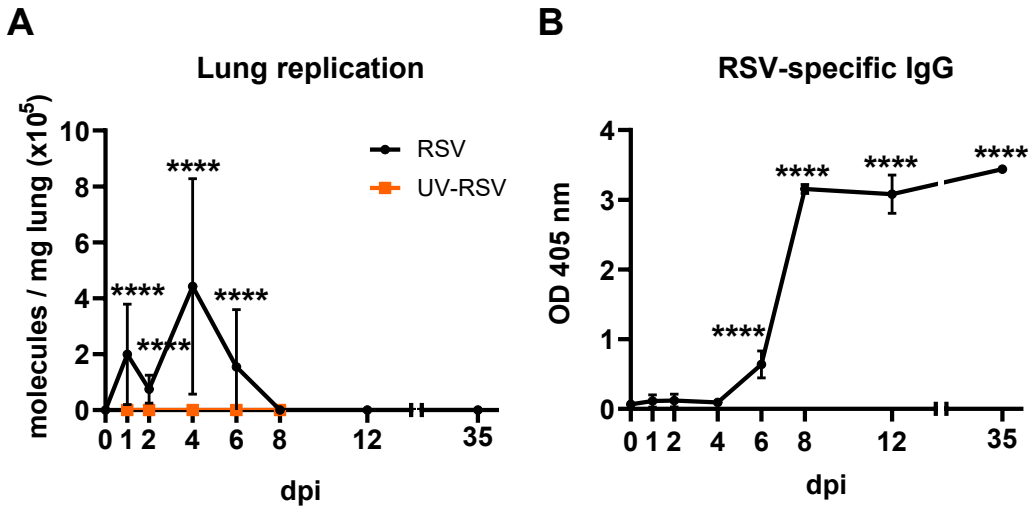

Figure 13: RSV A2 replicates in the lung until 4 dpi and induces virus-specific IgG response
Mice were infected with 1x10⁶ pfu RSV A2 and sacrificed at the indicated timepoints. Control mice were treated similarly with UV-inactivated virus and sacrificed at 1, 2, 4, 6 and 8 dpi. **A:** Detection of the replicative virus strain of N gene by qPCR. Molecules per mg lung were calculated based on a standard curve **B**: Measurement of RSV-specific IgG response by ELISA; n=3-10, Values are shown as mean ± SD, One-Way ANOVA vs 0 dpi; * p≤ 0,05, **** p≤0,0001, OD=optical density, dpi=days post infection, RSV=Respiratory syncytial virus

Airway inflammation was investigated in BAL cytospins (Figure 14 A) and started at 1 dpi with an early neutrophilic influx and increasing lymphocytes at 2 dpi and peaked between 6 and 12 dpi with elevated total BAL cells, lymphocytes and a second neutrophilic peak. Macrophages were not affected upon virus infection. In parallel with increasing numbers of leucocytes, inflammatory cytokines, especially IFNγ, were elevated and peaked at 6 dpi (Figure 14 B). At 35 dpi, airway inflammation reached a comparable level to 0 dpi, indicating that the infection has been cleared.

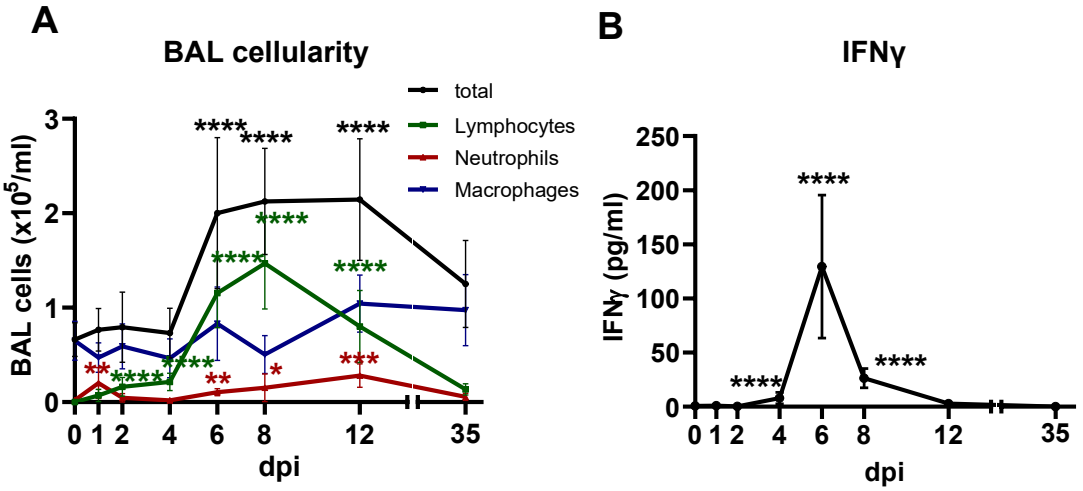

Figure 14: Airway inflammation peaks between 6 and 12 days after RSV A2 infection
Mice were infected with 1x10⁶ pfu RSV A2 or similarly treated with UV-inactivated virus and sacrificed at the indicated timepoints **A:** BAL cellularity **B:** Measurement of IFNγ in ELISA; n=3-10, Values are shown as mean

± SD, One-Way ANOVA vs 0 dpi; * p≤0,05, ** p≤0,01, *** p≤0,001, **** p≤0,0001, dpi=days post infection, BAL=bronchoalveolar lavage, IFN=Interferon

Furthermore, not only humoral response, but also T cell response could be shown upon viral infection. $CD4^+$/ $CD8^+$ ratio in the lung significantly decreased after 4 dpi and remained so until 12 dpi, in parallel with detection of activated $CD8^+$ $CD69^+$ T cells by means of flow cytometry (data not shown). Long-lasting $CD4^+$ and $CD8^+$ T effector memory cells were observed in the lung by flow cytometry (Figure 15 A). RSV-specific $CD8^+$ T cells were detected in the lung and mediastinal lymph nodes of infected animals by means of pentamer staining with the known MHC class I RSV T cell epitope $M2_{82\text{-}90}$, mainly in the effector phase at 12 dpi, but remained detectable until 35 dpi in the lung (Figure 15 B).

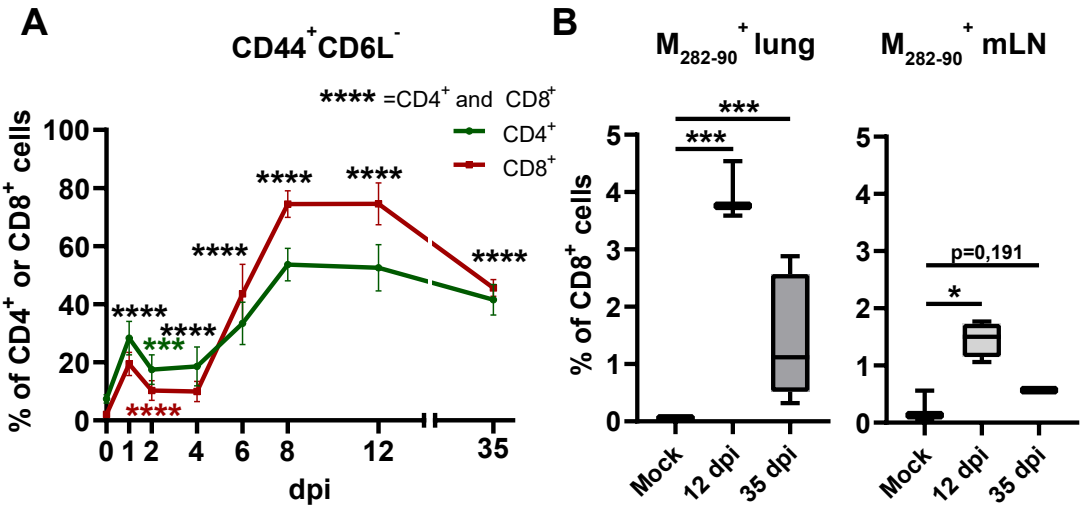

Figure 15: Virus infection induces long lasting T effector memory response in the lung as well as virus-specific T cells in lung and mediastinal lymph nodes
Mice were infected with $1x10^6$ pfu RSV A2 and sacrificed at the indicated timepoints **A:** Flow cytometry analysis of T effector memory cells in the lung **B:** Flow cytometry analysis of RSV-specific pentamer staining in lung and lymph nodes; n=3-5, Values are shown as mean ± SD, One-Way ANOVA vs 0 dpi or mock; * p≤0,05, *** p≤0,001, **** p≤0,0001, OD=optical density, dpi=days post infection, mLN=mediastinal lymph node

Lung inflammation was also investigated on the level of histology. Lung sections were stained for H&E for detection of inflammatory cells and virus presence was shown in parallel by means of immunofluorescence staining. Infiltrating inflammatory cells in the lung were observed at 1 dpi and increased until 6 dpi. Quantification of lung inflammation in H&E staining of the lung sections pointed out a similar degree of inflammation at 4 and 6 dpi, indicating a peak at this timepoint (Figure 16 A+B). Further timepoints were not quantified but no inflammatory cells were observed anymore in lung sections of 35 dpi. Additionally, virus presence could be

shown at 1 dpi in the airway epithelium and spread in the lung parenchyma between 2 and 6 dpi; 4 dpi is shown as an example in Figure 16 A.

In summary, RSV A2 infection resulted in increased inflammation in the BAL and lung, which mainly peaked between 4 and 12 dpi. At 35 dpi, the virus was cleared by the animals. Most importantly, long lasting virus-specific T cell response and generation of T_{EM}´s was induced.

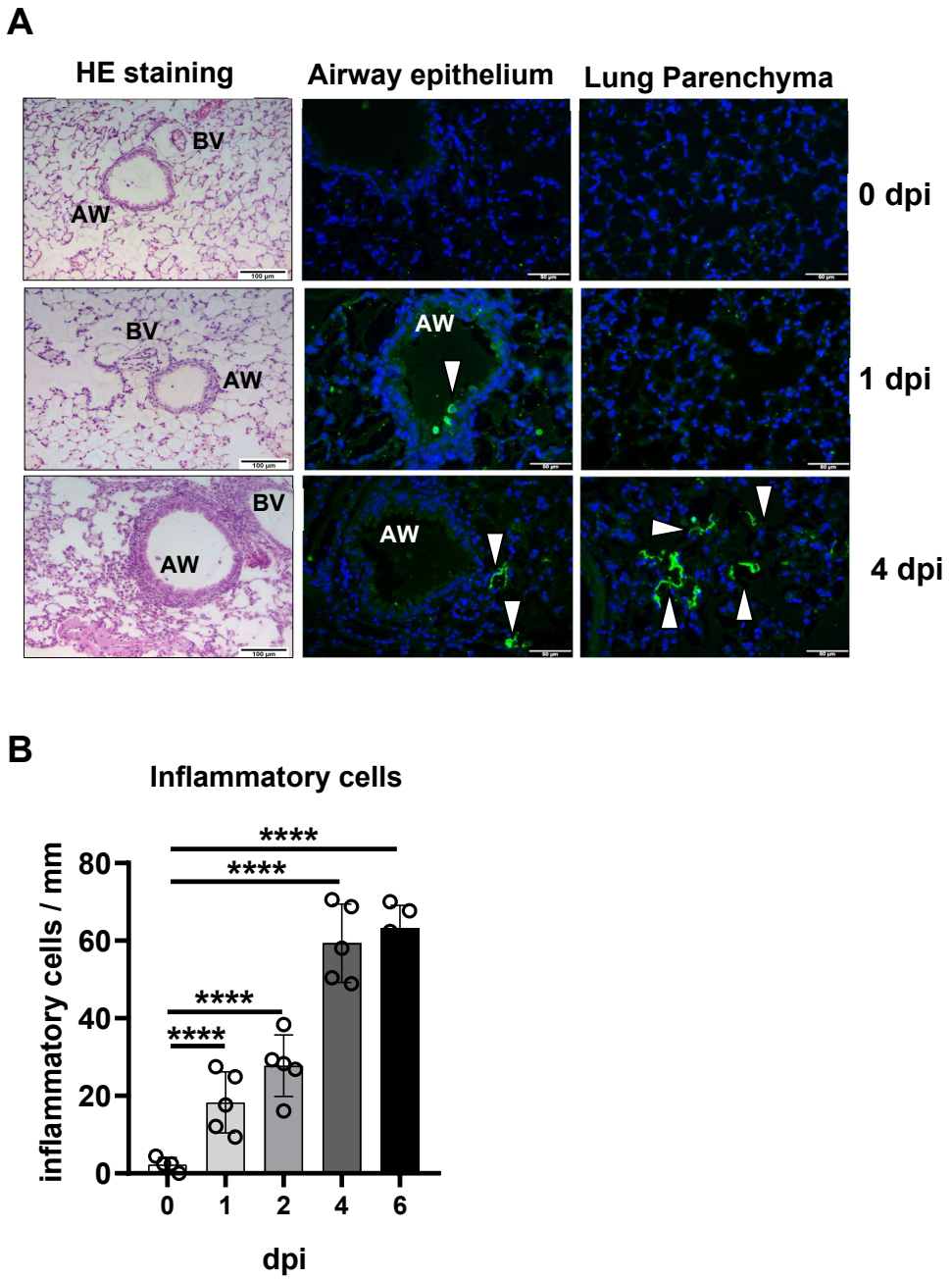

Figure 16: Lung inflammation can be observed in parallel with presence of RSV A2 in lung histology sections

Mice were infected with 1x10^6 pfu RSV A2 and sacrificed at the indicated timepoints **A:** H&E staining of lung histology sections and immunofluorescence staining of RSV (green) and DAPI staining for nuclei detection (blue). Arrow indicate virus presence. H&E staining: 200 x magnification, Immunofluorescence: 400 x magnification **B:** Lung inflammation scoring; n=3-5, Values are shown as mean ± SD, One-Way ANOVA vs 0dpi; **** p≤0,0001, dpi=days post infection, AW=airway, BV=blood vessel

4.4 Cross-reactivity between predicted RSV A2- and allergen-derived epitopes following viral infection and virus peptide immunization

4.4.1 *Ex-vivo* stimulation of splenocytes and lung cell homogenates with the predicted allergen peptides results in enhanced $CD8^+$ T cell response following RSV infection

Based on the aforementioned RSV A2 infection time course, 12 dpi was chosen as a timepoint for investigation of the effector phase and 35 dpi for investigation of the memory phase. Thus, assessing immunogenicity of the predicted virus peptides as well as cross-reactivity of the allergen counterparts at these timepoints after RSV A2 infection were performed next. Peptides that were positively tested *in-vitro* were used to create a pool of either virus-or allergen-derived peptides from the RSV A2 analysis (Table 23). *Ex-vivo* stimulation of lung cells of RSV-infected mice at 12 dpi resulted in a significant increase in $CD8^+$ $CD69^+$ activation as well as IFNγ-producing $CD8^+$ T cells compared to control stimulation with HBV_{28-39} and mock treated mice as determined by flow cytometry (Figure 17 A+B). Most importantly, this was observed with both the virus-and allergen peptide pool. Stimulation with UV-inactivated virus was used as positive control, inducing also activated- and IFNγ-producing $CD8^+$ T cells (Figure 17 C+D). At 35 dpi, activated $CD8^+$ $CD69^+$ T cells of splenocytes, but not lung cells (data not shown), remained elevated upon stimulation with the virus peptide pool, but not with the allergen peptide stimulation (Figure 18 A). Intracellular IFNγ was significantly increased in $CD8^+$ T cells when stimulated with the virus peptide pool compared to stimulation with HBV_{28-39} and mock animals (Figure 18 B). Importantly, allergen peptide stimulation also induced significantly elevated $CD8^+$ $IFN\gamma^+$ T cell response (Figure 18 B) compared to HBV_{28-39} stimulation and mock animals. Control stimulation with UV-inactivated virus significantly increased activation ($CD69^+$) and $IFN\gamma^+$ production in $CD8^+$ T cells compared to the negative control and mock animals (Figure 18 C+D).

Conclusively, immunogenicity of the predicted virus peptides and cross-reactive T cell response with the allergen peptides was shown at 12 dpi and 35 dpi, respectively.

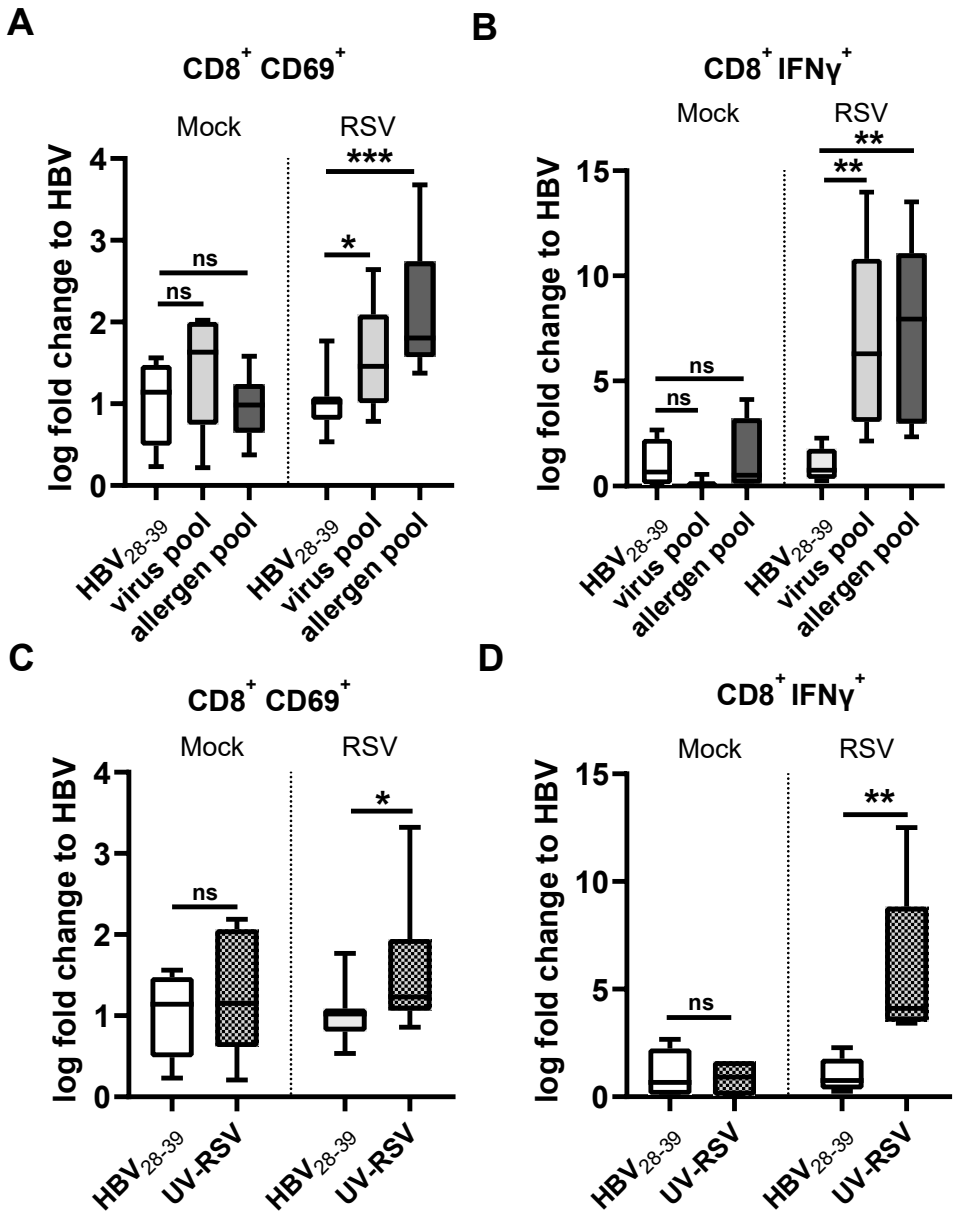

Figure 17: Enhanced CD8+ T cell activation and cytokine production upon *ex-vivo* stimuation with the predicted virus-and allergen derived peptides of RSV A2 primed lung cells at 12 dpi
Mice were infected with 1x10^6 pfu RSV A2 or mock infected and sacrificed at 12 dpi. Lung homogenates were used for *ex-vivo* stimulation with pools of the predicted virus-and allergen peptides or control antigens. **A, C:** Activation (CD69+) was measured after 24 h by flow cytometry. **B, D:** Intracellular IFNγ was measured after 24 h by flow cytometry; n=3-5, Values are shown as mean ± SD, A+B One-Way ANOVA vs HBV, C+D unpaired t-test; * p≤0,05, ** p≤0,01, *** p≤0,001, ns=not significant; RSV=respiratory syncytial virus, HBV=Hepatis B Virus

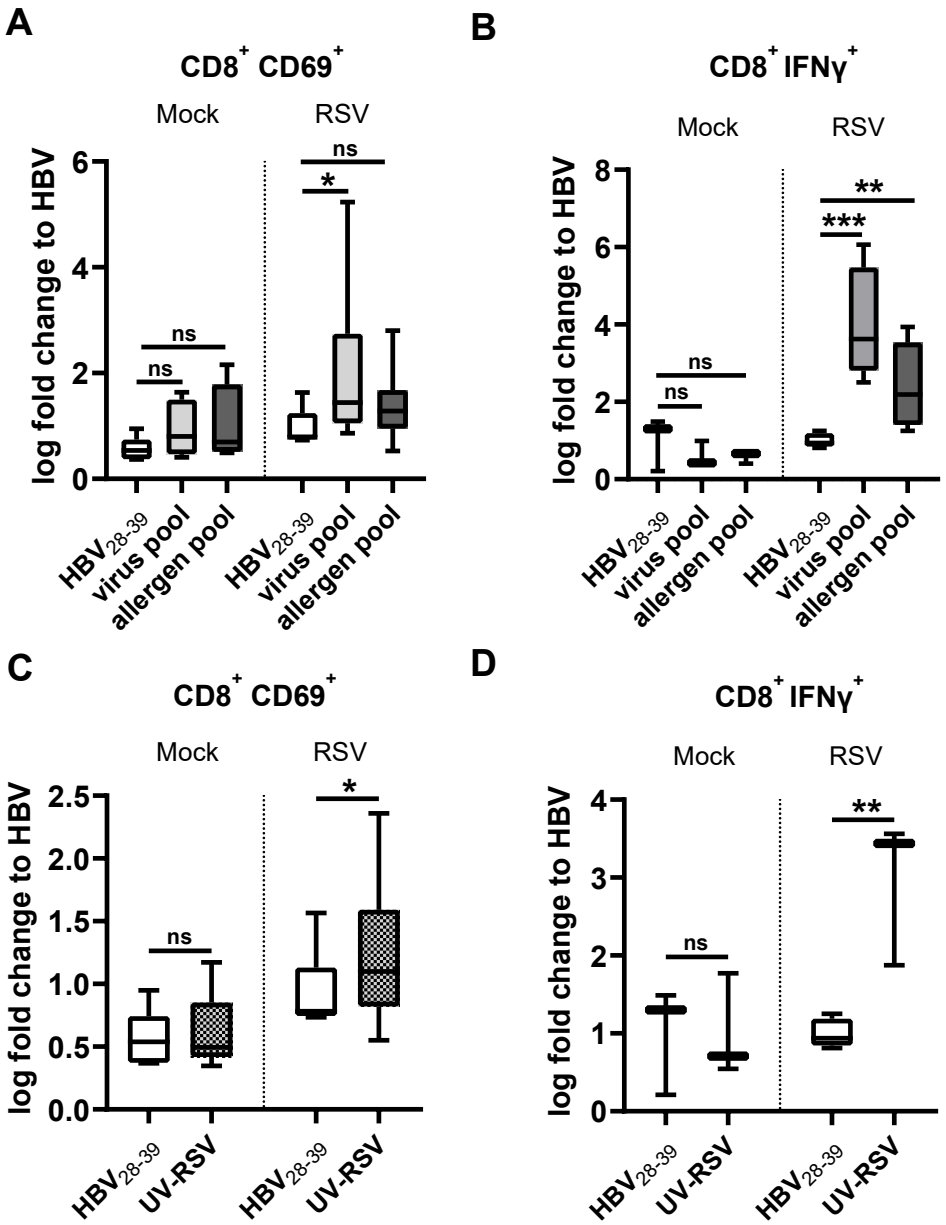

Figure 18: CD8+ T cells produce more intracellular cytokines upon *ex-vivo* stimulation with the predicted allergen peptide pool in RSV-primed splenocytes at 35 dpi
Mice were infected with 1x10^6 pfu RSV A2 or mock infected and sacrificed at 35 dpi. Spleen cells were used for *ex-vivo* stimulation with pools of the predicted virus-and allergen peptides or control antigens. **A, C:** Activation (CD69+) was measured after 24 h by flow cytometry. **B, D:** Intracellular IFNγ was measured after 24 h by flow cytometry; n=3-5, Values are shown as mean ± SD, A+B One-Way ANOVA vs HBV, C+D unpaired t-test; * p≤0,05, ** p≤0,01, ns=not significant, RSV=respiratory syncytial virus, HBV=Hepatis B Virus

4.4.2 Long-lasting virus- and allergen- double positive CD8+ memory T cells in the lung

Based on the *ex-vivo* peptide stimulation results described before (4.4.1) and the hypothesized importance of *Aspergillus fumigatus*, the predicted candidate epitope pair RSV A2 L$_{356-364}$ FYNSMLNNI/*Asp f* 4$_{192-200}$ WYGNSALTI was chosen for dual pentamer staining. Fluorescence labelled epitope-specific MHC class I pentamers were

produced, using two different fluorochromes for further discrimination. Virus, but also allergen-specific CD8+ T cells with an effector memory phenotype (CD44+ CD62L-) were detected in the lung already at the effector phase at 12 dpi and were still present at 35 dpi compared to mock animals. Most importantly, double positive cells for both epitopes could be identified at 12 dpi and remained elevated until 35 dpi (Figure 19).

Thus, although the T cells were primed for RSV, they were able to recognize allergen-specific peptides and furthermore, were also demonstrated to be double positive for virus- and allergen peptides.

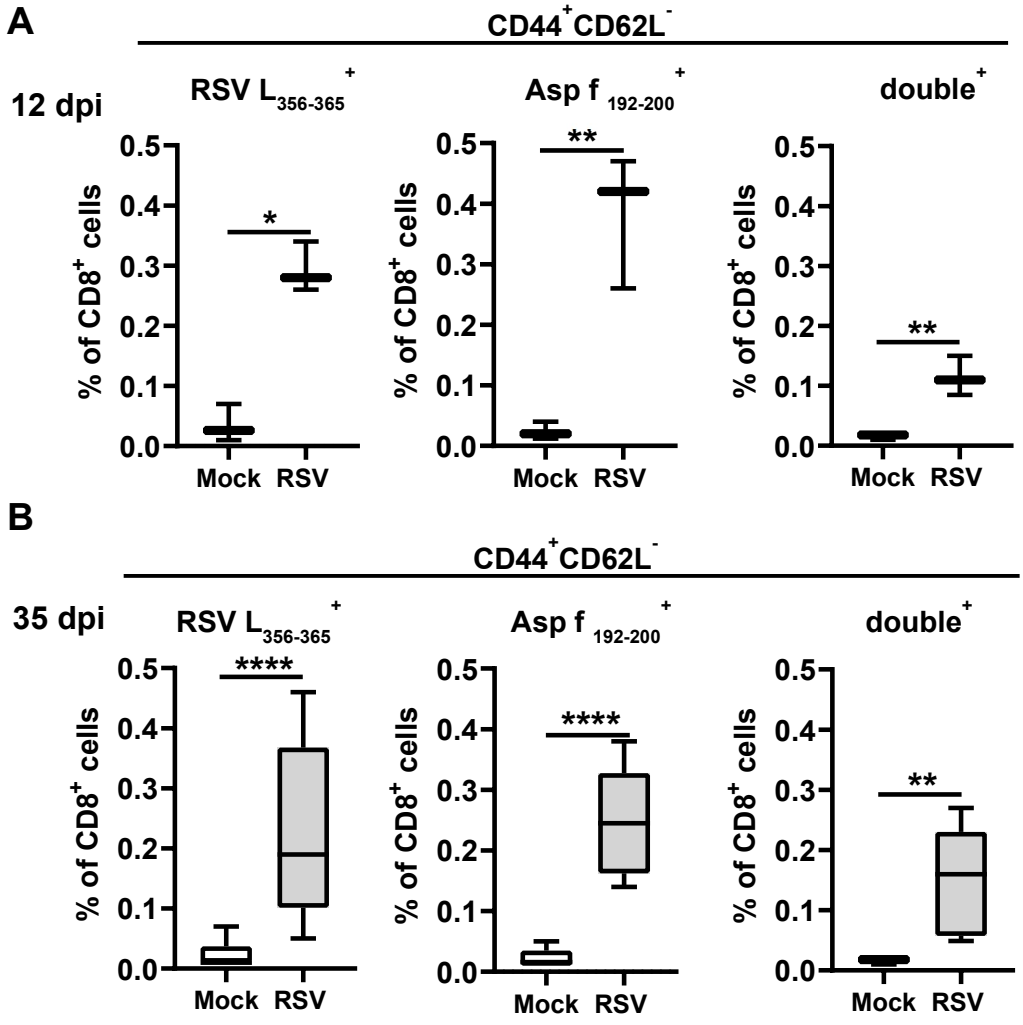

Figure 19: Dual pentamer staining of RSV-primed lung cells demonstrate long- lasting virus-and allergen specific CD8+ T cells

Mice were infected with 1x10^6 pfu RSV A2 or mock infected and sacrificed at 12 and 35 dpi. Lung cell homogenates were used for dual pentamer staining and flow cytometry analysis. **A:** Relative abundance of epitope specific CD8+ CD44+ C62L- T effector memory cells T cells at 12 dpi **B:** Relative abundance of epitope specific CD8+ CD44+ C62L- T effector memory cells T cells at 35 dpi; n=3-5, Values are shown as mean ± SD, unpaired t -test; * p≤0,05, ** p≤0,01, **** p≤0,0001; RSV=respiratory syncytial virus, dpi=days post infection

4.4.3 Cross-reactive T cell response to *Asp f*-derived epitopes in virus-peptide immunized mice

Aiming on further specifying the observed T cell response in RSV-infected animals, mice were immunized with a pool of virus peptides that were only predicted to cross-react with the *Asp f*-derived allergens (Table 14). These were selected based on the frequency of *Asp f*-derived candidates in the pool of peptides tested after RSV A2 infection, as well as the dual pentamer results, suggesting an important role for *Asp f* in cross-reactivity with RSV A2. *Ex-vivo* stimulation with the virus peptide pool resulted in increased activation (Figure 20 A), cytokine production (IFNγ and TNFα) (Figure 20 B, C) and proliferation (Figure 20 D) of $CD8^+$ T cells in spleen compared to control stimulation with HBV_{28-39}, confirming immunogenicity and successful immunization. However, stimulation of mock animals also led to increased activation. Importantly, significant increase of activation and proliferation was observed when stimulating with the *Asp f*-derived peptide pool compared to HBV_{28-39} (Figure 20 A, D). No response in mock animals was observed with this peptide pool. No altered abundance of cytokine producing T cells could be shown. Based on these results, *Aspergillus fumigatus* was chosen to be used as allergen in further *in-vivo* experiments to investigate a potentially protective effect of RSV A2 towards *Asp f*-induced experimental asthma.

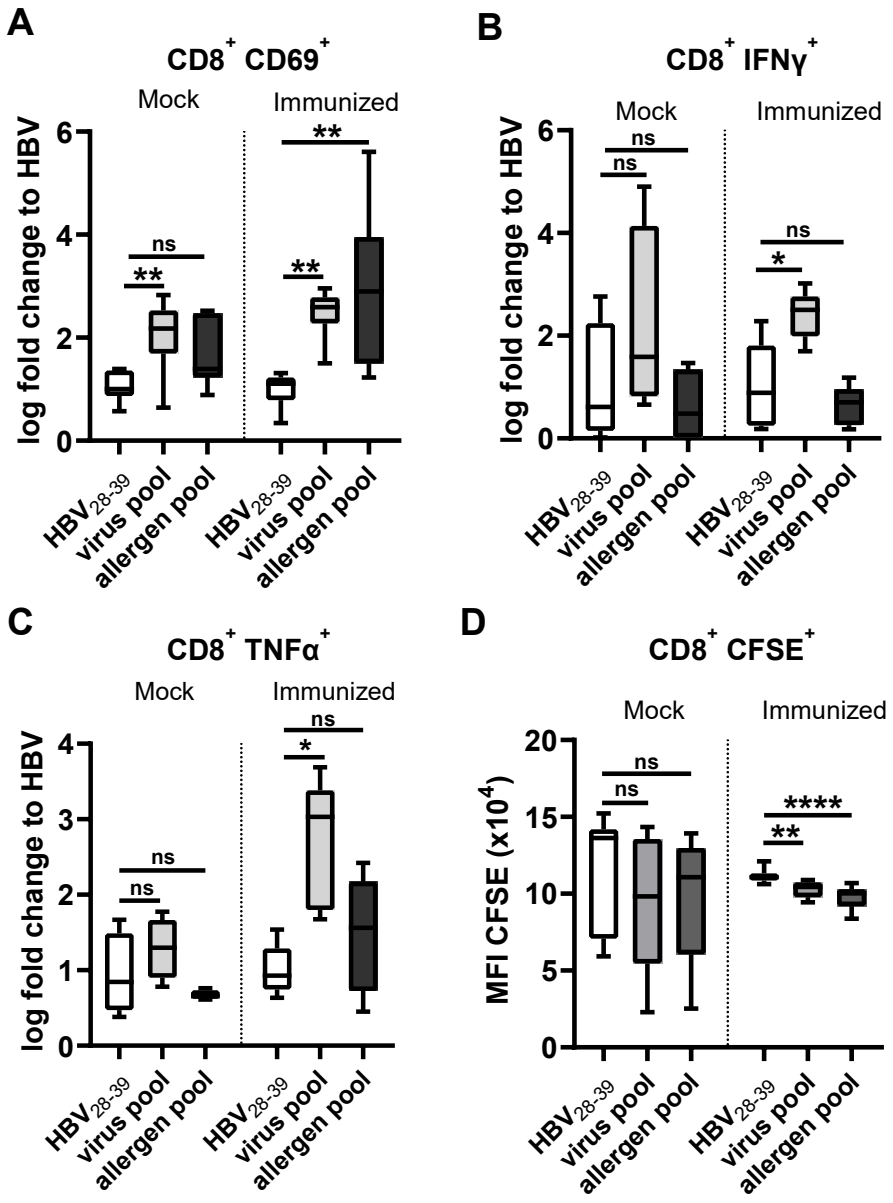

Figure 20: Predicted *Asp f*- derived peptides induce cross-reactive T cell response
Mice were immunized with a pool of the virus-derived peptides (Table 14) and spleen cells were stimulated *ex-vivo* with pools of the predicted virus-or allergen peptides, as well as control antigens. **A-C:** Activation ($CD69^+$) and intracellular cytokines of $CD8^+$ T cells were measured after 24 h stimulation by flow cytometry **D:** Proliferation (CFSE) of $CD8^+$ T cells was detected after 6 days stimulation by flow cytometry; n=4-6, Values are shown as mean ± SD, One-Way ANOVA vs HBV; * p≤0,05, ** p≤0,01, **** p≤0,0001, HBV=Hepatis B Virus, CFSE= Carboxyfluorescein succinimidyl ester

4.5 Prior RSV A2 infection attenuates T2 response in mice subjected to *Asp f*-induced experimental asthma

Cross-reactivity of the predicted RSV A2 and *Asp f*-derived peptides has been shown in the previous experiments. Thus, a potential protective effect of RSV A2 infection towards development of *Asp f*-induced experimental asthma was investigated in this experiment. Mice were infected with RSV A2 or mock infected and underwent an

Asp f-induced experimental asthma protocol or treated with control solution (Figure 21A). The asthma protocol was established during this thesis based on a protocol of Haczku et al. (Haczku et al., 2001). Allergen treatment started 35 dpi based on the RSV infection time course (4.3), choosing a timepoint where the infection has already been cleared but memory T cell response and virus-specific T cells are still available. Successful RSV infection was proven by means of immunoglobulin ELISA in serum of the mice (Figure 21 B). RSV-specific IgG could be detected in the groups with RSV A2 infection.

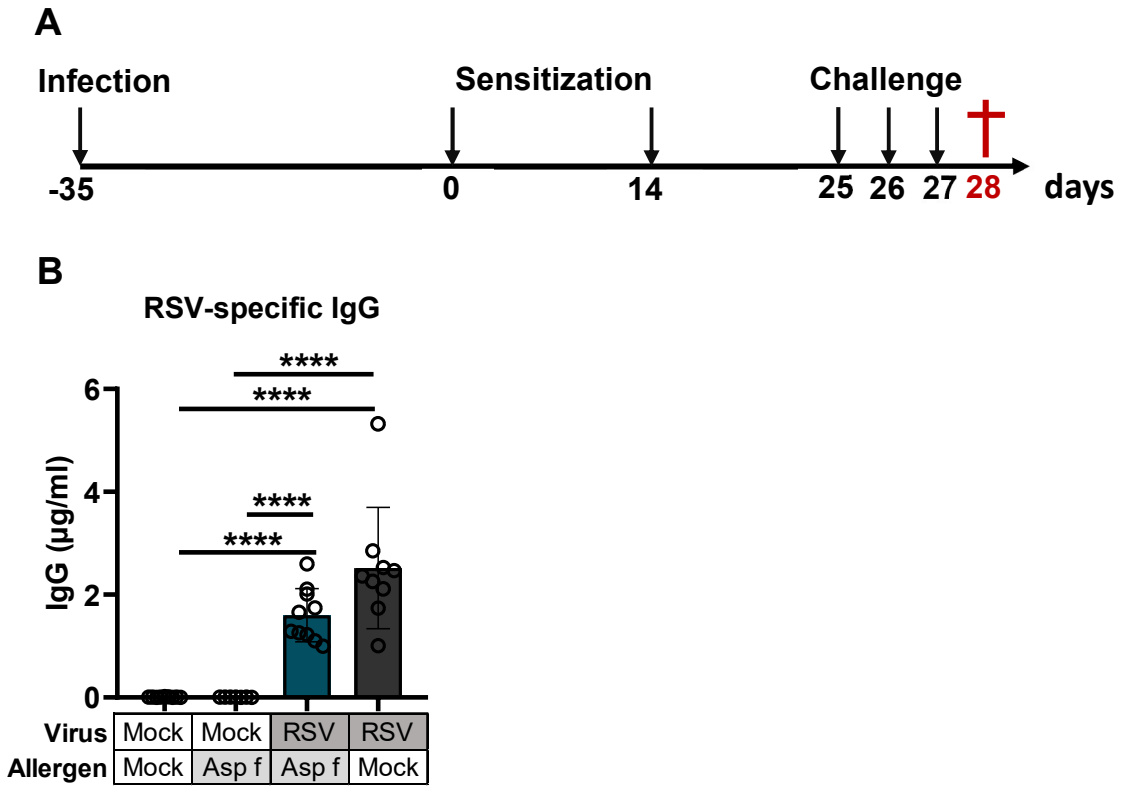

Figure 21: Experimental set-up and detection of immunoglobulins
Mice were infected with RSV A2 and subjected to an *Asp f*- induced experimental asthma protocol. **A:** Schematic experimental set-up **B**: Measurement of RSV-specific IgG levels by ELISA; n=8-10, Values are shown as mean ± SD, One-Way ANOVA multiple comparisons; **** p≤0,0001, RSV= respiratory syncytial virus, Asp f=*Aspergillus fumigatus*

Airway inflammation was investigated in BAL cytospins (Figure 22). *Asp f*-treatment induced increased numbers of total BAL cells, as well as lymphocytes, neutrophils and eosinophils compared to mock animals. While no difference was observed in numbers of total leucocytes in the BAL between the *Asp f*-treated mice with and without prior RSV A2 infection, eosinophils were significantly decreased in mice with prior infection compared to allergen treated animals only. Additionally, more

macrophages were observed in RSV/*Asp f* mice compared to Mock/*Asp f* animals, whereas the numbers of neutrophils were not affected.

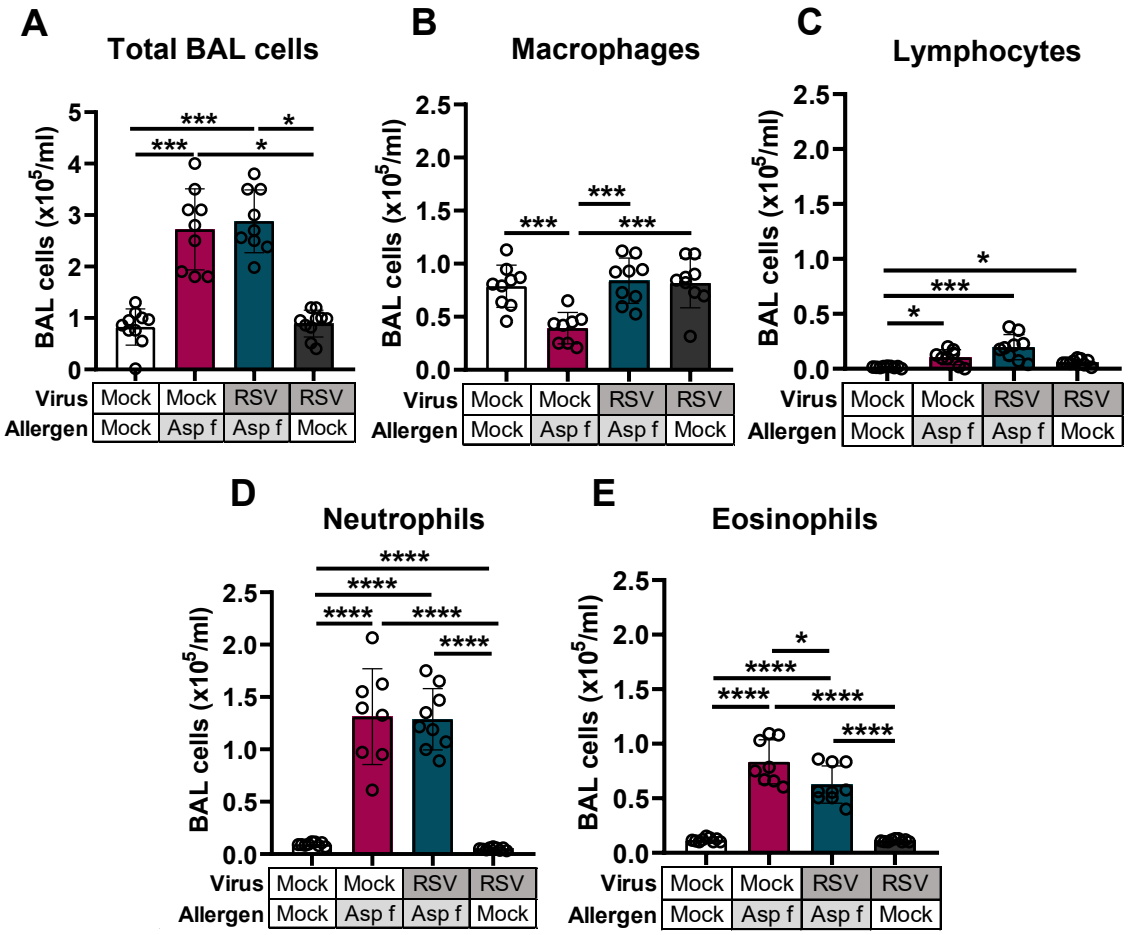

Figure 22: RSV A2 infection reduces eosinophilic response in BAL of *Asp f*- treated mice
Mice were infected with RSV A2 and subjected to an *Asp f*- induced experimental asthma protocol **A:** Cell count of total BAL cells **B-E:** Differential cell counting of BAL cell subsets; n=8-10, Values are shown as mean ± SD, One-Way ANOVA multiple comparisons; * p≤0,05, *** p≤0,001, **** p≤0,0001, RSV= respiratory syncytial virus, Asp f=*Aspergillus fumigatus*, BAL=bronchoalveolar lavage

Measurement of cytokines in BAL supernatant confirmed increased levels of the T2 cytokines IL-5 and IL-13 in mice that were subjected to the *Asp f*-induced experimental asthma protocol compared to mock animals. Upon prior RSV infection, significantly less levels of IL-13 could be detected compared to Mock/*Asp f* animals (Figure 23 B). Additionally, TNFα was significantly decreased in RSV/*Asp f* mice compared to Mock/*Asp f* animals (Figure 23 C).

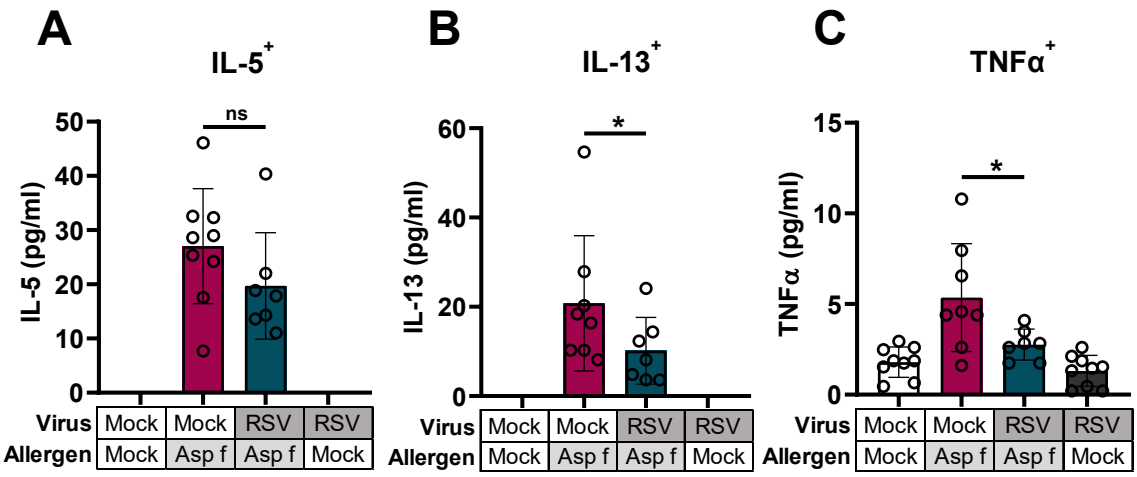

Figure 23: Cytokines are reduced in BAL supernatant of *Asp f*- treated mice upon RSV A2 infection
Mice were infected with RSV A2 and subjected to an *Asp f*- induced experimental asthma protocol. Cytokines were measured in BAL supernatant by CBA. Values for IL-5 and IL-13 in the control groups were out of range. Thus, t-test was performed for all cytokines comparing only Mock/*Asp f* and RSV/*Asp f* groups. n=7-10, Values are shown as mean ± SD, * p≤0,05, RSV= respiratory syncytial virus, Asp f=*Aspergillus fumigatus*

Next, different immune cell subsets and cytokine producing T cells were investigated in the lung. For this purpose, flow cytometry staining was used to analyze different markers in lung cell homogenates. Contrary to the BAL cell composition, abundance of neutrophils, but not eosinophils, was decreased in RSV/*Asp f* mice compared to Mock/*Asp f* mice (p=0,075) (Figure 24 E, F). No differences in the relative abundance of macrophages, dendritic cells or natural killer cells (NK cells) could be observed between the aforementioned groups (Figure 24 B-D). B cells showed an increasing trend in RSV/*Asp f* mice compared to Mock/*Asp f* mice (p=0,088) (Figure 24 A). The ratio of $CD4^+/CD8^+$ T cells increased in the *Asp f* groups, but no changes were observed after prior RSV A2 infection (data not shown).

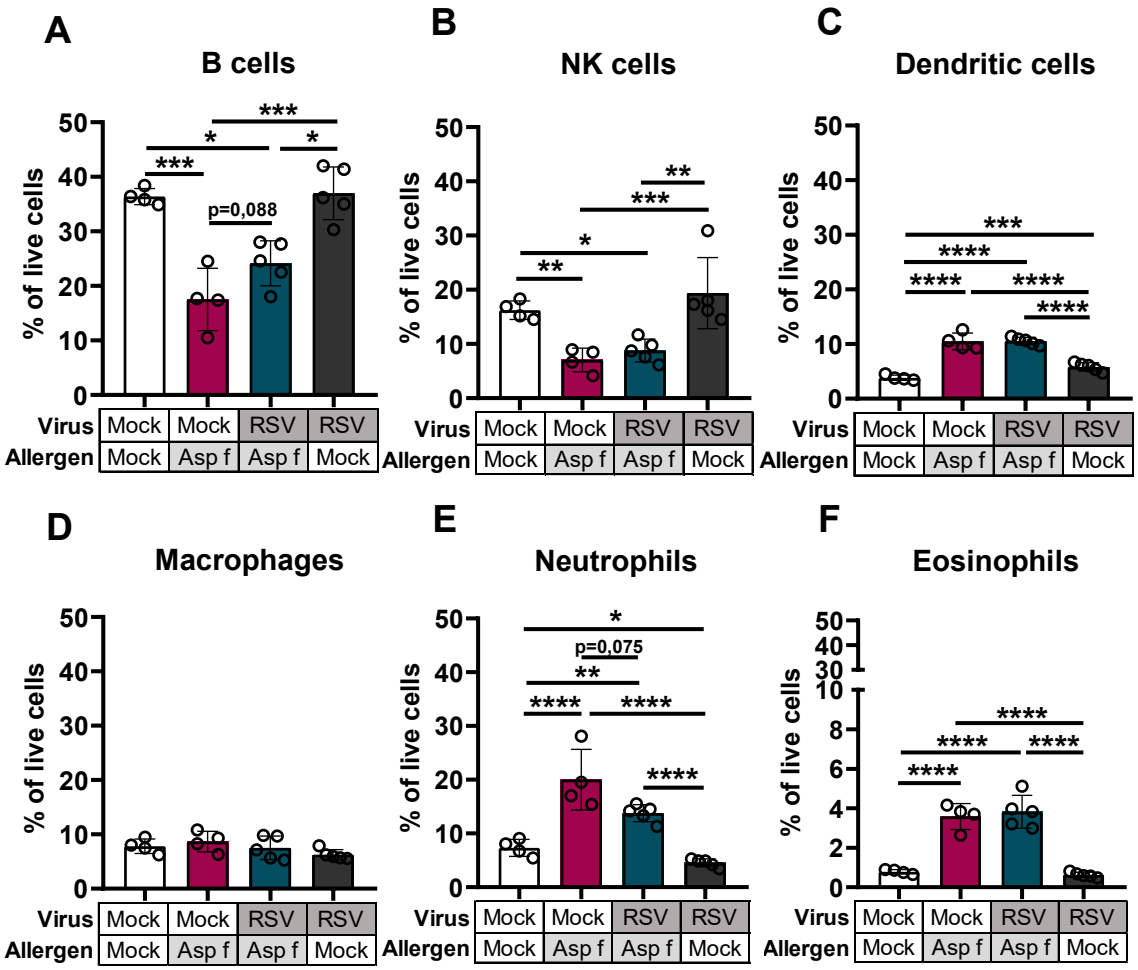

Figure 24: Immune cell composition in *Asp f*- treated mice is altered upon a prior RSV A2 infection
Mice were infected with RSV A2 and subjected to an *Asp f*- induced experimental asthma protocol. Lung cell homogenates were stained with different phenotypic markers for important immune cells subsets. Measurement by flow cytometry; Cells were defined as following **A:** B cells $B220^+$, **B:** NK cells $B220^-$ $CD27^+$, **C:** Dendritic cells $B220^-$ $CD27^-$ $CD11b^+$ $CD11c^+$ **D:** Macrophages $B220^-$ $CD27^-$ $CD11b^+$ $CD11c^-$ $Ly6G^-$ $SiglecF^-$ **E:** Neutrophils $B220^-$ $CD27^-$ $CD11b^+$ $CD11c^-$ $Ly6G^+$ **F:** Eosinophils $B220^-$ $CD27^-$ $CD11b^+$ $CD11c^-$ $Ly6G^-$ Siglec F^+; n=4-5, Values are shown as mean ± SD, One-Way ANOVA multiple comparisons ;* p≤0,05, ** p≤0,01, *** p≤0,001, **** p≤0,0001, RSV= respiratory syncytial virus, Asp f=*Aspergillus fumigatus*, NK cells= natural killer cells

Intracellular cytokines were measured in T cells by flow cytometry (Figure 25). *Asp f*-treatment increased the T2 cytokines IL-5 and IL-13. Prior RSV A2 infection resulted in a trend for less IL-5^+ $CD8^+$ (p=0,071) T cells compared to allergen treated animals without prior infection. No significant difference in the abundance of T2-biased $CD4^+$ T cells was observed, whereas no intracellular IL-13 could be detected at all in $CD8^+$ T cells. TNFα was highly decreased in both *Asp f*-treated groups but revealed no difference after prior RSV A2 infection (data not shown).
Summarizing, RSV A2 infection reduced the T2 response in lung and BAL and led to immune cell composition that show a less allergic phenotype compared to animals without prior infection.

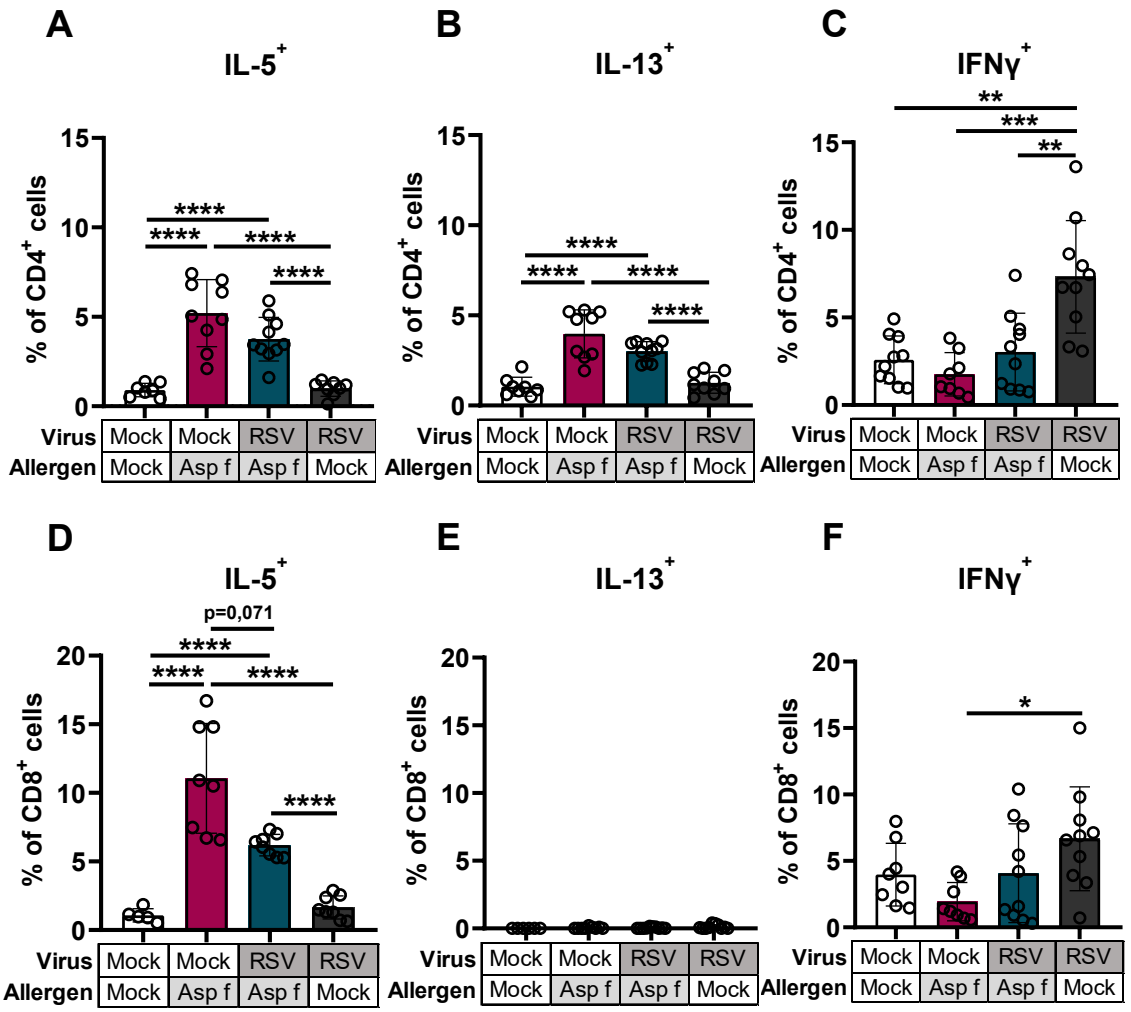

Figure 25: Reduced IL-5⁺ T cells in lung homogenates of RSV/*Asp f* mice
Mice were infected with RSV A2 and subjected to an *Asp f*-induced experimental asthma protocol. Lung cell homogenates were stained for intracellular cytokines in T cells and measured by flow cytometry. **A-C:** Intracellular cytokine detection in CD4⁺ T cells **D-F**: Intracellular cytokine detection in CD8⁺ T cells; n=8-10, Values are shown as mean ± SD, One-Way ANOVA multiple comparisons; * p≤0,05, ** p≤0,01, *** p≤0,001, **** p≤0,0001, RSV=respiratory syncytial virus, Asp f=*Aspergillus fumigatus*

Further, lung histology sections were investigated for inflammatory cells with H&E staining, as well as mucus-producing goblet cells with PAS staining. Representative pictures of each group are shown in Figure 26 A. Numbers of inflammatory cells between airways and blood vessels were quantified and PAS⁺ cells within an airway were scored (Figure 26 B, C). No inflammation was observed in Mock/Mock or RSV/Mock control groups. Inflammation around the airways and presence of goblet cells were shown in allergic asthmatic mice. Of note, significantly less inflammation and PAS⁺ cells were detected in *Asp f*-treated mice with prior RSV A2 infection compared to Mock/*Asp f* mice.

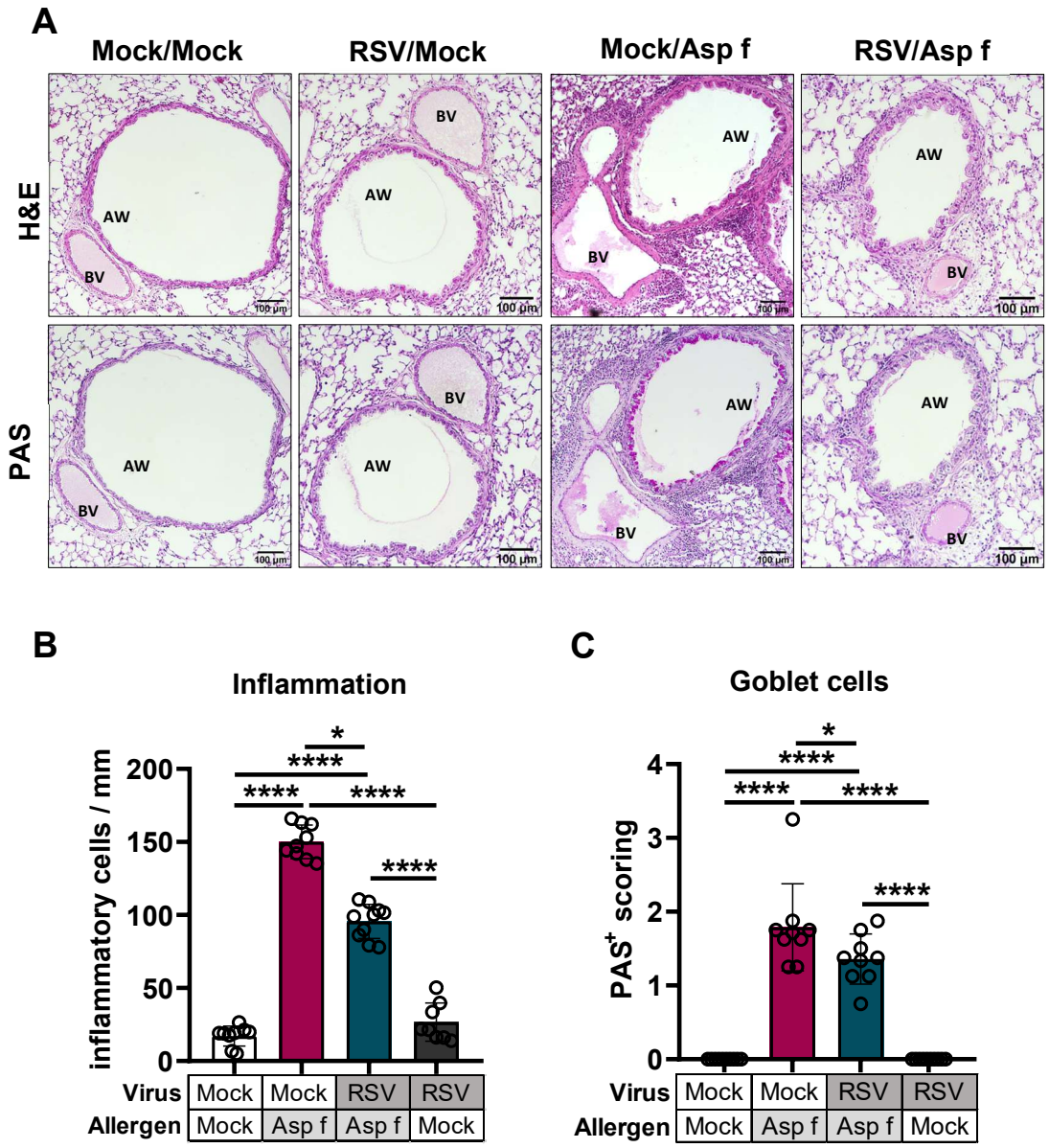

Figure 26: Lung inflammation and mucus production are reduced in RSV/*Asp f* mice
Mice were infected with RSV A2 and subjected to an *Asp f*-induced experimental asthma protocol. The left lobe of the lung was used for histological preparation and sections were stained for H&E and PAS staining. **A:** Representative pictures for each group for H&E (upper row) and PAS staining (lower row) **B:** Quantification of inflammatory cells between airway and blood vessel **C:** Scoring of PAS^+ cells within an airway; A minimum of 6 airways per animal were analyzed. n=8-10, Values are shown as mean ± SD, One-Way ANOVA multiple comparisons; * p≤0,05, *** p≤0,001, **** p≤0,0001, AW= airway, BV= blood vessel, RSV= respiratory syncytial virus, Asp f=*Aspergillus fumigatus*

4.5.1 Virome diversity and composition are altered in *Asp f*-induced experimental asthma

The results from the RSV/*Asp f* experiment in this thesis (4.5) showed an attenuated allergic inflammatory response of *Asp f*-induced experimental asthma when mice were previously infected with RSV A2. In addition to virus infections, commensal and non-pathological viruses are also thought to offer asthma protection. Thus, the role of airway virome composition in asthma development is currently intensively investigated (Choi et al., 2021). Therefore, the resident airway virome of *Asp f*-treated mice with and without prior RSV A2 infection were analyzed and a possible contribution of the virome in the observed asthma attenuation was investigated. Lung tissue and total BAL were used for sequencing and further analysis. When comparing the β-diversity (inter-community diversity) in the lung by means of Principal component Analysis (PCoA), control mice without experimental asthma grouped together and on the other hand, the *Asp f*-treated mice grouped together, showing a significant difference in virome diversity following allergen treatment. RSV infection did not seem to alter the virome diversity in lung at this late timepoint after initial infection. Samples of the BAL were more diverse and did not indicate such a clear grouping. However, a significant difference between RSV/Mock and Mock/*Asp f* was still observed. Interestingly, this difference was not observed in *Asp f* animals which were previously treated with RSV A2. Thus, *Asp f*-treatment altered the virome diversity in lung tissue and to a lower extent in BAL samples, but prior RSV infection did not influence the β-diversity of the virome in allergic asthmatic mice.

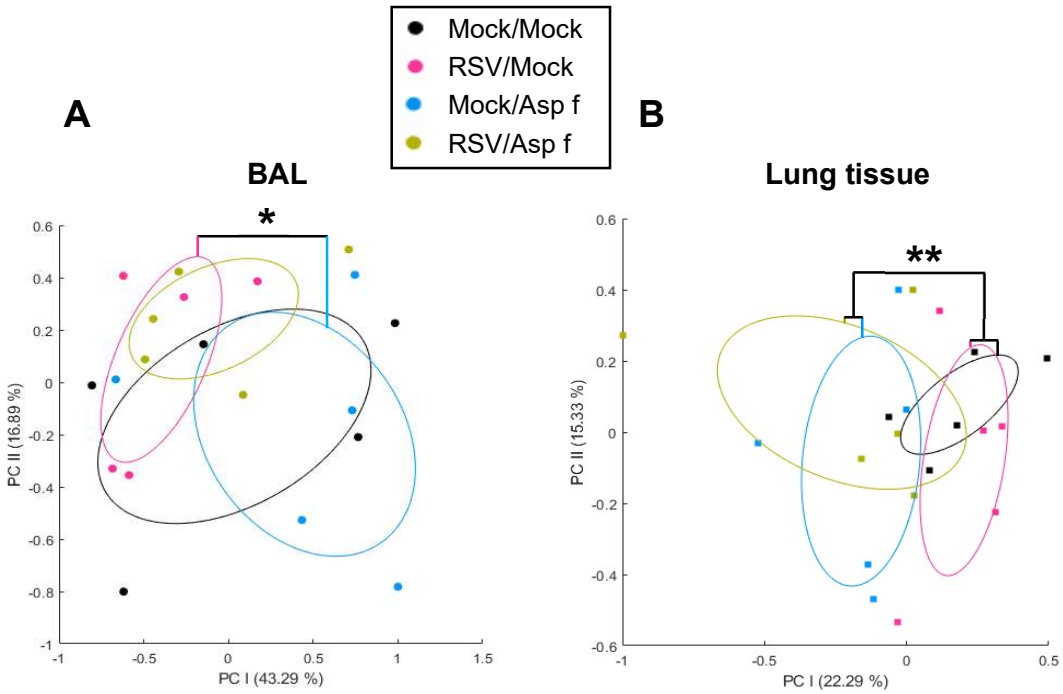

Figure 27: Principal Component Analysis (PCoA) reveals differences in lung tissue between asthmatic and non-asthmatic groups of animals
β diversity of the virome composition is represented in PCoA. **A:** BAL samples **B:** lung tissue; Significance was calculated using NPM ANOVA on the Bray-Curtis dissimilarity. * p≤0,05, ** p≤0,01; BAL=bronchoalvelolar lavage, RSV=respiratory syncytial virus, Asp f=*Aspergillus fumigatus*

As a next step, the intra-community diversity of each group (α-diversity) was measured by the Shannon Index (Figure 28). Interestingly, BAL samples revealed generally lower diversity in all groups when compared to lung tissue. No statistical difference could be observed between the different groups in BAL samples, although a trend of decreasing diversity in Mock/*Asp f* mice compared to control mice could be seen, whereas the index of diversity in mice with additional previous RSV infection is again on the same level as the control mice. In lung tissue, a clear difference with a p value of 0,051 was detected in control mice compared to asthma groups. This is in concordance with the results of the PCoA of β-diversity, showing an effect of allergen treatment on the virome. These results also confirm that RSV infection did not change virome diversity. Taken together, allergen treatment with *Asp f* altered the α- and β-diversity of the virome, mainly in lung tissue, whereas RSV infection was not observed to influence these parameters.

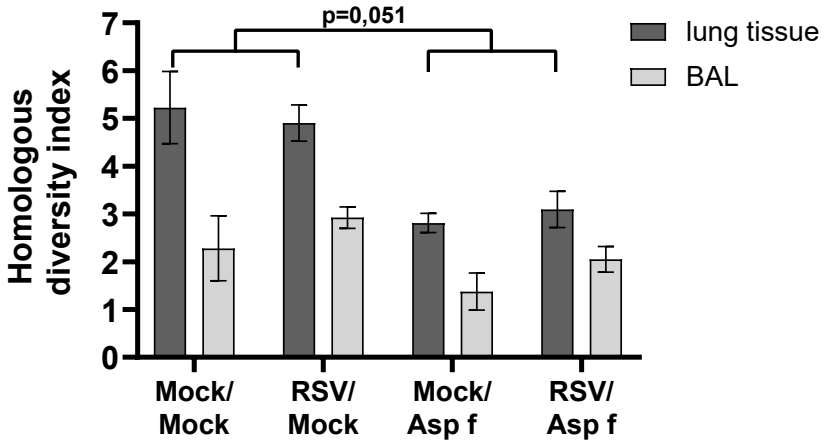

Figure 28: Lung samples contain higher virome diversity compared to BAL, which is reduced in asthmatic mice
Representation of the homologous virus diversity index (HVDI), which was measured by Shannon Index. Significance was calculated by a two-tailed t test. RSV=respiratory syncytial virus, Asp f=*Aspergillus fumigatus*, BAL=bronchoalveolar lavage

Virome composition was analyzed in more detail in order to specify the virus families which were responsible for the reduced diversity. Additionally, in spite of the non-changing diversity between the *Asp f*-groups, virome composition between the allergen groups with and without prior RSV infection might still be altered and was therefore investigated. The heatmap in Figure 29 A represents differences of the log-normalized abundance of all detected virus families in lung tissue, ranking the most abundant ones from top to bottom. *Herpesviridae* were found to be most abundant in all groups, followed by *Heunggongviridae*, several unclassified viruses, *Baculoviridae* and *Pararnavirdidae*. The overall reduction in diversity could be confirmed with this heatmap, indicating several virus families that were reduced in mice with *Asp f*-induced experimental asthma compared to mock animals. When quantifying the abundance of the viruses, significantly less *Shotokuvirae* and *Helvetiavirae* were found in *Asp f*-mice compared to the control mice, as well as a trend of reduced abundance of *Marseilleviridae* (Figure 23 B-D). No differences between RSV/*Asp f* mice compared to Mock/*Asp f* mice were observed, although a slight trend of increasing abundance of *Shotokuvirae* in RSV/*Asp f* mice compared to Mock/*Asp f* mice should be mentioned.

In line with the calculated diversity index, less virus families were detected in BAL samples compared to lung tissue when comparing abundance of single virus families (data not shown). However, some virus families displayed trends of reduced abundance upon *Asp f*-treatment compared to RSV/Mock mice, especially *Nudivirae*

(p=0,064). Differences between Mock/*Asp f* and RSV/*Asp f* groups were not observed. Thus, allergen treatment led to reduced virome diversity in lung tissue, specifically seen in the *Helvetiavirae*, *Shotokuvirae* and *Marseilleviridae* viral families.

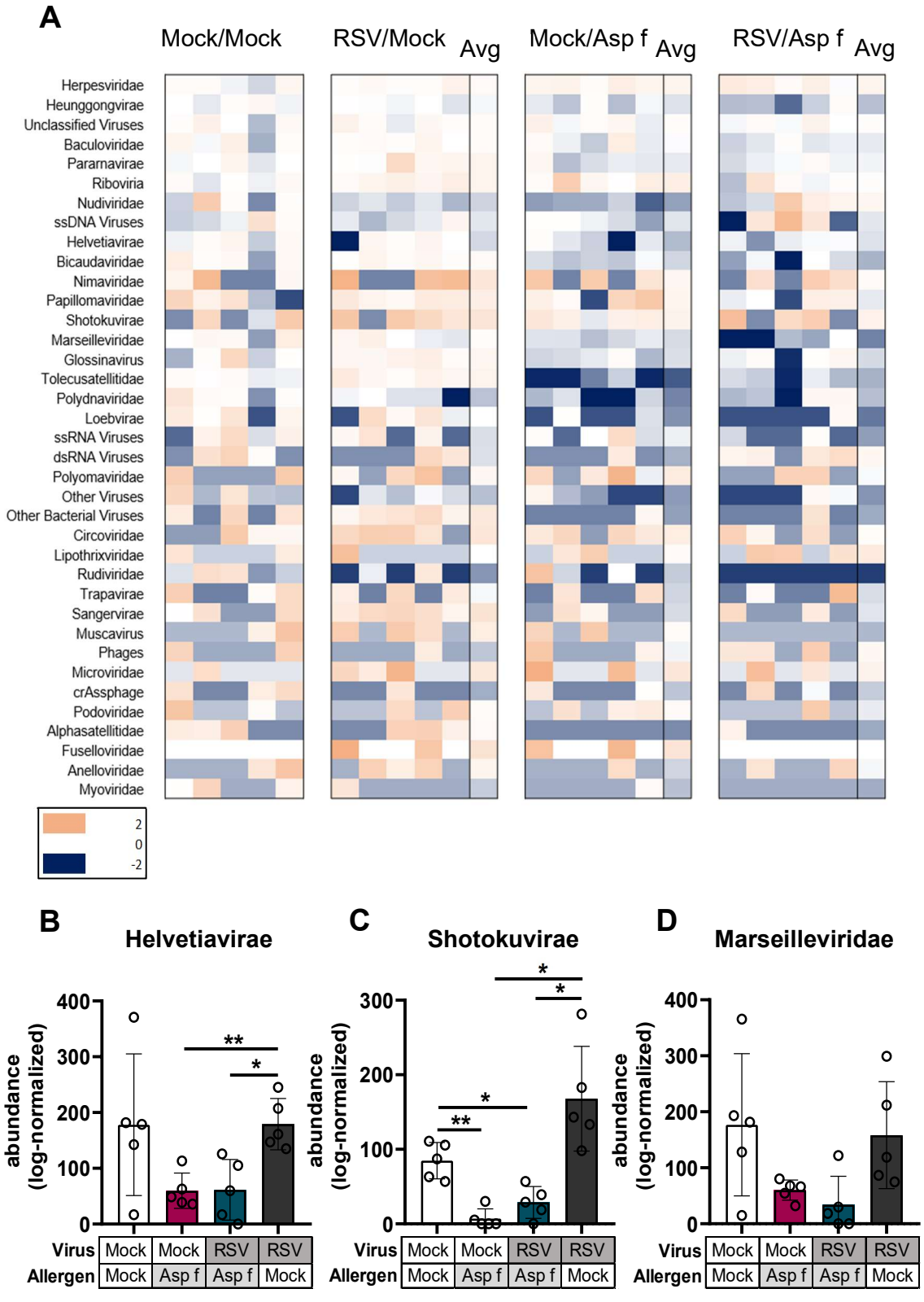

Figure 29: Virome composition is altered upon allergen treatment in lung tissue of mice

A: Heat map of the differences between each logarithm of viral family abundance minus the average of the 5 control samples (Mock/Mock). Avg columns describe the average of the 5 samples for the respective group minus the average of the respective Mock/Mock samples. **B-D:** Log-normalized abundance of indicated virus families. Statistics were calculated by Brown-Forsythe and Welch ANOVA test; Avg=Average, Asp f=*Aspergillus fumigatus*, RSV=respiratory syncytial virus

4.6 Predicted cross-reactive T cell epitopes are partly responsible for virus-mediated attenuation of *Asp f*-induced experimental asthma

RSV infection attenuated different hallmarks of asthma in the *Asp f*-induced experimental asthma model, including reduction of eosinophils in the BAL, less T2 cytokines in the BAL and lung, as well as significantly less inflammation and mucus production in lung histology (4.5). Next, the previously identified cross-reactive virus-derived peptides (Table 14) were used in combination with the *Asp f*-induced asthma protocol (Figure 30 A). With this experiment, the contribution of these cross-reactive peptides towards attenuation of asthma should be investigated.

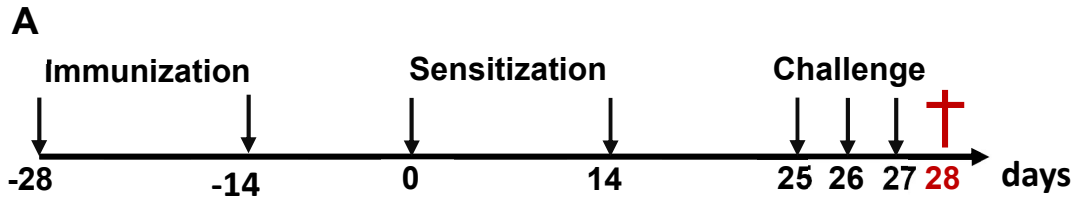

Figure 30: Experimental set-up
Mice were immunized with a pool of RSV A2 derived peptides (Table 14) before subjecting to the *Asp f*-induced experimental asthma protocol. Schematic representation of the experimental set-up.

BAL cells were investigated in cytospins. Numbers of eosinophils in the BAL were significantly reduced in mice that were treated with the virus peptide pool (VPP) before subjecting to the asthma protocol, compared to mice only treated with *Asp f* (Figure 31 E). Neither differences in macrophages, lymphocytes, neutrophils nor in total BAL cell numbers were detected between Mock/*Asp f* and VPP/*Asp f* mice (Figure 31 A-D).

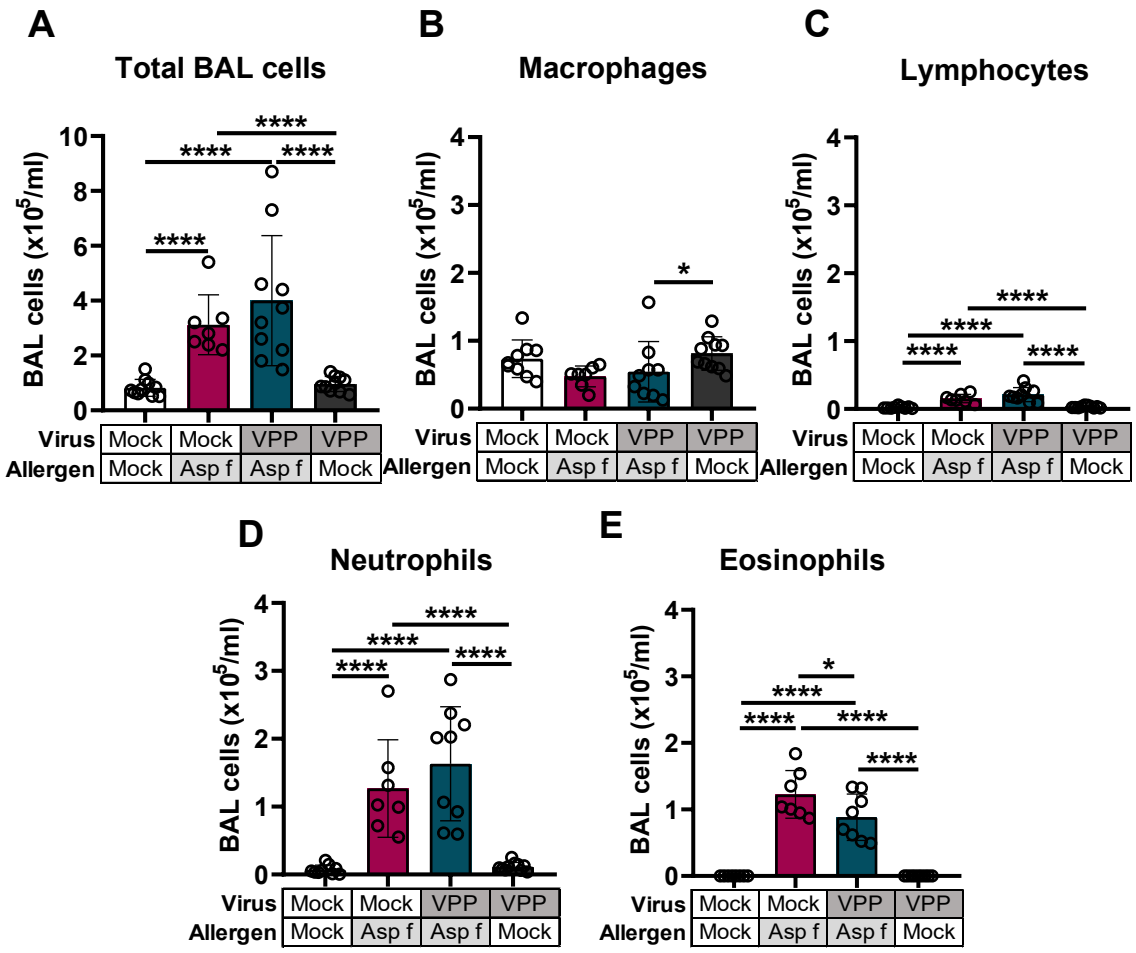

Figure 31: Virus peptide immunization reduces numbers of eosinophils in the BAL of *Asp f*-treated mice
Mice were immunized with a pool of RSV A2 derived peptides (Table 14) before subjecting to the *Asp f*-induced experimental asthma protocol. **A:** Cell count of total BAL cells **B-E:** Differential cell counting of BAL cell subsets; n=6-10, Values are shown as mean ± SD, One-Way ANOVA multiple comparisons; * p≤0,05, **** p≤0,0001, VPP=virus peptide pool, Asp f=*Aspergillus fumigatus*, BAL=Bronchoalveolar lavage

Next, immune cell subsets and cytokines in lung homogenates were measured by flow cytometry. With respect to *Asp f*-induced allergic airway inflammation (AAI), abundance of immune cells was in line with the previous experiment. Mainly, B cells and NK cells were significantly reduced, neutrophils and eosinophils were significantly increased compared to mock animals. However, no effect of a previous virus peptide immunization towards AAI could be detected in any cell subsets (Figure 32).

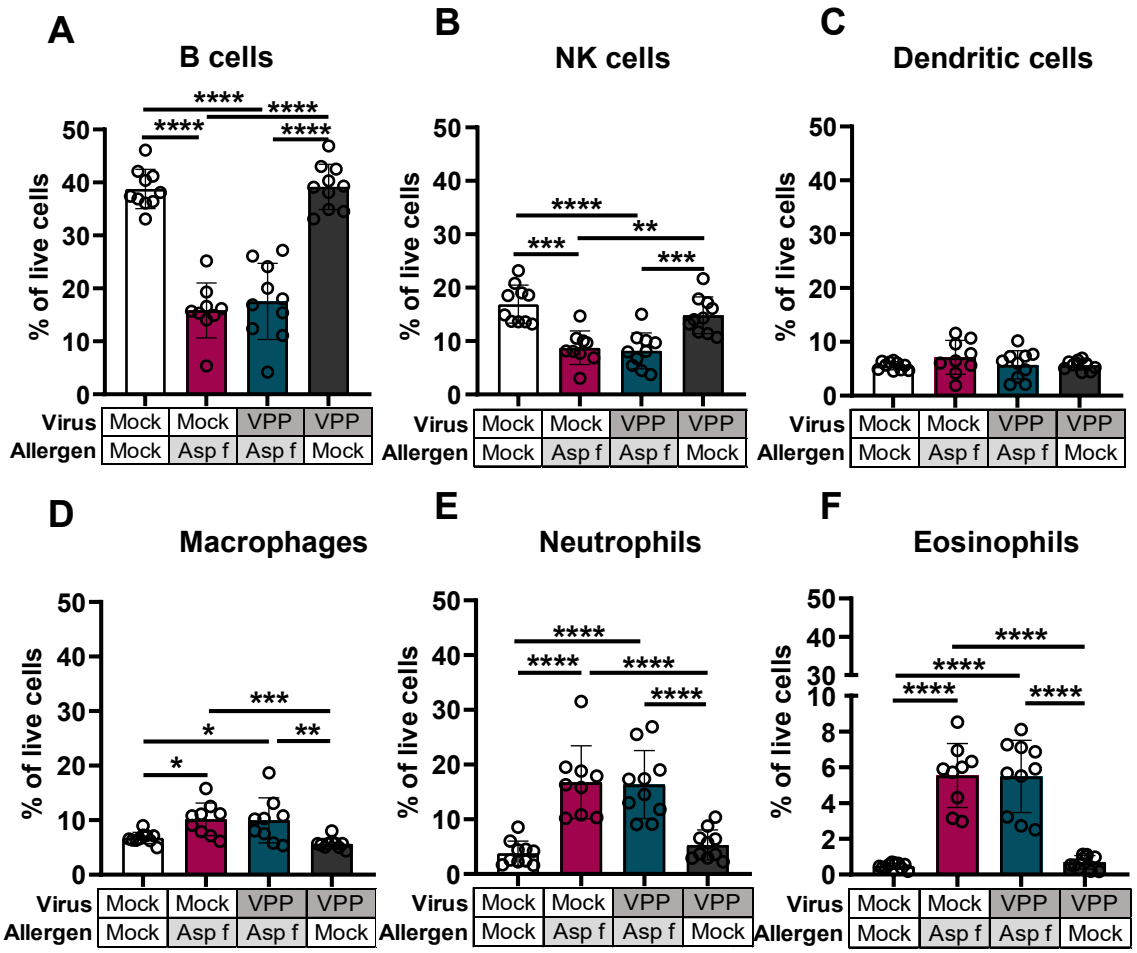

Figure 32: Immune cells in the lung are not affected by virus peptide immunization
Mice were immunized with a pool of RSV A2 derived peptides (Table 14) before subjecting to the *Asp f*- induced experimental asthma protocol. Lung cell homogenates were stained with different phenotypic markers for important immune cells subsets. Measurement by flow cytometry; Cells were defined as following: **A:** B cells B220$^+$, **B:** NK cells B220$^-$ CD27$^+$, **C:** Dendritic cells B220$^-$ CD27$^-$ CD11b$^+$ CD11c$^+$ **D:** Macrophages B220$^-$ CD27$^-$ CD11b$^+$ CD11c$^-$Ly6G$^-$SiglecF$^-$ **E:** Neutrophils B220$^-$ CD27$^-$ CD11b$^+$ CD11c$^-$ Ly6G$^+$ **F:** Eosinophils B220$^-$ CD27$^-$ CD11b$^+$CD11c$^-$ Ly6G$^-$ Siglec F$^+$; n=6-10, Values are shown as mean ± SD, One-Way ANOVA multiple comparisons; * p≤0,05, ** p≤0,01, *** p≤0,001, **** p≤0,0001, VPP=virus peptide pool, Asp f=*Aspergillus fumigatus*, NK cells=natural killer cells

When measuring intracellular cytokines in T cells of lung cell homogenates by flow cytometry, virus peptide immunization did not significantly affect intracellular T2 cytokines (IL-5 and IL-13) in CD4$^+$ and CD8$^+$ T cells of *Asp f*-treated mice compared to Mock/*Asp f* mice (Figure 33 A, B, D, E). However, a trend for reduced IL-5$^+$ CD8$^+$ Tcells (p=0,164) was observed in VPP/*Asp f* mice compared to Mock/*Asp f* mice. Importantly, IFNγ$^+$ CD8$^+$ T cells showed a trend for increase (p=0,058) when comparing the aforementioned groups (Figure 33 F).

Thus, virus peptides did not influence immune cell compositions in the lung but showed a trend for an increase of the T1 cytokine IFNγ and decreased abundance of IL-5$^+$ CD8$^+$ T cells compared to AAI mice without prior immunization.

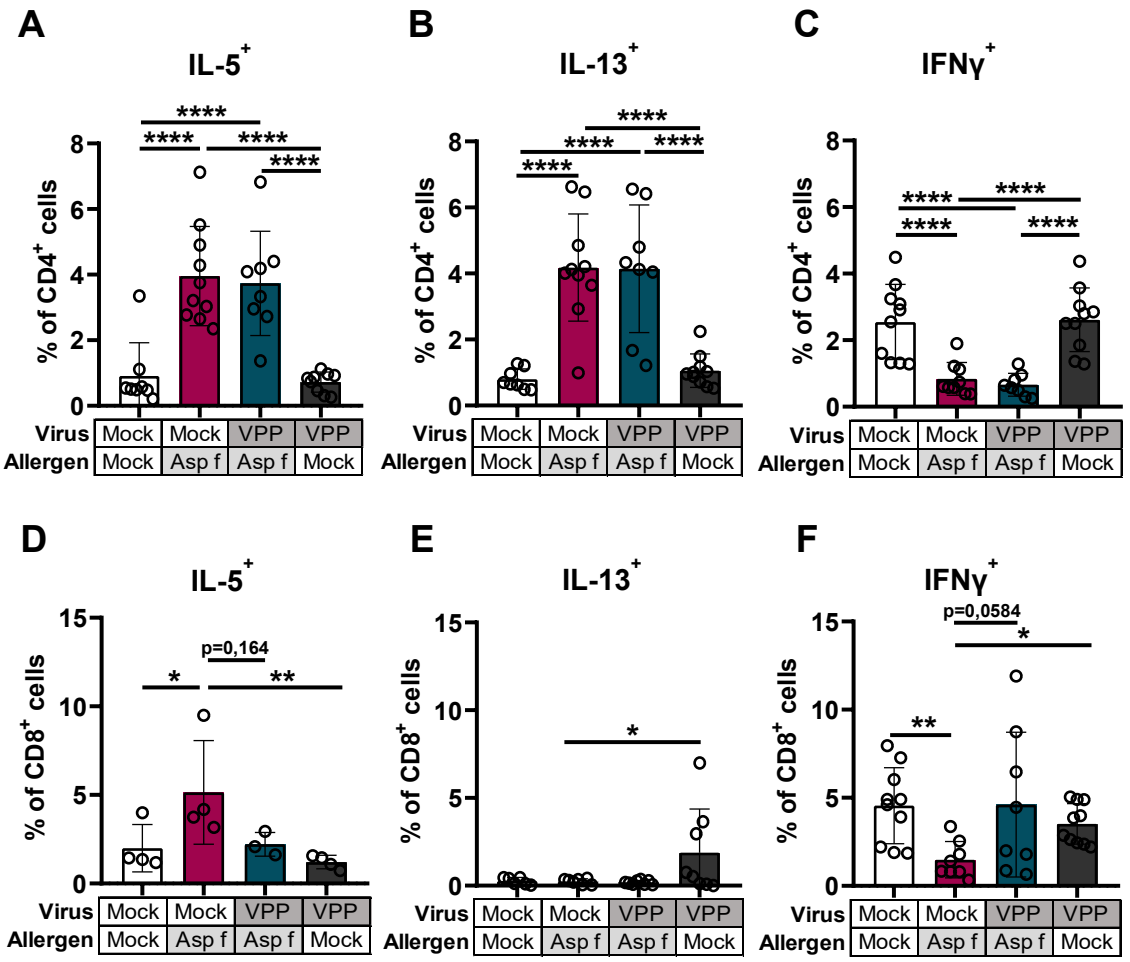

Figure 33: Virus peptide immunization increases intracellular IFNγ in CD8⁺ T cells
Mice were immunized with a pool of RSV A2 derived peptides (Table 14) before subjecting to the *Asp f*- induced experimental asthma protocol. Lung cell homogenates were stained for intracellular cytokines in T cells and measured by flow cytometry. **A-C:** Intracellular cytokine detection in CD4⁺ T cells **D-F**: Intracellular cytokine detection in CD8⁺ T cells; n=4-10, Values are shown as mean ± SD, One-Way ANOVA multiple comparisons; * p≤0,05, ** p≤0,01, **** p≤0,0001, VPP=virus peptide pool, Asp f=*Aspergillus fumigatus*

Inflammation and mucus-producing goblet cells were analyzed in lung histology sections. *Asp f*-treatment induced high inflammation and elevated numbers of goblet cell compared to control mice. In contrast to RSV infection, previous virus peptide immunization did not reduce any of these parameters in asthmatic mice (Figure 34), thus, not conferring a benefit for the mice.

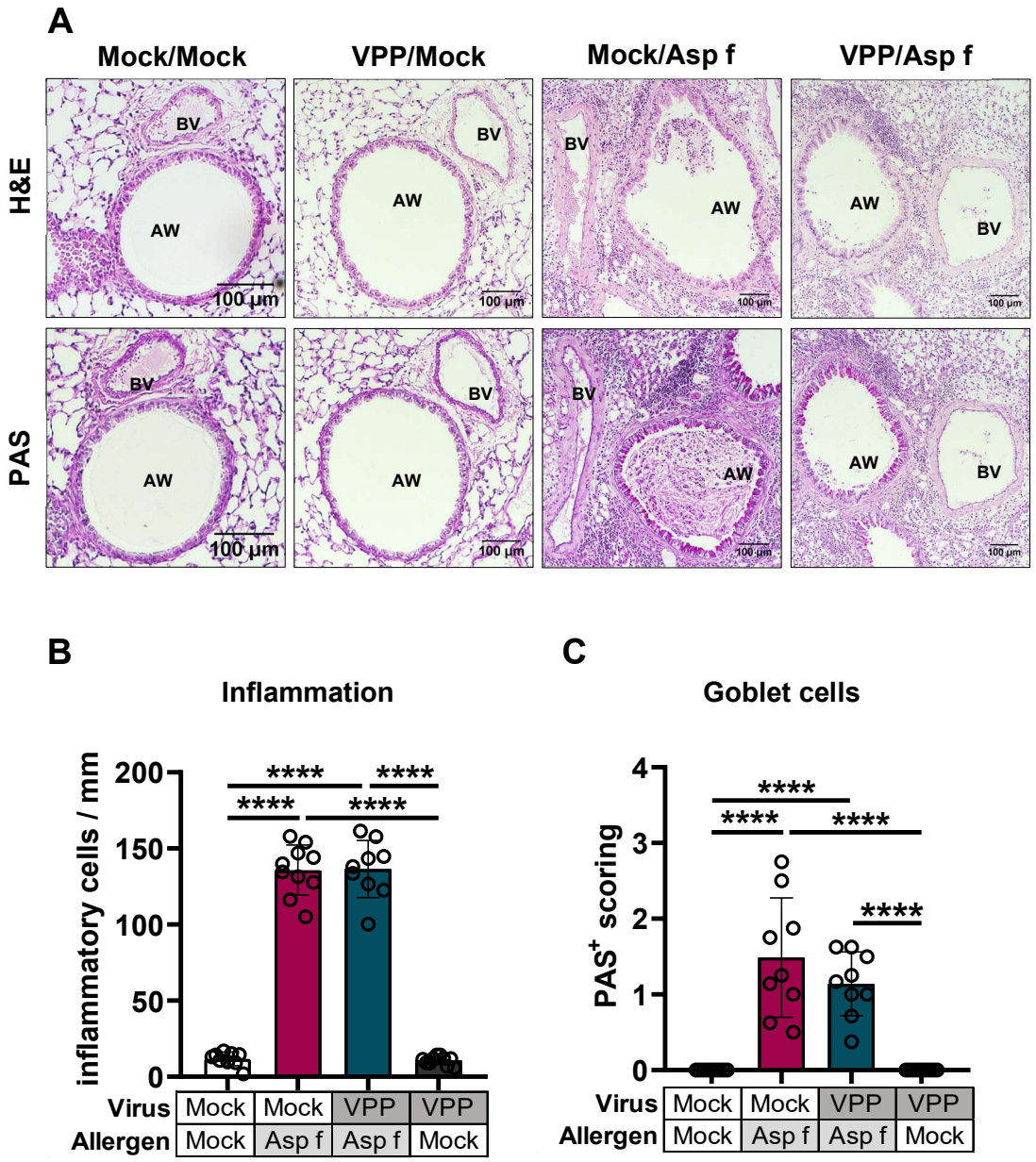

Figure 34: Lung histology is not altered in VPP/*Asp f* group compared to Mock/*Asp f*
Mice were immunized with a pool of RSV A2 derived peptides (Table 14) before subjecting to the *Asp f*-induced experimental asthma protocol. The left lobe of the lung was used for histological preparation and sections were stained for H&E and PAS staining. **A:** Representative pictures for each group for H&E (upper row) and PAS staining (lower row) **B:** Quantification of inflammatory cells between airway and blood vessel **C:** Scoring of PAS⁺ cells within an airway; A minimum of 6 airways per animal were analyzed. n=9-10, Values are shown as mean ± SD, One-Way ANOVA multiple comparisons; **** p≤0,0001, AW=airway, BV=blood vessel, VPP=virus peptide pool, Asp f=*Aspergillus fumigatus*

4.7 Beneficial heterologous immune response against allergens is also induced by prior influenza vaccination

It has been shown that an influenza A virus infection protected mice from subsequent development of experimental asthma in a murine model (Skevaki et al., 2018). Besides of investigating a potential protective effect of other RNA viruses, such as RSV A2, the observed effect of IAV should also be transferred into a more clinical context by using influenza vaccination instead of virus infection. Therefore, the *in-silico* analysis was performed with the influenza strains of the seasonal quadrivalent influenza vaccine (QIV) and candidate peptide pairs were tested *in-vitro*. Positive candidates were used for further *ex-vivo* stimulation assays and a potential protective effect of QIV immunization towards development of HDM-induced experimental asthma was investigated and is presented in the next sections.

4.7.1 Intraperitoneal vaccination of mice with the seasonal quadrivalent influenza vaccine induces B- and T cell response

Before the candidate peptide pairs could be evaluated in *ex-vivo* stimulation assays, a suitable mouse model of QIV immunization had to be established. Since the underlying hypothesis in this project is based on T cell epitopes and T cell-mediated heterologous immunity, it was important to be able to induce not only B cell response, but also T cell immunity in the mice, especially T_{EM} response. A mouse model of i.p. immunization once a week for three consecutive weeks was used (Figure 35 A). Mice were sacrificed 35 days after the last immunization in order to induce memory T cell response. QIV-specific IgG production was evident by means of ELISA measurement from serum of immunized mice compared to mock immunized mice (Figure 35 B). By means of pentamer staining with the known immunogenic influenza peptide $HA_{533-541}$, which was also confirmed to be included in the used vaccine, induction of long-lasting influenza-specific $CD8^+$ T cells in spleen and cervical lymph nodes were shown (Figure 35 C, D). Additionally, significant induction of $CD4^+$ (spleen) and $CD8^+$ (cervical lymph nodes) T effector memory cells ($CD44^+$ $CD62L^-$) were detected by flow cytometry analysis compared to mock animals (Figure 35 E, F). Intracellular cytokine staining of splenocytes revealed a reduction of IL-5^+ $CD8^+$ T cells, as well as

an increase of IFNγ⁺ CD4⁺ T cells in QIV immunized mice when comparing to mock-immunized animals (data not shown).

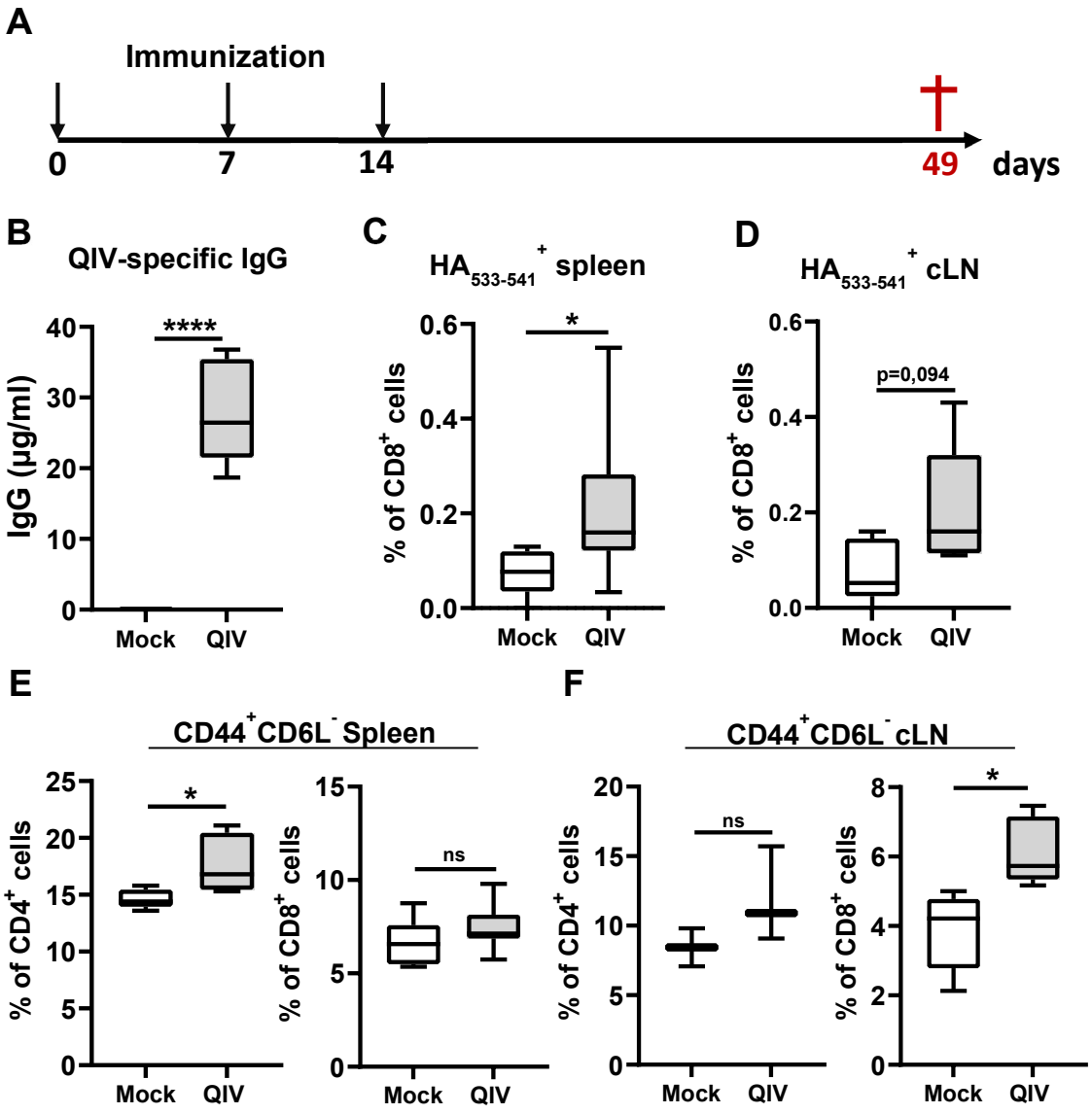

Figure 35: Immunization with QIV in mice induces T- and B cell response
Mice were immunized intraperitoneally with QIV or mock immunized with a control solution and sacrificed 35 days after the last treatment. **A:** Schematic representation of the experimental set-up **B:** Detection of IgG levels in serum by ELISA **C, D**: Measurement of IV-specific $HA_{533-541}$⁺ CD8⁺ T cells in spleen cells and cells of cervical lymph nodes by means of pentamer staining in flow cytometry **E, F:** Measurement of CD44⁺ CD62⁻ T effector memory cells in spleen and cervical lymph nodes by flow cytometry; n=5-10, Values are shown as mean ± SD, unpaired t test; * p≤0,05, **** p≤0,0001, ns=not significant, QIV=quadrivalent influenza vaccine, cLN=cervical lymph node

4.7.2 Predicted virus-and allergen derived T cell epitopes induce activation of CD8+ T cells upon *ex-vivo* stimulation of splenocytes from influenza-vaccinated mice

Immunogenicity of the predicted virus-derived peptides and cross-reactivity of the allergen derived peptides was investigated in an *ex-vivo* stimulation assay. For the generation of the peptide pools, all peptides that were positively tested *in-vitro* for MHC binding were used (Table 24). Immunogenicity of the virus peptides was confirmed by induction of CD8+ CD69+ activated T cells in splenocytes. Importantly, stimulation with the allergen peptide pool resulted in significantly increased activated CD8+ T cells compared to control stimulation with $HBV_{28-39,}$ which was not seen in mock animals (Figure 36 A). As positive controls, stimulation with the vaccine itself, as well as a commercially available peptide pool from influenza HA protein also induced CD8+ CD69+ T cells compared to control stimulation (Figure 36 B). Measurement of proliferation and intracellular cytokines did not point out additional T cell response towards the peptide pools (data not shown). Thus, immunogenicity and cross-reactivity of the predicted virus- and allergen peptide pools could be shown on the level of T cell activation.

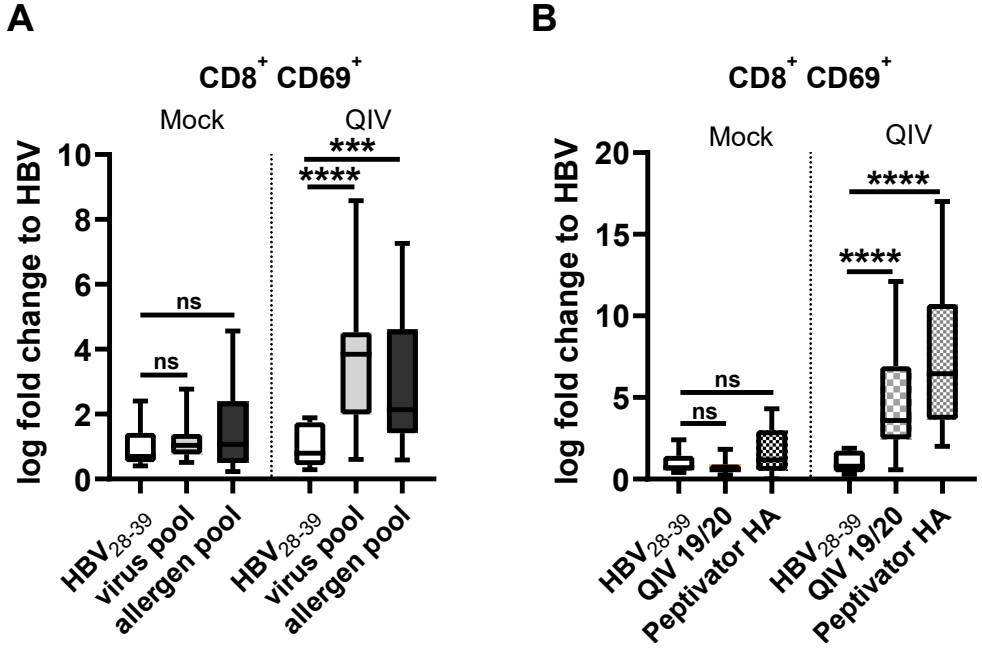

Figure 36: Predicted peptide pools induce activation of CD8+ T cells in spleen cells of QIV immunized mice

Mice were immunized intraperitoneally with QIV or mock immunized with a control solution and sacrificed 35 days after the last treatment. Spleen cells were used for *ex-vivo* stimulation with **(A)** peptide pools or **(B)** control antigens, CD8+ CD69+ T cells were measured by flow cytometry; n=5-10, Values are shown as mean ± SD, One-

Way ANOVA vs HBV; **** p≤ 0,0001, ns=not significant, QIV=quadrivalent influenza vaccine, cLN=cervical lymph node, HA=hemagglutinin, HBV=Hepatitis B Virus

4.7.3 Influenza vaccination reduces eosinophilic airway inflammation and mucus production in mice with HDM-induced experimental asthma

Next, a potential protective effect of influenza vaccination with the QIV towards experimental asthma was investigated. The protection of influenza virus infection was previously shown in OVA-induced experimental asthma, but also when using HDM (Skevaki et al., 2018). Additionally, several predicted candidate allergen peptides from the *in-silico* analysis were derived from HDM (Table 24). Based on this, combination of QIV immunization and HDM-induced experimental asthma was chosen (Figure 37 A). Humoral immune response to the QIV was confirmed by increased levels of QIV-specific IgG in QIV-immunized animals compared to mock animals (Figure 37 B).

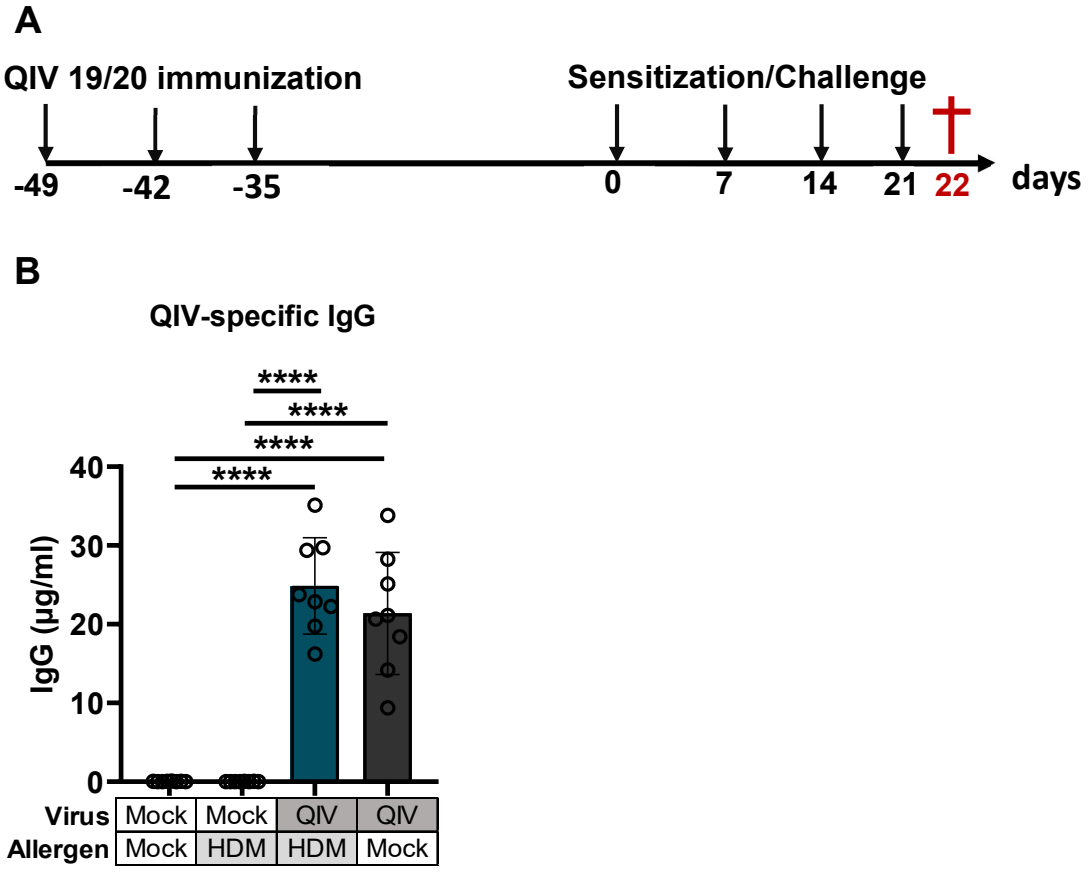

Figure 37: Experimental set-up and detection of immunoglobulins
Mice were immunized intraperitoneally with QIV and subjected to an HDM-induced experimental asthma model 35 days after the last immunization. **A:** Schematic representation of the experimental set-up **B:** Measurement of QIV-specific IgG by ELISA; n=6-8, Values are shown as mean ± SD, One-Way ANOVA multiple comparisons; **** p≤0,0001**,** QIV=quadrivalent influenza vaccine, HDM=house dust mite

Differential BAL cell counting confirmed allergic airway inflammation in HDM-treated mice, showing increased numbers of total BAL cells, lymphocytes, neutrophils and eosinophils, whereas the numbers macrophages decreased compared to mock animals (Figure 38). Mice previously treated with QIV revealed significantly reduced numbers of eosinophils in asthmatic mice, as well as increased numbers of macrophages that were comparable again to mock animals.

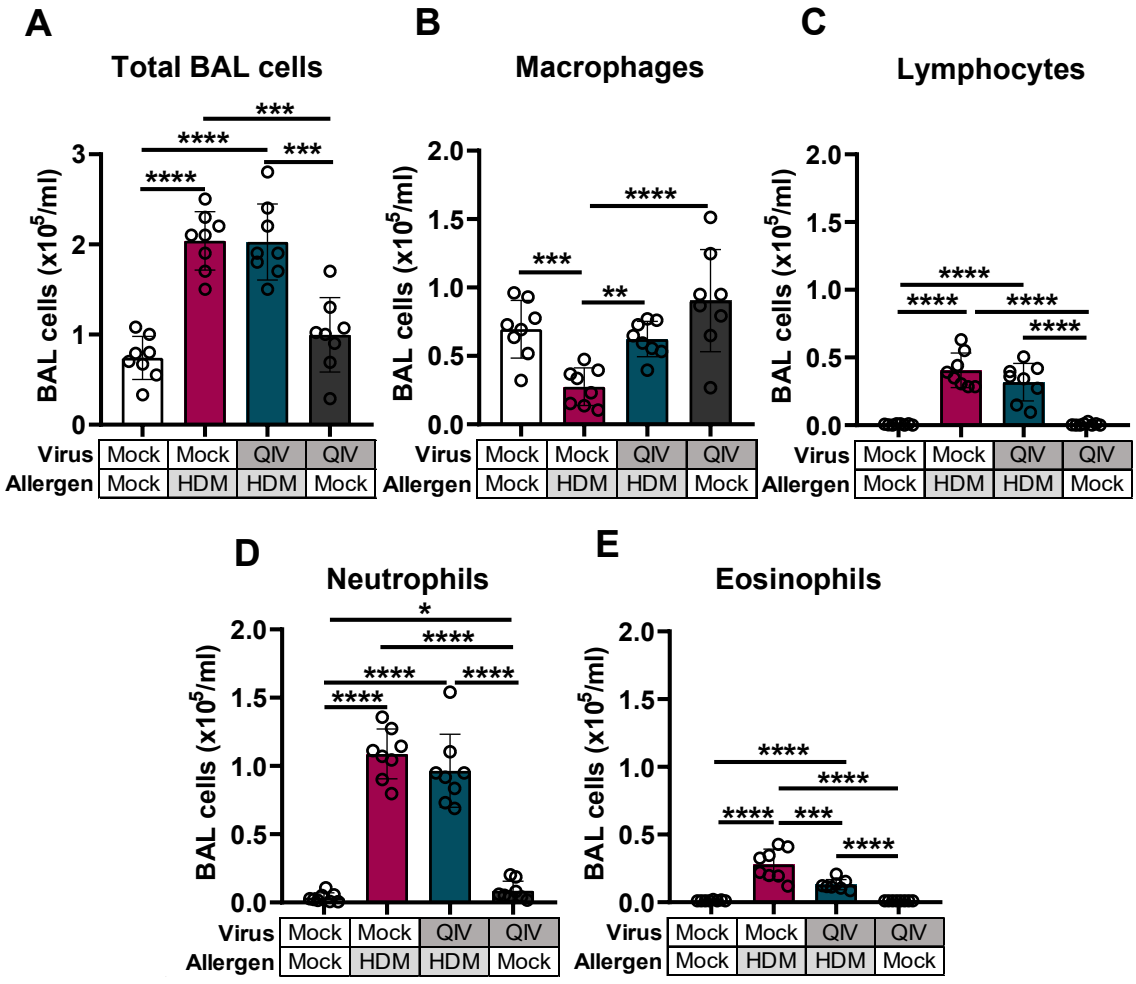

Figure 38: Influenza vaccination in mice reduces eosinophilia in BAL of HDM- treated animals
Mice were immunized intraperitoneally with QIV and subjected to an HDM-induced experimental asthma model 35 days after the last immunization. **A:** Cell count of total BAL cells **C-F:** Differential cell counting of BAL cell subsets; n=8, Values are shown as mean ± SD, One-Way ANOVA multiple comparisons; * p≤0,05, ** p≤0,01, *** p≤0,001, **** p≤0,0001**,** QIV=quadrivalent influenza vaccine, HDM=house dust mite, BAL=bronchoalveolar lavage

In addition, cytokines in the BAL supernatant were measured by CBA. The T2 cytokines IL-5 and IL-13 were significantly elevated in HDM-treated mice compared to control animals but did not alter after influenza vaccination (Figure 39 A, B). However, TNFα almost significantly increased (p=0,0508) when mice were previously immunized with QIV, compared to asthmatic mice alone (Figure 39 C).

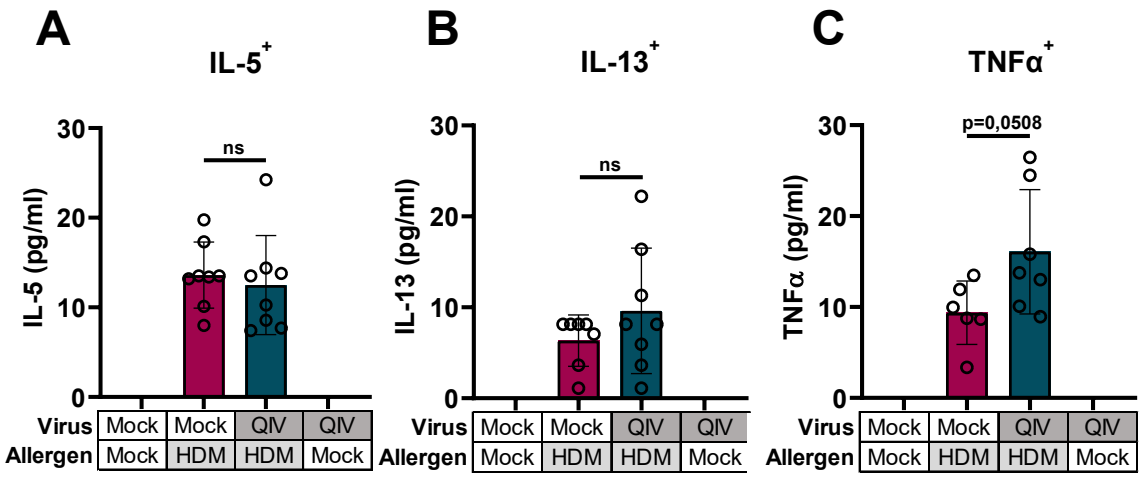

Figure 39: Increased TNFα but no changes in T2 cytokines in HDM-treated mice upon QIV immunization
Mice were immunized intraperitoneally with QIV and subjected to an HDM- induced experimental asthma model 35 days after the last immunization. Cytokines were measured in BAL supernatant by CBA. Values in the control groups were out of range. Thus, t-test was performed for all cytokines comparing only Mock/HDM and QIV/HDM groups. n=6-8, Values are shown as mean ± SD, QIV=quadrivalent influenza vaccine, HDM=house dust mite

A potential effect of QIV immunization on different immune cell subsets in the lung of HDM-treated mice was investigated by flow cytometry staining (Figure 40). Abundance of B cells, NK cells and dendritic cells was decreased in HDM-induced allergic asthma, whereas macrophages, neutrophils and eosinophils were elevated compared to mock animals. QIV/HDM mice showed significant decrease in relative numbers of macrophages compared to Mock/HDM mice. In addition, a trend for increased abundance of B cells (p=0,073) in asthmatic mice with prior QIV treatment was observed compared to mice only treated with HDM, as well as significantly elevated abundance of NK cells when comparing these groups. Abundance of eosinophils and neutrophilic were not significantly altered in the aforementioned groups.

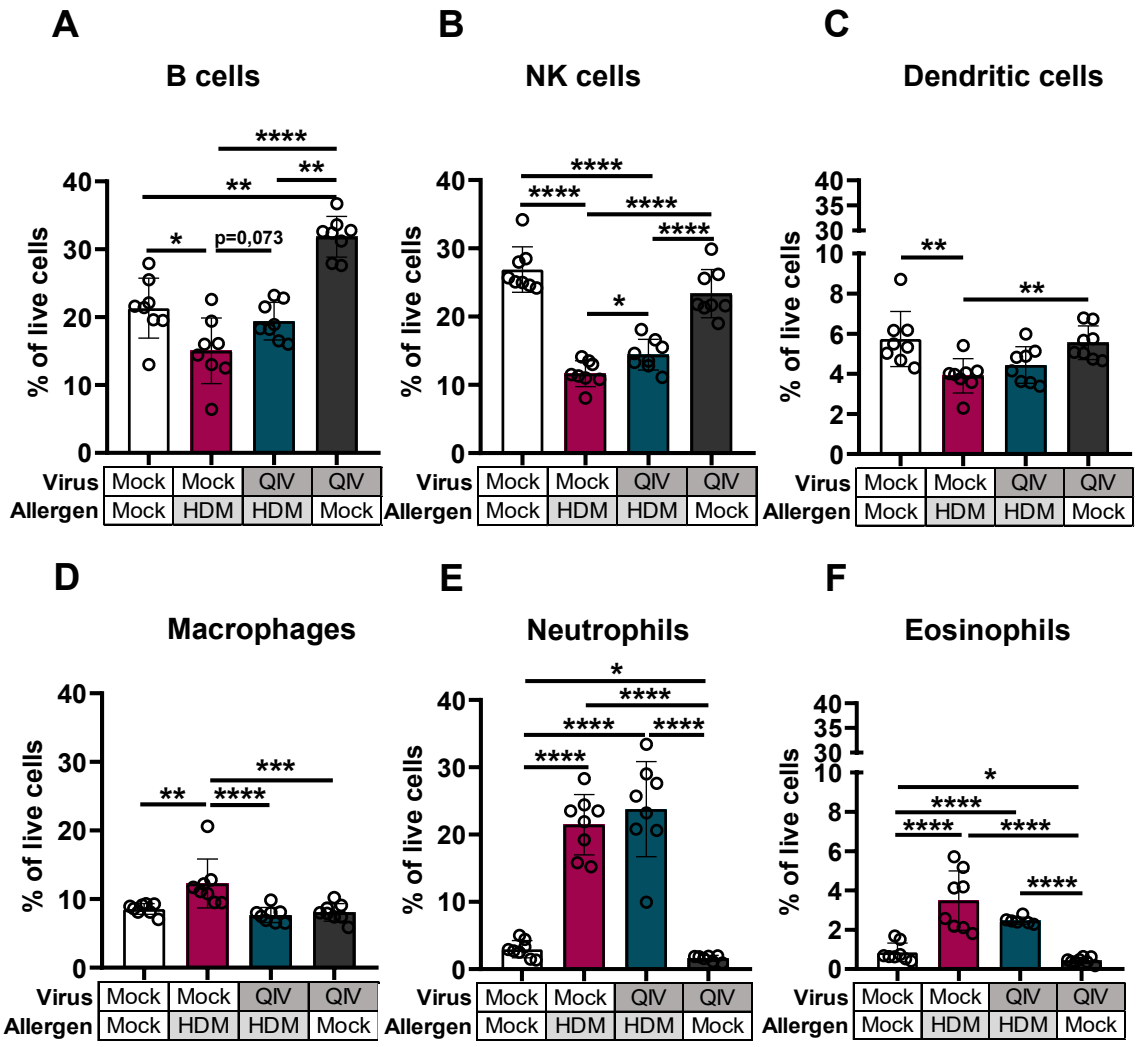

Figure 40: Altered abundance of immune cell subsets in the lung of QIV/HDM mice compared to Mock/HDM animals

Mice were immunized intraperitoneally with QIV and subjected to an HDM-induced experimental asthma model 35 days after the last immunization. Lung cell homogenates were stained with different phenotypic markers for important immune cells subsets. Measurement by flow cytometry; Cells were defined as following: **A:** B cells $B220^+$, **B:** NK cells $B220^-$ $CD27^+$, **C:** Dendritic cells $B220^-$ $CD27^-$ $CD11b^+$ $CD11c^+$ **D:** Macrophages $B220^-$ $CD27^-$ $CD11b^+$ $CD11c^-$ $Ly6G^-$ $SiglecF^-$ **E:** Neutrophils $B220^-$ $CD27^-$ $CD11b^+$ $CD11c^-$ $Ly6G^+$ **F:** Eosinophils $B220^-$ $CD27^-$ $CD11b^+$ $CD11c^-$ $Ly6G^-$ Siglec F^+; n=6-8, Values are shown as mean ± SD, One-Way ANOVA multiple comparisons; * p≤0,05, ** p≤0,01, *** p≤0,001, **** p≤0,0001, QIV=quadrivalent influenza vaccine, HDM house dust mite, NK cells=natural killer cells

T2 inflammation of HDM treatment was also confirmed by intracellular cytokine staining of lung cell homogenates, revealing increased levels of IL-5, IL-13 and IFNγ in $CD4^+$ T cells. When mice were previously immunized with QIV, abundance of cytokine producing T cells were not significantly altered in both, $CD4^+$ and $CD8^+$ T cells. IL-13 was not detected at all in $CD8^+$ T cells (Figure 41).

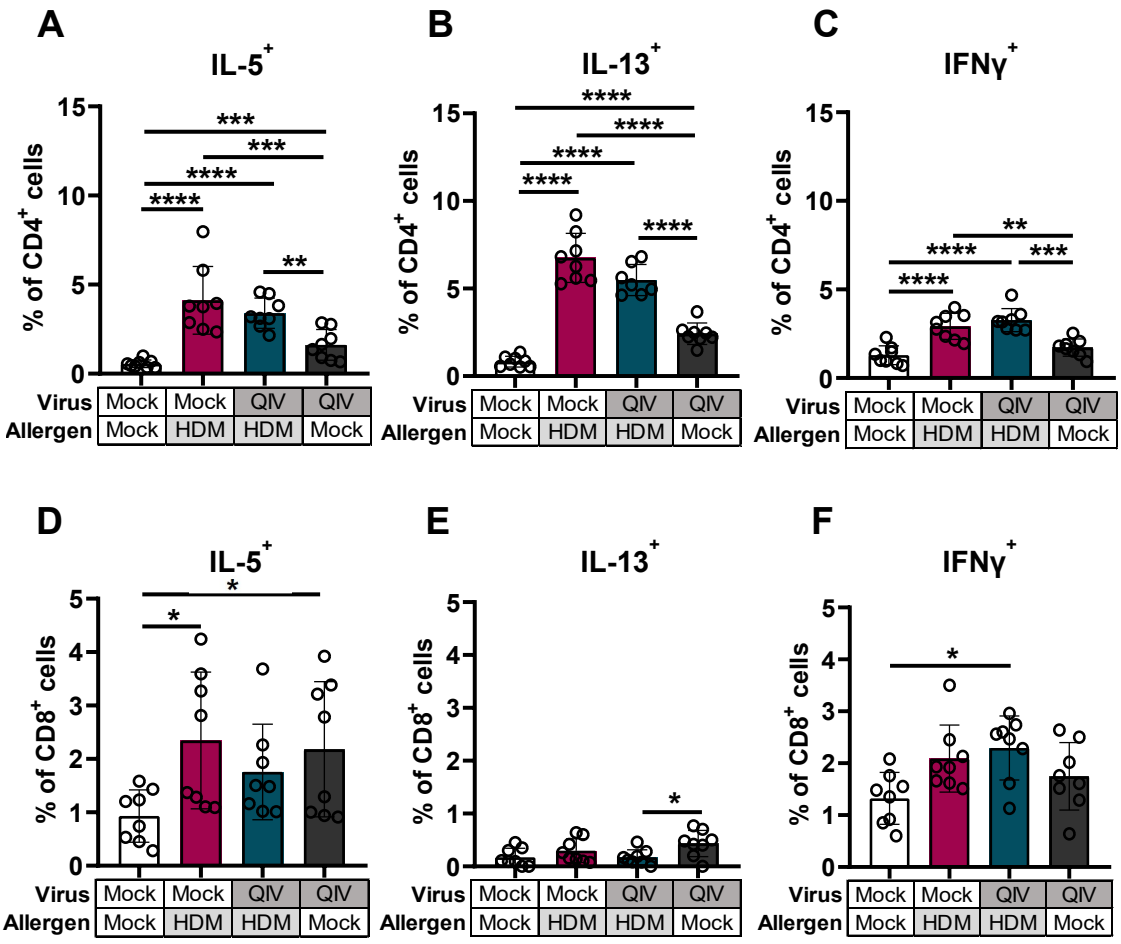

Figure 41: Relative abundance of cytokine producing T cells is not altered in the lung of QIV/HDM-treated mice compared to Mock/HDM animals
Mice were immunized intraperitoneally with QIV and subjected to an HDM-induced experimental asthma model 35 days after the last immunization. Lung cell homogenates were stained for intracellular cytokines in T cells and measured by flow cytometry. **A-C:** Intracellular cytokine detection in $CD4^+$ T cells **D-F**: Intracellular cytokine detection in $CD8^+$ T cells, n=6-8, Values are shown as mean ± SD, One-Way ANOVA multiple comparisons; * p≤0,05, ** p≤0,01, *** p≤0,001, **** p≤0,0001, QIV=quadrivalent influenza vaccine, HDM=house dust mite

Additionally, HDM-induced allergic response resulted in lung inflammation and mucus production, whereas control animals displayed a normal state of lung histology. Most importantly, prior QIV immunization significantly attenuated this airway inflammation and mucus secretion compared to Mock/HDM animals. Representative pictures from each group are shown in Figure 42 A, quantification of inflammatory cells (Figure 42 B) and scoring of PAS^+ cells (Figure 42 C) confirmed these observations.

Inferring, immunization of mice with the seasonal influenza vaccine resulted in reduced eosinophilic response in BAL and attenuated inflammation and mucus production in lung histology.

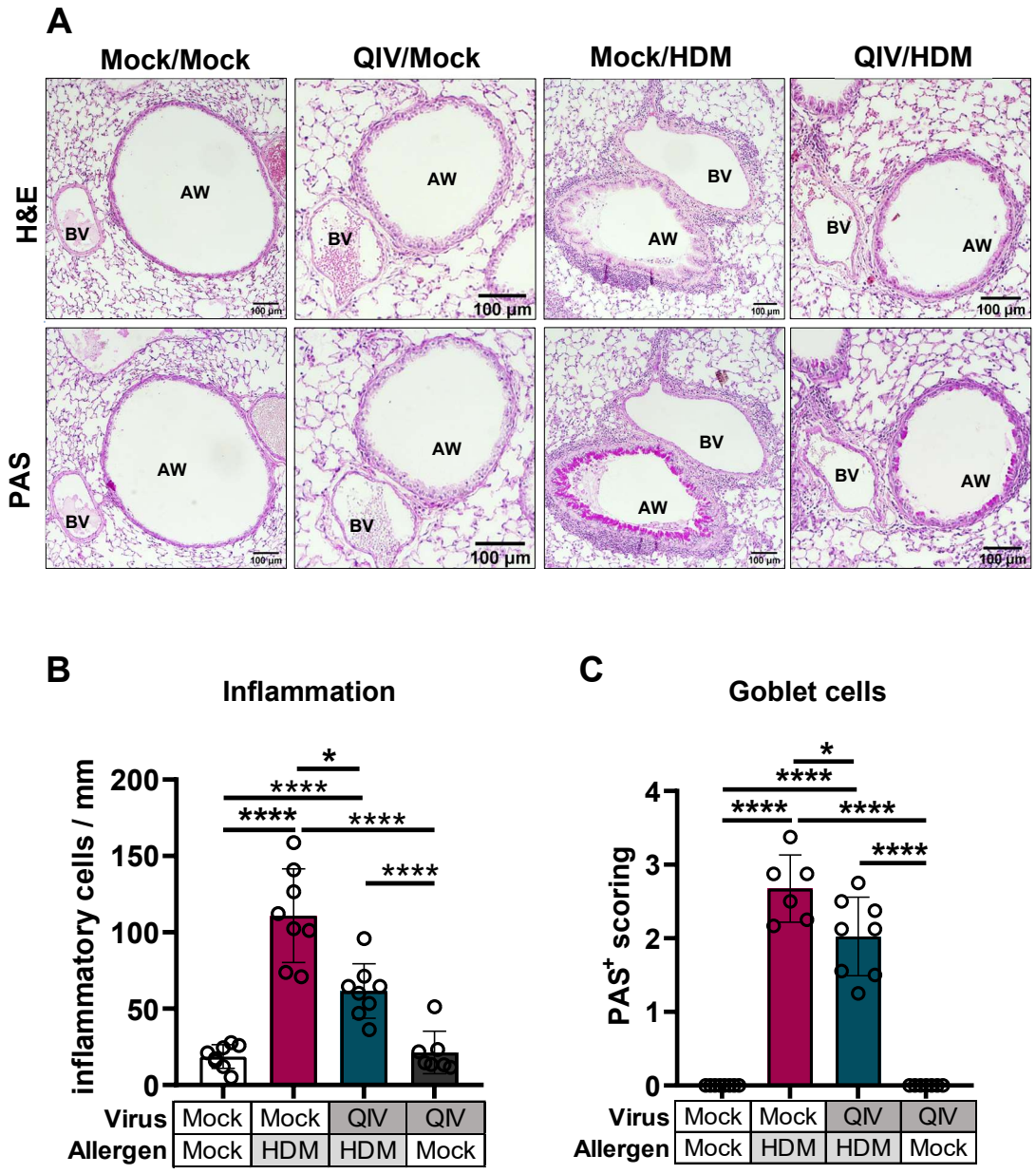

Figure 42: Influenza vaccination significantly reduces lung inflammation and mucus secretion in lung histology sections of HDM-treated mice
Mice were immunized intraperitoneally with QIV and subjected to an HDM-induced experimental asthma model 35 days after the last immunization. The left lobe of the lung was used for histological preparation and sections were stained for H&E and PAS staining. **A:** Representative pictures for each group for H&E (upper row) and PAS staining (lower row) **B:** Quantification of inflammatory cells between airway and blood vessel **C:** Scoring of PAS^+ cells within an airway; A minimum of 6 airways per animal were analyzed, n=6-8, Values are shown as mean ± SD, One-Way ANOVA multiple comparisons; * p≤0,05, **** p≤0,0001, QIV=quadrivalent influenza vaccine, HDM=house dust mite

5. Discussion

Asthma is one of the major chronic inflammatory disorders, affecting about 262 million people worldwide (World Health Organization, 2021). The role of viruses with regard to asthma is still controversial. On the one hand, respiratory viruses, mainly RV and RSV, are known to be a major risk factor for asthma development and exacerbations in childhood (Holgate et al., 2015). On the other hand, viruses were shown to induce protective effects on allergic diseases, supporting the "hygiene hypothesis" (Bach, 2002). Our group was able to show an IAV-mediated protection over development of experimental asthma in murine models of OVA and HDM, which was dependent on T effector memory cells. A first *in-silico* approach identified potentially cross-reactive T cell epitopes between the used influenza strain and ovalbumin, which were then confirmed to induce cross-reactive T cell response *ex-vivo* (Skevaki et al., 2018). Therefore, the aim of this work was to investigate whether heterologous immunity is a broadly applicable concept between several RNA viruses and allergens. A comprehensive *in-silico* approach identified potentially cross-reactive T cell epitopes between clinically relevant viruses and allergens. Cross-reactive T cell response of these epitope pairs was validated in *ex-vivo* stimulation assays and dual pentamer staining. Virus-induced attenuation of experimental asthma confirmed heterologous immune response and most importantly this was also observed in a translational setting with prior QIV immunization. This provides the first systematic and comprehensive immunoinformatic approach identifying and validating cross-reactive T cells originating from the distinct antigenic sources of virus and allergens and demonstrating asthma attenuation by virus infection and vaccination.

5.1 A suitable RSV infection model for investigation of heterologous T cell response was established

Heterologous immune response is known to require immune memory in order to alter the immune response to a subsequent exposure with a different pathogen. One mechanism of heterologous immune response is TCR-mediated cross-reactivity. Upon recognition of similar or even less similar peptides by the TCR, memory T cells are expanded and subsequently result in an altered immune response (Pusch et al.,

2018, Selin et al., 1998). Thus, in order to study T cell-mediated heterologous immunity, induction of memory T cells in a mouse model is required.

The human RSV is mainly separated into two major subgroups, A and B, differing only in their glycoprotein (Vandini et al., 2017). The RSV strain A2 is widely used in mouse models to study RSV infection. Virus susceptibility differs between mouse strains due to their genetic background and the Balb/c mouse strain is the most commonly used model for RSV infection, as it shows intermediate susceptibility (Altamirano-Lagos et al., 2019). Infection patterns being similar to RSV infection in childhood were observed with an infection model of $7{,}4x10^5$ pfu/mouse (Kast et al., 2017). Mouse models of higher infection doses, such as $1x10^7$ pfu, were demonstrated to induce a chronic disease (Jafri et al., 2004). As variations in virus propagation and titration protocols may occur between different scientific groups, many different infection doses are used in the literature. Therefore, we used a mouse model of an infection dose of $1x10^6$ pfu/mouse, aiming on inducing acute infection and memory T cell response, but not resulting in chronic inflammation. Virus replication in the lung was shown to rapidly increase until 4-6 dpi before declining again, being in line with data from the literature for both lower virus doses (Taylor et al., 1984) as well as higher doses (Graham et al., 1988). This was also confirmed by direct detection of RSV in the lung by immunofluorescence staining, where most of the virus signal was detected at 4 and 6 dpi. RSV is known to mainly infect ciliated cells of the epithelium, bronchi and broncheoli, thus being found only scattered in the lung parenchyma (Smith et al., 2014). At 1 dpi the virus could only be detected on the apical side of the airway epithelium and further spread into the lung parenchyma, which is in line with data from cell culture (Zhang et al., 2002). The acute phase of infection was shown to peak between 6 and 12 dpi and most importantly, long lasting T effector memory response was induced. Moreover, virus-specific $CD8^+$ T cells in the lung and mediastinal lymph nodes were detected at two timepoints. Mice showed no weight loss and acute virus infection was completely cleared by the animals at 35 dpi. Thus, RSV A2 infection of Balb/c mice with a dose of $1x10^6$ pfu was deemed suitable for further experiments. The acute phase of infection was defined at 12 dpi, showing elevated inflammation but also RSV-specific $CD8^+$ T cells, whereas the memory phase was defined at 35 dpi, having a memory phenotype but no signs of acute infection.

5.2 An immunoinformatics approach identified cross-reactive T cell epitope pairs between RNA viruses and environmental allergens

We developed a bioinformatics pipeline for prediction of potentially cross-reactive T cell epitopes between proteins of distinct antigenic sources. This pipeline takes MHC binding affinity as well as sequence homology into consideration. Prediction of T cell epitopes is of great interest especially in the field of diagnostics, development of therapeutics and peptide-based vaccines (Dhanda et al., 2018). Therefore, several online tools are available, aiming at identifying immunogenic epitopes which are able to stimulate T cells. Immunogenicity is dependent on antigen processing, recognition by a cognate TCR and MHC binding, the latter being the most critical characteristic (Sanchez-Trincado et al., 2017). Hence, we combined *in-silico* MHC binding prediction with an *in-vitro* MHC stabilization assay, selecting only candidate pairs with both epitopes forming a stable bond with the mouse H-2-Kd MHC class I molecule.

Epitope cross-reactivity can exist between structurally unrelated antigens with little sequence homology (Welsh et al., 2010). Similarity of physicochemical properties of amino acids is also associated with a higher probability for cross-reactivity in an *in-silico* approach (Frankild et al., 2008). Therefore, not only the degree of sequence identity between T cell epitopes should be considered in such prediction tools for cross-reactivity, but also amino acid properties. This has been done in the developed pipeline from this work. Additionally, T cells have a preference for aromatic and large amino acid residues, such as Isoleucine, Phenylalanine, and Tryptophan. Furthermore, the position of those amino acids in non-anchor parts (position 4-6) is important (Calis et al., 2013). Thermodynamic interactions between the MHC complex and the respective TCR clonotype also display a critical factor for immunogenicity (Ogishi, Yotsuyanagi, 2019). Therefore, these criteria are also included in prediction of immunogenicity in different tools, such as the “Repitope” R package (Ogishi, Yotsuyanagi, 2019) or the The Immune Epitope Database (IEDB) class I immunogenicity tool (Calis et al., 2013). Thus, the lack of including such a tool for prediction of immunogenicity in our pipeline represents a limitation and could be added for further studies.

The pair combined scores for aero- and food- allergens scored quite similar in the performed analyses, therefore not preferring one or the other group of allergens to be able to induce cross-reactive T cell response with virus epitopes. This is especially interesting when considering a higher association between respiratory virus infections and allergic asthma based on inhaled allergens compared to food allergy. A possible relationship between respiratory viruses and food allergy is suggested in some studies, however, gastrointestinal tract infections might be more relevant in the context of food allergy (Cheung, Grayson, 2012). Still, inhaled food allergens were also described to induce respiratory symptoms, especially wheat (Emons, van Gerth Wijk, 2018). Importantly, allergen epitopes predicted to potentially cross-react with RV1b-derived virus epitopes in our *in-silico* approach frequently derived from wheat in the context of food allergens, supporting a possible importance of virus-food allergen interactions as well. These interactions could be further investigated based on the performed *in-silico* predictions of different viruses.

Of note, less candidates were predicted for MHC class II and the predicted pairs ranked much lower compared to MHC class I predicted epitope pairs in all analyses. Due to their variation in the peptide-binding groove, presented peptides for MHC class I are recognized by $CD8^+$ T cells and presented peptides for MHC class II are recognized by $CD4^+$ T cells (Wieczorek et al., 2017). $CD8^+$ T cells are the major cell subset in anti-viral immune response (Schmidt, Varga, 2018). The first step in the bioinformatics pipeline is T cell epitope prediction for the virus proteins. In a second step, these predicted epitopes are aligned against all allergen proteins. Only fitting allergen proteins were used for subsequent allergen epitope prediction. Due to the T1-mediated anti-viral immune response, virus epitope prediction might have resulted in more predicted MHC class I epitopes rather than MHC class II, which might have resulted in a bias for MHC class I rather than MHC class II prediction. Therefore, investigating an effect of the predicted MHC class II-derived epitope pairs would also be interesting with respect to asthma protection.

The epitopes from the allergen counterpart were further assessed in an additional scoring system, investigating clinical relevance, abundance of an allergen source and conservation criteria. Allergen epitopes deriving from allergens of the protein families cupin and lipoprotein were predicted most frequently within the top 30

candidate pairs for both mouse MHC and human HLA background for RV1b, RSV A2 and QIV 19/20. The cupin superfamily belongs to the group of plant seed storage proteins, including major nut-derived allergens, such as peanut, cashew and hazelnut (Scala et al., 2018). Although such allergens are mainly associated with food allergy, they can also result in the so called "pollen-food syndrome". This is for example known for hazelnut, showing high cross-reactivity to birch pollen proteins, thereby resulting in rhinitis/asthma during pollen season (Calamelli et al., 2021). Importantly, allergen-derived epitopes from hazelnut were also predicted for both aero- and food- allergens in our *in-silico* analysis. Lipoproteins include vitellogenins from egg yolk (Amo et al., 2010), fish (Shimizu et al., 2009), bees and wesps (Blank et al., 2013) and mites (Thomas et al., 2002), most of them being characterized as minor allergens. However, *Der p* 14, the lipoprotein allergen component from HDM, was also described to contribute to severe mite-related allergic rhinitis and asthma in patients from the German Multicenter Allergy Study (MAS cohort). Although allergen sensitization against *Der p* 14 and other minor allergens started later in the evolution of IgE-sensitization against *Der p* allergen components and the prevalence of *Der p* 14-IgE was lower compared to major allergens, patients with IgE-sensitization against both major and minor allergens showed significantly higher prevalence of asthma and allergic rhinitis (Posa et al., 2017). Of note, *Der p* 14-derived allergen epitopes were frequently predicted to potentially cross-react with influenza strains from QIV.

Interestingly, candidate allergen epitopes for RSV A2 mouse prediction derived from a high diversity of allergen protein families, suggesting a high probability of RSV epitopes to cross-react with different allergens. Indeed, *ex-vivo* stimulation of lung and spleen cells from RSV-infected animals revealed cross-reactive T cell response when using a pool of all *in-vitro* positively tested epitope pairs, deriving from different allergenic sources. Importantly, allergen-peptide stimulation induced IFNγ response at both timepoints after infection. Clearance of respiratory virus infections is characterized by IFNγ and T1 response, resulting in long-lasting memory T cells which are activated upon a second infection (Openshaw, Chiu, 2013). Thus, such T1-primed memory cells might have cross-recognized the allergen peptides and resulted in the same T1 response.

Epitopes derived from *Asp f* were most frequent in the top five pairs and the allergen component *Asp f* 4 does also represent a major allergen. *Asp f* 5 shows closely related homologs to other *Aspergillus* strains, suggesting a high degree of cross-reactivity (Bowyer et al., 2006, Matricardi et al., 2016). Notably, direct cross-reactivity for the predicted RSV A2 $L_{356\text{-}364}$ FYNSMLNNI /*Asp f* $4_{192\text{-}200}$ WYGNSALTI candidate pair was demonstrated by dual pentamer staining in $CD8^+$ T effector memory lung cells of RSV-infected mice. Additional functional T cell assays in splenocytes of virus peptide immunized mice supported the findings of cross-reactivity between the predicted RSV A2- and *Asp f-* derived T cell epitopes. So far, virus-specific T cell cross-reactivity was only demonstrated for other antigens, including distinct virus subtypes (Clute et al., 2005, Vali et al., 2011), autoantigens (Wucherpfennig, Strominger, 1995), and alloantigens (D'Orsogna et al., 2010). Our group recently identified cross-reactive T cell epitopes between IAV and OVA, inducing IFNγ and IL-2 response upon *ex-vivo* stimulation in ELISPOT assay as well as attenuation of experimental asthma (Skevaki et al., 2018). Indeed, the ability of cross-reactivity is a prerequisite of our immune system to manage the amount of non-self-peptides, overshadowing the TCR repertoire (Sewell, 2012). The advanced and comprehensive *in-silico* prediction used in this work, combined with *in-vitro* selection and *ex-vivo* stimulation, extended this concept to other RNA viruses and a broad range of environmental allergens.

Interestingly, candidate epitope pairs deriving from RV1b achieved the lowest pair combined score compared to RSV A2 or QIV candidate pairs and, additionally, were less prone for MHC binding. Thus, they were not further investigated. Of note, barely any human RV-specific $CD8^+$ T epitopes have been identified so far. Gomez-Perosanz et al. were the first ones identifying and validating nine immunogenic and conserved human RV A and RV C $CD8^+$ T cell epitopes by means of a computational approach combined with functional T cell assays in human peripheral blood mononuclear cells (PBMCs) (Gomez-Perosanz et al., 2021). The low pair combined scores for RV1b-derived candidate pairs might also indicate restricted cross-reactivity between RV1b epitopes and allergens. This would imply less heterologous immune response, being in line with the fact that RV1b is the most common cause for asthma exacerbations in childhood (Jackson et al., 2008), therefore not resulting in an altered immune response in the direction of asthma protection.

The described bioinformatics pipeline and additional scoring system were also used to predict potentially cross-reactive T cell epitopes between SARS-CoV-2 and allergens on the background of the most important human HLA class alleles. The high variety of allergen sources indicates a high probability of heterologous immune response between SARS-CoV-2 and allergen derived T cell epitopes. A link between these epitope pairs and the outcome in immune response against SARS-CoV-2 and allergy in human PBMCs remains to be investigated experimentally. So far, atopy and asthma were not linked with a more severe outcome of COVID-19, suggesting a potential protective role of such cross-reactive T cell epitopes (Carli et al., 2021). This is also supported by a report from the data of the UK biobank, demonstrating a higher risk of non-atopic patients for a severe COVID-19 outcome (Zhu et al., 2020). In line with this, a recent study demonstrated less Angiotensin-converting enzyme 2 (AEC2) receptors in nasal epithelial cells from atopic asthmatic children compared to non-atopic and non-asthmatic children (Jackson et al., 2020). Importantly, heterologous immune response of SARS-CoV-2 specific T cell epitopes towards common cold coronaviruses were described recently (Braun et al., 2020, Grifoni et al., 2020). Thus, aeroallergen sensitization may shape the outcome of COVID-19 through cross-reactive T cells, thereby preventing an overwhelming T1 response (Balz et al., 2021). This would complement our hypothesis of heterologous immune response not only in the direction of asthma protection by a previous virus infection, but also suggests an inverse relationship.

5.3 Type 2 immune response in experimental asthma is attenuated by preceding virus infection

In order to investigate the outcome of the observed virus-induced heterologous immune response, the influence of RSV infection on the development of *Asp f*-induced experimental asthma was investigated. Allergen epitopes derived from *Asp f* were represented most frequently in the top five candidate list for RSV A2. Additionally, *Asp f* 4 is considered a major allergen and is included in routine diagnostic assays and *Asp f* 5 has been found to be important for airway remodeling and inflammation in a murine model (Namvar et al., 2015). Allergy against fungi, including *Asp f*, are highly associated with asthma (Woolnough et al., 2018) and rates of *Asp f*-sensitized

individuals are higher in asthmatic patients compared to non-asthmatics (Kespohl, Raulf, 2019). Virus peptide immunization with the peptides predicted to potentially cross-react with *Asp f*-derived allergen peptides confirmed cross-reactive T cell response between RSV A2- and *Asp f*- derived peptides and dual pentamer staining demonstrated direct cross-reactivity. Due to these criteria, a potential protective effect of prior RSV A2 infection towards development of *Asp f*-induced experimental asthma was chosen to be investigated in this project.

Allergic asthma is characterized by eosinophil hyperplasia, increase of T2 cytokines and airway inflammation (Suraya et al., 2021). Importantly, an attenuation of these hallmarks of asthma was observed by a previous RSV infection in our mouse model. Specifically, reduced numbers of eosinophils were observed in the BAL when comparing allergic asthmatic mice with prior RSV infection and such without virus infection. In addition, RSV infection led to a trend of reduced abundance of IL-5$^+$ T cells in the lung of RSV/*Asp f* animals compared to Mock/*Asp f* mice. Indeed, IL-5 is known to recruit and activate eosinophils and neutrophils (Holgate et al., 2015). This also matches to the trend for reduced abundance of neutrophils in the lung of RSV/*Asp f* mice compared to Mock/*Asp f* mice.

In fact, the trend for reduction of IL-5$^+$ T cells in the lungs of RSV/*Asp f* mice was observed in CD8$^+$ T cells. Indeed, CD8$^+$ T cells are known to secrete both, T1 (Tc1 cells) and T2 (Tc2 cells) cytokines (Maggi et al., 1994, Seder, Le Gros, 1995). Additionally, a time-dependent role of CD8$^+$ T cells was demonstrated in allergen sensitized animals. At an early sensitization step, these cells induce a protective effect by antagonizing T2 development through IFNγ production, whereas after allergen challenge they adapt the Tc2 profile (Stock et al., 2004). Thus, virus infection might have suppressed the development of T2-like CD8$^+$ T cells in allergen sensitized mice. In combination with the data from the *ex-vivo* stimulation assays, this might have been promoted by RSV-specific T1-primed CD8$^+$ memory cells, recognizing the cross-reactive allergen-derived peptides, thereby altering the immune system and more specifically, shaping also the differentiation of CD8$^+$ T cells.

In addition to IL-5, IL-13 represents a major T2 cytokine in type-2 immune responses. In asthma development, IL-13 promotes airway remodeling, among other things by driving goblet cell hyperplasia and mucus production, thereby leading to

airway hyperresponsiveness (Gandhi et al., 2016, Suraya et al., 2021). Significantly reduced concentrations of IL-13 in the BAL of RSV/*Asp f* mice were observed compared to Mock/*Asp f* animals. In line with the functional capacity of IL-13, prior RSV infection resulted in less mucus-producing goblet cells in the lungs of mice with experimental asthma.

Histologically, lungs of asthmatic patients are characterized by multiple chronic changes that describe airway remodeling. This includes not only mucus production, but also smooth muscle hyperplasia and deposition of extracellular matrix components, resulting in airway wall thickening (Busse, Lemanske, 2001). Previous RSV infection significantly reduced abundance of mucus producing goblet cells and peribronchial inflammation in the experimental asthma model. This suggests an overall reduction of airway remodeling and therefore a clinical benefit for the mice due to the previous virus infection. Thus, investigating the airway wall thickening in a next step would provide a better understanding of the extent of attenuated airway remodeling in these mice. Additionally, airway remodeling is associated with airway hyperresponsiveness (Suraya et al., 2021). It represents a pathophysiological consequence of airway inflammation and therefore an important clinical parameter, which is also measured for diagnosis of asthma (Buhl et al., 2021, Deng et al., 2013). Reduction of airway hyperresponsiveness was also previously proven in the IAV-mediated protection over development experimental asthma in a murine model of OVA (Skevaki et al., 2018); thus, the impact of RSV infection on this clinical parameter remains to be investigated in order to fully conclude on the extent of asthma attenuation.

Heterologous immune response is a broadly accepted concept and more studies arise demonstrating that virus infection may also alter inflammatory responses not being related to infections, such as allergic asthma. Several studies investigated heterogenous consequence of previous virus infections towards AAI induction (Wu et al., 2020). Enhanced airway sensitization was demonstrated by Al-Garawi et al., showing an increase in the allergic asthma phenotype of HDM-induced experimental asthma in previously IAV-infection animals, resulting in enhanced airway inflammation and production of T2 cytokines, IgE-response and airway remodeling. In this study, mice were infected at the age of eight days and allergen sensitization started

seven days later (Al-Garawi et al., 2011). You et al. observed similar effects with RSV infection prior to an HDM-induced experimental asthma model when infecting 7 days old mice (You et al., 2006). Increased eosinophilic response and inflammation to HDM-treatment were also shown in previously RSV-infected mice when starting the virus infection at the age of four weeks with a virus infection dose of $2x10^6$ pfu (Keegan et al., 2016). The aforementioned studies showed enhanced allergic airway inflammation in AAI mice with prior virus infection. However, our group previously demonstrated IAV-mediated asthma protection in a murine model of OVA- and HDM- induced experimental asthma (Skevaki et al., 2018). The data presented in this thesis support these findings. In contrast to the aforementioned studies, virus infections in our experiments were performed at an adult age of 6-8 weeks old mice, whereas these studies mainly infected 7-8 days old mice. Such virus infections in infant mice correlate with virus infection in early infancy as a risk factor for allergic asthma. Thus, the age of virus infection may influence the heterologous outcome towards allergen exposure. Additionally, higher infection doses of the virus may also increase airway inflammation, as Keegan et al. used also older mice at the age of 4 weeks, but the RSV infection dose was two times higher compared to the one used in this research project. Indeed, other groups also demonstrated partly favorable altered immune response upon virus infection towards AAI in mice. A suppression of airway eosinophilia and T2-response by influenza infection was also already shown in an OVA-model of airway inflammation but not T2-inflammation in the lung, having also not resulted in reduction of goblet cells and AHR (Wohlleben et al., 2003). Recently, Wu et al. supported an altered effect of IAV PR8 infection towards AAI in OVA-treated mice when starting allergen sensitization two weeks after virus infection. Less T2-cells were observed in the lungs of such animals as well as increased numbers of B cells, which is in alignment with our data. A strong increase in bronchial and alveolar hyperplasia was observed in previously infected animals subjected to the OVA-model compared to OVA-mice alone, supporting the concept of trained immunity (Wu et al., 2020). Taken together, age of infection, infection dose and time period until exposure to the allergen might contribute to the outcome of an altered immune response, resulting in enhanced or attenuated allergic asthma.

The observed asthma attenuation by viral infection provides evidence of heterologous immunity between different (RNA)-viruses and environmental allergens,

thereby supporting the previously investigated IAV-mediated asthma protection and extending the hygiene hypothesis, which up to now was mainly associated with bacterial exposure so far.

5.3.1 Changes in lung virome composition may also contribute to heterologous immune response

The human microbiota has gained high interest in the past years and its balance is known to be important for a stable immune system. The microbiota consists of bacteria, viruses, fungi and archaea, being highly diverse, stable, resistant and resilient (Barcik et al., 2020). The human virome includes eukaryotic viruses and bacteriophages (Abeles, Pride, 2014). A disbalance of the microbiota is associated with respiratory diseases, including asthma and cystic fibrosis (Wypych et al., 2019). Extending the hygiene hypothesis, commensal and non-pathogenic viruses are suggested to reduce the risk of asthma development, although the mechanisms are not yet understood. Compared to the microbiome, the human virome has been less intensively studied so far (Choi et al., 2021). Thus, it was of high interest to study the airway virome of allergen-treated animals and to further investigate a possible influence of RSV infection on the virome of such animals, which might contribute to an altered immune response.

Indeed, the β-diversity in the lung of *Asp f*-treated mice was altered compared to control mice. This was also observed in human lung of asthmatic patients compared to healthy controls and further increased with disease severity (Choi et al., 2021). Interestingly, the α-diversity of animals treated with *Asp f* decreased in the lung (p=0,051), and to a lower extent also in BAL samples. Reduced virus families in the lung included *Helvetiavirae*, *Shotokuvirae* and *Marseillevirae*. In addition, a trend of increasing abundance of *Shotokuvirae* was observed following RSV infection and allergen treatment compared to allergen treatment alone, although the statistical difference is weak. Importantly, the kingdom of *Shotokuvirae* also includes the virus family of *Redondoviridae*, which is highly associated with severe COVID-19 (Merenstein et al., 2021). *Redondoviridae* were recently introduced as a new virus family, being found selectively in the lung and oro-pharyngeal samples and were associated with periodontal disease (Abbas et al., 2019). Thus, a possible role of this virus family in human asthmatic patients might still be investigated. Several commensal

viruses are associated with a potential protective role for wheezing and rhinitis in human, especially *Anelloviridae*, but also *Caudovirales* and *Picornaviridae* (Tay et al., 2021). *Anelloviridae*, specifically the prototype torquetenovirus (TTV), constitute approximately 70 % of the human virome and can be found in the blood and several tissues and organs. Different studies demonstrated increased activity of eosinophils in patients with high levels of TTV, as well as reduced circulating $CD4^+$ T cells and increased levels of B cells. A correlation between TTV loads and impaired lung function was demonstrated in children with bronchiectasis as well (Freer et al., 2018). However, *Anelloviridae* were not found to be highly abundant in *Asp f*-treated mice. Interestingly, *Herpesviridae* were found to be the most abundant population in asthmatic patients, being able to serve as a biomarker, whereas bacteriophages were shown to be reduced (Choi et al., 2021). Of note, *Herpesviridae* represented the most abundant virus family in healthy lungs and a tendency in increase in *Herpesviridae* was as well observed upon allergen treatment, although not significantly.

The low sample number of five animals represent a limitation of this study, which might have led to less obvious and significant results when comparing allergic asthmatic mice with and without prior RSV infection. Thus, an influence of virus infection on the lung airway composition contributing to the attenuation of experimental asthma by heterologous immune response cannot be confirmed with these results and further analyses with more animals are needed to support the hypothesis. Complex interactions in the upper respiratory tract between the microbiome and virome of healthy children were observed in several studies, making associations between microbiota and respiratory diseases even more complex (van den Bergh et al., 2012). Therefore, associating the virome with the microbiome in a virus-mediated asthma protection model would also give insights into these mechanisms.

5.4 Immunization with the predicted RSV-derived peptides partially contribute to attenuation of experimental asthma

Having observed attenuation of different hallmarks of asthma by RSV infection, the impact of the predicted cross-reactive T cell epitopes was investigated. Similar to RSV infection, *Asp f*-treated mice with a previous virus-peptide immunization showed reduced numbers of eosinophils in the BAL compared to asthmatic mice

alone. Notably, a trend for decreased abundance of IL5$^+$ CD8$^+$ T cells and increasing abundance of CD8$^+$ IFNγ producing T cells were observed in the lung when comparing the aforementioned groups. This indicates an induction of T1 responses mediated by the virus peptides, shaping the immune response upon recognition of the cross-reactive allergen peptides. However, this may not be sufficient to confer protection or attenuation of experimental asthma, as no changes were also observed in lung histology. A possible explanation for this may be the small numbers of peptides included in the virus peptide pool. These represented the top candidates predicted from the *in-silico* analysis. Many other RSV/*Asp f*-derived epitope pairs were predicted to potentially be cross-reactive, whereby these resulted in heterologous immune response upon RSV infection, as the whole virus does include several peptides. Thus, performing immunization with a mega pool of predicted peptides may lead to a more attenuating effect.

In addition, one might hypothesize an induction of additional mechanisms by viral infection or whole protein immunization which contribute to asthma attenuation or protection, displaying complex interactions rather than a T cell-mediated effect alone. T cell-mediated cross-reactivity represents only one potential mechanism of heterologous immunity. Memory B cells are as well known to be activated upon exposure to heterologous antigens, thereby inducing an immune response. This could also lead to protection against secondary infection, as it has been shown for distinct influenza strains, but also for infections with different flaviviruses (Leach et al., 2019, Wong et al., 2020). Indeed, relative abundance of total B cells was slightly increased in previously infected and influenza vaccinated mice compared to allergen treated mice without virus infection or vaccination. In addition, ILCs are discussed to contribute to innate immune memory, thereby altering the immune response upon a secondary antigenic exposure (Martin, 2014). As ILC2s display a major cell type in type 2 inflammation, a contribution of these cells in heterologous immune response of virus-induced asthma protection would be highly interesting. First measurements of ILC2s by flow cytometry revealed differences in the abundance of these cells in the lung of *Asp f*-treated mice (data not shown), promoting the intention for additional experiments focusing on these cell subsets.

Vaccines inducing T cell-mediated heterologous immunity are of high interest in the field of vaccine development, conferring high effectiveness and broad cross-reactive immune responses. Such peptide-based vaccines are currently being investigated for DENV and ZIKA virus among others. Antonelli et al. developed a vaccine construct based on *in-silico* predictions of conserved $CD4^+$ and $CD8^+$ T cell epitopes from ZIKV and confirmed T cell response in previously exposed individuals (Antonelli et al., 2022). Another group predicted functional and serotype-cross-reactive $CD8^+$ T cell epitopes from DENV and the resulting vaccine construct elicited $CD8^+$ T cell response in DENV-positive patients. Importantly, memory T cell response was also observed in ZIKV-positive patients (Reguzova et al., 2021). Currently, developing a cross-protective vaccine against SARS-CoV-2 and arising mutants is of high interest, which could be achieved by inducing a cross-reactive memory T cell response. A recently published approach identified several highly conserved $CD4^+$ and $CD8^+$ T cell epitopes from different SARS-CoV-2 proteins being able to bind to different HLA alleles and not being conserved among the human genome. The authors claim a higher positivity rate when using this approach and its possible implication for T cell-based vaccines (Meyers et al., 2021). Another group identified the epitope $N^{361-369}$ as a dominant $CD8^+$ T cell epitope and two TCRs specific for this epitope were found to display cross-reactivity to several $N^{361-369}$ mutants. This epitope was able to be endogenously processed and presented, thereby leading to a $CD8^+$ T cell response (Hu et al., 2022). Such a T cell-based vaccine approach eliciting immune response towards heterosubtypic virus strains is also of great interest for influenza in order to overcome the annual adaption of the vaccine. The peptide-based vaccine candidate FLU-v has recently finished the clinical trial phase IIb and is supposed to act as a broad-spectrum vaccine. So far, it offered protection to a challenge with the H1N1/2009 pandemic strain in healthy individuals. Recruitment of elderly and challenge with heterosubtypic virus strains remains to be investigated (Pleguezuelos et al., 2020). Several other vaccine candidates are being identified by computational approaches, including artificial antigenic constructs based on conserved epitopes, thus, providing promising approaches for future cross-reactive vaccines (Bazhan et al., 2020).

5.5 T2 inflammation is attenuated in experimental asthma via prior influenza vaccination

Inactivated influenza vaccines and the live-attenuated influenza vaccine (LAIV) represent the only two licensed influenza vaccines so far. Both induce mainly HA-directed neutralizing antibodies, whereby the LAIV is also known to elicit cross-reactive T cell response against conserved influenza proteins (Hoft et al., 2011, Schmidt, Lapuente, 2021). However, due to its low efficiency in some patients, the LAIV is only recommended in Germany for children aged 2-17 years (Falkenhorst et al., 2013). In order to use the best translational approach for a broad range of patients, the inactivated influenza vaccine was used in this project; more precisely, the quadrivalent influenza vaccine 2019/2020. A mass spectrometry analysis (data not shown) confirmed the presence of the predicted epitopes from the QIV 19/20 *in-silico* analysis within this vaccine and indicated also the presence of other influenza proteins besides of HA, mainly NP, M1 and NA. Booster vaccination is often used in mice to enhance the immune response (Groves et al., 2018, Han et al., 2019). In this project, performing triple immunization with a two-weeks interval induced long-lasting influenza-specific T cells as well as effector memory T cells in both, spleen and lymph nodes. Importantly, cellular response was proven for $CD4^+$ and $CD8^+$ T cells. In human, the inactivated vaccine is known to elicit only $CD4^+$ T cells. These cells are mainly responsible for supporting B cells, but also promote anti-viral immune response. However, influenza-specific $CD8^+$ T cells are mostly directed against internal viral proteins, being able to provide heterosubtypic cross-protection (Jansen et al., 2019). Thus, induction of influenza-specific $CD8^+$ T cells was necessary in this project to study heterologous immune response and was confirmed by pentamer staining.

Cross-reactive T cell response was also demonstrated for virus peptides from influenza strains of the QIV 19/20 and a pool of allergen-derived peptides, including HDM, but also other allergen sources. However, *ex-vivo* stimulation only resulted in activated $CD8^+$ T cells but not in T1 cytokine response. Yet, cross-reactivity for influenza-derived peptides and HDM-derived peptides was demonstrated for the second time (Skevaki et al., 2018), suggesting a high probability of heterologous immune response between these unrelated pathogens. Indeed, allergy to HDM is highly

associated with asthma burden (Kovac et al., 2007). As already discussed in 5.2, *Der p* 14 epitopes have been frequently predicted to potentially cross-react with epitopes from influenza strains of QIV. *Der p* 14 allergens also contribute to a synergistic effect of major and minor *Der p* allergens, increasing allergy and asthma prevalence and burden (Posa et al., 2017). Due to these aspects, a potentially protective effect of prior QIV immunization towards HDM-induced experimental asthma was investigated.

Similar to a prior RSV infection towards *Asp f*-induced experimental asthma, an attenuation of different hallmarks of asthma upon QIV immunization towards HDM-induced experimental asthma was also demonstrated in this setting. More specifically, reduced eosinophilia in the BAL was observed in QIV/HDM mice compared to Mock/HDM animals, but no changes in T2 cytokines were found in the BAL when comparing the aforementioned groups. However, higher levels of TNFα were detected in the BAL of allergic asthmatic mice with prior QIV immunization compared to Mock/HDM mice, suggesting a stronger T1 response induced by the vaccination. Additionally, no significant differences in the abundance of cytokine producing T cells were detected in the lungs of QIV/HDM vs Mock/HDM mice. However, prior QIV immunization resulted in less mucus-producing goblet cells in the lungs of mice with experimental asthma. This indicates a clinically relevant benefit for these mice, which was induced by the vaccination. It remains to be investigated whether a reduction of IL-13 or IL-5 might at least be detected at mRNA level in QIV/HDM animals compared to Mock/HDM mice. Annual vaccination with the seasonal influenza vaccine is recommended by the Advisory Committee on Immunization Practice to prevent asthma exacerbations by influenza infections (Velasco-Medina et al., 2021, World Health Organiszation, 2012). Of note, some recent studies also associated influenza vaccination with a lower risk for asthma burden and prevalence. Lower asthma prevalence in influenza vaccinated children in the US was demonstrated, although asthma severity was not assessed (Hou, Silverberg, 2021). A 13- years retrospective study from Taiwan demonstrated a lower risk for asthma development in patients with atopic dermatitis with influenza vaccination compared to those patients without this vaccination. As asthma is also associated with other diseases, including allergic rhinitis, this group suggests an overall beneficial effect of influenza vaccination on allergic diseases (Li et al., 2021b). The observed QIV-associated

asthma attenuation in the HDM-induced mouse model support these data and the implication of inducing a T1-shift to reduce atopic disorders in predisposed children.

Compared to the previously observed protective effect of an influenza infection observed by our group, QIV immunization resulted in attenuation of HDM-induced experimental asthma, but not complete protection. This might be due to the chosen route of application, as well as the use of the inactivated vaccine instead of LAIV. However, while establishing the QIV immunization model, intranasal application did not improve T cell response compared to intraperitoneal application (data not shown). Nonetheless, nasal application mimics the route of virus infection more closely, as the LAIV is also administered. The virus in the LAIV nasal spray can replicate to some extent in the upper respiratory tract (Fischer et al., 2015), inducing mucosal antibodies and, more importantly, cross-reactive T cell response against divergent influenza subtypes (Hoft et al., 2011). Therefore, repeating the experiment with the use of the LAIV would display if this vaccine also induces stronger heterologous immune response against allergens compared to the QIV.
Indeed, epidemiological studies revealed an overall beneficial effect of live attenuated vaccines towards mortality, but also unrelated infections and other diseases. This was demonstrated for example for the measles vaccine (Aaby et al., 2003, Aaby et al., 2012), BCG (Bacillus Calmette–Guérin) vaccine against tuberculosis and the vaccinia vaccine against poxs (Aaby et al., 2006, Villumsen et al., 2009), as well as the oral polio vaccine (Aaby et al., 2004). Such non-specific effects often were sex-specific, primed by maternal vaccinations and increased with booster vaccinations (Higgins et al., 2016, Jensen et al., 2016). Additionally, age-dependent differences in cytokine responses were observed when stimulating blood samples of BCG-vaccinated individuals of different age with several bacteria or TLR ligands (Freyne et al., 2018, Nissen et al., 2018). Most recently, protective effects of the BCG vaccine towards COVID-19 were suggested in different epidemiological studies and clinical trials. One clinical trial investigated BCG as a potential therapeutic for hospitalized COVID-19 patients, resulting in a beneficial outcome for these patients (Padmanabhan et al., 2020). In addition, another study with BCG-revaccinated individuals revealed a significantly lower risk for SARS-CoV-2 infection compared to the control group (Tsilika et al., 2021). Heterologous immune response, including innate

immune response as well as T cell-mediated effects, is suggested as a possible mechanism for such unrelated vaccine effects (Blok et al., 2015, Jensen et al., 2016). Indeed, sequence homology between BCG and SARS-CoV-2 was identified and cross-reactivity towards SARS-CoV-2 epitopes was demonstrated *in-vitro* in BCG-primed T cells (Eggenhuizen et al., 2021). These data support the hypothesis and findings of this project with respect to a possible beneficial effect of influenza vaccination towards asthma and other allergic diseases.

5.6 Conclusion and outlook

This research project provides the first systematic and comprehensive immunoinformatic approach for identification and characterization of cross-reactive T cell epitopes deriving from the distinct antigenic sources of viruses and allergens. The *in-silico* pipeline predicted several potentially cross-reactive T cell epitopes between environmental allergens and clinically relevant viruses, including SARS-CoV-2, RSV A2, RV1b and influenza strains from the seasonal quadrivalent influenza vaccine 2019/2020. This pipeline in combination with the scoring system for clinical relevance provides a tool for any future prediction to extend such studies. In addition, the *in-vitro* MHC stabilization assay investigated MHC binding of the predicted epitopes before using such peptides in further experiments, offering an additional validation step. *Ex-vivo* T cell stimulation assays and dual pentamer staining confirmed cross-reactivity of the predicted epitope pairs, which was shown in RSV-infected and RSV-derived peptide immunized animals, as well as influenza vaccinated mice. Virus-induced attenuation of experimental asthma was demonstrated with RSV A2 infection, but also in a setting with prior QIV immunization. Peptide immunization with RSV-derived peptides was not sufficient to induce the same extent of asthma attenuation as observed with virus infection but resulted in an increased T1 response. Virome analyses of lung samples of RSV infected and allergen-treated mice provided first insights into an altered virome composition upon allergen treatment, which needs to be further investigated in order to confirm also an influence of prior RSV infection on the virome of allergic asthmatic mice.

The results of this thesis confirmed heterologous immunity as a broadly applicable concept between different (RNA)-viruses and environmental allergens.

Furthermore, the findings extend the hygiene hypothesis and protective effects of respiratory viruses towards asthma development. Of note, the extent of asthma attenuation may differ for specific viruses and in relation to different allergens, suggesting that different cross-reactive T cells may shape the outcome of allergic diseases. The data support the need for peptide-based vaccines and an importance of inducing T cell-mediated heterologous immune response in this context, resulting in broad-protective vaccine response. However, further experiments are needed to broaden the underlying of the mechanisms and to transfer this concept to the human setting.

In order to gain deeper insight into the mechanisms of the observed virus induced attenuation of allergic asthma, single cell analyses of lung cells will provide hints for underlying molecular mechanisms. Additionally, investigation of the TCR repertoire of lung $CD8^+$ T effector memory cells is planned to point out unique TCR clonotypes, which might be responsible for the observed T cell-mediated heterologous immune responses. Ultimately, TCR sequencing of pentamer-FACS-sorted antigen-specific T cells would provide evidence on relevant TCR clonotypes.
In addition, the influence of virus infection on the airway virome composition of allergic asthmatic mice and its possible contribution to an altered immune response could be further investigated as an additional mechanism.
In order to transfer the findings of this work into the human context, transgenic human HLA mice represent good models to form a bridge between mouse data and further experiments with human samples. In this context, vaccination of such mice with the QIV would be of major interest in a clinical context. We have already identified potentially cross-reactive T cell epitopes between the influenza strains of the seasonal QIV and allergens on the background of the most frequent human HLA alleles. With the help of a T2-cell-line based HLA stabilization assay and available transfectants for HLA alleles, such candidate peptide pairs could also be validated for MHC binding in a similar way as it has been done using the RMA-S cells. Based on the predicted candidate pairs and the allergen counterpart, a potential protective effect of QIV immunization on the development of experimental asthma could then be investigated in the setting of human HLA alleles. However, investigating a potentially protective effect of RSV infection as well as virus peptide immunization towards asthma development in the context of transgenic human HLA mice would

provide a basis for peptide-based vaccines inducing heterologous immune responses.

Ultimately, based on the results of the transgenic mice, PBMCs of non-atopic and atopic patients with relevant allergies could be assessed in *ex-vivo* stimulation assays using the cross-reactive virus- and allergen-derived peptide pools at different timepoints before and after influenza vaccination. By doing this, cross-reactive T cells could be further characterized and differences between healthy and atopic patients could be investigated. If such cross-reactive T cell populations are accentuated following exposure to RNA virus antigens and if their functional output presents increasing T1 responses, this points a promising direction towards peptide-based vaccines with anti-viral and anti-allergic potential. Immunization of atopic individuals with such virus antigens might potentially display a preventive strategy to reduce harmful allergic responses.

Additionally, with respect to the SARS-CoV-2 pandemic, it would be of high interest to investigate whether patients with cross-reactive allergen-specific T cells have a different response to SARS-CoV-2, which is currently investigated in our group. Therefore, potentially cross-reactive T cell epitopes were already predicted in this thesis using the *in-silico* pipeline and scoring system. In addition, patients were already recruited and screened for relevant allergies based on the allergenic source of the predicted epitopes. Upcoming stimulation experiments of PBMCs of allergic vs. non-allergic patients with or without SARS-CoV-2 infection could demonstrate a potential heterologous outcome of SARS-CoV-2 infection based on cross-reactive T cell epitopes.

6. Summary

Asthma is one of the major chronic inflammatory disorders worldwide. Respiratory virus infections and exposure to allergens are important risk factors for asthma development. Our group previously demonstrated an influenza-mediated protective effect over experimental asthma in a murine model, which was dependent on cross-reactive T effector memory cells. The hypothesis of this research work was that virus-mediated heterologous immune response is a broadly applicable concept for several respiratory viruses and environmental allergens. This immune response may be mediated by cross-reactive virus-specific memory T cells, which react in a T1-driven immune response upon allergen exposure. In order to test this hypothesis, a comprehensive *in-silico* pipeline for prediction of potentially cross-reactive T cell epitope pairs between several respiratory viruses and allergens was developed, taking MHC binding affinity and sequence similarity of the T cell epitopes into consideration. An additional scoring system further characterized and prioritized the allergen counterpart based on clinical relevance and conservation criteria. Mouse Balb/c MHC class I epitope pairs were validated for MHC stabilization in an *in-vitro* assay and binder pairs were used for further *ex-vivo* and *in-vivo* experiments. Using an RSV A2 infection model, *ex-vivo* T cell stimulation assays of lung cells and splenocytes confirmed immunogenicity of the predicted virus peptides as well as cross-reactivity of the corresponding allergen peptides. Additionally, dual pentamer staining of lung cells of RSV-infected mice with the predicted candidate pair RSV A2 $L_{356\text{-}364}$ FYNSMLNNI/*Asp f* $4_{192\text{-}200}$ WYGNSALTI revealed virus- and allergen- specific $CD8^+$ T effector memory cells, as well as double positive T cells. Based on this result and the fact that several predicted candidate pairs derived from *Aspergillus fumigatus* (*Asp f),* mice were immunized with a pool of RSV A2-derived peptides that were predicted to cross-react with *Asp f*-derived peptides. *Ex-vivo* stimulation of splenocytes with the predicted *Asp f*-derived peptides resulted in increased proliferation, activation and cytokine production of $CD8^+$ T cells. Subsequently, a potentially protective effect of RSV A2 infection towards development of *Asp f*-induced experimental asthma was investigated. A preceding RSV infection resulted in less eosinophils and T2 cytokines in the BAL of allergic asthmatic animals compared to those without virus infection, as well as a trend for reduced abundance

neutrophils and T2-biased $CD8^+$ T cells in the lung. Additionally, lung histology sections confirmed less mucus-producing goblet cells and inflammation.

In order to investigate the contribution of the predicted cross-reactive T cell epitopes in the attenuation of the allergic asthmatic response, mice were immunized with the predicted RSV-derived peptides and subsequently subjected to the *Asp f*-mouse model. These animals had lower numbers of eosinophils in the BAL, displayed a trend for reduced $IL5^+$ $CD8^+$ T cells and increased abundance of $IFN\gamma^+$ $CD8^+$ T cells in the lung compared to allergic asthmatic mice without prior peptide immunization.

In addition to RSV A2, candidate epitope pairs for the virus strains of the seasonal quadrivalent influenza vaccine 2019/2020 (QIV) were predicted and validated *in-vitro*. A mouse model of influenza vaccination was established, inducing both humoral response and virus-specific T cell response. Mice were vaccinated with the QIV and *ex-vivo* stimulation of splenocytes with the predicted allergen peptides resulted in increased induction of activated $CD8^+$ $CD69^+$ T cells compared to control stimulation and mock animals. Subsequently, QIV immunization was combined with an HDM-induced experimental asthma model and, similarly to the RSV/*Asp f* model, hallmarks of allergic asthma were attenuated, including numbers of eosinophils, lung inflammation and mucus production.

In summary, these data confirm virus-induced heterologous immune responses towards environmental allergens, which result in attenuation of allergen-mediated experimental asthma. Several epidemiologically relevant respiratory RNA viruses play a role in this regard. A more extensive virus peptide pool may be needed to induce the same degree of attenuation with peptide immunization versus virus infection. Further experiments using human biomaterial for investigation of cross-reactive T cell populations among asthmatic and healthy individuals who have or have not been vaccinated against influenza or following specific virus infections would support the translational potential of our findings. Evidence in this regard will have important implications for future peptide vaccination strategies, inducing dual antiviral and anti-allergic potential.

7. Zusammenfassung

Asthma ist eine der bedeutendsten chronischen Entzündungserkrankungen weltweit. Infektionen mit respiratorischen Viren sowie die Expositionen mit Allergenen stellen wichtige Risikofaktoren für die Entwicklung von Asthma dar. Unsere Arbeitsgruppe hat kürzlich einen Influenzavirus-vermittelten protektiven Effekt gegenüber experimentellem Asthma in einem Mausmodell gezeigt, welcher abhängig von kreuzreaktiven T-Effektor-Gedächtniszellen war. Die Hypothese dieser Forschungsarbeit war, dass die virusvermittelte heterologe Immunantwort ein breit anwendbares Konzept für verschiedene Atemwegsviren und Umweltallergene ist. Diese Immunantwort könnte durch kreuzreaktive virusspezifische T-Gedächtniszellen vermittelt werden, die bei Allergenexposition mit einer T1-gesteuerten Immunantwort reagieren. Um diese Hypothese zu untersuchen, wurde eine umfangreiche *in-silico* Pipeline zur Vorhersage von potenziellen kreuzreaktiven T-Zell Epitoppaaren entwickelt. Diese berücksichtigt sowohl die MHC Bindungsaffinität, als auch die Sequenzähnlichkeit von den T-Zell Epitopen. Ein zusätzliches Bewertungssystem charakterisierte und priorisierte das Allergengegenstück basierend auf klinischer Relevanz. Die MHC Bindung der vorhergesagten Maus Balb/c MHC Klasse I Epitoppaare wurde in einem *in-vitro* Experiment validiert und positive Bindungspaare wurden für fortfolgende *ex-vivo* und *in-vivo* Analysen verwendet. Mit Hilfe von *ex-vivo* Stimulationsversuchen in einem RSV Mausmodell konnten Immunogenität der vorhergesagten Viruspeptide, sowie Kreuzreaktivität der korrespondierenden Allergenpeptide in Lungen- und Milzzellen bestätigt werden. Zusätzlich zeigte eine duale Pentamer-Färbung mit dem vorhergesagten Kandidatenpaar RSV A2 $L_{356\text{-}364}$ FYNSMLNNI/Asp f $_{4192\text{-}200}$ WYGNSALTI virus- und allergenspezifische sowie doppelt positive $CD8^+$ T-Effektor-Gedächtniszellen in Lungenzellen von RSV-infizierten Mäusen. Basierend auf diesem Ergebnis und der Tatsache, dass mehrere vorhergesagte Kandidatenpaare von *Aspergillus fumigatus* (*Asp f*) stammen, wurden Mäuse mit einem Pool von RSV A2 stammenden Peptiden immunisiert, von denen vorhergesagt wurde, dass sie mit von *Asp f* stammenden Peptiden kreuzreagieren. Die *ex-vivo* Stimulation von Milzzellen mit den vorhergesagten Allergenpeptiden führte zu einer erhöhten Proliferation, Aktivierung und Zytokinproduktion von $CD8^+$ T-Zellen. Daraufhin wurde ein potenziell protektiver Effekt einer RSV A2 Infektion auf die Entwicklung von *Asp f*-induziertem experimentellem Asthma untersucht. Eine vorrangehende Virusinfektion führte zu weniger Eosinophilen und T2-assoziierten Zytokinen in der BAL in allergisch asthmatischen Mäusen im Vergleich zu solchen ohne

Virusinfektion, sowie einem Trend für eine reduzierte Häufigkeit von Neutrophilen und T2-assoziierten $CD8^+$ T-Zellen in der Lunge. Des Weiteren konnte in Lungenhistologie-Schnitten eine verringerte Anzahl an Schleim-produzierende Becherzellen und weniger Entzündung detektiert werden. Um den Einfluss der vorhergesagten kreuzreaktiven T-Zell-Epitope zur Abschwächung der allergischen Reaktion zu untersuchen, wurden Mäuse mit den vorhergesagten, von RSV stammenden Peptiden immunisiert und anschließend dem *Asp f*-Mausmodell unterzogen. Diese Tiere wiesen im Vergleich zu Mäusen mit allergischem Asthma ohne vorherige Peptidimmunisierung eine geringere Anzahl an Eosinophilen in der BAL auf, sowie eine leichte Verringerung von IL-5^+ $CD8^+$ T Zellen und einer erhöhten Häufigkeit von IFNγ^+ $CD8^+$ T-Zellen in Lungenzellen.

Neben RSV A2 wurden Epitoppaare für die Virusstämme des saisonalen quadrivalenten Influenza-Impfstoffs 2019/2020 (QIV) vorhergesagt und *in-vitro* validiert. Ein Mausmodell der Influenza-Impfung wurde etabliert, welches sowohl eine Antikörperantwort als auch eine virusspezifische T-Zell-Antwort induziert. Eine *ex-vivo* Stimulation von Milzzellen mit den vorhergesagten Allergenpeptiden führte zu einer erhöhten relativen Häufigkeit aktivierter $CD8^+$ $CD69^+$ T-Zellen im Vergleich zu dem Kontrollstimulus in QIV immunisierten Mäusen und nicht-immunisierten Tieren. Anschließend wurde die QIV-Immunisierung mit einem HDM-induzierten experimentellen Asthmamodell kombiniert und eine Reduktion verschiedener Merkmale von allergischem Asthma wurde hier ähnlich wie in dem RSV/*Asp f* Modell beobachtet, einschließlich der Anzahl von Eosinophilen, Lungenentzündung und Schleimproduktion.

Zusammenfassend bestätigen diese Daten eine virusinduzierte heterologe Immunantworten auf Umweltallergene, die zu einer Abschwächung des Allergen-vermittelten experimentellen Asthmas führen. Dabei spielen mehrere epidemiologisch relevante respiratorische RNA-Viren eine Rolle. Ein erweiterter Virus-Peptidpool könnte erforderlich sein, um den gleichen Grad an Reduktion des allergischen Asthmas mit einer Peptid-Immunisierung gegenüber einer Virusinfektion zu induzieren. Weitere Experimente mit menschlichem Biomaterial zur Untersuchung kreuzreaktiver T-Zell-Populationen bei Asthmatikern und gesunden Personen, mit oder ohne Influenza Impfung, oder nach spezifischen Virusinfektionen, würden das translationale Potenzial unserer Ergebnisse unterstützen. Beweise in dieser Hinsicht könnten wichtige Implikationen für zukünftige Impfstrategien mit Peptiden haben, welche eine doppelte anti-virale und anti-allergische Antwort induzieren.

8. References

Aaby, P.; Bhuiya, A.; Nahar, L.; Knudsen, K.; Francisco, A. de; Strong, M. The survival benefit of measles immunization may not be explained entirely by the prevention of measles disease: a community study from rural Bangladesh. *International journal of epidemiology* **2003,** *32* (1), 106–116. DOI: 10.1093/ije/dyg005.

Aaby, P.; Gustafson, P.; Roth, A.; Rodrigues, A.; Fernandes, M.; Sodemann, M.; Holmgren, B.; Benn, C. S.; Garly, M.-L.; Lisse, I. M.; Jensen, H. Vaccinia scars associated with better survival for adults. An observational study from Guinea-Bissau. *Vaccine* **2006,** *24* (29-30), 5718–5725. DOI: 10.1016/j.vaccine.2006.04.045.

Aaby, P.; Martins, C. L.; Garly, M.-L.; Rodrigues, A.; Benn, C. S.; Whittle, H. The optimal age of measles immunisation in low-income countries: a secondary analysis of the assumptions underlying the current policy. *BMJ open* **2012,** *2* (4). DOI: 10.1136/bmjopen-2011-000761.

Aaby, P.; Rodrigues, A.; Biai, S.; Martins, C.; Veirum, J. E.; Benn, C. S.; Jensen, H. Oral polio vaccination and low case fatality at the paediatric ward in Bissau, Guinea-Bissau. *Vaccine* **2004,** *22* (23-24), 3014–3017. DOI: 10.1016/j.vaccine.2004.02.009.

Abbas, A. A.; Taylor, L. J.; Dothard, M. I.; Leiby, J. S.; Fitzgerald, A. S.; Khatib, L. A.; Collman, R. G.; Bushman, F. D. Redondoviridae, a Family of Small, Circular DNA Viruses of the Human Oro-Respiratory Tract Associated with Periodontitis and Critical Illness. *Cell host & microbe* **2019,** *25* (5), 719-729.e4. DOI: 10.1016/j.chom.2019.04.001.

Abeles, S. R.; Pride, D. T. Molecular bases and role of viruses in the human microbiome. *Journal of molecular biology* **2014,** *426* (23), 3892–3906. DOI: 10.1016/j.jmb.2014.07.002.

Al-Garawi, A.; Fattouh, R.; Botelho, F.; Walker, T. D.; Goncharova, S.; Moore, C.-L.; Mori, M.; Erjefalt, J. S.; Chu, D. K.; Humbles, A. A.; Kolbeck, R.; Stampfli, M. R.; O'Byrne, P. M.; Coyle, A. J.; Jordana, M. Influenza A facilitates sensitization to house dust mite in infant mice leading to an asthma phenotype in adulthood. *Mucosal immunology* **2011,** *4* (6), 682–694. DOI: 10.1038/mi.2011.35.

Altamirano-Lagos, M. J.; Díaz, F. E.; Mansilla, M. A.; Rivera-Pérez, D.; Soto, D.; McGill, J. L.; Vasquez, A. E.; Kalergis, A. M. Current Animal Models for Understanding the

Pathology Caused by the Respiratory Syncytial Virus. *Frontiers in microbiology* **2019,** *10*, 873. DOI: 10.3389/fmicb.2019.00873.

Amo, A.; Rodríguez-Pérez, R.; Blanco, J.; Villota, J.; Juste, S.; Moneo, I.; Caballero, M. L. Gal d 6 is the second allergen characterized from egg yolk. *Journal of agricultural and food chemistry* **2010,** *58* (12), 7453–7457. DOI: 10.1021/jf101403h.

Andreatta, M.; Karosiene, E.; Rasmussen, M.; Stryhn, A.; Buus, S.; Nielsen, M. Accurate pan-specific prediction of peptide-MHC class II binding affinity with improved binding core identification. *Immunogenetics* **2015,** *67* (11-12), 641–650. DOI: 10.1007/s00251-015-0873-y.

Antonelli, A. C. B.; Almeida, V. P.; Castro, F. O. F. de; Silva, J. M.; Pfrimer, I. A. H.; Cunha-Neto, E.; Maranhão, A. Q.; Brígido, M. M.; Resende, R. O.; Bocca, A. L.; Fonseca, S. G. In silico construction of a multiepitope Zika virus vaccine using immunoinformatics tools. *Scientific reports* **2022,** *12* (1), 53. DOI: 10.1038/s41598-021-03990-6.

Arstila, T. P.; Casrouge, A.; Baron, V.; Even, J.; Kanellopoulos, J.; Kourilsky, P. A direct estimate of the human alphabeta T cell receptor diversity. *Science (New York, N.Y.)* **1999,** *286* (5441), 958–961. DOI: 10.1126/science.286.5441.958.

Bach, J.-F. The effect of infections on susceptibility to autoimmune and allergic diseases. *The New England journal of medicine* **2002,** *347* (12), 911–920. DOI: 10.1056/NEJMra020100.

Bach, J.-F. The hygiene hypothesis in autoimmunity: the role of pathogens and commensals. *Nature reviews. Immunology* **2018,** *18* (2), 105–120. DOI: 10.1038/nri.2017.111.

Balz, K.; Kaushik, A.; Chen, M.; Cemic, F.; Heger, V.; Renz, H.; Nadeau, K.; Skevaki, C. Homologies between SARS-CoV-2 and allergen proteins may direct T cell-mediated heterologous immune responses. *Scientific reports* **2021,** *11* (1), 4792. DOI: 10.1038/s41598-021-84320-8.

Balz, K.; Trassl, L.; Härtel, V.; Nelson, P. P.; Skevaki, C. Virus-Induced T Cell-Mediated Heterologous Immunity and Vaccine Development. *Front. Immunol.* **2020,** *11*, 513. DOI: 10.3389/fimmu.2020.00513.

Barcik, W.; Boutin, R. C. T.; Sokolowska, M.; Finlay, B. B. The Role of Lung and Gut Microbiota in the Pathology of Asthma. *Immunity* **2020,** *52* (2), 241–255. DOI: 10.1016/j.immuni.2020.01.007.

Barnett, L. A.; Fujinami, R. S. Molecular mimicry: a mechanism for autoimmune injury. *FASEB journal : official publication of the Federation of American Societies for Experimental Biology* **1992,** *6* (3), 840–844. DOI: 10.1096/fasebj.6.3.1740233.

Barrios, C.; Brawand, P.; Berney, M.; Brandt, C.; Lambert, P. H.; Siegrist, C. A. Neonatal and early life immune responses to various forms of vaccine antigens qualitatively differ from adult responses: predominance of a Th2-biased pattern which persists after adult boosting. *European journal of immunology* **1996,** *26* (7), 1489–1496. DOI: 10.1002/eji.1830260713.

Bazhan, S. I.; Antonets, D. V.; Starostina, E. V.; Ilyicheva, T. N.; Kaplina, O. N.; Marchenko, V. Y.; Volkova, O. Y.; Bakulina, A. Y.; Karpenko, L. I. In silico design of influenza a virus artificial epitope-based T-cell antigens and the evaluation of their immunogenicity in mice. *Journal of biomolecular structure & dynamics* [Online] **2020**, 1–17.

Betts, R. J.; Kemeny, D. M. CD8+ T cells in asthma: friend or foe? *Pharmacology & therapeutics* **2009,** *121* (2), 123–131. DOI: 10.1016/j.pharmthera.2008.09.001.

Beuther, D. A.; Sutherland, E. R. Overweight, obesity, and incident asthma: a meta-analysis of prospective epidemiologic studies. *Am J Respir Crit Care Med* **2007,** *175* (7), 661–666. DOI: 10.1164/rccm.200611-1717OC.

Birmingham, J. M.; Gillespie, V. L.; Srivastava, K.; Li, X.-M.; Busse, P. J. Influenza A infection enhances antigen-induced airway inflammation and hyperresponsiveness in young but not aged mice. *Clinical and experimental allergy : journal of the British Society for Allergy and Clinical Immunology* **2014,** *44* (9), 1188–1199. DOI: 10.1111/cea.12365.

Blank, S.; Seismann, H.; McIntyre, M.; Ollert, M.; Wolf, S.; Bantleon, F. I.; Spillner, E. Vitellogenins are new high molecular weight components and allergens (Api m 12 and Ves v 6) of Apis mellifera and Vespula vulgaris venom. *PloS one* **2013,** *8* (4), e62009. DOI: 10.1371/journal.pone.0062009.

Blok, B. A.; Arts, R. J. W.; van Crevel, R.; Benn, C. S.; Netea, M. G. Trained innate immunity as underlying mechanism for the long-term, nonspecific effects of vaccines. *Journal of leukocyte biology* **2015,** *98* (3), 347–356. DOI: 10.1189/jlb.5RI0315-096R.

Bowyer, P.; Fraczek, M.; Denning, D. W. Comparative genomics of fungal allergens and epitopes shows widespread distribution of closely related allergen and

epitope orthologues. *BMC genomics* **2006,** *7*, 251. DOI: 10.1186/1471-2164-7-251.

Braun, J.; Loyal, L.; Frentsch, M.; Wendisch, D.; Georg, P.; Kurth, F.; Hippenstiel, S.; Dingeldey, M.; Kruse, B.; Fauchere, F.; Baysal, E.; Mangold, M.; Henze, L.; Lauster, R.; Mall, M. A.; Beyer, K.; Röhmel, J.; Voigt, S.; Schmitz, J.; Miltenyi, S.; Demuth, I.; Müller, M. A.; Hocke, A.; Witzenrath, M.; Suttorp, N.; Kern, F.; Reimer, U.; Wenschuh, H.; Drosten, C.; Corman, V. M.; Giesecke-Thiel, C.; Sander, L. E.; Thiel, A. SARS-CoV-2-reactive T cells in healthy donors and patients with COVID-19. *Nature* **2020,** *587* (7833), 270–274. DOI: 10.1038/s41586-020-2598-9.

Braun-Fahrländer, C.; Gassner, M.; Grize, L.; Neu, U.; Sennhauser, F. H.; Varonier, H. S.; Vuille, J. C.; Wüthrich, B. Prevalence of hay fever and allergic sensitization in farmer's children and their peers living in the same rural community. SCARPOL team. Swiss Study on Childhood Allergy and Respiratory Symptoms with Respect to Air Pollution. *Clinical and experimental allergy : journal of the British Society for Allergy and Clinical Immunology* **1999,** *29* (1), 28–34. DOI: 10.1046/j.1365-2222.1999.00479.x.

Brigham, E. P.; West, N. E. Diagnosis of asthma: diagnostic testing. *International Forum of Allergy and Rhinology* **2015,** *5 Suppl 1* (S1), S27-30. DOI: 10.1002/alr.21597.

Bufe, A.; Gehlhar, K.; Grage-Griebenow, E.; Ernst, M. Atopic phenotype in children is associated with decreased virus-induced interferon-alpha release. *International archives of allergy and immunology* **2002,** *127* (1), 82–88. DOI: 10.1159/000048173.

Buhl, R.; Bals, R.; Baur, X.; Berdel, D.; Criée, C.-P.; Gappa, M.; Gillissen, A.; Greulich, T.; Haidl, P.; Hamelmann, E.; Horak, F.; Kardos, P.; Kenn, K.; Klimek, L.; Korn, S.; Magnussen, H.; Nowak, D.; Pfaar, O.; Rabe, K. F.; Riedler, J.; Ritz, T.; Schultz, K.; Schuster, A.; Spindler, T.; Taube, C.; Vogelmeier, C.; Leupoldt, A. von; Wantke, F.; Wildhaber, J.; Worth, H.; Zacharasiewicz, A.; Lommatzsch, M. S2k-Leitlinie zur Diagnostik und Therapie von Patienten mit Asthma – Addendum 2020. *Pneumologie (Stuttgart, Germany)* **2021,** *75* (3), 191–200. DOI: 10.1055/a-1352-0296.

Burke, H.; Leonardi-Bee, J.; Hashim, A.; Pine-Abata, H.; Chen, Y.; Cook, D. G.; Britton, J. R.; McKeever, T. M. Prenatal and passive smoke exposure and incidence of

asthma and wheeze: systematic review and meta-analysis. *Pediatrics* **2012,** *129* (4), 735–744. DOI: 10.1542/peds.2011-2196.

Busse, W. W.; Lemanske, R. F. Asthma. *The New England journal of medicine* **2001,** *344* (5), 350–362. DOI: 10.1056/NEJM200102013440507.

Buus, S.; Lauemøller, S. L.; Worning, P.; Kesmir, C.; Frimurer, T.; Corbet, S.; Fomsgaard, A.; Hilden, J.; Holm, A.; Brunak, S. Sensitive quantitative predictions of peptide-MHC binding by a 'Query by Committee' artificial neural network approach. *Tissue antigens* **2003,** *62* (5), 378–384. DOI: 10.1034/j.1399-0039.2003.00112.x.

Calamelli, E.; Trozzo, A.; Di Blasi, E.; Serra, L.; Bottau, P. Hazelnut Allergy. *Medicina (Kaunas, Lithuania)* **2021,** *57* (1). DOI: 10.3390/medicina57010067.

Calis, J. J. A.; Maybeno, M.; Greenbaum, J. A.; Weiskopf, D.; Silva, A. D. de; Sette, A.; Keşmir, C.; Peters, B. Properties of MHC class I presented peptides that enhance immunogenicity. *PLoS computational biology* **2013,** *9* (10), e1003266. DOI: 10.1371/journal.pcbi.1003266.

Camacho, C.; Coulouris, G.; Avagyan, V.; Ma, N.; Papadopoulos, J.; Bealer, K.; Madden, T. L. BLAST+: architecture and applications. *BMC Bioinformatics* **2009,** *10*, 421. DOI: 10.1186/1471-2105-10-421.

Cantani, A. The growing genetic links and the early onset of atopic diseases in children stress the unique role of the atopic march: a meta-analysis. *Journal of investigational allergology & clinical immunology* **1999,** *9* (5), 314–320.

Carli, G.; Cecchi, L.; Stebbing, J.; Parronchi, P.; Farsi, A. Is asthma protective against COVID-19? *Allergy* **2021,** *76* (3), 866–868. DOI: 10.1111/all.14426.

Cheung, D. S.; Grayson, M. H. Role of viruses in the development of atopic disease in pediatric patients. *Current allergy and asthma reports* **2012,** *12* (6), 613–620. DOI: 10.1007/s11882-012-0295-y.

Choi, S.; Sohn, K.-H.; Jung, J.-W.; Kang, M.-G.; Yang, M.-S.; Kim, S.; Choi, J.-H.; Cho, S.-H.; Kang, H.-R.; Yi, H. Lung virome: New potential biomarkers for asthma severity and exacerbation. *The Journal of allergy and clinical immunology* **2021,** *148* (4), 1007-1015.e9. DOI: 10.1016/j.jaci.2021.03.017.

Cianferoni, A. Non-IgE Mediated Food Allergy. *CPR* **2020,** *16* (2), 95–105. DOI: 10.2174/1573396315666191031103714.

Clute, S. C.; Watkin, L. B.; Cornberg, M.; Naumov, Y. N.; Sullivan, J. L.; Luzuriaga, K.; Welsh, R. M.; Selin, L. K. Cross-reactive influenza virus-specific CD8+ T cells

contribute to lymphoproliferation in Epstein-Barr virus-associated infectious mononucleosis. *The Journal of clinical investigation* **2005,** *115* (12), 3602–3612. DOI: 10.1172/JCI25078.

Coca, A. F.; Cooke, R. A. On the Classification of the Phenomena of Hypersensitiveness. *The Journal of Immunology* **1923,** *8* (3), 163.

Cock, P. J. A.; Antao, T.; Chang, J. T.; Chapman, B. A.; Cox, C. J.; Dalke, A.; Friedberg, I.; Hamelryck, T.; Kauff, F.; Wilczynski, B.; Hoon, M. J. L. de. Biopython: freely available Python tools for computational molecular biology and bioinformatics. *Bioinformatics (Oxford, England)* **2009,** *25* (11), 1422–1423. DOI: 10.1093/bioinformatics/btp163.

Debarry, J.; Garn, H.; Hanuszkiewicz, A.; Dickgreber, N.; Blümer, N.; Mutius, E. von; Bufe, A.; Gatermann, S.; Renz, H.; Holst, O.; Heine, H. Acinetobacter lwoffii and Lactococcus lactis strains isolated from farm cowsheds possess strong allergy-protective properties. *The Journal of allergy and clinical immunology* **2007,** *119* (6), 1514–1521. DOI: 10.1016/j.jaci.2007.03.023.

Deng, Y.; Guan, M.; Xie, X.; Yang, X.; Xiang, H.; Li, H.; Zou, L.; Wei, J.; Wang, D.; Deng, X. Geniposide inhibits airway inflammation and hyperresponsiveness in a mouse model of asthma. *International immunopharmacology* **2013,** *17* (3), 561–567. DOI: 10.1016/j.intimp.2013.06.028.

Dhanda, S. K.; Karosiene, E.; Edwards, L.; Grifoni, A.; Paul, S.; Andreatta, M.; Weiskopf, D.; Sidney, J.; Nielsen, M.; Peters, B.; Sette, A. Predicting HLA CD4 Immunogenicity in Human Populations. *Front. Immunol.* **2018,** *9*, 1369. DOI: 10.3389/fimmu.2018.01369.

D'Orsogna, L. J. A.; Roelen, D. L.; Doxiadis, I. I. N.; Claas, F. H. J. Alloreactivity from human viral specific memory T-cells. *Transplant immunology* **2010,** *23* (4), 149–155. DOI: 10.1016/j.trim.2010.06.008.

Dulek, D. E.; Peebles, R. S. Viruses and asthma☆. *Biochimica et Biophysica Acta. General Subjects* **2011,** *1810* (11), 1080–1090. DOI: 10.1016/j.bbagen.2011.01.012.

Edwards, M. R.; Strong, K.; Cameron, A.; Walton, R. P.; Jackson, D. J.; Johnston, S. L. Viral infections in allergy and immunology: How allergic inflammation influences viral infections and illness. *The Journal of allergy and clinical immunology* **2017,** *140* (4), 909–920. DOI: 10.1016/j.jaci.2017.07.025.

Ege, M. J.; Mayer, M.; Normand, A.-C.; Genuneit, J.; Cookson, W. O. C. M.; Braun-Fahrländer, C.; Heederik, D.; Piarroux, R.; Mutius, E. von. Exposure to environmental microorganisms and childhood asthma. *The New England journal of medicine* **2011,** *364* (8), 701–709. DOI: 10.1056/NEJMoa1007302.

Eggenhuizen, P. J.; Ng, B. H.; Chang, J.; Fell, A. L.; Cheong, R. M. Y.; Wong, W. Y.; Gan, P.-Y.; Holdsworth, S. R.; Ooi, J. D. BCG Vaccine Derived Peptides Induce SARS-CoV-2 T Cell Cross-Reactivity. *Front. Immunol.* **2021,** *12*, 692729. DOI: 10.3389/fimmu.2021.692729.

Elong Ngono, A.; Shresta, S. Cross-Reactive T Cell Immunity to Dengue and Zika Viruses: New Insights Into Vaccine Development. *Front. Immunol.* **2019,** *10*, 1316. DOI: 10.3389/fimmu.2019.01316.

Emons, J. A. M.; van Gerth Wijk, R. Food Allergy and Asthma: Is There a Link? *Current treatment options in allergy* **2018,** *5* (4), 436–444. DOI: 10.1007/s40521-018-0185-1.

Fahy, J. V. Type 2 inflammation in asthma--present in most, absent in many. *Nature reviews. Immunology* **2015,** *15* (1), 57–65. DOI: 10.1038/nri3786.

Falkenhorst, G.; Harder, T.; Remschmidt, C.; Terhardt, M.; Zepp, F.; Ledig, T.; Wicker, S.; Keller-Stanislawski, B.; Mertens, T. Background paper to the recommendation for the preferential use of live-attenuated influenza vaccine in children aged 2-6 years in Germany. *Bundesgesundheitsblatt, Gesundheitsforschung, Gesundheitsschutz* **2013,** *56* (11), 1557–1564. DOI: 10.1007/s00103-013-1844-9.

Fischer, W. A.; King, L. S.; Lane, A. P.; Pekosz, A. Restricted replication of the live attenuated influenza A virus vaccine during infection of primary differentiated human nasal epithelial cells. *Vaccine* **2015,** *33* (36), 4495–4504. DOI: 10.1016/j.vaccine.2015.07.023.

Frankild, S.; Boer, R. J. de; Lund, O.; Nielsen, M.; Kesmir, C. Amino acid similarity accounts for T cell cross-reactivity and for "holes" in the T cell repertoire. *PloS one* **2008,** *3* (3), e1831. DOI: 10.1371/journal.pone.0001831.

Freer, G.; Maggi, F.; Pifferi, M.; Di Cicco, M. E.; Peroni, D. G.; Pistello, M. The Virome and Its Major Component, Anellovirus, a Convoluted System Molding Human Immune Defenses and Possibly Affecting the Development of Asthma and Respiratory Diseases in Childhood. *Frontiers in microbiology* **2018,** *9*, 686. DOI: 10.3389/fmicb.2018.00686.

Freyne, B.; Donath, S.; Germano, S.; Gardiner, K.; Casalaz, D.; Robins-Browne, R. M.; Amenyogbe, N.; Messina, N. L.; Netea, M. G.; Flanagan, K. L.; Kollmann, T.; Curtis, N. Neonatal BCG Vaccination Influences Cytokine Responses to Toll-like Receptor Ligands and Heterologous Antigens. *The Journal of infectious diseases* **2018,** *217* (11), 1798–1808. DOI: 10.1093/infdis/jiy069.

Gandhi, N. A.; Bennett, B. L.; Graham, N. M. H.; Pirozzi, G.; Stahl, N.; Yancopoulos, G. D. Targeting key proximal drivers of type 2 inflammation in disease. *Nature reviews. Drug discovery* **2016,** *15* (1), 35–50. DOI: 10.1038/nrd4624.

Gartler, S. M. Apparent Hela cell contamination of human heteroploid cell lines. *Nature* **1968,** *217* (5130), 750–751. DOI: 10.1038/217750a0.

Gavala, M. L.; Bashir, H.; Gern, J. E. Virus/allergen interactions in asthma. *Current allergy and asthma reports* **2013,** *13* (3), 298–307. DOI: 10.1007/s11882-013-0344-1.

Geerdink, R. J.; Pillay, J.; Meyaard, L.; Bont, L. Neutrophils in respiratory syncytial virus infection: A target for asthma prevention. *The Journal of allergy and clinical immunology* **2015,** *136* (4), 838–847. DOI: 10.1016/j.jaci.2015.06.034.

Gent, J. F.; Kezik, J. M.; Hill, M. E.; Tsai, E.; Li, D.-W.; Leaderer, B. P. Household mold and dust allergens: exposure, sensitization and childhood asthma morbidity. *Environmental Research* **2012,** *118*, 86–93. DOI: 10.1016/j.envres.2012.07.005.

Gill, M. A.; Liu, A. H.; Calatroni, A.; Krouse, R. Z.; Shao, B.; Schiltz, A.; Gern, J. E.; Togias, A.; Busse, W. W. Enhanced plasmacytoid dendritic cell antiviral responses after omalizumab. *The Journal of allergy and clinical immunology* **2017,** *141* (5), 1735-1743.e9. DOI: 10.1016/j.jaci.2017.07.035.

Global Initiative for Asthma - GINA. Reports - Global Initiative for Asthma - GINA: https://ginasthma.org/wp-content/uploads/2021/05/GINA-Main-Report-2021-V2-WMS.pdf. https://ginasthma.org/reports/ (accessed September 28, 2021).

Gomez-Perosanz, M.; Sanchez-Trincado, J. L.; Fernandez-Arquero, M.; Sidney, J.; Sette, A.; Lafuente, E. M.; Reche, P. A. Human rhinovirus-specific CD8 T cell responses target conserved and unusual epitopes. *FASEB journal : official publication of the Federation of American Societies for Experimental Biology* **2021,** *35* (1), e21208. DOI: 10.1096/fj.202002165R.

Graham, B. S.; Perkins, M. D.; Wright, P. F.; Karzon, D. T. Primary respiratory syncytial virus infection in mice. *Journal of medical virology* **1988,** *26* (2), 153–162. DOI: 10.1002/jmv.1890260207.

Grifoni, A.; Pham, J.; Sidney, J.; O'Rourke, P. H.; Paul, S.; Peters, B.; Martini, S. R.; Silva, A. D. de; Ricciardi, M. J.; Magnani, D. M.; Silveira, C. G. T.; Maestri, A.; Costa, P. R.; de-Oliveira-Pinto, L. M.; Azeredo, E. L. de; Damasco, P. V.; Phillips, E.; Mallal, S.; Silva, A. M. de; Collins, M.; Durbin, A.; Diehl, S. A.; Cerpas, C.; Balmaseda, A.; Kuan, G.; Coloma, J.; Harris, E.; Crowe, J. E.; Stone, M.; Norris, P. J.; Busch, M.; Vivanco-Cid, H.; Cox, J.; Graham, B. S.; Ledgerwood, J. E.; Turtle, L.; Solomon, T.; Kallas, E. G.; Watkins, D. I.; Weiskopf, D.; Sette, A. Prior Dengue Virus Exposure Shapes T Cell Immunity to Zika Virus in Humans. *Journal of virology* **2017,** *91* (24). DOI: 10.1128/JVI.01469-17.

Grifoni, A.; Weiskopf, D.; Ramirez, S. I.; Mateus, J.; Dan, J. M.; Moderbacher, C. R.; Rawlings, S. A.; Sutherland, A.; Premkumar, L.; Jadi, R. S.; Marrama, D.; Silva, A. M. de; Frazier, A.; Carlin, A. F.; Greenbaum, J. A.; Peters, B.; Krammer, F.; Smith, D. M.; Crotty, S.; Sette, A. Targets of T Cell Responses to SARS-CoV-2 Coronavirus in Humans with COVID-19 Disease and Unexposed Individuals. *Cell* **2020,** *181* (7), 1489-1501.e15. DOI: 10.1016/j.cell.2020.05.015.

Groves, H. T.; McDonald, J. U.; Langat, P.; Kinnear, E.; Kellam, P.; McCauley, J.; Ellis, J.; Thompson, C.; Elderfield, R.; Parker, L.; Barclay, W.; Tregoning, J. S. Mouse Models of Influenza Infection with Circulating Strains to Test Seasonal Vaccine Efficacy. *Front. Immunol.* **2018,** *9*, 126. DOI: 10.3389/fimmu.2018.00126.

Guarnieri, M.; Balmes, J. R. Outdoor air pollution and asthma. *The Lancet* **2014,** *383* (9928), 1581–1592. DOI: 10.1016/S0140-6736(14)60617-6.

Haahtela, T. A biodiversity hypothesis. *Allergy* **2019,** *74* (8), 1445–1456. DOI: 10.1111/all.13763.

Haczku, A.; Atochina, E. N.; Tomer, Y.; Chen, H.; Scanlon, S. T.; Russo, S.; Xu, J.; Panettieri, R. A.; Beers, M. F. Aspergillus fumigatus-induced allergic airway inflammation alters surfactant homeostasis and lung function in BALB/c mice. *American journal of respiratory cell and molecular biology* **2001,** *25* (1), 45–50. DOI: 10.1165/ajrcmb.25.1.4391.

Hammad, H.; Lambrecht, B. N. The basic immunology of asthma. *Cell* **2021,** *184* (6), 1469–1485. DOI: 10.1016/j.cell.2021.02.016.

Han, H.; Roan, F.; Ziegler, S. F. The atopic march: current insights into skin barrier dysfunction and epithelial cell-derived cytokines. *Immunological reviews* **2017,** *278* (1), 116–130. DOI: 10.1111/imr.12546.

Han, H. J.; Song, M.-S.; Park, S.-J.; Byun, H. Y.; Robles, N. J. C.; Ha, S.-H.; Choi, Y. K. Efficacy of A/H1N1/2009 split inactivated influenza A vaccine (GC1115) in mice and ferrets. *Journal of microbiology (Seoul, Korea)* **2019,** *57* (2), 163–169. DOI: 10.1007/s12275-019-8504-1.

Hanski, I.; Hertzen, L. von; Fyhrquist, N.; Koskinen, K.; Torppa, K.; Laatikainen, T.; Karisola, P.; Auvinen, P.; Paulin, L.; Mäkelä, M. J.; Vartiainen, E.; Kosunen, T. U.; Alenius, H.; Haahtela, T. Environmental biodiversity, human microbiota, and allergy are interrelated. *Proceedings of the National Academy of Sciences of the United States of America* **2012,** *109* (21), 8334–8339. DOI: 10.1073/pnas.1205624109.

Haspeslagh, E.; Heyndrickx, I.; Hammad, H.; Lambrecht, B. N. The hygiene hypothesis: immunological mechanisms of airway tolerance. *Current Opinion in Immunology* **2018,** *54*, 102–108. DOI: 10.1016/j.coi.2018.06.007.

Heinrich, J.; Hoelscher, B.; Frye, C.; Meyer, I.; Wjst, M.; Wichmann, H. E. Trends in prevalence of atopic diseases and allergic sensitization in children in Eastern Germany. *The European respiratory journal* **2002,** *19* (6), 1040–1046. DOI: 10.1183/09031936.02.00261802.

Hertzen, L. von; Hanski, I.; Haahtela, T. Natural immunity. Biodiversity loss and inflammatory diseases are two global megatrends that might be related. *EMBO reports* **2011,** *12* (11), 1089–1093. DOI: 10.1038/embor.2011.195.

Higgins, J. P. T.; Soares-Weiser, K.; López-López, J. A.; Kakourou, A.; Chaplin, K.; Christensen, H.; Martin, N. K.; Sterne, J. A. C.; Reingold, A. L. Association of BCG, DTP, and measles containing vaccines with childhood mortality: systematic review. *BMJ (Clinical research ed.)* **2016,** *355*, i5170. DOI: 10.1136/bmj.i5170.

Hill, D. A.; Grundmeier, R. W.; Ram, G.; Spergel, J. M. The epidemiologic characteristics of healthcare provider-diagnosed eczema, asthma, allergic rhinitis, and food allergy in children: a retrospective cohort study. *BMC pediatrics* **2016,** *16*, 133. DOI: 10.1186/s12887-016-0673-z.

Hill, D. A.; Spergel, J. M. The atopic march: Critical evidence and clinical relevance. *Annals of allergy, asthma & immunology : official publication of the American*

College of Allergy, Asthma, & Immunology **2018,** *120* (2), 131–137. DOI: 10.1016/j.anai.2017.10.037.

Hinks, T. S. C.; Hoyle, R. D.; Gelfand, E. W. CD8+ Tc2 cells: underappreciated contributors to severe asthma. *European respiratory review : an official journal of the European Respiratory Society* **2019,** *28* (154). DOI: 10.1183/16000617.0092-2019.

Hoft, D. F.; Babusis, E.; Worku, S.; Spencer, C. T.; Lottenbach, K.; Truscott, S. M.; Abate, G.; Sakala, I. G.; Edwards, K. M.; Creech, C. B.; Gerber, M. A.; Bernstein, D. I.; Newman, F.; Graham, I.; Anderson, E. L.; Belshe, R. B. Live and inactivated influenza vaccines induce similar humoral responses, but only live vaccines induce diverse T-cell responses in young children. *The Journal of infectious diseases* **2011,** *204* (6), 845–853. DOI: 10.1093/infdis/jir436.

Holgate, S. T. Innate and adaptive immune responses in asthma. *Nat Med* **2012,** *18* (5), 673–683. DOI: 10.1038/nm.2731.

Holgate, S. T.; Wenzel, S.; Postma, D. S.; Weiss, S. T.; Renz, H.; Sly, P. D. Asthma. *Nature Reviews. Disease Primers* **2015,** *1* (1). DOI: 10.1038/nrdp.2015.25.

Hoof, I.; Peters, B.; Sidney, J.; Pedersen, L. E.; Sette, A.; Lund, O.; Buus, S.; Nielsen, M. NetMHCpan, a method for MHC class I binding prediction beyond humans. *Immunogenetics* **2009,** *61* (1), 1–13. DOI: 10.1007/s00251-008-0341-z.

Hou, A.; Silverberg, J. I. Increasing rates of influenza vaccination were associated with lower asthma prevalence in United States children. *Allergy* **2021,** *76* (7), 2273–2275. DOI: 10.1111/all.14790.

Hu, C.; Shen, M.; Han, X.; Chen, Q.; Li, L.; Chen, S.; Zhang, J.; Gao, F.; Wang, W.; Wang, Y.; Li, T.; Li, S.; Huang, J.; Wang, J.; Zhu, J.; Chen, D.; Wu, Q.; Tao, K.; Da Pang; Jin, A. Identification of cross-reactive CD8+ T cell receptors with high functional avidity to a SARS-CoV-2 immunodominant epitope and its natural mutant variants. *Genes & diseases* **2022,** *9* (1), 216–229. DOI: 10.1016/j.gendis.2021.05.006.

Huber, M.; Lohoff, M. Change of paradigm: CD8+ T cells as important helper for CD4+ T cells during asthma and autoimmune encephalomyelitis. *Allergo journal international* **2015,** *24* (1), 8–15. DOI: 10.1007/s40629-015-0038-4.

Hulin, M.; Caillaud, D.; Annesi-Maesano, I. Indoor air pollution and childhood asthma: variations between urban and rural areas. *Indoor Air* **2010,** *20* (6), 502–514. DOI: 10.1111/j.1600-0668.2010.00673.x.

Jackson, D. J.; Busse, W. W.; Bacharier, L. B.; Kattan, M.; O'Connor, G. T.; Wood, R. A.; Visness, C. M.; Durham, S. R.; Larson, D.; Esnault, S.; Ober, C.; Gergen, P. J.; Becker, P.; Togias, A.; Gern, J. E.; Altman, M. C. Association of respiratory allergy, asthma, and expression of the SARS-CoV-2 receptor ACE2. *The Journal of allergy and clinical immunology* **2020,** *146* (1), 203-206.e3. DOI: 10.1016/j.jaci.2020.04.009.

Jackson, D. J.; Evans, M. D.; Gangnon, R. E.; Tisler, C. J.; Pappas, T. E.; Lee, W.-M.; Gern, J. E.; Lemanske, R. F. Evidence for a Causal Relationship between Allergic Sensitization and Rhinovirus Wheezing in Early Life. *Am J Respir Crit Care Med* **2012,** *185* (3), 281–285. DOI: 10.1164/rccm.201104-0660OC.

Jackson, D. J.; Gangnon, R. E.; Evans, M. D.; Roberg, K. A.; Anderson, E. L.; Pappas, T. E.; Printz, M. C.; Lee, W.-M.; Shult, P. A.; Reisdorf, E.; Carlson-Dakes, K. T.; Salazar, L. P.; DaSilva, D. F.; Tisler, C. J.; Gern, J. E.; Lemanske, R. F. Wheezing rhinovirus illnesses in early life predict asthma development in high-risk children. *American journal of respiratory and critical care medicine* **2008,** *178* (7), 667–672. DOI: 10.1164/rccm.200802-309OC.

Jackson, D. J.; Lemanske, R. F. The Role of Respiratory Virus Infections in Childhood Asthma Inception. *Immunology and Allergy Clinics of North America* **2010,** *30* (4), 513–522. DOI: 10.1016/j.iac.2010.08.004.

Jafri, H. S.; Chavez-Bueno, S.; Mejias, A.; Gomez, A. M.; Rios, A. M.; Nassi, S. S.; Yusuf, M.; Kapur, P.; Hardy, R. D.; Hatfield, J.; Rogers, B. B.; Krisher, K.; Ramilo, O. Respiratory syncytial virus induces pneumonia, cytokine response, airway obstruction, and chronic inflammatory infiltrates associated with long-term airway hyperresponsiveness in mice. *The Journal of infectious diseases* **2004,** *189* (10), 1856–1865. DOI: 10.1086/386372.

Jansen, J. M.; Gerlach, T.; Elbahesh, H.; Rimmelzwaan, G. F.; Saletti, G. Influenza virus-specific CD4+ and CD8+ T cell-mediated immunity induced by infection and vaccination. *Journal of clinical virology : the official publication of the Pan American Society for Clinical Virology* **2019,** *119*, 44–52. DOI: 10.1016/j.jcv.2019.08.009.

Jartti, T.; Gern, J. E. Role of viral infections in the development and exacerbation of asthma in children. *The Journal of allergy and clinical immunology* **2017,** *140* (4), 895–906. DOI: 10.1016/j.jaci.2017.08.003.

Jensen, K. J.; Benn, C. S.; van Crevel, R. Unravelling the nature of non-specific effects of vaccines-A challenge for innate immunologists. *Seminars in immunology* **2016,** *28* (4), 377–383. DOI: 10.1016/j.smim.2016.05.005.

Kabashima, K. Pathomechanism of atopic dermatitis in the perspective of T cell subsets and skin barrier functions – "Which comes first, the chicken or the egg?". *Dermatologica Sinica* **2012,** *30* (4), 142–146. DOI: 10.1016/j.dsi.2012.07.003.

Kast, J. I.; McFarlane, A. J.; Głobińska, A.; Sokolowska, M.; Wawrzyniak, P.; Sanak, M.; Schwarze, J.; Akdis, C. A.; Wanke, K. Respiratory syncytial virus infection influences tight junction integrity. *Clinical and experimental immunology* **2017,** *190* (3), 351–359. DOI: 10.1111/cei.13042.

Keegan, A. D.; Shirey, K. A.; Bagdure, D.; Blanco, J.; Viscardi, R. M.; Vogel, S. N. Enhanced allergic responsiveness after early childhood infection with respiratory viruses: Are long-lived alternatively activated macrophages the missing link? *Pathogens and disease* **2016,** *74* (5). DOI: 10.1093/femspd/ftw047.

Kespohl, S.; Raulf, M. Mold Sensitization in Asthmatic and Non-asthmatic Subjects Diagnosed with Extract-Based Versus Component-Based Allergens. *Advances in experimental medicine and biology* **2019,** *1153*, 79–89. DOI: 10.1007/5584_2019_342.

Koch, S.; Sopel, N.; Finotto, S. Th9 and other IL-9-producing cells in allergic asthma. *Semin Immunopathol* **2017,** *39* (1), 55–68. DOI: 10.1007/s00281-016-0601-1.

Koczulla, A. R.; Vogelmeier, C. F.; Garn, H.; Renz, H. New concepts in asthma: clinical phenotypes and pathophysiological mechanisms. *Drug discovery today* **2017,** *22* (2), 388–396. DOI: 10.1016/j.drudis.2016.11.008.

Kovac, K.; Dodig, S.; Tjesić-Drinković, D.; Raos, M. Correlation between asthma severity and serum IgE in asthmatic children sensitized to Dermatophagoides pteronyssinus. *Archives of medical research* **2007,** *38* (1), 99–105. DOI: 10.1016/j.arcmed.2006.07.007.

Krishnamoorthy, N.; Khare, A.; Oriss, T. B.; Raundhal, M.; Morse, C.; Yarlagadda, M.; Wenzel, S. E.; Moore, M. L.; Peebles, R. S.; Ray, A.; Ray, P. Early infection with respiratory syncytial virus impairs regulatory T cell function and increases susceptibility to allergic asthma. *Nat Med* **2012,** *18* (10), 1525–1530. DOI: 10.1038/nm.2896.

Kuruvilla, M. E.; Lee, F. E.-H.; Lee, G. B. Understanding Asthma Phenotypes, Endotypes, and Mechanisms of Disease. *Clinical reviews in allergy & immunology* **2019a,** *56* (2), 219–233. DOI: 10.1007/s12016-018-8712-1.

Kuruvilla, M. E.; Vanijcharoenkarn, K.; Shih, J. A.; Lee, F. E.-H. Epidemiology and risk factors for asthma. *Respiratory medicine* **2019b,** *149*, 16–22. DOI: 10.1016/j.rmed.2019.01.014.

Labrosse, R.; Graham, F.; Caubet, J.-C. Non-IgE-Mediated Gastrointestinal Food Allergies in Children: An Update. *Nutrients* **2020,** *12* (7), 2086. DOI: 10.3390/nu12072086.

Lambrecht, B. N.; Hammad, H. The immunology of asthma. *Nature immunology* **2015,** *16* (1), 45–56. DOI: 10.1038/ni.3049.

Lambrecht, B. N.; Hammad, H. The immunology of the allergy epidemic and the hygiene hypothesis. *Nature immunology* **2017,** *18* (10), 1076–1083. DOI: 10.1038/ni.3829.

Lau, S.; Illi, S.; Platts-Mills, T. A. E.; Riposo, D.; Nickel, R.; Grüber, C.; Niggemann, B.; Wahn, U. Longitudinal study on the relationship between cat allergen and endotoxin exposure, sensitization, cat-specific IgG and development of asthma in childhood--report of the German Multicentre Allergy Study (MAS 90). *Allergy* **2005,** *60* (6), 766–773. DOI: 10.1111/j.1398-9995.2005.00781.x.

Le Bert, N.; Tan, A. T.; Kunasegaran, K.; Tham, C. Y. L.; Hafezi, M.; Chia, A.; Chng, M. H. Y.; Lin, M.; Tan, N.; Linster, M.; Chia, W. N.; Chen, M. I.-C.; Wang, L.-F.; Ooi, E. E.; Kalimuddin, S.; Tambyah, P. A.; Low, J. G.-H.; Tan, Y.-J.; Bertoletti, A. SARS-CoV-2-specific T cell immunity in cases of COVID-19 and SARS, and uninfected controls. *Nature* **2020,** *584* (7821), 457–462. DOI: 10.1038/s41586-020-2550-z.

Leach, S.; Shinnakasu, R.; Adachi, Y.; Momota, M.; Makino-Okamura, C.; Yamamoto, T.; Ishii, K. J.; Fukuyama, H.; Takahashi, Y.; Kurosaki, T. Requirement for memory B-cell activation in protection from heterologous influenza virus reinfection. *International immunology* **2019,** *31* (12), 771–779. DOI: 10.1093/intimm/dxz049.

Lee, J.-U.; Kim, J. D.; Park, C.-S. Gene-Environment Interactions in Asthma: Genetic and Epigenetic Effects. *Yonsei Medical Journal* **2015,** *56* (4), 877–886. DOI: 10.3349/ymj.2015.56.4.877.

Lemanske, R. F.; Jackson, D. J.; Gangnon, R. E.; Evans, M. D.; Li, Z.; Shult, P. A.; Kirk, C. J.; Reisdorf, E.; Roberg, K. A.; Anderson, E. L.; Carlson-Dakes, K. T.; Adler, K. J.;

Gilbertson-White, S.; Pappas, T. E.; DaSilva, D. F.; Tisler, C. J.; Gern, J. E. Rhinovirus illnesses during infancy predict subsequent childhood wheezing. *The Journal of allergy and clinical immunology* **2005,** *116* (3), 571–577. DOI: 10.1016/j.jaci.2005.06.024.

Leynaert, B.; Neukirch, C.; Kony, S.; Guénégou, A.; Bousquet, J.; Aubier, M.; Neukirch, F. Association between asthma and rhinitis according to atopic sensitization in a population-based study. *Journal of Allergy and Clinical Immunology* **2004,** *113* (1), 86–93. DOI: 10.1016/j.jaci.2003.10.010.

León, B. T Cells in Allergic Asthma: Key Players Beyond the Th2 Pathway. *Current allergy and asthma reports* **2017,** *17* (7), 43. DOI: 10.1007/s11882-017-0714-1.

Li, H.; Wang, H.; Sokulsky, L.; Liu, S.; Yang, R.; Liu, X.; Zhou, L.; Li, J.; Huang, C.; Li, F.; Lei, X.; Jia, H.; Cheng, J.; Li, F.; Yang, M.; Zhang, G. Single-cell transcriptomic analysis reveals key immune cell phenotypes in the lungs of patients with asthma exacerbation. *The Journal of allergy and clinical immunology* **2021a,** *147* (3), 941–954. DOI: 10.1016/j.jaci.2020.09.032.

Li, K. H.; Leong, P.-Y.; Tseng, C.-F.; Wang, Y. H.; Wei, J. C.-C. Influenza Vaccination Is Associated With Lower Incidental Asthma Risk in Patients With Atopic Dermatitis: A Nationwide Cohort Study. *Front. Immunol.* **2021b,** *12*, 729501. DOI: 10.3389/fimmu.2021.729501.

Ljunggren, H. G.; Stam, N. J.; Ohlén, C.; Neefjes, J. J.; Höglund, P.; Heemels, M. T.; Bastin, J.; Schumacher, T. N.; Townsend, A.; Kärre, K. Empty MHC class I molecules come out in the cold. *Nature* **1990,** *346* (6283), 476–480. DOI: 10.1038/346476a0.

Maggi, E.; Giudizi, M. G.; Biagiotti, R.; Annunziato, F.; Manetti, R.; Piccinni, M. P.; Parronchi, P.; Sampognaro, S.; Giannarini, L.; Zuccati, G.; Romagnani, S. Th2-like CD8+ T cells showing B cell helper function and reduced cytolytic activity in human immunodeficiency virus type 1 infection. *The Journal of experimental medicine* **1994,** *180* (2), 489–495. DOI: 10.1084/jem.180.2.489.

Mari, A.; Rasi, C.; Palazzo, P.; Scala, E. Allergen databases: current status and perspectives. *Current allergy and asthma reports* **2009,** *9* (5), 376–383. DOI: 10.1007/s11882-009-0055-9.

Mari, A.; Scala, E. Allergome: a unifying platform. *Arbeiten aus dem Paul-Ehrlich-Institut (Bundesamt fur Sera und Impfstoffe) zu Frankfurt a.M* [Online] **2006,** No. 95, 29-39; discussion 39-40.

Mari, A.; Scala, E.; Palazzo, P.; Ridolfi, S.; Zennaro, D.; Carabella, G. Bioinformatics applied to allergy: allergen databases, from collecting sequence information to data integration. The Allergome platform as a model. *Cellular immunology* **2006,** *244* (2), 97–100. DOI: 10.1016/j.cellimm.2007.02.012.

Martin, S. F. Adaptation in the innate immune system and heterologous innate immunity. *Cellular and molecular life sciences : CMLS* **2014,** *71* (21), 4115–4130. DOI: 10.1007/s00018-014-1676-2.

Mason, D. A very high level of crossreactivity is an essential feature of the T-cell receptor. *Immunology Today* **1998,** *19* (9), 395–404. DOI: 10.1016/s0167-5699(98)01299-7.

Mathurin, K. S.; Martens, G. W.; Kornfeld, H.; Welsh, R. M. CD4 T-cell-mediated heterologous immunity between mycobacteria and poxviruses. *Journal of virology* **2009,** *83* (8), 3528–3539. DOI: 10.1128/JVI.02393-08.

Matricardi, P. M.; Kleine-Tebbe, J.; Hoffmann, H. J.; Valenta, R.; Hilger, C.; Hofmaier, S.; Aalberse, R. C.; Agache, I.; Asero, R.; Ballmer-Weber, B.; Barber, D.; Beyer, K.; Biedermann, T.; Bilò, M. B.; Blank, S.; Bohle, B.; Bosshard, P. P.; Breiteneder, H.; Brough, H. A.; Caraballo, L.; Caubet, J. C.; Crameri, R.; Davies, J. M.; Douladiris, N.; Ebisawa, M.; EIgenmann, P. A.; Fernandez-Rivas, M.; Ferreira, F.; Gadermaier, G.; Glatz, M.; Hamilton, R. G.; Hawranek, T.; Hellings, P.; Hoffmann-Sommergruber, K.; Jakob, T.; Jappe, U.; Jutel, M.; Kamath, S. D.; Knol, E. F.; Korosec, P.; Kuehn, A.; Lack, G.; Lopata, A. L.; Mäkelä, M.; Morisset, M.; Niederberger, V.; Nowak-Węgrzyn, A. H.; Papadopoulos, N. G.; Pastorello, E. A.; Pauli, G.; Platts-Mills, T.; Posa, D.; Poulsen, L. K.; Raulf, M.; Sastre, J.; Scala, E.; Schmid, J. M.; Schmid-Grendelmeier, P.; van Hage, M.; van Ree, R.; Vieths, S.; Weber, R.; Wickman, M.; Muraro, A.; Ollert, M. EAACI Molecular Allergology User's Guide. *Pediatr Allergy Immunol* **2016,** *27 Suppl 23*, 1–250. DOI: 10.1111/pai.12563.

Matricardi, P. M.; Rosmini, F.; Ferrigno, L.; Nisini, R.; Rapicetta, M.; Chionne, P.; Stroffolini, T.; Pasquini, P.; D'Amelio, R. Cross sectional retrospective study of prevalence of atopy among Italian military students with antibodies against hepatitis A virus. *BMJ (Clinical research ed.)* **1997,** *314* (7086), 999–1003. DOI: 10.1136/bmj.314.7086.999.

Matricardi, P. M.; Rosmini, F.; Panetta, V.; Ferrigno, L.; Bonini, S. Hay fever and asthma in relation to markers of infection in the United States. *The Journal of*

allergy and clinical immunology **2002,** *110* (3), 381–387. DOI: 10.1067/mai.2002.126658.

Matricardi, P. M.; Rosmini, F.; Riondino, S.; Fortini, M.; Ferrigno, L.; Rapicetta, M.; Bonini, S. Exposure to foodborne and orofecal microbes versus airborne viruses in relation to atopy and allergic asthma: epidemiological study. *BMJ (Clinical research ed.)* **2000,** *320* (7232), 412–417. DOI: 10.1136/bmj.320.7232.412.

Mebrahtu, T. F.; Feltbower, R. G.; Greenwood, D. C.; Parslow, R. C. Childhood body mass index and wheezing disorders: a systematic review and meta-analysis. *Pediatr Allergy Immunol* **2015,** *26* (1), 62–72. DOI: 10.1111/pai.12321.

Merenstein, C.; Liang, G.; Whiteside, S. A.; Cobián-Güemes, A. G.; Merlino, M. S.; Taylor, L. J.; Glascock, A.; Bittinger, K.; Tanes, C.; Graham-Wooten, J.; Khatib, L. A.; Fitzgerald, A. S.; Reddy, S.; Baxter, A. E.; Giles, J. R.; Oldridge, D. A.; Meyer, N. J.; Wherry, E. J.; McGinniss, J. E.; Bushman, F. D.; Collman, R. G. Signatures of COVID-19 Severity and Immune Response in the Respiratory Tract Microbiome. *mBio* **2021,** *12* (4), e0177721. DOI: 10.1128/mBio.01777-21.

Meyers, L. M.; Gutiérrez, A. H.; Boyle, C. M.; Terry, F.; McGonnigal, B. G.; Salazar, A.; Princiotta, M. F.; Martin, W. D.; Groot, A. S. de; Moise, L. Highly conserved, non-human-like, and cross-reactive SARS-CoV-2 T cell epitopes for COVID-19 vaccine design and validation. *NPJ vaccines* **2021,** *6* (1), 71. DOI: 10.1038/s41541-021-00331-6.

Miethe, S.; Karsonova, A.; Karaulov, A.; Renz, H. Obesity and asthma. *The Journal of allergy and clinical immunology* **2020,** *146* (4), 685–693. DOI: 10.1016/j.jaci.2020.08.011.

Moutaftsi, M.; Peters, B.; Pasquetto, V.; Tscharke, D. C.; Sidney, J.; Bui, H.-H.; Grey, H.; Sette, A. A consensus epitope prediction approach identifies the breadth of murine T(CD8+)-cell responses to vaccinia virus. *Nature biotechnology* **2006,** *24* (7), 817–819. DOI: 10.1038/nbt1215.

Namvar, S.; Warn, P.; Farnell, E.; Bromley, M.; Fraczek, M.; Bowyer, P.; Herrick, S. Aspergillus fumigatus proteases, Asp f 5 and Asp f 13, are essential for airway inflammation and remodelling in a murine inhalation model. *Clinical and experimental allergy : journal of the British Society for Allergy and Clinical Immunology* **2015,** *45* (5), 982–993. DOI: 10.1111/cea.12426.

Narasaraju, T.; Yang, E.; Samy, R. P.; Ng, H. H.; Poh, W. P.; Liew, A.-A.; Phoon, M. C.; van Rooijen, N.; Chow, V. T. Excessive neutrophils and neutrophil extracellular traps contribute to acute lung injury of influenza pneumonitis. *The American journal of pathology* **2011,** *179* (1), 199–210. DOI: 10.1016/j.ajpath.2011.03.013.

National Institute for Health and Care Excellence.: Quality Standard for Asthma. https://www.nice.org.uk/guidance/qs25 (accessed September 28, 2021).

Nelde, A.; Bilich, T.; Heitmann, J. S.; Maringer, Y.; Salih, H. R.; Roerden, M.; Lübke, M.; Bauer, J.; Rieth, J.; Wacker, M.; Peter, A.; Hörber, S.; Traenkle, B.; Kaiser, P. D.; Rothbauer, U.; Becker, M.; Junker, D.; Krause, G.; Strengert, M.; Schneiderhan-Marra, N.; Templin, M. F.; Joos, T. O.; Kowalewski, D. J.; Stos-Zweifel, V.; Fehr, M.; Rabsteyn, A.; Mirakaj, V.; Karbach, J.; Jäger, E.; Graf, M.; Gruber, L.-C.; Rachfalski, D.; Preuß, B.; Hagelstein, I.; Märklin, M.; Bakchoul, T.; Gouttefangeas, C.; Kohlbacher, O.; Klein, R.; Stevanović, S.; Rammensee, H.-G.; Walz, J. S. SARS-CoV-2-derived peptides define heterologous and COVID-19-induced T cell recognition. *Nature immunology* **2021,** *22* (1), 74–85. DOI: 10.1038/s41590-020-00808-x.

Nielsen, M.; Lund, O. NN-align. An artificial neural network-based alignment algorithm for MHC class II peptide binding prediction. *BMC Bioinformatics* **2009,** *10*, 296. DOI: 10.1186/1471-2105-10-296.

Nielsen, M.; Lundegaard, C.; Worning, P.; Lauemøller, S. L.; Lamberth, K.; Buus, S.; Brunak, S.; Lund, O. Reliable prediction of T-cell epitopes using neural networks with novel sequence representations. *Protein science : a publication of the Protein Society* **2003,** *12* (5), 1007–1017. DOI: 10.1110/ps.0239403.

Nissen, T. N.; Birk, N. M.; Blok, B. A.; Arts, R. J. W.; Andersen, A.; Kjærgaard, J.; Thøstesen, L. M.; Hoffmann, T.; Jeppesen, D. L.; Nielsen, S. D.; Kofoed, P.-E.; Stensballe, L. G.; Aaby, P.; Ruhwald, M.; Netea, M. G.; Benn, C. S.; Pryds, O. Bacillus Calmette-Guérin vaccination at birth and in vitro cytokine responses to non-specific stimulation. A randomized clinical trial. *European journal of clinical microbiology & infectious diseases : official publication of the European Society of Clinical Microbiology* **2018,** *37* (1), 29–41. DOI: 10.1007/s10096-017-3097-2.

Ogishi, M.; Yotsuyanagi, H. Quantitative Prediction of the Landscape of T Cell Epitope Immunogenicity in Sequence Space. *Front. Immunol.* **2019,** *10*, 827. DOI: 10.3389/fimmu.2019.00827.

Openshaw, P. J.; Chiu, C. Protective and dysregulated T cell immunity in RSV infection☆. *Current Opinion in Virology* **2013,** *3* (4), 468–474. DOI: 10.1016/j.coviro.2013.05.005.

Padmanabhan, U.; Mukherjee, S.; Borse, R.; Joshi, S.; Deshmukh, R. *Phase II Clinical trial for Evaluation of BCG as potential therapy for COVID-19*, 2020.

Papi, A.; Brightling, C.; Pedersen, S. E.; Reddel, H. K. Asthma. *The Lancet* **2018,** *391* (10122), 783–800. DOI: 10.1016/S0140-6736(17)33311-1.

Peters, B.; Sette, A. Generating quantitative models describing the sequence specificity of biological processes with the stabilized matrix method. *BMC Bioinformatics* **2005,** *6*, 132. DOI: 10.1186/1471-2105-6-132.

Pfefferle, P. I.; Teich, R.; Renz, H. The Immunological Basis of the Hygiene Hypothesis. In *Allergy Frontiers: Epigenetics, Allergens and Risk Factors*; Pawankar, R., Holgate, S. T., Rosenwasser, L. J., Eds.; Springer Japan: Tokyo, 2009; pp 325–348. DOI: 10.1007/978-4-431-72802-3_19.

Pleguezuelos, O.; James, E.; Fernandez, A.; Lopes, V.; Rosas, L. A.; Cervantes-Medina, A.; Cleath, J.; Edwards, K.; Neitzey, D.; Gu, W.; Hunsberger, S.; Taubenberger, J. K.; Stoloff, G.; Memoli, M. J. Efficacy of FLU-v, a broad-spectrum influenza vaccine, in a randomized phase IIb human influenza challenge study. *NPJ vaccines* **2020,** *5* (1), 22. DOI: 10.1038/s41541-020-0174-9.

Polosa, R.; Knoke, J. D.; Russo, C.; Piccillo, G.; Caponnetto, P.; Sarvà, M.; Proietti, L.; Al-Delaimy, W. K. Cigarette smoking is associated with a greater risk of incident asthma in allergic rhinitis. *The Journal of allergy and clinical immunology* **2008,** *121* (6), 1428–1434. DOI: 10.1016/j.jaci.2008.02.041.

Posa, D.; Perna, S.; Resch, Y.; Lupinek, C.; Panetta, V.; Hofmaier, S.; Rohrbach, A.; Hatzler, L.; Grabenhenrich, L.; Tsilochristou, O.; Chen, K.-W.; Bauer, C.-P.; Hoffman, U.; Forster, J.; Zepp, F.; Schuster, A.; Wahn, U.; Keil, T.; Lau, S.; Vrtala, S.; Valenta, R.; Matricardi, P. M. Evolution and predictive value of IgE responses toward a comprehensive panel of house dust mite allergens during the first 2 decades of life. *The Journal of allergy and clinical immunology* **2017,** *139* (2), 541-549.e8. DOI: 10.1016/j.jaci.2016.08.014.

Prescott, S. L.; Macaubas, C.; Holt, B. J.; Smallacombe, T. B.; Loh, R.; Sly, P. D.; Holt, P. G. Transplacental priming of the human immune system to environmental allergens: universal skewing of initial T cell responses toward the Th2 cytokine

profile. *Journal of immunology (Baltimore, Md. : 1950)* [Online] **1998,** *160* (10), 4730–4737. https://pubmed.ncbi.nlm.nih.gov/9590218/.

Pusch, E.; Renz, H.; Skevaki, C. Respiratory virus-induced heterologous immunity: Part of the problem or part of the solution? *Allergo Journal : interdisziplinare Zeitschrift fur Allergologie und Umweltmedizin : Organ der Deutschen Gesellschaft fur Allergie- und Immunitatsforschung* **2018,** *27* (3), 28–45. DOI: 10.1007/s15007-018-1580-4.

Radauer, C.; Bublin, M.; Wagner, S.; Mari, A.; Breiteneder, H. Allergens are distributed into few protein families and possess a restricted number of biochemical functions. *The Journal of allergy and clinical immunology* **2008,** *121* (4), 847-52.e7. DOI: 10.1016/j.jaci.2008.01.025.

Rahimi, R. A.; Nepal, K.; Cetinbas, M.; Sadreyev, R. I.; Luster, A. D. Distinct functions of tissue-resident and circulating memory Th2 cells in allergic airway disease. *The Journal of experimental medicine* **2020,** *217* (9). DOI: 10.1084/jem.20190865.

Regateiro, F. S.; Botelho Alves, P.; Moura, A. L.; Azevedo, J. P.; Regateiro, D. T. The diverse roles of T cell subsets in asthma. *European annals of allergy and clinical immunology* **2021,** *53* (5), 201–208. DOI: 10.23822/EurAnnACI.1764-1489.177.

Reguzova, A.; Fischer, N.; Müller, M.; Salomon, F.; Jaenisch, T.; Amann, R. A Novel Orf Virus D1701-VrV-Based Dengue Virus (DENV) Vaccine Candidate Expressing HLA-Specific T Cell Epitopes: A Proof-of-Concept Study. *Biomedicines* **2021,** *9* (12). DOI: 10.3390/biomedicines9121862.

Renz, H.; Skevaki, C. Early life microbial exposures and allergy risks: opportunities for prevention. *Nature reviews. Immunology* **2021,** *21* (3), 177–191. DOI: 10.1038/s41577-020-00420-y.

Robinson, D. S. Regulatory T cells and asthma. *Clinical and experimental allergy : journal of the British Society for Allergy and Clinical Immunology* **2009,** *39* (9), 1314–1323. DOI: 10.1111/j.1365-2222.2009.03301.x.

Romagnani, S. Immunologic influences on allergy and the TH1/TH2 balance. *Journal of Allergy and Clinical Immunology* **2004,** *113* (3), 395–400. DOI: 10.1016/j.jaci.2003.11.025.

Rook, G. A. W. Review series on helminths, immune modulation and the hygiene hypothesis: the broader implications of the hygiene hypothesis. *Immunology* **2009,** *126* (1), 3–11. DOI: 10.1111/j.1365-2567.2008.03007.x.

Rook, G. A. W.; Adams, V.; Hunt, J.; Palmer, R.; Martinelli, R.; Brunet, L. R. Mycobacteria and other environmental organisms as immunomodulators for immunoregulatory disorders. *Springer seminars in immunopathology* **2004,** *25* (3-4), 237–255. DOI: 10.1007/s00281-003-0148-9.

Saffarzadeh, M.; Juenemann, C.; Queisser, M. A.; Lochnit, G.; Barreto, G.; Galuska, S. P.; Lohmeyer, J.; Preissner, K. T. Neutrophil extracellular traps directly induce epithelial and endothelial cell death: a predominant role of histones. *PloS one* **2012,** *7* (2), e32366. DOI: 10.1371/journal.pone.0032366.

Salo, P. M.; Arbes, S. J.; Crockett, P. W.; Thorne, P. S.; Cohn, R. D.; Zeldin, D. C. Exposure to multiple indoor allergens in US homes and its relationship to asthma. *The Journal of allergy and clinical immunology* **2008,** *121* (3), 678-684.e2. DOI: 10.1016/j.jaci.2007.12.1164.

Sanchez-Trincado, J. L.; Gomez-Perosanz, M.; Reche, P. A. Fundamentals and Methods for T- and B-Cell Epitope Prediction. *Journal of immunology research* **2017,** *2017*, 2680160. DOI: 10.1155/2017/2680160.

Scala, E.; Villalta, D.; Meneguzzi, G.; Giani, M.; Asero, R. Storage molecules from tree nuts, seeds and legumes: relationships and amino acid identity among homologue molecules. *European annals of allergy and clinical immunology* **2018,** *50* (4), 148–155. DOI: 10.23822/EurAnnACI.1764-1489.54.

Schäfer, T.; Vieluf, D.; Behrendt, H.; Krämer, U.; Ring, J. Atopic eczema and other manifestations of atopy: results of a study in East and West Germany. *Allergy* **1996,** *51* (8), 532–539. DOI: 10.1111/j.1398-9995.1996.tb04665.x.

Schmidt, A.; Lapuente, D. T Cell Immunity against Influenza: The Long Way from Animal Models Towards a Real-Life Universal Flu Vaccine. *Viruses* **2021,** *13* (2). DOI: 10.3390/v13020199.

Schmidt, M. E.; Varga, S. M. The CD8 T Cell Response to Respiratory Virus Infections. *Front. Immunol.* **2018,** *9*, 678. DOI: 10.3389/fimmu.2018.00678.

Seder, R. A.; Le Gros, G. G. The functional role of CD8+ T helper type 2 cells. *The Journal of experimental medicine* **1995,** *181* (1), 5–7. DOI: 10.1084/jem.181.1.5.

Selin, L. K.; Varga, S. M.; Wong, I. C.; Welsh, R. M. Protective heterologous antiviral immunity and enhanced immunopathogenesis mediated by memory T cell populations. *The Journal of experimental medicine* **1998,** *188* (9), 1705–1715. DOI: 10.1084/jem.188.9.1705.

Seneviratne, S. L.; Jones, L.; King, A. S.; Black, A.; Powell, S.; McMichael, A. J.; Ogg, G. S. Allergen-specific CD8(+) T cells and atopic disease. *The Journal of clinical investigation* **2002,** *110* (9), 1283–1291. DOI: 10.1172/JCI15753.

Sewell, A. K. Why must T cells be cross-reactive? *Nature reviews. Immunology* **2012,** *12* (9), 669–677. DOI: 10.1038/nri3279.

Sharma, S.; Thomas, P. G. The two faces of heterologous immunity: protection or immunopathology. *Journal of leukocyte biology* **2014,** *95* (3), 405–416. DOI: 10.1189/jlb.0713386.

Shimizu, Y.; Nakamura, A.; Kishimura, H.; Hara, A.; Watanabe, K.; Saeki, H. Major allergen and its IgE cross-reactivity among salmonid fish roe allergy. *Journal of agricultural and food chemistry* **2009,** *57* (6), 2314–2319. DOI: 10.1021/jf8031759.

Skevaki, C.; Hudemann, C.; Matrosovich, M.; Möbs, C.; Paul, S.; Wachtendorf, A.; Alashkar Alhamwe, B.; Potaczek, D. P.; Hagner, S.; Gemsa, D.; Garn, H.; Sette, A.; Renz, H. Influenza-derived peptides cross-react with allergens and provide asthma protection. *The Journal of allergy and clinical immunology* **2018,** *142* (3), 804–814. DOI: 10.1016/j.jaci.2017.07.056.

Slon Campos, J. L.; Mongkolsapaya, J.; Screaton, G. R. The immune response against flaviviruses. *Nature immunology* **2018,** *19* (11), 1189–1198. DOI: 10.1038/s41590-018-0210-3.

Smith, C. M.; Kulkarni, H.; Radhakrishnan, P.; Rutman, A.; Bankart, M. J.; Williams, G.; Hirst, R. A.; Easton, A. J.; Andrew, P. W.; O'Callaghan, C. Ciliary dyskinesia is an early feature of respiratory syncytial virus infection. *The European respiratory journal* **2014,** *43* (2), 485–496. DOI: 10.1183/09031936.00205312.

Smits, H. H.; Hiemstra, P. S.; Da Prazeres Costa, C.; Ege, M.; Edwards, M.; Garn, H.; Howarth, P. H.; Jartti, T.; Jong, E. C. de; Maizels, R. M.; Marsland, B. J.; McSorley, H. J.; Müller, A.; Pfefferle, P. I.; Savelkoul, H.; Schwarze, J.; Unger, W. W. J.; Mutius, E. von; Yazdanbakhsh, M.; Taube, C. Microbes and asthma: Opportunities for intervention. *The Journal of allergy and clinical immunology* **2016,** *137* (3), 690–697. DOI: 10.1016/j.jaci.2016.01.004.

Sridhar, S.; Begom, S.; Bermingham, A.; Hoschler, K.; Adamson, W.; Carman, W.; Bean, T.; Barclay, W.; Deeks, J. J.; Lalvani, A. Cellular immune correlates of protection against symptomatic pandemic influenza. *Nat Med* **2013,** *19* (10), 1305–1312. DOI: 10.1038/nm.3350.

Steffen, M.; Krieg, P.; Pernfuss, M.; Sauer, E.; Eisinger, V.; Sauer, G. Growth dynamics of a latent primate papovavirus. *Journal of virology* **1980,** *35* (3), 865–875. DOI: 10.1128/JVI.35.3.865-875.1980.

Stensballe, L. G.; Simonsen, J. B.; Thomsen, S. F.; Larsen, A.-M. H.; Lysdal, S. H.; Aaby, P.; Kyvik, K. O.; Skytthe, A.; Backer, V.; Bisgaard, H. The causal direction in the association between respiratory syncytial virus hospitalization and asthma. *The Journal of allergy and clinical immunology* **2009,** *123* (1), 131-137.e1. DOI: 10.1016/j.jaci.2008.10.042.

Stern, J.; Pier, J.; Litonjua, A. A. Asthma epidemiology and risk factors. *Semin Immunopathol* [Online] **2020,** *42* (1), 5–15. https://link.springer.com/article/10.1007/s00281-020-00785-1.

Stock, P.; Kallinich, T.; Akbari, O.; Quarcoo, D.; Gerhold, K.; Wahn, U.; Umetsu, D. T.; Hamelmann, E. CD8(+) T cells regulate immune responses in a murine model of allergen-induced sensitization and airway inflammation. *European journal of immunology* **2004,** *34* (7), 1817–1827. DOI: 10.1002/eji.200324623.

Stokes, K. L.; Currier, M. G.; Sakamoto, K.; Lee, S.; Collins, P. L.; Plemper, R. K.; Moore, M. L. The respiratory syncytial virus fusion protein and neutrophils mediate the airway mucin response to pathogenic respiratory syncytial virus infection. *Journal of virology* **2013,** *87* (18), 10070–10082. DOI: 10.1128/JVI.01347-13.

Strachan, D. P. Hay fever, hygiene, and household size. *BMJ (Clinical research ed.)* **1989,** *299* (6710), 1259–1260. DOI: 10.1136/bmj.299.6710.1259.

Sullivan, A.; Hunt, E.; MacSharry, J.; Murphy, D. M. 'The Microbiome and the Pathophysiology of Asthma'. *Respiratory research* **2016,** *17* (1), 163. DOI: 10.1186/s12931-016-0479-4.

Sun, F.; Liang, Y.; Lin, M.; Tan, C.; Chen, M.; Tu, C.; Shi, H.; Li, Y.; Yu, J.; Liu, J. Regulatory T cell deficiency in patients with eosinophilic asthma. *The Journal of asthma : official journal of the Association for the Care of Asthma* [Online] **2021**, 1–9.

Suraya, R.; Nagano, T.; Katsurada, M.; Sekiya, R.; Kobayashi, K.; Nishimura, Y. Molecular mechanism of asthma and its novel molecular target therapeutic agent. *Respiratory investigation* **2021,** *59* (3), 291–301. DOI: 10.1016/j.resinv.2020.12.007.

Tay, C. J. X.; Le Ta, D. H.; Ow Yeong, Y. X.; Yap, G. C.; Chu, J. J. H.; Lee, B. W.; Tham, E. H. Role of Upper Respiratory Microbiota and Virome in Childhood Rhinitis and Wheeze: Collegium Internationale Allergologicum Update 2021. *International*

archives of allergy and immunology **2021,** *182* (4), 265–276. DOI: 10.1159/000513325.

Taylor, G.; Stott, E. J.; Hughes, M.; Collins, A. P. Respiratory syncytial virus infection in mice. *Infection and immunity* **1984,** *43* (2), 649–655. DOI: 10.1128/iai.43.2.649-655.1984.

The universal protein resource (UniProt). *Nucleic acids research* **2008,** *36* (Database issue), D190-5. DOI: 10.1093/nar/gkm895.

Thomas, W. R.; Smith, W.-A.; Hales, B. J.; Mills, K. L.; O'Brien, R. M. Characterization and immunobiology of house dust mite allergens. *International archives of allergy and immunology* **2002,** *129* (1), 1–18. DOI: 10.1159/000065179.

Toskala, E.; Kennedy, D. W. Asthma risk factors. *International Forum of Allergy and Rhinology* **2015,** *5* (Suppl 1), S11-6. DOI: 10.1002/alr.21557.

Tsilika, M.; Taks, E.; Dolianitis, K.; Kotsaki, A.; Leventogiannis, K.; Damoulari, C.; Kostoula, M.; Paneta, M.; Adamis, G.; Papanikolaou, I. C.; Stamatelopoulos, K.; Bolanou, A.; Katsaros, K.; Delavinia, C.; Perdios, I.; Pandi, A.; Tsiakos, K.; Proios, N.; Kalogianni, E.; Delis, I.; Skliros, E.; Akinosoglou, K.; Perdikouli, A.; Poulakou, G.; Milionis, H.; Athanassopoulou, E.; Kalpaki, E.; Efstratiou, L.; Perraki, V.; Papadopoulos, A.; Netea, M. G.; Giamarellos-Bourboulis, E. J. *ACTIVATE-2: A DOUBLE-BLIND RANDOMIZED TRIAL OF BCG VACCINATION AGAINST COVID19 IN INDIVIDUALS AT RISK*, 2021.

Vali, B.; Tohn, R.; Cohen, M. J.; Sakhdari, A.; Sheth, P. M.; Yue, F. Y.; Wong, D.; Kovacs, C.; Kaul, R.; Ostrowski, M. A. Characterization of cross-reactive CD8+ T-cell recognition of HLA-A2-restricted HIV-Gag (SLYNTVATL) and HCV-NS5b (ALYDVVSKL) epitopes in individuals infected with human immunodeficiency and hepatitis C viruses. *Journal of virology* **2011,** *85* (1), 254–263. DOI: 10.1128/JVI.01743-10.

van den Bergh, M. R.; Biesbroek, G.; Rossen, J. W. A.; Steenhuijsen Piters, W. A. A. de; Bosch, A. A. T. M.; van Gils, E. J. M.; Wang, X.; Boonacker, C. W. B.; Veenhoven, R. H.; Bruin, J. P.; Bogaert, D.; Sanders, E. A. M. Associations between pathogens in the upper respiratory tract of young children: interplay between viruses and bacteria. *PloS one* **2012,** *7* (10), e47711. DOI: 10.1371/journal.pone.0047711.

van Regenmortel, M. H. V. Specificity, polyspecificity, and heterospecificity of antibody-antigen recognition. *Journal of molecular recognition : JMR* **2014,** *27* (11), 627–639. DOI: 10.1002/jmr.2394.

Vandini, S.; Biagi, C.; Lanari, M. Respiratory Syncytial Virus: The Influence of Serotype and Genotype Variability on Clinical Course of Infection. *International journal of molecular sciences* **2017,** *18* (8). DOI: 10.3390/ijms18081717.

Velasco-Medina, A. A.; García-León, M. L.; Velázquez-Sámano, G.; Wong-Chew, R. M. The cellular and humoral immune response to influenza vaccination is comparable in asthmatic and healthy subjects. *Human vaccines & immunotherapeutics* **2021,** *17* (1), 98–105. DOI: 10.1080/21645515.2020.1759995.

Verschoor, D.; Gunten, S. von. Allergy and Atopic Diseases: An Update on Experimental Evidence. *International archives of allergy and immunology* **2019,** *180* (4), 235–243. DOI: 10.1159/000504439.

Villumsen, M.; Sørup, S.; Jess, T.; Ravn, H.; Relander, T.; Baker, J. L.; Benn, C. S.; Sørensen, T. I. A.; Aaby, P.; Roth, A. Risk of lymphoma and leukaemia after bacille Calmette-Guérin and smallpox vaccination: a Danish case-cohort study. *Vaccine* **2009,** *27* (49), 6950–6958. DOI: 10.1016/j.vaccine.2009.08.103.

Waldeck, W.; Sauer, G. New oncogenic papova virus from primate cells. *Nature* **1977,** *269* (5624), 171–173. DOI: 10.1038/269171a0.

Wark, P. A. B.; Ramsahai, J. M.; Pathinayake, P.; Malik, B.; Bartlett, N. W. Respiratory Viruses and Asthma. *Seminars in respiratory and critical care medicine* **2018,** *39* (1), 45–55. DOI: 10.1055/s-0037-1617412.

Welsh, R. M.; Che, J. W.; Brehm, M. A.; Selin, L. K. Heterologous immunity between viruses. *Immunological reviews* **2010,** *235* (1), 244–266. DOI: 10.1111/j.0105-2896.2010.00897.x.

Welsh, R. M.; Selin, L. K. No one is naive: the significance of heterologous T-cell immunity. *Nature reviews. Immunology* **2002,** *2* (6), 417–426. DOI: 10.1038/nri820.

Wenzel, S. E. Asthma phenotypes: the evolution from clinical to molecular approaches. *Nat Med* **2012,** *18* (5), 716–725. DOI: 10.1038/nm.2678.

Wichmann, H. E. Possible explanation for the different trends of asthma and allergy in East and West Germany. *Clinical and experimental allergy : journal of the British Society for Allergy and Clinical Immunology* **1996,** *26* (6), 621–623.

Wieczorek, M.; Abualrous, E. T.; Sticht, J.; Álvaro-Benito, M.; Stolzenberg, S.; Noé, F.; Freund, C. Major Histocompatibility Complex (MHC) Class I and MHC Class II Proteins: Conformational Plasticity in Antigen Presentation. *Front. Immunol.* **2017,** *8*, 292. DOI: 10.3389/fimmu.2017.00292.

Wohlleben, G.; Müller, J.; Tatsch, U.; Hambrecht, C.; Herz, U.; Renz, H.; Schmitt, E.; Moll, H.; Erb, K. J. Influenza A virus infection inhibits the efficient recruitment of Th2 cells into the airways and the development of airway eosinophilia. *Journal of immunology (Baltimore, Md. : 1950)* **2003,** *170* (9), 4601–4611. DOI: 10.4049/jimmunol.170.9.4601.

Wong, R.; Belk, J. A.; Govero, J.; Uhrlaub, J. L.; Reinartz, D.; Zhao, H.; Errico, J. M.; D'Souza, L.; Ripperger, T. J.; Nikolich-Zugich, J.; Shlomchik, M. J.; Satpathy, A. T.; Fremont, D. H.; Diamond, M. S.; Bhattacharya, D. Affinity-Restricted Memory B Cells Dominate Recall Responses to Heterologous Flaviviruses. *Immunity* **2020,** *53* (5), 1078-1094.e7. DOI: 10.1016/j.immuni.2020.09.001.

Woodruff, P. G.; Modrek, B.; Choy, D. F.; Jia, G.; Abbas, A. R.; Ellwanger, A.; Koth, L. L.; Arron, J. R.; Fahy, J. V. T-helper type 2-driven inflammation defines major subphenotypes of asthma. *Am J Respir Crit Care Med* **2009,** *180* (5), 388–395. DOI: 10.1164/rccm.200903-0392OC.

Woolnough, K.; Craner, M.; Pashley, C. H.; Wardlaw, A. J. rAsp f3 and rAsp f4 are associated with bronchiectasis in allergic fungal airways disease. *Annals of allergy, asthma & immunology : official publication of the American College of Allergy, Asthma, & Immunology* **2018,** *120* (3), 325–326. DOI: 10.1016/j.anai.2017.10.026.

World Health Organiszation. Vaccines against influenza WHO position paper – November 2012. *Releve epidemiologique hebdomadaire* **2012,** *87* (47), 461–476.

World Health Organization: Chronic Respiratory Diseases - Asthma. https://www.who.int/news-room/q-a-detail/chronic-respiratory-diseases-asthma (accessed September 28, 2021).

Wu, P.; Dupont, W. D.; Griffin, M. R.; Carroll, K. N.; Mitchel, E. F.; Gebretsadik, T.; Hartert, T. V. Evidence of a Causal Role of Winter Virus Infection during Infancy in Early Childhood Asthma. *Am J Respir Crit Care Med* **2008,** *178* (11), 1123–1129. DOI: 10.1164/rccm.200804-579OC.

Wu, Q.; Jorde, I.; Kershaw, O.; Jeron, A.; Bruder, D.; Schreiber, J.; Stegemann-Koniszewski, S. Resolved Influenza A Virus Infection Has Extended Effects on Lung Homeostasis and Attenuates Allergic Airway Inflammation in a Mouse Model. *Microorganisms* **2020,** *8* (12). DOI: 10.3390/microorganisms8121878.

Wucherpfennig, K. W.; Strominger, J. L. Molecular mimicry in T cell-mediated autoimmunity: Viral peptides activate human T cell clones specific for myelin basic protein. *Cell* **1995,** *80* (5), 695–705. DOI: 10.1016/0092-8674(95)90348-8.

Wypych, T. P.; Wickramasinghe, L. C.; Marsland, B. J. The influence of the microbiome on respiratory health. *Nature immunology* **2019,** *20* (10), 1279–1290. DOI: 10.1038/s41590-019-0451-9.

Yang, L.; Fu, J.; Zhou, Y. Research Progress in Atopic March. *Front. Immunol.* **2020,** *11*, 1907. DOI: 10.3389/fimmu.2020.01907.

Yao, Y.; Chen, C.-L.; Di Yu; Liu, Z. Roles of follicular helper and regulatory T cells in allergic diseases and allergen immunotherapy. *Allergy* **2021,** *76* (2), 456–470. DOI: 10.1111/all.14639.

You, D.; Becnel, D.; Wang, K.; Ripple, M.; Daly, M.; Cormier, S. A. Exposure of neonates to respiratory syncytial virus is critical in determining subsequent airway response in adults. *Respiratory research* **2006,** *7*, 107. DOI: 10.1186/1465-9921-7-107.

Yuan, R.; Yu, J.; Jiao, Z.; Li, J.; Wu, F.; Yan, R.; Huang, X.; Chen, C. The Roles of Tissue-Resident Memory T Cells in Lung Diseases. *Front. Immunol.* **2021,** *12*, 710375. DOI: 10.3389/fimmu.2021.710375.

Zens, K. D.; Chen, J. K.; Farber, D. L. Vaccine-generated lung tissue-resident memory T cells provide heterosubtypic protection to influenza infection. *JCI insight* **2016,** *1* (10). DOI: 10.1172/jci.insight.85832.

Zhang, L.; Peeples, M. E.; Boucher, R. C.; Collins, P. L.; Pickles, R. J. Respiratory syncytial virus infection of human airway epithelial cells is polarized, specific to ciliated cells, and without obvious cytopathology. *Journal of virology* **2002,** *76* (11), 5654–5666. DOI: 10.1128/JVI.76.11.5654-5666.2002.

Zhao, J.; Zhao, J.; Mangalam, A. K.; Channappanavar, R.; Fett, C.; Meyerholz, D. K.; Agnihothram, S.; Baric, R. S.; David, C. S.; Perlman, S. Airway Memory CD4(+) T Cells Mediate Protective Immunity against Emerging Respiratory Coronaviruses. *Immunity* **2016,** *44* (6), 1379–1391. DOI: 10.1016/j.immuni.2016.05.006.

Zhu, Z.; Hasegawa, K.; Ma, B.; Fujiogi, M.; Camargo, C. A.; Liang, L. Association of asthma and its genetic predisposition with the risk of severe COVID-19. *The Journal of allergy and clinical immunology* **2020,** *146* (2), 327-329.e4. DOI: 10.1016/j.jaci.2020.06.001.

9. Supplementary figures

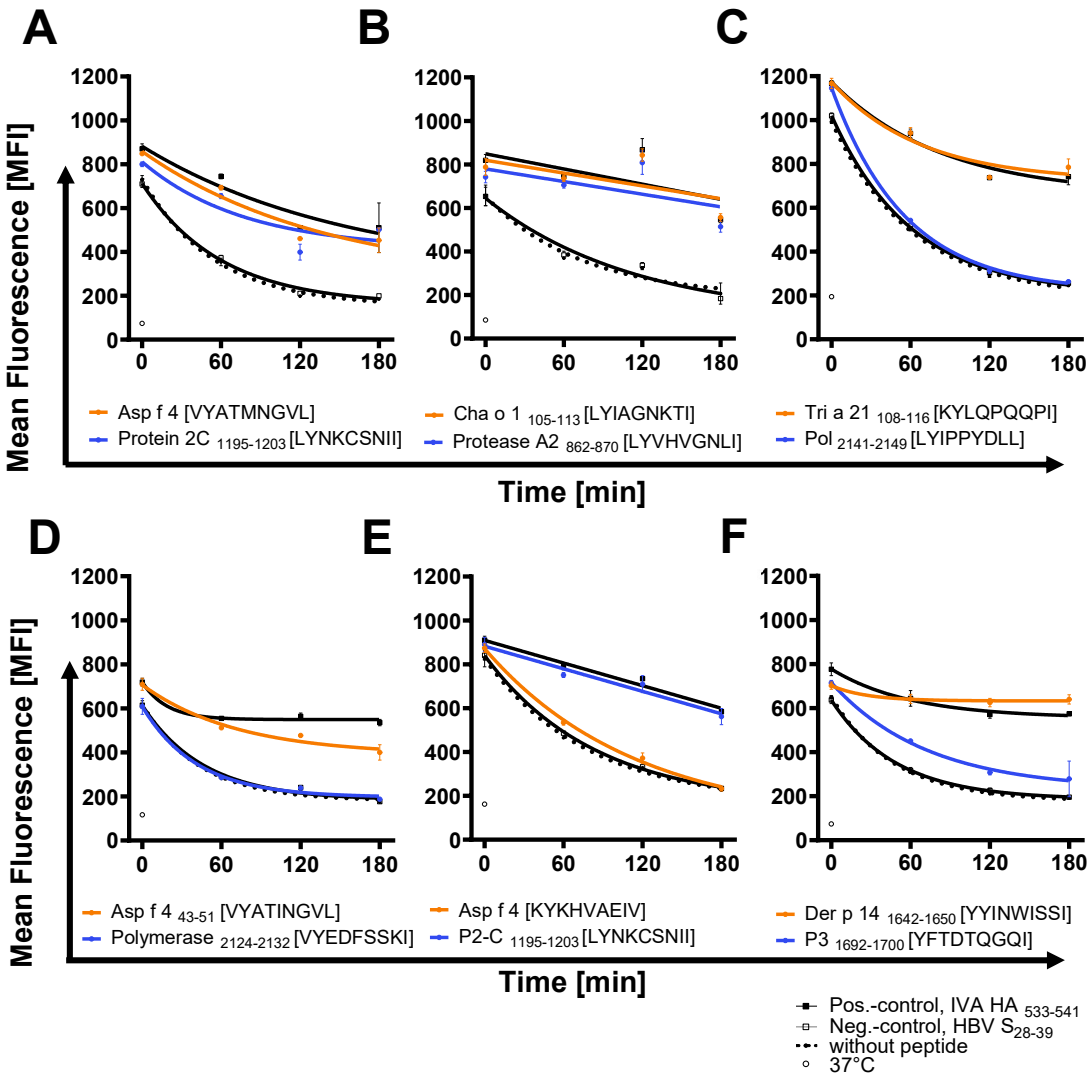

Figure 43: Binding of predicted RV1b peptides to the mouse Balb/c H-2-Kd MHC molecule *in-vitro*
H-2-Kd expressing RMA-S cells were incubated with 10 µM of the respective peptides of RV1b analysis or control peptides for 3 h at 26 °C. Mean fluorescence intensity of H-2-Kd expression was measured by flow cytometry and are shown as ± SD, n=3 **A-B:** strong binder pairs **C-F:** non-binder pairs; IVA HA=Hemagglutinin of Influenza A virus, HBV S=surface protein of Hepatitis B virus

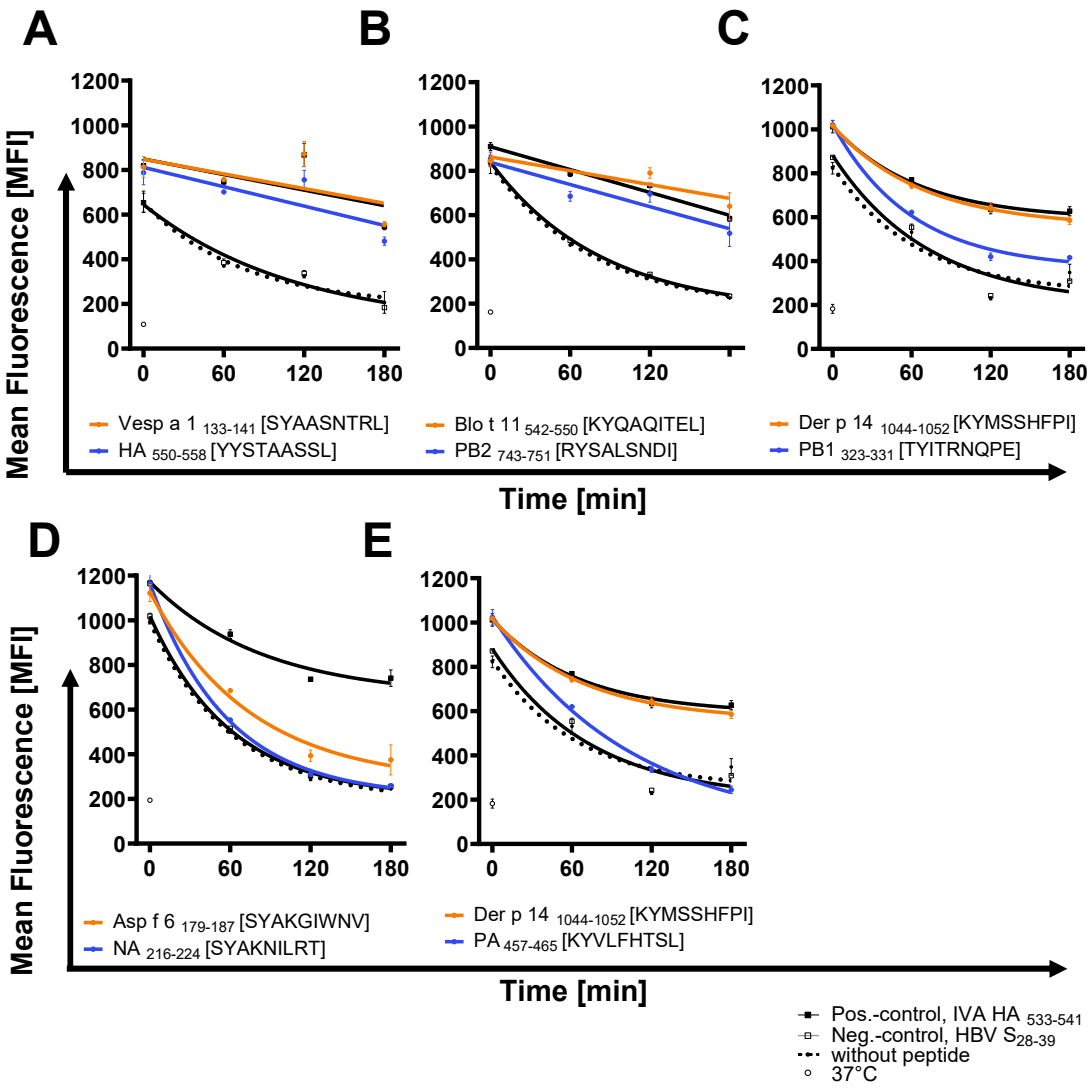

Figure 44: Binding of predicted QIV 19/20 peptides to the mouse Balb/c H-2-Kd MHC molecule *in-vitro*
H-2-Kd expressing RMA-S cells were incubated with 10 µM of the respective peptides of QIV 19/20 analysis or control peptides for 3 h at 26 °C. Mean fluorescence intensity of H-2-Kd expression was measured by flow cytometry and are shown as ± SD, n=3 **A-B:** strong binder pairs **C:** weak binder pair **D-E:** non-binder pairs; IVA HA=Hemagglutinin of Influenza A virus, HBV S=surface protein of Hepatitis B virus

10. Appendix

a. Verzeichnis der akademischen Lehrer/-innen
b. Danksagung

Verzeichnis der akademischen Lehrer

Meine akademischen Lehrer und Lehrerinnen der Justus-Liebig-Universität waren:

Althaus, Becker, Bindereif, Dammann, Dorresteijn, Ehlers, Ekschmitt, Friedhoff, Goesman, Göttlich, Holz, Hughes, Klug, Lakes-Harlan, Leers, Martin, Renkawitz, Schmitz, Schindler, Sträßer, Trenczek, Wilke, Wolters, Wissemann, Ziemek

Danksagung

Zum Schluss möchte ich mich noch bei allen bedanken, die mich auf dem Weg zu meiner Promotion begleitet haben und diese ermöglicht haben.
Ein ganz besonderer Dank gilt **Prof. Dr. Harald Renz** und **PD Dr. Chrysanthi Skevaki** für die Möglichkeit, an solch einem interessanten und abwechslungsreichen Thema zu arbeiten, sowie für die vielen wissenschaftlichen Diskussionen während dieser Zeit. Liebe **Chrysanthi**, ich danke dir besonders dafür, dass du dir immer Zeit für mich genommen hast. Zusätzlich möchte ich mich für die Möglichkeit bedanken, an so vielen nationalen und internationalen Kongressen teilzunehmen und mir so einen wissenschaftlichen Austausch zu ermöglichen.
Ein weiterer Dank geht an **Prof. David Pride** und **Dr. Roland Liu** von der UCSD für die Kooperation und Unterstützung mit den Virome Analysen.
Außerdem möchte ich mich bei **Prof. Franz Cemic** und **Vanessa Heger** für die Kooperation und Hilfe bei den *in-silico* Analysen bedanken.
Bei **Dr. Jochen Wilhelm** möchte ich mich für die Hilfe bei der statistischen Auswertung bedanken und bei **Dr. Hervé Luche** für die Hilfe bei der Auswertung von FACS Daten.
Ein riesiges Dankeschön geht an **alle aktuellen und ehemaligen Mitglieder** des Instituts, die mich tatkräftig bei den vielen Experimenten unterstützt haben und ohne die so manche Versuchstage in dem Ausmaß nicht funktioniert hätten. Solch ein Zusammenhalt und gegenseitige Unterstützung sind nicht selbstverständlich! Außerdem bedanke ich mich für die tolle Atmosphäre und die vielen lustigen Momente, Weihnachtsfeiern und Pizzaessen 😊 Ganz besonders bedanken möchte ich mich bei
…. **Kim und Sarah**, ich bin sehr dankbar, dass wir von Anfang an so ein gutes Team waren! Ich danke euch für all eure Hilfe, für die neuen Ideen und Problemlösungen aber auch für die Freundschaft, die sich entwickelt hat und natürlich dafür, dass ich Karl behalten durfte 😉
…. all den Studenten, die ich mitbetreuen durfte- **Lilith, Anita, Valerie und Max**, ihr wart eine riesige Unterstützung, ich danke euch für die Mitarbeit in diesem Projekt und für euer Vertrauen!

…. **Nicole und Thomas**, ich verdanke euch mein ganzes tierexperimentelles Wissen und das Erlernen der meisten Methoden! Ich danke euch für die unendlichen Stunden im Tierstall, die oft sehr spontane Hilfe und all eure Unterstützung!
…. **Sara**, ich bin so dankbar für alles, was du für mich getan hast! Ich danke dir für die viele Unterstützung mit unserem lieblings-TCR-Sequencing und natürlich für all deine andere Hilfe zu jeder Tages- und Nachtzeit und ganz besonders für dein immer offenes Ohr und die vielen freundschaftlichen aber auch wissenschaftlichen Gespräche, ewigen Telefonate und langen Sprachnachrichten 😉!
…. **Laura** und **Philipp** für all die Unterstützung bei den bioinformatischen Auswertungen, **Bilal** für all die beantworteten Fragen und Problemlösungen, **Thilo** für das immer offene Ohr im Büro und die Hilfe bei den Prep´s und **Julia** für die seelisch-moralische Unterstützung bei einem Kaffee oder gutem griechischem Essen!
Ein weiterer Dank geht an **Dr. Hartmann Raifer**, danke, dass du immer noch ein Zeitslot für mich gefunden hast und vielen Dank für all deine Hilfe beim Panel-Design, Auswertungen oder sonstigen Problemen!
Ein großes Dankeschön geht auch an **Sara, Lena**, **Hannah, Sarah und Sina** für´s Korrekturlesen dieser Arbeit!
Natürlich geht auch ein riesiges Dankeschön an **all meine lieben Mädels**! Ihr habt mich immer motiviert, hattet stets ein offenes Ohr für mich und habt mit den vielen schönen gemeinsamen Momenten für den perfekten Ausgleich gesorgt. Ich danke euch von Herzen für eure Freundschaft und dafür, dass ihr immer für mich da seid!

Und wie immer das Beste zum Schluss- **meine Familie und meine bessere Hälfte Jan**, die mich tagtäglich auf diesem Weg begleitet und unterstützt haben und immer für mich da sind! **Liebe Mama, lieber Achim**, ohne euch wäre all das nicht möglich gewesen und dafür danke ich euch von Herzen. Ich bin sehr dankbar, so eine tolle Familie zu haben und zu wissen, dass ich immer auf euch zählen kann!
Mein liebster **Jan**, du hast mich selbst nach den längsten Labortagen zum Lächeln gebracht, stets motiviert, immer die richtigen Worte gefunden oder mich einfach in den Arm genommen und mich in jeglicher Hinsicht unterstützt. Ich danke dir für jede Sekunde mit dir, für deine Liebe und dafür, dass wir das perfekte Team sind und ich mich immer auf dich verlassen kann!